Differential Packaging of Outer Membrane Proteins of Enterotoxigenic *Escherichia coli* into Outer Membrane Vesicles under Oxidative Stress Conditions Reveals a Potential Mechanism for Vesicle Cargo Selectivity

by

Nichole Orench-Rivera

Department of Biochemistry
Duke University Medical School

Date: _____
Approved:

_____
Margarethe Kuehn, Advisor

_____
Richard G. Brennan

_____
Michael S. Boyce

_____
Sudarshan Rajagopal

_____
Christopher V. Nicchitta

Dissertation submitted in partial fulfillment of
the requirements for the degree of Doctor
of Philosophy in the Department of
Biochemistry in the Graduate School
of Duke University

2020

ABSTRACT

Differential Packaging of Outer Membrane Proteins of Enterotoxigenic *Escherichia coli* into Outer Membrane Vesicles under Oxidative Stress Conditions Reveals a Potential Mechanism for Vesicle Cargo Selectivity

by

Nichole Orench-Rivera

Department of Biochemistry
Duke University Medical School

Date: _____
Approved:

_____
Margarethe Kuehn, Advisor

_____
Richard G. Brennan

_____
Michael S. Boyce

_____
Sudarshan Rajagopal

_____
Christopher V. Nicchitta

An abstract of a dissertation submitted in partial fulfillment of the requirements for the degree of Doctor of Philosophy in the Department of Biochemistry in the Graduate School of Duke University

2020

Copyright by
Nichole Orench-Rivera
2020

Abstract

Outer membrane vesicles (OMVs) are spherical structures that bud from the outer membrane (OM) of bacteria containing OM and periplasmic material. They are known to be produced by all bacteria studied to date and play important roles in inter-bacterial communication, bacterial-host interactions, toxin delivery, survival, nutrient acquisition, and biofilm development. The process of OMV production is known to be genetically regulated and selective cargo packaging into bacterial vesicles has been reported and implicated in many biological processes. While much is known about how cargo gets incorporated into vesicles in eukaryotic systems, the mechanism behind cargo selectivity in bacteria has remained largely unexplored. In this study we aimed to characterize preferential sorting trends in OMV packaging in *Escherichia coli* under oxidative stress, and investigate the mechanism behind selective sorting into OMVs. Proteomic analysis of outer membrane (OM) and OM vesicle fractions from enterotoxigenic *E. coli* (ETEC) revealed significant differences in protein abundance in the OMV and OM fractions for cultures shifted to oxidative stress conditions. Analysis of sequences of proteins preferentially packaged into OMVs showed that proteins with oxidizable residues were more packaged into OMVs in comparison with those retained in the membrane. In addition, the results indicated two distinct classes of OM-associated proteins were differentially packaged into OMVs as a function of peroxide treatment

and we observed a slight increase in periplasmic content. Implementing a Bayesian hierarchical model, OM lipoproteins were determined to be preferentially exported during stress whereas integral OM proteins were preferentially retained in the cell. We first inquired whether this sorting was due to the need of the cell to discard or retain OM proteins and tested oxidative stress sensitivity of mutants of lipoproteins and integral proteins. We hypothesized that mutants of lipoproteins would not be more sensitive than integral proteins however both groups showed increased sensitivity. Therefore, this did not explain this preferential sorting. We next wondered if selectivity was dependent on gene expression. By mining gene expression databases and performing qRT-PCR we found the sorting to be independent of transcriptional regulation of the proteins upon oxidative stress. We were also able to validate these preferential sorting trends of lipoproteins vs integral proteins using randomly selected protein candidates from the different cargo classes. We also observed that a shift to oxidative stress conditions improved the fitness of bacteria to a secondary oxidative challenge, suggesting the differential sorting resulted in an OMV-mediated remodeling of the OM during stress. Together, our data showed that oxidative stress induced a differential sorting of proteins into OMVs and OM of *E. coli* and that OMV production might serve as a disposal mechanism for the cell to rid itself of oxidized proteins. Since our data revealed that the preferentially retained proteins were those known to have ties to other cell envelope components, a hypothetical functional and mechanistic basis for

cargo selectivity was tested using OmpA as a model. A full-length and a truncated version of OmpA were used to test whether physical tethering to the cell is a determinant for protein retention in the OM. Quantifying OMV protein packaging of both OmpA constructs revealed a basic mechanism for cargo selectivity into OMVs. We show that the untethered version of OmpA was more likely to be exported than the tethered version and that this preferential selection was exacerbated under oxidative stress. The findings of this study provide insight into the dynamics of bacterial cargo selection and membrane remodeling during stress as well as propose and test a mechanism for cargo incorporation in *E. coli*.

Dedication

I dedicate this work to my *familia*. My parents Bruno and Albilda, and my sister, Zoé, along with my husband Austin and his family, have been a constant source of support and encouragement.

Contents

Abstract iv

List of Tables xiii

List of Figures xiv

Acknowledgements xvi

1. Introduction 1

1.1 Model organisms: Escherichia coli and Enterotoxigenic Escherichia coli (ETEC) ..2

1.1.1 *Escherichia coli* 2

1.1.2 Enterotoxigenic *Escherichia coli* 2

1.2 Cell envelope architecture in Gram-negative bacteria 5

1.2.6 Lipoproteins 7

1.2.7 OM and IM Integral proteins 9

1.2.8 Connections in the cell envelope 10

1.3 Outer membrane vesicles (OMVs) 11

1.3.1 OMV Biogenesis 12

1.3.2 OMV functions 15

1.3.2.1 Inter-bacterial communication 16

1.3.2.2 Bacteria-host interactions 17

1.3.2.3 Delivery of virulence factors 18

1.3.2.4 Survival and nutrient acquisition 19

1.3.2.5 Horizontal gene transfer 23

1.3.2.6 Biofilms....24

1.3.3 Quantification of OMVs....25

1.4 OMV composition and cargo selectivity....27

1.4.1 Mechanisms of vesicle cargo loading....31

1.5 Environment impacts on OMV content, function, and production....39

1.5.1 Iron availability....42

1.5.2 Biofilm versus planktonic lifestyle....44

1.5.3 Oxygen availability and pH....45

1.5.4 SOS response and antibiotic exposure....47

1.5.5 Host factors....51

1.5.6 Growth phase and media composition....54

1.5.7 Implications for OMV studies....57

1.6 OMVs and membrane remodeling....57

1.7 Oxidative stress and OMVs....58

1.7.1 Oxidative stress and the bacterial response....60

1.8 Summary and project aims....65

2. Outer membrane associated proteins are differentially packaged into outer membrane vesicles by *Escherichia coli* during an environmental shift to oxidative stress conditions.67

2.1 Summary....67

2.2 Introduction....68

2.3 Developing a protocol for monitoring changes in OMV packaging....71

2.4 Proteomic analysis of ETEC OMVs produced under unstressed and oxidative stress conditions....75

2.4.1 Proteomic data identification and annotation process 76

2.4.2 Outer membrane proteins are selectively packaged in enterotoxigenic *Escherichia coli* OMVs under unstressed environmental conditions 78

2.4.3 Oxidative stress alters the packaging of outer membrane-associated OMV cargo in enterotoxigenic *Escherichia coli* 78

2.5 Statistical model reveals differential sorting of lipoproteins and integral proteins during stress conditions 83

2.5.1 Bayesian Hierarchical models 83

2.6 No correlation is observed between packaging of proteins into OMVs and gene expression under stress conditions.....87

2.7 K-12 E. coli knockout mutants of lipoproteins and integral proteins do not show patterns of differential sensitivity to H_2O_2 90

2.8 Validation of differential OM-associated protein class sorting upon oxidative stress.....92

2.9 OMVs carry oxidized, functionally altered cargo and slightly increased periplasmic content, possibly dependent on gene expression 95

2.9.1 Oxidative stress causes a slight increase in OMV periplasmic cargo and this is possibly correlated with gene expression.....95

2.9.2 OMV cargo is more oxidatively modified in response to stress 100

2.9.3 Oxidative stress reduces OMV cytotoxicity 101

2.10 Remodeled membrane confers fitness advantage to the bacteria upon secondary challenge.....103

2.11 Discussion.....104

3. Uncovering a mechanism for OMV cargo selection based on physical tethering to the bacterial cell wall 109

3.1 Summary 109

3.2 Introduction 109

3.3 Gene Ontology analysis reveals preferentially retained OM proteins during oxidative stress are enriched in categories related to transport and iron homeostasis 112

3.4 Implementing OmpA as a model protein for testing tethering as a mechanism for OMV incorporation or exclusion of proteins during stress 114

3.5 Selective packaging of truncated OmpA compared to full-length OmpA into OMVs is exacerbated with oxidative stress.....116

3.6 Discussion.....118

4. Materials and methods 121

4.1 Culture conditions.....121

4.2 Sytox Green sensitivity assay 121

4.3 OMV isolation.....122

4.4 OM isolation.....122

4.5 Periplasm isolation.....123

4.6 OMV quantification 124

4.7 OMV and OM sample purification and preparation for proteomics 124

4.8 Proteomic analysis 125

4.9 Statistical analysis and model for protein sorting from proteomic dataset.....126

4.10 Statistics for non-proteomic data 127

4.11 Gene expression data from the GEO database 127

4.12 Detection of carbonyl-modified proteins.....127

4.13 qRT-PCR 128

4.14 Plasmid constructs 129

4.15 Immunoblot for validation of protein packaging into OMVs 134

5. Conclusions.....137

5.1 Future directions and impact on the field 140

5.2 Moving the OMV field forward 141

Appendix A 143

Abbreviations used in this text.....143

Appendix B 144

Supplementary tables 144

References 197

Biography.....229

List of Tables

Table 1: Studies were enrichment or exclusion of OMV cargo was observed. 28

Table 2 Environmental changes demonstrated to affect vesiculation (e.g. levels, activity or contents) 41

Table 3: Selective OM retention and OMV packaging with and without stress, and change in selectivity after oxidative stress for OM-associated proteins.....79

Table 4: Preferentially retained OM-associated proteins are enriched in transport and iron homeostasis GO categories 113

Table 5: qRT-PCR primers used in this study.....129

Table 6: Protein constructs used in this study 130

Table 7: Summary of recent proteomic analyses of OMV composition[1] 144

Table 8: Recent studies were lipid analysis was performed on OMVs and/or DNA presence was detected in vesicle samples. 150

Table 9: Localization of proteins with 2 or more peptides 151

Table 10: Summary of all OM-associated proteins detected in proteomic analysis of OM and OMV samples from untreated and peroxide-treated cultures 180

Table 11: GO Category analysis of OM-associated proteins at least 2-fold more retained or exported with oxidative stress 192

List of Figures

Figure 1: Architecture of the Gram-negative cell envelope. 5

Figure 2: Outer membrane vesicle. 12

Figure 3: Summary of current OMV biogenesis models. 15

Figure 4: Summary of OMV functions. 16

Figure 5: Mechanisms of cargo selection in bacterial systems. 32

Figure 6: Mechanisms of cargo selection in eukaryotes. 33

Figure 7: Environment shifts elicit changes in functional roles for OMVs. 40

Figure 8: The oxidative stress response in Gram-negative bacteria. 62

Figure 9: Shift conditions do not compromise membrane integrity or bacterial cell growth. 72

Figure 10: H_2O_2 treatment oxidizes protein in ETEC. 73

Figure 11: Oxidative stress does not alter vesicle production in ETEC. 74

Figure 12: Representative SDS-PAGE gels of gradient purified OMV and OM fractions. 75

Figure 13: Proteomic data identification and annotation process. 76

Figure 14: Subcellular localization of proteins in OM and OMV preparations from untreated and treated cultures. 77

Figure 15: Bayesian estimates and posterior distributions for treatment effect on OMV packaging of protein groups. 86

Figure 16: Oxidative stress causes a preferential export of lipoproteins into OMVs and a preferential retention of integral proteins in the OM of enterotoxigenic *Escherichia coli*. . 87

Figure 17: Results from mining GEO profile GSE4735 and validation in ETEC of selected genes. 89

Figure 18: Sensitivity of *E. coli* K-12 OM lipoprotein and integral protein mutants to H_2O_2. 91

Figure 19: OM localization, and treatment and membrane integrity assays for lipoprotein and integral proteins used in this study. 93

Figure 20: Validation of preferential packaging of lipoproteins into OMVs upon oxidative stress. 94

Figure 21: Oxidative stress increases the periplasmic content of OMVs. 98

Figure 22: Results from mining GEO profile GSE4735 and validation in ETEC of selected periplasmic genes. 99

Figure 23: Cargo contains a higher amount of oxidizable residues and it is more oxidatively modified in response to stress. 101

Figure 24: Oxidative stress reduces OMV cytotoxicity. 102

Figure 25: Remodeled membrane confers fitness advantage to the bacteria upon secondary challenge. 103

Figure 26: Overview of OmpA structure. 115

Figure 27: Proper localization and folding of tagged OmpA constructs in the OM and OMVs. 116

Figure 28: Selective packaging of truncated OmpA compared to full-length OmpA into OMVs is exacerbated with oxidative stress. 117

Figure 29: Summary for the selective OMV packaging of untethered cargo into OMVs in unstressed and stressed conditions. 120

Figure 30: Lipoprotein constructs used in this study. 132

Figure 31: Integral protein constructs used in this study. 133

Figure 32: Representative blot for OMV packaging of tagged constructs. 136

Acknowledgements

I acknowledge research support from NIH, NIGMS grant R01-GM099471. I thank the Duke Proteomics Core Facility and the Duke Core Facilities Voucher program for facilitating this investigation. I especially thank Matthew W. Foster, and M. Arthur Moseley, respectively, for collecting and analyzing the MS data and for proteomic facility scientific oversight. I also acknowledge the statistical support from A. Talbot; Dr. Tanneke den Blaauwen (University of Amsterdam) for generously providing the OmpA constructs; Dr. Richard Brennan for providing funding for gene synthesis orders from GenScript; and Carmen Schwechheimer for initiating the data-collection for Table 7 and 8 of proteomic references. Many thanks to all previous and current members of the Kuehn Lab, my committee members, and my advisor Meta J. Kuehn, for their support, feedback and many fruitful discussions.

1. Introduction

More than half a century ago, while studying products released by cultures of *Escherichia coli* under lysine-limiting conditions, D.G. Bishop and Elizabeth Work discovered what they described as "extracellular lipoglycopeptides" (Bishop and Work 1965). It wasn't until later that these structures were identified as outer membrane vesicles (OMVs) and found to be ubiquitously secreted by bacterial species. Today, it is known OMVs are key players in bacterial metabolism, nutrient acquisition, cell to cell communication and even antibacterial defense.

The overuse of antibiotics has caused an increase in antibiotic-resistant strains and according to the CDC's Antibiotic Resistance Threats in the United States report, more than 2.8 million antibiotic-resistant infections occur in the U.S. each year, resulting in more than 35,000 deaths (CDC 2019). Recently, OMVs have begun to be employed as vaccine platforms and some OMV-based vaccines are available (Gnopo et al. 2017; Irene et al. 2019). An understanding of the mechanisms of OMV production, specifically the process of cargo loading into vesicles, can inform the development of OMV-based vaccines to prevent bacterial infections.

1.1 Model organisms: Escherichia coli *and Enterotoxigenic* Escherichia coli *(ETEC)*

1.1.1 *Escherichia coli*

Escherichia coli is a Gram-negative, aero-anaerobic, rod-shaped bacteria that inhabits the lower intestine of vertebrates (Tenaillon et al. 2010). It provides its host with vitamin K_2, (Bentley and Meganathan 1982) which is crucial for blood clotting and calcium metabolism, and conveys protection against colonization of pathogenic bacteria in the gut (Hudault, Guignot, and Servin 2001).

Since its discovery by German-Austrian microbiologist and pediatrician Theodor Escherich, *E. coli* has become the most studied microorganism (Escherich 1989). Its rise as a model organism came as a result of its quick growth, availability of non-pathogenic strains, and its ease of isolation from humans (Blount 2015). *E. coli* is widely used for gene cloning due to its high efficiency of DNA transfer via plasmids, and is ideal for recombinant protein production (Cronan 2014). In 1997, the complete genome of *E. coli* non-pathogenic strain K-12 was sequenced (Blattner et al. 1997). This remarkable achievement took six years and since then has greatly increased our understanding of this model bacterium.

1.1.2 Enterotoxigenic *Escherichia coli*

Enterotoxigenic *E. coli* (ETEC) is the name given to a group of pathogenic *E. coli* which produce toxins that ultimately cause diarrhea. ETEC is contracted through the

ingestion of contaminated food or drinks and remains the major cause of traveler's diarrhea. Its discovery dates back to Calcutta, India in 1956 where it was isolated from children and adults who suffered from a cholera-like illness (De, Bhattacharya, and Sarkar 1956). Its hardiness and adaptability allows it to inhabit a wide variety of ecological niches such as environmental water, and the surface of leaves and fruits (Gonzales-Siles and Sjöling 2016).

The ETEC strain used in this study is *E. coli* O78:H11 strain H10407, phylogroup A. Strain H10407 is an ETEC isolate from an adult with cholera-like symptoms in Dacca, Bangladesh (Evans and Evans 1973). Its chromosome is most closely related to those of non-pathogenic *E. coli* strains (including *E. coli* K-12) and its virulence genes are located in plasmids. It has been suggested that this isolate was a commensal isolate that acquired plasmids with virulence genes, and became pathogenic (Crossman et al. 2010).

The major virulence factor of ETEC H10407 is heat-labile (LT) enterotoxin which is released after colonization of the small intestine. LT is an 87.5 kDa holotoxin with two subunits, a 27kDa A subunit surrounded by five identical binding B subunits of 11.7 kDa each. The A subunit contains two domains linked by a disulfide bridge, A1 and A2. A1 is the active toxin and A2 anchors to the B subunits (Bhunia 2018; Sixma et al. 1991; Merritt et al. 1994; Fleckenstein et al. 2010). Both subunits are produced with N-terminal signal peptides that get cleaved during Sec-dependent translocation across the inner membrane (IM) to the periplasm via the general secretory pathway (Connell et al. 1995;

Sandkvist et al. 1997; Hirst and Holmgren 1987). For many years it was thought that ETEC did not secrete LT and that the toxin remained in the periplasm. Studies later showed that while LT was not detected in the soluble ETEC culture supernatants, it was found associated with bacterial OMVs (Wai et al. 2003; Gankema et al. 1980; Horstman and Kuehn 2000) and that the mature holotoxin is then transported out of the periplasm, across the outer membrane (OM) via a type II protein secretion pathway (Sandkvist et al. 1997; Tauschek et al. 2002; Horstman and Kuehn 2002). After export, LT can remain associated with the OM due to the affinity of its B subunits for lipopolysaccharide (LPS) on the surface of *E. coli* via its B subunits. (Horstman and Kuehn 2002; Horstman, Bauman, and Kuehn 2004).

After host colonization, using a distinct binding site from its LPS-binding site, the LT B subunits can bind irreversibly to the GM1 ganglioside on the surface of epithelial cells (Lencer, Hirst, and Holmes 1999; Spangler 1992) triggering endocytosis of the holotoxin. The A1 domain of the A subunit is then translocated across the host plasma membrane to interact with ADP-ribosylating factors to ADP-ribosylate the GTPase Gsα (Tsai et al. 1987), causing its inactivation. This activates adenylate cyclase resulting in increases in cyclic AMP and subsequent stimulation of chloride secretion in the crypt cells and inhibition of neutral sodium chloride in the villus tips (Sears and Kaper 1996). This causes an increase in the absorptive capacity of the bowel, triggering diarrhea (Qadri et al. 2005; Sack et al. 1971).

ETEC H10407 is known to produce a higher amount of vesicles in comparison to its nonpathogenic counterpart K-12 *E. coli* (Horstman and Kuehn 2002). Its OMV yield facilitates studies of OMV cargo selection in *E. coli* by providing higher amounts of OMVs for proteomic characterization and biochemical assays.

1.2 Cell envelope architecture in Gram-negative bacteria

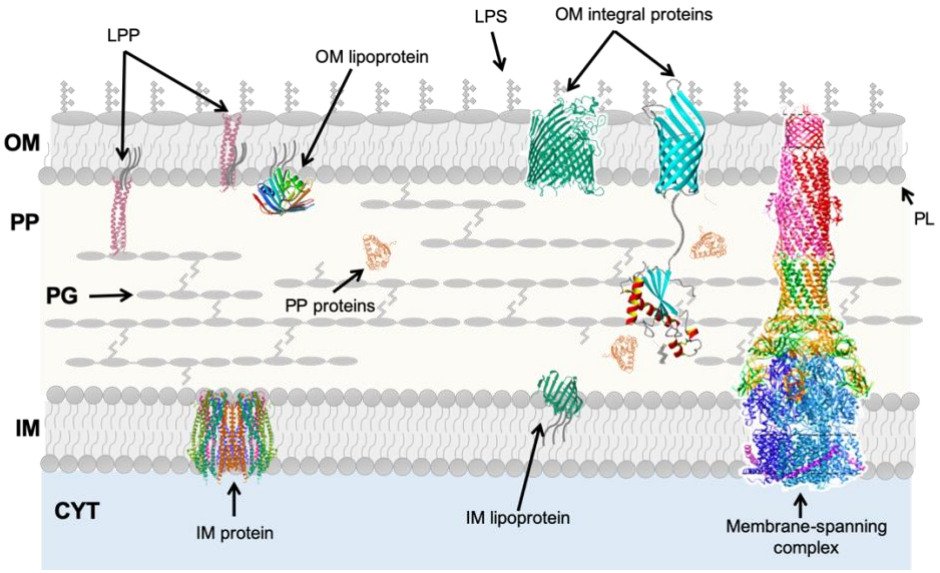

Figure 1: Architecture of the Gram-negative cell envelope.

OM, outer membrane; PP, periplasm; PG, peptidoglycan; IM, inner membrane, CYT, cytoplasm; LPP, Braun's lipoprotein; LPS, lipopolysaccharide; PL, phospholipids. OmpA structure from (Ishida, Garcia-Herrero, and Vogel 2014); AcrAB-TolC by (Wang et al. 2017); LolB (lipoprotein), PDB 1IWM; ExbB/ExbD from PDB 5ZFV; FhuA from PDB 2GRX; OmpX from PDB 1QJ8.

The cell envelope of Gram-negative bacteria is the outermost barrier against environmental stressors. Its unique architecture is complex and every component

contributes to bacteria's innate ability to adapt, thrive and survive in different conditions. it is composed of an inner membrane (IM), a periplasmic space, cell wall and an outer membrane (OM), all which play important roles in maintaining the cells integrity and barrier capabilities (Fig. 1). Knowledge of the nuances of the cell envelope structure is important for understanding OMV structure and biogenesis.

The IM, also known as the cytoplasmic membrane, is a phospholipid bilayer that surrounds the cytoplasm in Gram-negative bacteria. In *E. coli*, its main phospholipids are phosphatidyl ethanolamine and phosphatidyl glycerol, with smaller amounts of phosphatidyl serine and cardiolipin (Raetz and Dowhan 1990). The IM of Gram-negative bacteria is populated with many proteins that have crucial functions in energy production, lipid biosynthesis, protein secretion and transport (Silhavy, Kahne, and Walker 2010).

Between the IM and OM lies the periplasmic space. This aqueous compartment is densely packed with proteins that function in sugar transport, amino acid transport, and chemotaxis, as well as chaperone-like proteins that aid in envelope biogenesis (Silhavy, Kahne, and Walker 2010). The periplasm is an oxidizing environment and it serves as an important site for protein folding with proteins that allow for disulfide bond formation and isomerization (Missiakas and Raina 1997).

Within the periplasmic space is the peptidoglycan (PG) cell wall. This polymeric structure is composed of repeating glycan strands of N-acetyl glucosamine-N-acetyl

muramic (NAG-NAM) acid residues, crosslinked by short peptides (Vollmer, Blanot, and De Pedro 2008). The peptidoglycan is crucial for cell shape and serves as a scaffold for anchoring of proteins such as outer membrane protein A (OmpA) (Park 2011) and Braun's lipoprotein (Lpp) (Braun 1975). It is also involved in cell growth and division (Vollmer, Blanot, and De Pedro 2008).

The OM of Gram-negative bacteria is the outer most layer of the cell envelope. It is an asymmetrical bilayer where the outer leaflet is composed of lipopolysaccharide (LPS) while the inner one is phospholipids with a lipid composition similar to that of lipids in the IM (Hobot 2015). It contains a wide array of proteins, including porins and lipoproteins that aid in communication and signaling between the cell and its environment.

LPS is found in the outer leaflet of the Gram-negative OM and is anchored on the glycolipid lipid A. LPS consists of a lipid moiety, lipid A, covalently bound to a chain of sugar residues (Raetz 1993). These sugar residues are polysaccharides and oligosaccharide chains (O-antigen) that are antigenic and vary between bacterial species (Hobot 2015).

1.2.6 Lipoproteins

Bacterial lipoproteins are membrane-anchored proteins that serve a wide variety of functions including roles in cell division, virulence, nutrient uptake, signal transduction, adhesion, conjugation, antibiotic resistance, and transport. In pathogens,

they aid in colonization, invasion and evasion of host defenses, as well as immunomodulation (Kovacs-Simon, Titball, and Michell 2011). There are three enzymes in the IM involved in lipoprotein biosynthesis, the preprolipoprotein diacylglyceryl transferase (Lgt), prolipoprotein signal peptidase (Lsp) and apolipoprotein *N*-acyltransferase (Lnt) (Nakayama, Kurokawa, and Lee 2012). Lipoproteins are initially translated as pre-lipoproteins with an N-terminal signal and a conserved sequence at the C terminus called the lipobox. This sequence is modified through the covalent attachment of a diacylglycerol group to the thiol group on the side chain of the cysteine residue by Lgt (Nakayama, Kurokawa, and Lee 2012; Narita and Tokuda 2017). After addition of the lipid moiety, Lsp cleaves the signal sequence leaving the lipobox cysteine as the terminal residue (Nakayama, Kurokawa, and Lee 2012; Narita and Tokuda 2017). Finally, the cleaved prolipoprotein is further modified by the attachment of an amide-linked acyl group to the N-terminal cysteine (Noland et al. 2017) by Lnt. The diacylglycerol group and the amino-terminal acyl group provide anchoring to the membrane (Noland et al. 2017; Nakayama, Kurokawa, and Lee 2012; Narita and Tokuda 2017).

Lipoproteins can remain in the IM or become OM-localized. The LolCDE ATP-binding cassette transporter releases the OM-targeted lipoproteins from the IM and directs them into a complex with the periplasmic chaperone LolA (Narita and Tokuda 2006; Narita et al. 2002; Ito et al. 2006). LolB, an OM lipoprotein, then facilitates

incorporation the new lipoprotein into the OM (Narita and Tokuda 2017; Szewczyk and Collet 2016; Okuda and Tokuda 2011). Presence of an IM retention signal maintains lipoproteins in the IM (Masuda, Matsuyama, and Tokuda 2002; Sakamoto et al. 2010). In *E. coli*, this signal consists of a highly conserved aspartic aid at the +2 position of the mature lipoprotein and it is not recognized by LolCDE, leaving these proteins in the IM (Miyamoto and Tokuda 2007). Absence of this signal promotes the targeting of lipoproteins towards the Lol transport pathway to become OM-localized (Masuda, Matsuyama, and Tokuda 2002; Sakamoto et al. 2010).

1.2.7 OM and IM Integral proteins

Integral proteins are proteins embedded in the phospholipid bilayer. Integral OM proteins, typically called outer membrane proteins (OMPs), make up approximately 3% of the bacterial genome (Wimley 2003; Rollauer et al. 2015). OM Integral membrane proteins feature a β-barrel architecture in the membrane with loops between strains on the periplasmic side and large, extended loops on the extracellular side (Koebnik, Locher, and Van Gelder 2000). They are highly stable due to their particular structure and have many roles in virulence such as adhesion, nutrient uptake, and siderophore uptake (DiRienzo, Nakamura, and Inouye 1978). In contrast to OM integral proteins, IM integral proteins typically contain long hydrophobic transmembrane α-helices (Walther, Rapaport, and Tommassen 2009).

1.2.8 Connections in the cell envelope

Physical connections between the OM and PG; OM proteins and PG; and membrane spanning complexes with ties to the IM and PP components; all contribute to the structural integrity of the cell envelope and have crucial roles in bacterial physiology. The OM-lipoprotein Lpp, or Braun's lipoprotein can be found free (albeit anchored to the OM by its lipid group) as well as covalently bound to PG (Braun and Rehn 1969; Braun 1975; Cascales et al. 2002). Cells lacking Lpp or with mutations preventing its anchoring to PG exhibit high OMV production, are hypersensitive to toxic compounds and show overall membrane instability (Suzuki et al. 1978; Vadillo-Rodriguez, Schooling, and Dutcher 2009; Yem and Wu 1978)

OmpA is a major protein in the *E. coli* OM and is considered important for structural integrity of the OM along with Lpp (Wang 2002). OmpA contains a β-barrel transmembrane domain and a domain that non-covalently binds to PG and contributes to the stability of the OM (Wang 2002; Ortiz-Suarez et al. 2016; Park 2011).

Multi-protein complexes that span the OM and IM also provide connectivity in the cell envelope. The flagellar machine, for instance, is composed of about two dozen proteins some of which are in the IM, the periplasm and the OM. Some components of trans-envelope complexes even have muramidase activity to penetrate the PG layer (Kojima and Blair 2004). The periplasm-spanning, integral IM-TonB protein is required for many receptors and drug efflux machinery. Such TonB-dependent receptors mediate

transport of macromolecules such as siderophores across the OM and use energy derive from the TonB-ExbB-ExbD complex located in the IM (Noinaj et al. 2010; Celia et al. 2016; Pawelek et al. 2006; Shultis et al. 2006). In *E. coli*, efflux pumps belonging to the Resistance -nodulation-division (RND) family are multi-protein complexes important for antimicrobial resistance and they are formed by complexes between periplasmic proteins that belong to the membrane-fusion-protein (MFP) and OM channels facilitating the export of drugs out of the cell (Nikaido 1998). For example, the AcrAB-TolC system is composed of an IM (AcrB), an OM channel (TolC), and an adaptor protein (AcrA) (Nikaido and Takatsuka 2009; Pagès and Amaral 2009; Pos 2009).

1.3 Outer membrane vesicles (OMVs)

OMVs are spherical, proteo-lipidic nanostructures, ranging in 50-250 nm in size, that are produced from the OM of bacteria (Fig. 2). OMVs can carry material from the OM as well as the periplasmic space and they have multiple roles in bacterial physiology and pathogenesis. All bacteria studied to date produce vesicles and the process of OMV biogenesis is known to be genetically regulated (Bodero, Pilonieta, and Munson 2007; Kitagawa et al. 2010; Kulp et al. 2015; Nevermann et al. 2019; van der Westhuizen et al. 2019). While much is known about OMV function, many mechanistic questions remain regarding the OMV-mediated secretion process.

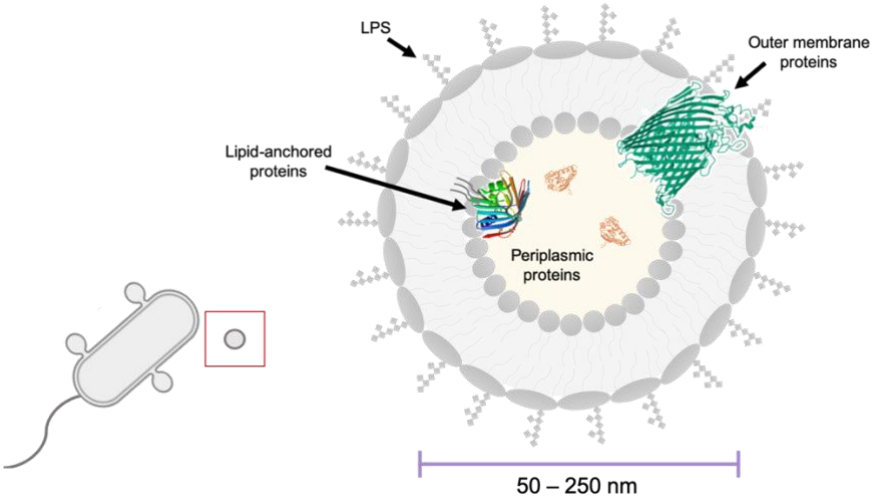

Figure 2: Outer membrane vesicle.

1.3.1 OMV Biogenesis

The biogenesis of OMVs has been widely studied. Studies reveal the mechanism of OMV budding and subsequent release varies greatly depending on bacterial species and environmental conditions. However, there are currently several proposed models for OMV secretion (Fig. 3), some of which are derived from studies of mutants of bacterial strains with OMV secretion phenotypes. Many studies have shown that OMV production is a genetically controlled process. Some studies have focused on specific genes modulating OMV production (Bodero, Pilonieta, and Munson 2007; van der Westhuizen et al. 2019; Kitagawa et al. 2010). Others such as a screen of transposon mutants with vesiculation phenotypes (McBroom et al. 2006) and a genome-wide assessment of vesicle production in *E.* coli, (Kulp et al. 2015) as well as in *S. enterica*

(Nevermann et al. 2019) have expanded the OMV field by identifying groups of genes that regulate OMV production in bacteria.

Lpp (Braun's lipoprotein) crosslinks and PG remodeling are key contributors to modulation of OMV production (Schwechheimer, Rodriguez, and Kuehn 2015; Schwechheimer, Kulp, and Kuehn 2014). These studies showed that the amount of crosslinking in the cell envelope correlates with the production of OMVs, suggesting more crosslinks decreases OMV production while the loss of crosslinks increases it. The amount of crosslinking can be modulated not only by the presence of Lpp, but also by localized PG degradation or synthesis. In this mechanism of OMV biogenesis, the amount of crosslinking in the cell envelope, by either Lpp or PG, can modulate OMV budding.

Another mechanism found to modulate OMV production in bacteria is periplasmic pressure. Studies in *E. coli* have suggested accumulation of misfolded proteins or overexpression of proteins, exerts pressure on the OM, driving OMV formation. In this mechanism, vesiculation serves as a disposal mechanism, allowing the cell to rid itself of unneeded or damaged material (Schwechheimer and Kuehn 2013).

The bi-layer couple model is an OMV biogenesis mechanism observed in *Pseudomonas aeruginosa*. The model involves molecules such as the *Pseudomonas* quinolone signal (PQS) which intercalate into lipids in the outer leaflet of the OM,

promoting vesicle production by inducing curvature at the surface (Schertzer and Whiteley 2012; Florez et al. 2017).

In the case of *Haemophilus influenzae*, deletion or repression of the VacJ/Yrb ABC phospholipid transport system, was shown to cause an accumulation of phospholipids in the outer leaflet of the OM resulting in increased OMV production (Roier et al. 2016). This study revealed a mechanism in which PL accumulation in the OM causes an asymmetric expansion of the outer leaflet leading to OM budding (Roier et al. 2016).

A study on *S. enterica* serovar Typhimurium suggested a mechanism of OMV production based on lipid A deacylation (Elhenawy et al. 2016). When the authors overexpressed PagL they observed an increase in vesiculation in *S. enterica*, and an associated enrichment of deacylated lipid A in OMVs. In this case OMV production is thought to be driven by the change in lipid A topology that forces the OM to bulge outwards promoting curvature and subsequent OMV formation (Elhenawy et al. 2016). Whether this mechanism occurs in wildtype cells (without PagL overexpression) is currently unknown.

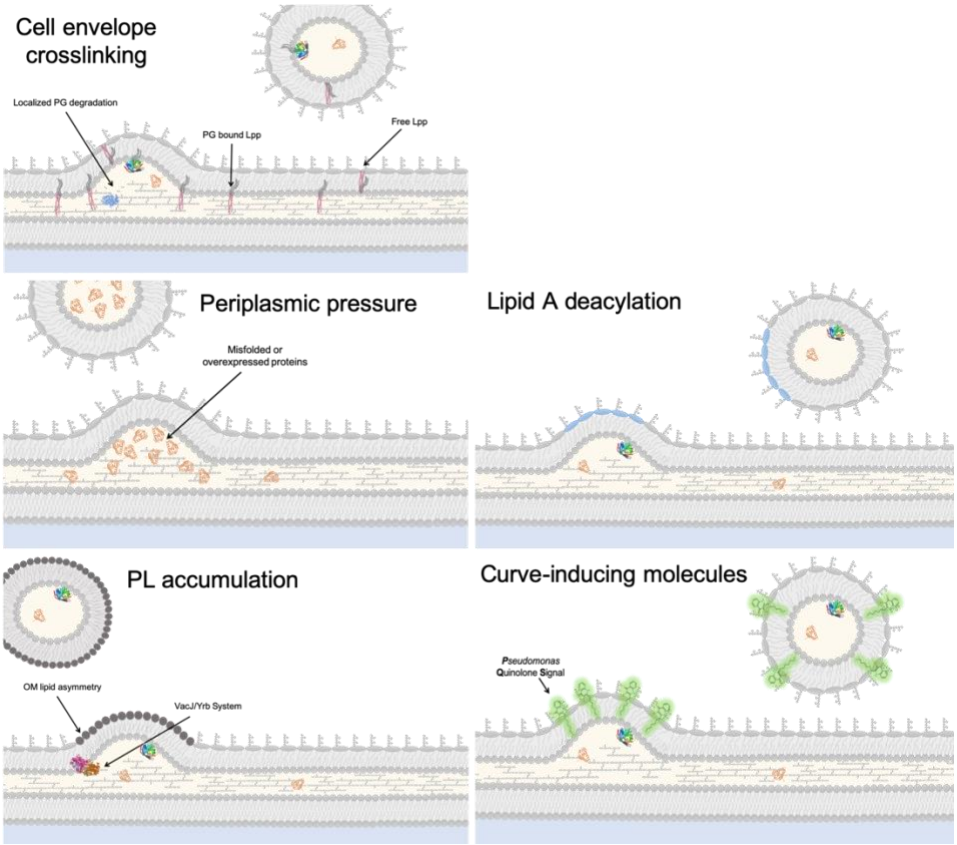

Figure 3: Summary of current OMV biogenesis models.

OMV biogenesis in bacteria can occur due to envelope crosslinking (Schwechheimer, Rodriguez, and Kuehn 2015; Schwechheimer, Kulp, and Kuehn 2014), periplasmic pressure (Schwechheimer and Kuehn 2013), PL (phospholipid) accumulation (Roier et al. 2016), Lipid A deacylation (Elhenawy et al. 2016), or aided by curve-inducing molecules (Schertzer and Whiteley 2012; Florez et al. 2017).

1.3.2 OMV functions

The most investigated aspect of OMV biology is OMV function (Fig. 4). As a secretion mechanism, OMV allow bacteria to secrete insoluble molecules in a protected environment and allow for enzymes to travel in a concentrated and targeted form (Kulp

and Kuehn 2010). Their stability contributes to their wide variety of roles in bacterial interactions as well as bacterial-host interactions.

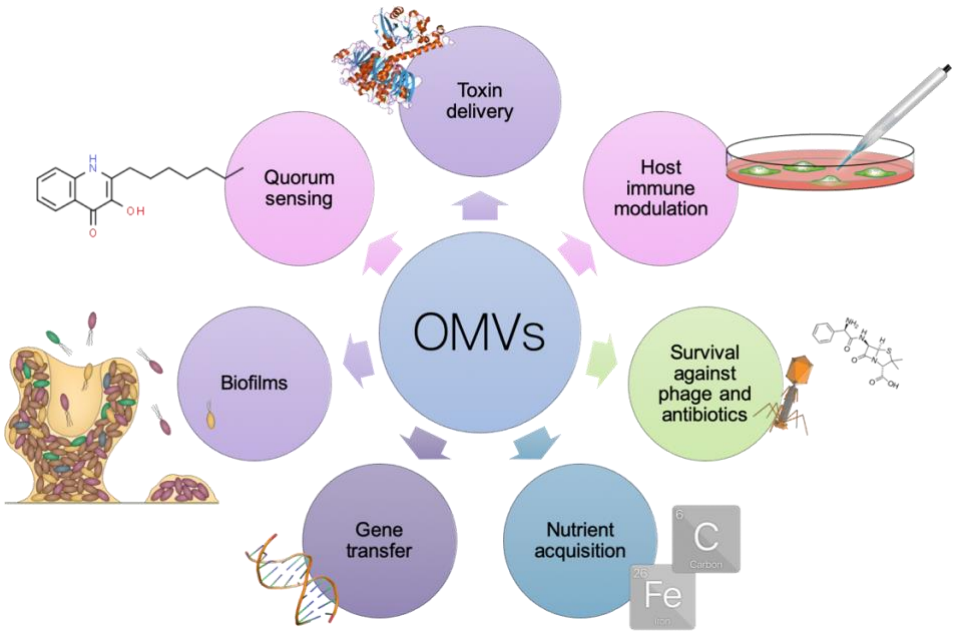

Figure 4: Summary of OMV functions.

Figures for this diagram were adapted or obtained from several sources: Biofilm (McDougald, et al. 2012); PQS (Hodgkinson, et al. 2011); toxin (Bioinformatics services | European Bioinformatics Institute, 2020); cell dish (OBOE IPR, 2020); antibiotic penicillin and phage (Wikipedia, 2020); C and Fe elements (4,625,000+ free and premium vector icons in SVG, PNG, CSH and AI format., 2020).

1.3.2.1 Inter-bacterial communication

OMVs have important roles in inter-bacterial communication. Many bacteria secrete small molecules to communicate with each other in a process called quorum sensing (QS) and by this process bacteria produce and release molecules that increase in

concentration as a function of cell density (Miller and Bassler 2001). Both Gram-positive and Gram-negative bacteria regulate a variety of process through QS, including, virulence, motility, and biofilm formation (Miller and Bassler 2001). OMVs have been observed to play a role in quorum sensing in several studies (Toyofuku 2019). In *P. aeruginosa*, the Pseudomonas quinolone signal (PQS) can trigger OMV formation and it was also been observed to be packaged into vesicles to be used by other bacterial cells (Mashburn-Warren et al. 2008; Schertzer and Whiteley 2012; Mashburn and Whiteley 2005). In the case of *Paracoccus denitrificans* a nitrate reducing bacterium, vesicles were observed to carry C16-HSL (Toyofuku et al. 2017), an acyl-homoserine lactone (AHL) important for quorum sensing. Thus, OMVs can contribute to bacterial communication by acting as delivery mechanisms for molecules crucial for cell to cell signaling.

1.3.2.2 Bacteria-host interactions

Within their biological hosts, bacteria are known to secrete OMVs and many studies have outlined their effect on modulating bacterial-host interactions (Kuehn and Kesty 2005). For example, OMVs are known to elicit host immune responses. OMV proteins, lipids, as well as vesicle-bound cargo, can elicit pro- or anti-inflammatory effects on the host (Bonnington and Kuehn 2013). While many studies have highlighted the contribution of OMVs to the modulation of the mammalian immune response, recent studies have also shown that OMVs can also modulate the plant immune response (McMillan, et al. 2020).

Bacteria employ a wide variety of proteins and molecules, some of which are OMV-associated (Bonnington and Kuehn 2013), to adhere to host cells, colonize tissues and in some cases invade cells during infection (Pizarro-Cerdá and Cossart 2006). OM proteins, for example, can confer adhesive properties to OMVs. While a study in *Actinobacillu*s vesicles showed that OMVs enhanced the ability of the parent cells to adhere to epithelial cells, the mechanism by which it influences adherence of the *Actinobacillus* cells is unknown (Meyer and Fives-Taylor 1994). In other cases, the adhesive properties of the OMVs can negatively impact bacterial adherence to host cells as it was the case with *Borrelia burgdoferi* vesicles which were shown to compete with the parent bacterium for host receptors in human umbilical vein endothelial cells (Shoberg and Thomas 1993).

1.3.2.3 Delivery of virulence factors

It has been observed that OMVs can carry and delivery virulence factors, including toxins, to host cells, aiding bacteria in the development of infection. A wide variety of toxins such LT from ETEC; Shiga toxin from Shiga-toxin-producing *E. coli* (STEC); NarE from *Neisseria meningitidis*; hemolysin from extraintestinal *E.* coli (ExPEC); VacA from *H.* pylory; leukotoxin from *Actinobacillus actinomycetemcomitans*; and cytotoxins from *Xenorhabdus nematophilus*, have been found to associated with OMVs (Ellis and Kuehn 2010). In a *P. aeruginosa* study purified OMVs delivered multiple virulence factors such as β-lactamase, alkaline phosphatase, hemolytic phospholipase C

(PlcH), and CFTR inhibitory factor (Cif) to the host plasma membrane (Bomberger et al. 2009) confirming OMVs can be serve as delivery vehicles for virulence factors in *P. aeruginosa*. Delivery of virulence factors via OMVs is also observed in enterohemorrhagic *E. coli* (EHEC) O157, a human pathogen responsible for hemolytic uremic syndrome (HUS) and bloody diarrhea (Nguyen and Sperandio 2012). Bielaszewska et al found that EHEC OMVs carried many virulence factors including Shiga toxin 2a (Stx2a), cytolethal distending toxin V (CdtV), EHEC hemolysin and flagellin which were internalized by host cells resulting in cell death (Bielaszewska et al. 2017). Notable for the work in this thesis, OMVs from ETEC, carry the major toxin LT (Wai et al. 2003; Gankema et al. 1980; Horstman and Kuehn 2000) and enable for targeted delivery and entry of this enterotoxin into host cells (Kesty et al. 2004; Chutkan and Kuehn 2011). These studies highlight the potential of OMVs as vehicles for delivery of virulence factors and toxins to host cells.

1.3.2.4 Survival and nutrient acquisition

In a screen of *E. coli* transposon mutants with vesiculation phenotypes, McBroom et al. observed an enrichment for genes from the σ^E envelope stress response pathway (McBroom et al. 2006). Additional studies showed that misfolded proteins are targeted as vesicle cargo suggesting OMVs as a mechanism for alleviating a toxic accumulation of misfolded proteins in the periplasm (McBroom and Kuehn 2007). The same study showed that hypervesiculating mutants of *E. coli* are less sensitive to stressors than

hypovesiculating mutants of *E. coli* (McBroom and Kuehn 2007). This data was the first to show that OMVs were important for bacterial viability. Follow up studies by Schwechheimer and Kuehn showed that an accumulation of proteins in the periplasm caused by the absence of the protease DegP drives the production of OMVs containing misfolded proteins (Schwechheimer and Kuehn 2013).

Studies of the proteomes of OMVs have shown that vesicles can carry proteins that can aid in nutrient acquisition and transfer to neighboring cells. For instance, in *Bacteroides succinogenes*, a cellulolytic bacterium in the rumen of cattle and sheep (Montgomery, Berdena, and Stahl 1988), hydrolytic enzymes such as cellulase and xylanase associate with vesicles (Forsberg, Beveridge, and Hellstrom 1981). This suggests that OMVs can possess cellulolytic and activities to provide a sugar source for surrounding microbes that cannot degrade polymers (Forsberg, Beveridge, and Hellstrom 1981). Recently, in *Pseudomonas putida*, a Gram-negative bacterium found in soil and water, Salvachúa et al. found that OMVs contained enzymes that catabolize lignin-derived aromatic compounds when grown in lignin-rich media (Salvachúa et al. 2020). OMVs have also been shown to possess metal scavenging properties since they have been shown to carry proteins that aid in metal binding (Prados-Rosales et al. 2011). A study by Prados-Rosales et al. showed the siderophore mycobactin was packaged into OMVs of iron-limited *Mycobacterium tuberculosis*. This supports the idea of vesicles as iron-scavenging agents (Prados-Rosales et al. 2014). Furthermore, OMVs from *M.*

tuberculosis enriched in mycobactin helped deliver iron to neighboring cells (Prados-Rosales et al. 2014).

There are also several studies consistent with the idea of OMVs absorbing antibiotics in the environment and improving bacterial survival. Manning and Kuehn showed that hypervesiculation was protective against antibiotics that target the OM (Manning and Kuehn 2011). This showed that OMVs can interact with antibiotic molecules (acting as decoy agents) and protect bacteria during treatment. In on *Moraxella catarrhalis* the antibiotic β-lactamase was found to be enzymatically active in OMVs and a preincubation of amoxicillin with OMVs rescued several amoxicillin-susceptible strains including *M. catarrhalis*, *Streptococcus pneumoniae* and *H. influenzae* from β-lactam-induced killing (Schaar, Nordström, et al. 2011). Kulkarni et al. found that OMVs isolated from *E. coli* MG1655 were protective to *E. coli* against colistin and melittin (both membrane-targeting agents) and also conferred protection to *P. aeruginosa* and *Acinetobacter radioresistens* against those same compounds. In this case, degrading enzymes were found in the OMV proteome suggesting vesicles were able to degrade antibiotic molecules extracellularly to confer protection (Kulkarni, Nagaraj, and Jagannadham 2015). This mechanism of extracellular degradation of antibiotics, was also observed by the Devos group in *Stenotrophomonas maltophilia* (Devos et al. 2015; Devos et al. 2016). In *S. maltophilia*, OMVs released in response to the β-lactam antibiotic

imipenem contained β-lactamase (Devos et al. 2015) which was later found to be active and effective at degrading β-lactams (Devos et al. 2016).

Bacteriophages are viruses that infect bacteria and several studies have shown that OMVs can act as decoys to protect bacteria from phage infection. Manning and Kuehn observed that co-incubation of phage T4 with OMVs resulted in reduced infection caused by irreversible binding of the phage with the OMVs (Manning and Kuehn 2011). This binding was confirmed by electron microscopy showing complexes between T4 and OMVs (Manning and Kuehn 2011). Also, in cultures of *Prochlorococcus*, a marine cyanobacterium, vesicles were found to be co-purifying with phage particles. This suggested that in the marine environment, vesicles can also act as a phage-capture mechanism for bacteria (Biller et al. 2014) More recently, Reyes-Robles et al. found that OMVs from *V. cholerae* were able to neutralize three different virulent phages. For phage ICP1, the protection was mediated by the O-antigen in *V. cholerae* OMVs, while for ICP2 it was mediated by the OM porin OmpU (Reyes-Robles et al. 2018). This group was also able to visualize via cryo-electron tomography, the interactions between phages and OMVs (Reyes-Robles et al. 2018). Similar to the interactions observed between OMVs and antibiotics, OMVs can mediate bacterial protection against phages by binding and neutralizing phages in the surrounding environment.

1.3.2.5 Horizontal gene transfer

Genetic material has been found to be a component of some bacterial vesicles (Table 8) and the mechanism driving the incorporation of DNA or RNA into vesicles is currently poorly understood (Domingues and Nielsen 2017). Some studies suggest DNA becomes vesicle cargo as part of double-layered inner-outer membrane vesicles (I-OM) containing cytoplasmic content (Pérez-Cruz 2013), while others propose DNA is transported to the periplasm through a yet unknown mechanism, and becomes encapsulated (Renelli et al. 2004; Rumbo et al. 2011). For RNA, it is hypothesized that protein synthesis near the budding site results in incorporation of mRNA (Blenkiron et al. 2016). Regardless of the mechanism behind nucleic acid incorporation, OMVs have been implicated in horizontal gene transfer events (Fulsundar et al. 2014; Blesa and Berenguer 2015; Renelli et al. 2004; Rumbo et al. 2011; Sjöström et al. 2015). For example, in *Acinetobacter baumannii*, a strain expressing the plasmid-born carbapenemase gene $bla_{\text{OXA-24}}$, released OMVs that harbored this gene. Incubation of the OMVs with a carbapenem-suceptible *A. baumannii* resulted in full resistance and the plasmid was detected in the recipient cell (Rumbo et al. 2011). In *Acinetobacter baylyi* horizontal gene transfer was also observed when OMVs isolated from plasmid-containing donor cells were incubated with *E. coli* and transformation-deficient mutants of *A. baylyi* resulting in transformation of the recipient cells (Fulsundar et al. 2014). Delivery of genetic material via vesicles is believed to be beneficial for efficient transfer of material since it has been

observed that vesicles can provide protection to the genetic material against nucleases (Rumbo et al. 2011; Blesa and Berenguer 2015).

1.3.2.6 Biofilms

A biofilm is an aggregate of microorganisms and extracellular products in which cells are embedded in a matrix of extracellular polymeric substances (EPS), nucleic acids, OMVs, and other bacterial products that adhere that stick to each other and to a biotic or an abiotic surface (Vert et al. 2012; Schooling and Beveridge 2006). Several studies have focused on the role of OMVs in bacterial biofilms. In *Helicobacter pylori*, a bacterium commonly associated with gastritis, a unique OMV 22-kDa protein was found to be important for biofilm formation in a strain with a robust biofilm phenotype (TK1402) (Yonezawa et al. 2011). In *P. aeruginosa*, the OMV-associated leucine aminopeptidase PaAP was found to play a role in biofilm formation (Esoda and Kuehn 2019). A deletion of this protein greatly altered the microcolony composition of an early biofilm and OMVs from PaAP-expressing strains were able to complement the phenotype. In this case, this OMV-associated protein was found to mediate changes in early biofilm development (Esoda and Kuehn 2019). Other studies have also found evidence of vesicle components or vesicles themselves modulating biofilm formation (van Hoek 2013), influencing the overall structure of the biofilm (Murphy et al. 2014) or modulating the surface of cells to enhance biofilm development (Baumgarten, Sperling, et al. 2012).

1.3.3 Quantification of OMVs

There is a wide variety of analytical methods used to study OMV biogenesis and composition. The quantitative methods include counting particles by transmission electron microscopy (TEM), Nanoparticle tracking analysis (NTA), and Dynamic Light Scattering (DLS); quantification of lipid content using lipid probes such as FM4-64; and quantification of protein content by SDS-PAGE, and densitometry of OMPs, or assays of total protein by Bradford reagent or bicinchoninic-acid assays (Stewart 1980; McBroom et al. 2006; Schertzer, Brown, and Whiteley 2010; Van Der Pol et al. 2010; Sharpe, Kuehn, and Mason 2011; Wessel et al. 2013; Devos et al. 2015; Chen et al. 2016). Each of these methods has strengths and weaknesses.

Protein and lipid quantification are often used as proxies for amount of OMVs in a sample. A Bradford protein assay or bicinchoninic acid assay can be used to quantify total amount of protein per OMV sample and, the lipophilic styryl dye FM4-64 ((N-(3-Triethylammoniumpropyl)-4-(6-(4-(Diethylamino) Phenyl) Hexatrienyl) Pyridinium Dibromide), allows for OMV lipid quantification. Notably, growth conditions and genetic mutations can change lipid to protein ratios and composition in the bacterial membrane, skewing lipid- or protein-only-based quantitative comparisons of OMV production (McBroom et al. 2006). Furthermore, in many cases, samples do not consist of pure OMVs, so the use of total protein quantification in samples is reliable only if OMV purity has been established. Depending on the preparative method or culture

conditions, cell-free supernatants may be contaminated with protein from lysed cells, flagellin, cytoplasm, or IM fragments that co-pellet with OMVs upon ultracentrifugation. Density gradient purification of OMVs reduces contaminants but also impacts quantitative yield. Therefore, for the accurate quantitation of OMVs in impure samples, densitometry measurements of OMV-specific SDS-PAGE protein bands (e.g. OmpF/C for *E. coli*) can be used. However, if this method is being used to calculate OMV amount, the relative level of OMP expression in the cells must be taken into account.

Regardless of the quantification method, all OMV production data must be normalized to the number of bacteria in the culture, either by utilizing optical density (OD) or colony-forming units (CFUs). A combination of quantitative techniques is often useful to establish OMV production. For instance, OMV lipid quantification can be coupled to measurements of OMPs by SDS-PAGE and densitometry, and normalized to bacterial counts (Chutkan et al. 2013; Schwechheimer, Rodriguez, and Kuehn 2015; Roier et al. 2016).

Several techniques are employed for OMV counting. Transmission electron microscopy (TEM) is used for vesicle imaging and has nanometer resolution which allows for distinguishing between the relative abundance of vesicles and non-vesicle material (Rikkert et al. 2019). TEM is often used to determine vesicle size, heterogeneity in vesicle size, and to confirm vesicle membrane integrity and purity of the sample.

Nanoparticle tracking analysis (NTA) is often used as to the most up-to-date method for counting vesicles. NTA is based on the movement of nanoparticles in solution according to Brownian motion (Bachurski et al. 2019). It can size particles from 30 to 1000 nm and it combines laser light scattering microscopy with a camera, enabling the visualization and recording of the particles in solution (Filipe, Hawe, and Jiskoot 2010). Size, and concentration of vesicles can be obtained using this technique and it provides information at the single-particle level. Combined with surface-charge measurement, it can provide more information about vesicle properties. Dynamic Light Scattering (DLS) is also a common technique used for characterizing OMVs. Its principle is based on directing a monochromatic laser light through a solution (Yennawar et al. 2016). It provides information about vesicle size and polydispersity (heterogeneity of sizes) (Palmieri et al. 2014). With additional analyses, DLS can also provide OMV hydrodynamic radius (Pencer and Hallett 2003). These OMV counting techniques provide information about different OMV properties. However, given the heterogeneity of OMV sizes in different bacterial strains and growth conditions, the ability to distinguish between protein complexes and vesicles can become an issue.

1.4 OMV composition and cargo selectivity

While some studies might suggest OMV cargo is randomly incorporated into vesicles, many studies have shown that there is selectivity in cargo incorporation into bacterial vesicles and that this occurs in many strains (Table 1).

Table 1: Studies were enrichment or exclusion of OMV cargo was observed.

Strain	Enrichment	Depletion	Reference
A. actinomycetemcomitans	Leukotoxin	n/a	(Kato, Kowashi, and Demuth 2002)
P. gingivalis	Gingipains	OM proteins PG0694, PG0695	(Glowczyk et al. 2017)
	Virulence factors	Proteins with OmpA-binding motifs and TonB-dependent receptors	(Veith et al. 2014)
Enterotoxigenic *E. coli*	Heat-labile enterotoxin	-	(Horstman and Kuehn 2000)
F. nucleatum	Virulence factor FadA	Autotransporters	(Liu et al. 2019).
B. thetaiotaomicron	Alpha-amylase SusG and other lipoproteins	TonB-dependent receptor SusC	(Valguarnera et al. 2018).
S. marcescens	Several OMPs (OmpA, W and X)	TolC, LptD, maltoporin and YaeT	(McMahon et al. 2012)
H. pylori	Several bacterial proteins	-	(Zavan et al. 2019)

Generally, studies of OMV composition focus on identifying OMV proteins and lipids, along with their relative abundance. This can be achieved using qualitative methods to identify the components (Table 7) and quantitative methods to obtain protein and lipid abundances (Ong and Mann 2005), including mass spectrometry, thin layer chromatography, biochemical detection and activity assays. To identify OMV cargo enrichment and subsequently study the mechanics and functional consequences of cargo selectivity, OMV content must be compared with purified OM and periplasmic

fractions to obtain a ratio representative of OMV packaging for a particular OMV component.

Several studies have highlighted that OMVs exhibit selective protein content and have shown that preferential packaging or exclusion of proteins from OMVs can contribute to bacterial virulence. For instance, *A. actinomycetemcomitans* was shown to secrete vesicles enriched in leukotoxin which were shown to be more toxic to human HL60 cells than isolated OM fractions (Kato, Kowashi, and Demuth 2002). In the case of *Porphyromonas gingivalis*, the proteases gingipains, which are known to modulate host immune responses (Glowczyk et al. 2017), were observed to selectively associate with OMVs while other OM proteins (such as PG0694 and PG0695) were excluded from vesicles (Haurat et al. 2011). Also in *P. gingivalis*, relative to the OM, an enrichment of virulence factors and exclusion of proteins with OmpA-binding motifs and TonB-dependent receptors was observed in OMVs (Veith et al. 2014). In ETEC, OMVs are selectively enriched for active heat-labile enterotoxin compared to other periplasmic cargo (Horstman and Kuehn 2000). Selective cargo of virulence factors was also demonstrated in *Fusobacteirum nucleatum,* where selective OMV incorporation of the virulence factor FadA and exclusion of some autotransporters was observed (Liu et al. 2019). These studies show that OMV cargo selectivity plays a role in bacterial virulence as vehicles for toxin delivery.

OMV cargo selectivity can also be beneficial for the cell to package proteins that other cells can utilize. In *Bacterioides thetaiotaomicron*, OMV enrichment of the alpha-amylase SusG, and other lipoproteins was observed under standard growth conditions, as well as an exclusion of TonB-dependent receptor SusC, compared to OM fractions (Valguarnera et al. 2018). SusG was shown to be active in OMVs and able to rescue the growth of bacterial cells unable to grown on starch as a carbon source (Valguarnera et al. 2018).

In other cases, OMV-enrichment of particular proteins has not been documented to serve a particular function for the bacterium. For *Serratia marcescens* enrichment of several OMPs (such as OmpA, OmpW and OmpX) and exclusion of other proteins such as TolC, LptD, maltoporin and YaeT was observed when OMVs were compared to OM fractions (McMahon et al. 2012). In *H. pylori*, OMV enrichment of several bacterial proteins was observed when compared to the *H. pylori* proteome (Zavan et al. 2019), showing OMV selectivity occurs during standard growth conditions.

OMV cargo selectivity can be particularly important for bacteria during environmental shifts. In *P. aeruginosa*, treatment with the epoxide epibromohydrin (EBH) resulted in an enrichment of the OM porin OprF and the protein Cif into OMVs (Ballok et al. 2014). Epoxides are toxic by-products of eukaryotic metabolism (Hayakawa et al. 1986) and Cif is an epoxide hydrolase, suggesting OMVs selectively package this protein to target host-derived epoxides during infection (Ballok et al. 2014).

While lipid analysis has been performed as part of several OMV composition studies (Table 8), very few studies have focused on OMV lipid selectivity. In *P. aeruginosa*, OMVs showed enrichment of negatively charged B-band forms of LPS compared to neutral A-band forms (Kadurugamuwa and Beveridge 1995). In contrast, Haurat et al. recently showed that in *P. gingivalis*, A-band form of LPS was enriched in OMVs compared to the OM (Haurat et al. 2011).

1.4.1 Mechanisms of vesicle cargo loading

Preferential packaging or exclusion of OMV cargo is an interesting feature of OMVs, and while cargo selectivity has been observed for several bacterial strains, not much is known about *how* cargo gets incorporated into the vesicles. Is cargo incorporation an active process, or does cargo selectivity result from particular sites of the envelope that are more prone to budding? Are there particular proteins that recruit cargo into vesicles? In the field of OMVs these questions are yet to be answered as only a few mechanisms have even been explored (Fig. 5). In eukaryotic vesicle systems, however, vesicle cargo selection has been widely studied (Fig. 6). Generally, mechanisms for cargo selection in both prokaryotic and eukaryotic systems involve bulk flow incorporation of cargo, signal sequence, or modification-dependent cargo selection, and incorporation via protein or lipid recruitment factors.

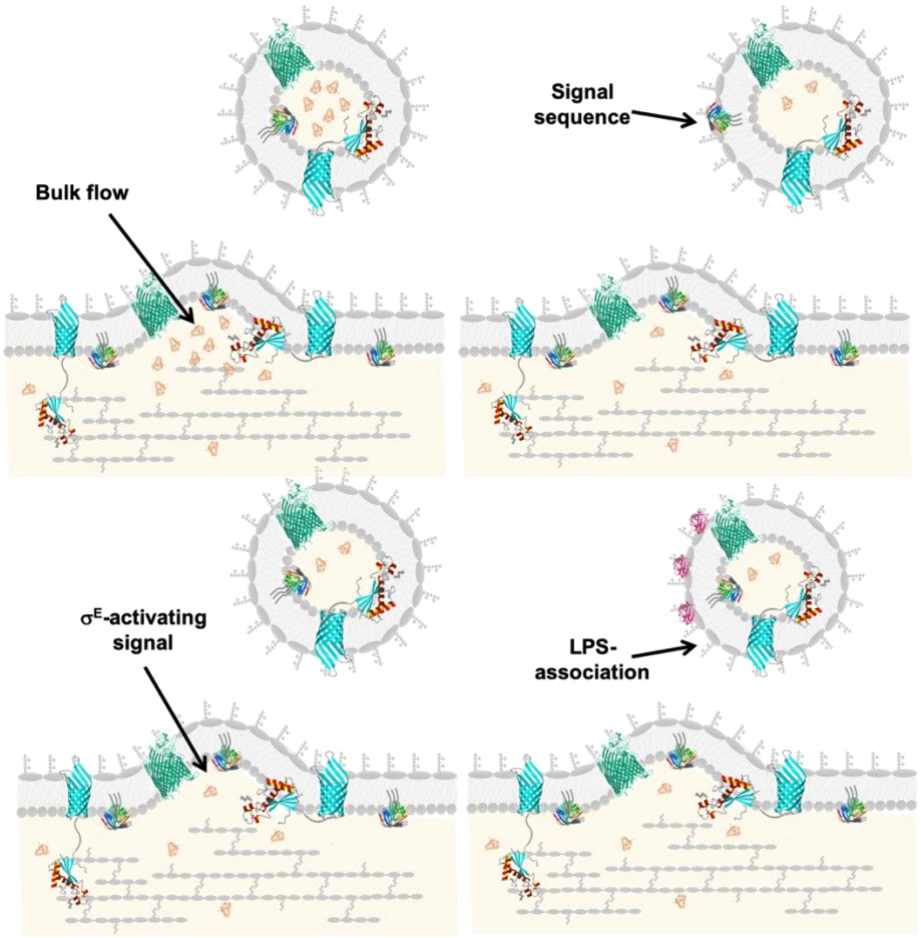

Figure 5: Mechanisms of cargo selection in bacterial systems.

In bacteria, cargo selection has been observed to occur by bulk flow (*E. coli*, *H. pylori*); determined by signal sequence (*B. thetaiotaomicron*), by an σ^E-activating signal (*E. coli*); or by association with LPS (*P. gingivalis*).

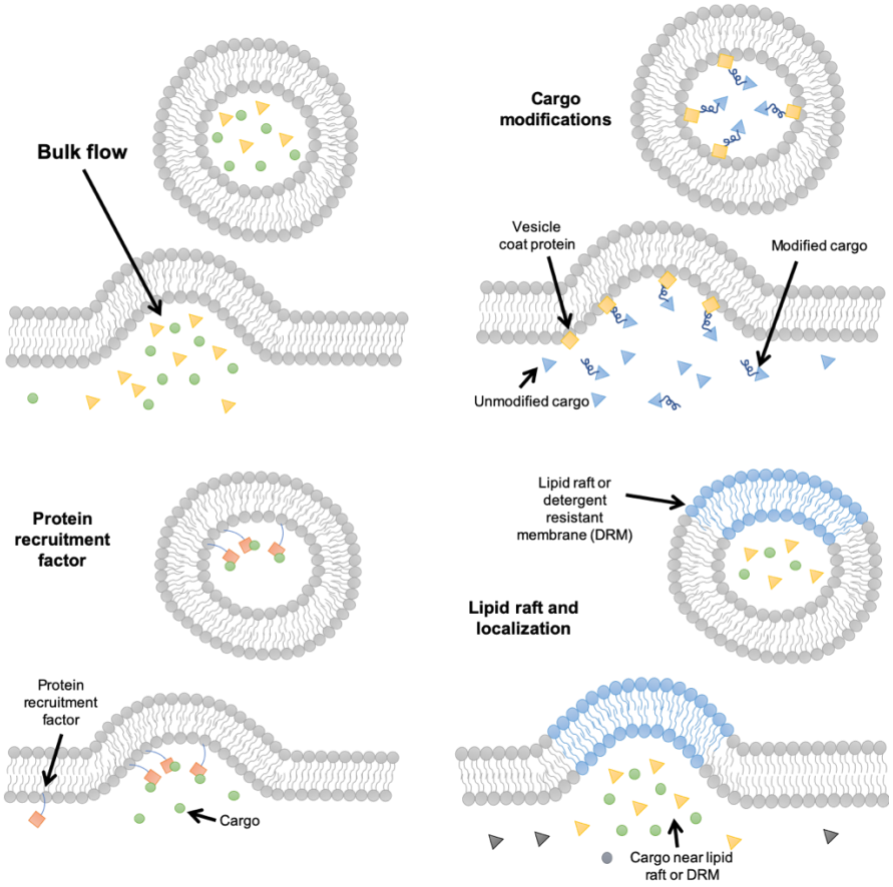

Figure 6: Mechanisms of cargo selection in eukaryotes.

In eukaryotic systems, cargo selection can occur by bulk flow (COPI and COPII systems); dictated by cargo modifications such as post-translational modifications, signal sequences or protein domains (exosomes, ESCRT system); by protein-recruitment factors (COPI and COPII systems, exosomes, shedding microvesicles); or in association with lipid rafts or detergent-resistant membranes (ESCRT system, exosomes).

Bulk flow incorporation of cargo is the random incorporation of proteins into vesicles. It likely occurs for proteins and lipids that are incorporated into vesicles based on their proximity to the budding site. This occurs in the case of *H. pylori* where mass spectroscopy analysis of vesicles revealed the majority of the OM proteins were

observed to be vesicle cargo (Olofsson, Vallström, et al. 2010). In the case of non-pathogenic *E. coli*, accumulation of misfolded proteins in the periplasm of a DegP (protease) mutant, or the overexpression of an envelope protein resulted in a corresponding high abundance of misfolded protein and envelope protein, respectively, as OMV cargo (Schwechheimer and Kuehn 2013), consistent with incorporation of proteins into vesicles by bulk flow and may be due to the presence of such proteins in the vicinity of the budding site as a result of overexpression or accumulation in the periplasm.

As in the bacterial system, bulk flow in eukaryotic vesicle systems occurs when proteins and lipids are incorporated by default (Barlowe and Helenius 2016). For example, in the COPI and II systems which are involved in protein traffic between the endoplasmic reticulum and the Golgi apparatus, p24 proteins (a conserved family of eukaryotic small integral membrane proteins) in the membrane force a delay in the budding event allowing for sorting of proteins to occur by bulk flow (Elrod-Erickson and Kaiser 1996).

In other cases, protein incorporation into vesicles can occur in a signal sequence-dependent manner. In a study of *B. thetaiotaomicron* OMVs, a negatively charged amino acid motif (LES) was found to be required for the surface exposure and subsequent OMV packaging of the alpha-amylase SusG (Valguarnera et al. 2018). This case exemplifies a selective cargo mechanism by which a particular motif in the protein

directs its incorporation into vesicles, however this mechanism might be exclusive for *B. thetaiotaomicron* due to the particular localization of its lipoproteins on the outer surface of the OM.

In non-pathogenic *E. coli*, McBroom and Kuehn showed that appending a σ^E activating stress signal to proteins determined their incorporation into OMVs (McBroom and Kuehn 2007). The σ^E-dependent stress response pathway is induced by heat or stressors that would generate unfolded cell envelope proteins (Alba and Gross 2004). This suggested a mechanism for how misfolded proteins get targeted for export in vesicles and is the only known signal for inclusion and enrichment of soluble bacterial proteins into OMVs (McBroom and Kuehn 2007).

In the field of eukaryotic vesicles, post-translational modifications, signal sequences or protein domains can determine the incorporation of proteins as vesicle cargo. In exosomes, the presence of a modular domain in Nedd4 family proteins (neural precursor cell expressed developmentally down-regulated protein 4), mediated protein-protein interactions with protein Ndfip1 (Nedd4 family-interacting protein 1) directing their incorporation into exosomes (as reviewed in (Anand et al. 2019)). In the endosomal sorting complexes required for transport (ESCRT) system, many studies have revealed that cargo sorting occurs through the recognition of ubiquitinated proteins (For reviews see (Schuh and Audhya 2014) and (Anand et al. 2019)). Other modifications such as SUMOylation (small ubiquitin related modifier), phosphorylation, glycosylation, and

citrullination (studies are needed to determine if citrullinated proteins are being selectively packaged) have been observed in exosomal cargo (reviewed in (Anand et al. 2019)). In those cases, protein modifications target cargo to be incorporated into vesicles.

Another mechanism by which cargo can become incorporated into vesicles is through recruitment factors. These recruitment molecules can either be protein or lipid recruitment factors. In the COPII system, proteins inside the vesicle budding site act as recruitment factors or anchors for other proteins get incorporated as cargo. Using tagged constructs of COPII system proteins Sar1 and Sec23, Aridor et al. found that the Sar1 protein and the Sec23-24 complex were required for cargo selection (Aridor et al. 1998; Kuehn, Herrmann, and Schekman 1998). Specifically, vesicular stomatitis virus G protein (VSV-G) is known to be recruited to the vesicular coat through interactions via its di-acidic motif (Nishimura and Balch 1997). Other studies showed that p24 proteins self-associate creating a domain in the membrane that serves as an attachment site for factors that get sorted into vesicles in the COPI and COPII systems (Dominguez et al. 1998; Lavoie et al. 1999). Similarly, in the COPI and COPII systems, proteins that coat the inside of the vesicle budding site are displaced by proteins with higher affinity to the vesicle coat. Only proteins with high affinity can displace p24 proteins, becoming cargo and excluding other proteins from being incorporated into the vesicle (Springer et al. 2000).

Protein sorting into exosomes can also via protein recruitment factors. This process is ESCRT-independent and aided by tetraspanins, proteins with four transmembrane domains that play diverse roles in cell biology and physiology (Charrin et al. 2014). The tetraspanins are known to cluster into microdomains at the membrane and they have been found to be enriched in exosomes. Many studies suggest they interact with exosome cargo and mediate its sorting into exosomes (see (Raposo and Stoorvogel 2013) for review). In the case of shedding microvesicles, which are plasma membrane-derived particles distinct from exosomes, the protein Arf6 (ADP-ribosylation factor 6) can influence the sorting of proteins by becoming activated along the plasma membrane acting as a recruitment factor (Donaldson 2003). In all of these cases, proteins at the budding site act as anchoring sites for cargo to attach and eventually get incorporated as vesicle cargo.

As mentioned previously, lipids can also aid in recruitment of vesicle cargo. In *P. gingivalis*, Haurat et al. showed that gingipains were found to be preferentially incorporated into vesicles by associating with A-LPS (negatively charged) molecules, demonstrating a mechanism by which a lipid can determine the enrichment of particular proteins into OMVs (Haurat et al. 2011). Incorporation of cargo into vesicles in some cases depends on *localization* of proteins in relation to the lipids in the membrane. For example, the incorporation of transmembrane glycoproteins via exosomes formed by the the ESCRT machinery is determined by their association with lipid rafts or detergent

resistant membranes (Staubach, Razawi, and Hanisch 2009). Lipid rafts, or lipid microdomains are cholesterol and sphingolipid-enriched membrane domains (Lajoie and Nabi 2010) that influence the distribution of receptors and other signaling molecules in the membrane (Castro et al. 2013). Further, in the formation of both ESCRT-dependent and ESCRT-independent extracellular vesicle formation, the inclusion of vesicle cargo in association with lipid rafts has been widely observed to occur for a variety of cargo. For instance, αB-crystallin, a small heat-shock protein found in exosomes, was located in detergent resistant membranes, together with caveolin-1, Hsp70, and flotillin-1 (Gangalum et al. 2011). In several studies, exosomal proteins such as signaling receptors and components important for the active lipid compound PGE_2 (Prostaglanding E_2) signaling (Lin et al. 2017), as well as AnxA2 (Annexin A2) (Valapala and Vishwanatha 2011) , TNFα (Tumor necrosis factor alpha) converting enzyme (Lee, Wittki, et al. 2013), and some chemokines (Chen et al. 2011), were found to be recruited to lipid rafts. In sum, the enrichment of protein cargo into extracellular vesicles by lipids can occur by either direct binding, or by recruitment to particular lipid domains of the pre-budding membrane.

In sum, there are only a few studies addressing OMV cargo loading while this process has been widely explored in eukaryotic vesicle systems. It is important to investigate this mechanism in bacterial systems in order to establish the general principles of cargo incorporation in the bacterial vesicle field. The inherent heterogeneity

and differences in bacterial strains used in OMV studies greatly impacts the ability of the field to establish commonalities and observe patterns in protein and lipid OMV loading mechanisms. However, not only differences in bacterial strains impact this goal, but also growth conditions. The bacterial environment is known to modulate bacterial physiology and metabolism, and along with it, OMV content, function and production in bacteria. Because of this, environmental conditions and shifts to stressful conditions is another factor to consider when exploring OMV cargo loading mechanisms.

1.5 Environment impacts on OMV content, function, and production

Environmental conditions have been observed to modulate OMV content and function, and many studies have focused on functional analyses of vesicles grown in specific conditions (e.g., a change in media or antibiotic exposure). These studies have revealed important roles for vesicles or vesicle secretion in that particular environment (Fig. 7 and Table 2).

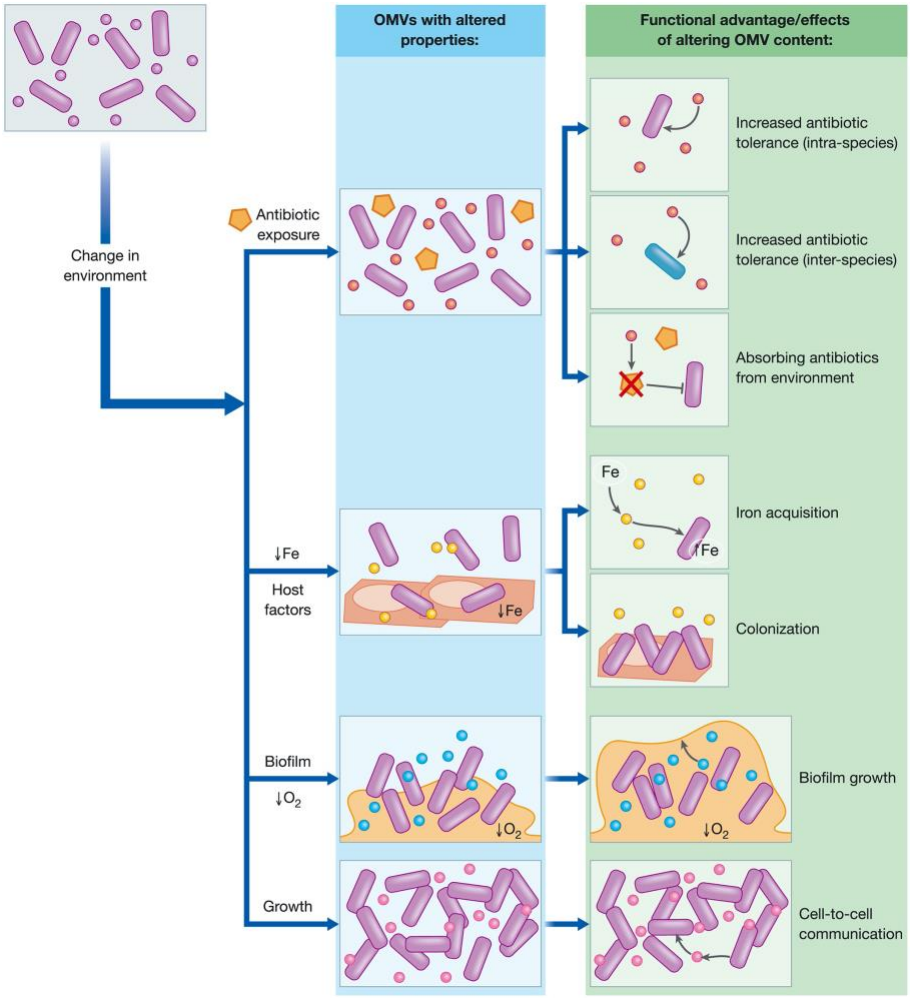

Figure 7: Environment shifts elicit changes in functional roles for OMVs.

Environment changes such as antibiotic exposure, release of host factors, low iron, transition to biofilm lifestyle, anaerobic conditions, and changes in growth phases can modulate OMV production. In many cases, OMVs produced upon a shift in environmental conditions exhibit functional roles that can help the mother cell or other bystander cells adapt to the new environment, survive future stressors, and/or interact with host cells or co-inhabitant cells differently (Orench-Rivera and Kuehn 2016).

Table 2 Environmental changes demonstrated to affect vesiculation (e.g. levels, activity or contents)

	Reference
Media	(Choi et al. 2014; Bager et al. 2013; Taboada et al. 2019)
Growth phase	(Tashiro et al. 2010; Zavan et al. 2019; Taboada et al. 2019)
Biofilm vs planktonic mode	(Park et al. 2015; Grande et al. 2015; Cooke et al. 2019)
Temperature	(Macdonald and Kuehn 2013; Fulsundar et al. 2014; Klimentova et al. 2019; Taheri et al. 2019)
Host cell factor	(Taheri et al. 2018; Metruccio et al. 2016; Ballok et al. 2014)
Antibiotic exposure	(Maredia et al. 2012; Devos et al. 2015; Devos et al. 2016; Macdonald and Kuehn 2013; Yun et al. 2018; Koeppen et al. 2019; Chiu et al. 2020; Kesavan et al. 2020; Chan, Shone, and Hesp 2017)
Anoxic conditions	(Toyofuku et al. 2013)
Iron depletion	(Keenan and Allardyce 2000; Veith et al. 2018; Chan, Shone, and Hesp 2017)
pH	(Klimentova et al. 2019; Lynch et al. 2019)
Oxidative stress	(Klimentova et al. 2019; Macdonald and Kuehn 2013; van de Waterbeemd et al. 2013; Chang et al. 2005; Toyofuku et al. 2012; Olofsson, Vallström, et al. 2010; Oliveira et al. 2015; Lekmeechai et al. 2018; Zielke et al. 2014)

Achieving a simple definition of OMV-related activities, even for those derived from a single species, will be impossible without including a caveat for changing environmental conditions. Growth phase, solid or liquid media, or the composition of the media are well known to affect virulence-associated bacterial traits such as adherence and toxin secretion, and impact membrane composition. Similarly, OMVs are complex entities composed of environmentally and temporally controlled factors. Therefore, it is important to elucidate the functional importance of OMVs produced in a particular environment to bacteria growing in that setting. In the following section, we highlight some examples demonstrating the environmental control of OMVs:

1.5.1 Iron availability

Iron is an essential element for bacterial survival; however, its bioavailability is strictly controlled within the host. Several reviews have highlighted the importance of iron acquisition during infection (Caza and Kronstad 2013; Ferreira et al. 2016), and in light of recent evidence, OMVs might potentially serve as vehicles for iron uptake during host invasion.

Evidence for environmental influence over OMV production for Mycobacterium tuberculosis comes from a study by Prados-Rosales et al. in which vesiculation was assayed in conditions of high and low iron concentration using minimal media (Prados-Rosales et al. 2014). While OMV size did not change significantly between both conditions, vesicle production was enhanced in iron-limiting conditions. Furthermore, OMVs from low iron conditions were enriched for the lipid siderophore mycobactin, whereas its precursor, with lower iron binding affinity, was the main siderophore found in OMVs from high iron conditions. Therefore, iron deprivation stimulated the production of OMVs enriched in the siderophore mycobactin, and these OMVs were also able to deliver iron to iron-deficient mutants of *M. tuberculosis*. The selective packaging of mycobactin in vesicles grown in iron-limiting conditions and the ability of these vesicles to donate iron and support the growth of mutants deficient in iron uptake suggest a crucial role for OMVs during nutrient-limited conditions.

In addition, many proteins associated with iron acquisition were found in biofilm OMVs of *P. aeruginosa* (Toyofuku et al. 2012). Given that iron-limiting conditions are also known to inhibit biofilm formation (Singh et al. 2002; Cai et al. 2010), iron uptake mechanisms in the OMVs might also be important for the transition from a planktonic to a biofilm lifestyle, allowing the bacteria to thrive in this type of community.

In the case of *H. pylori*, it was observed that iron-limiting conditions also caused a marked increase in vesicle production and influenced the expression of the OMV-associated virulence factor VacA. Reduced levels of VacA were found in vesicles from iron-limiting conditions, and iron salt was able to restore this decrease (Keenan and Allardyce 2000). Similarly, studies of OMV production by *H. influenzae*, *E. coli*, and *V. cholerae* found iron-limiting conditions corresponded to increased OMV production and that a deletion in the iron-sensitive *fur* transcription factor also lead to increased OMV levels (Roier et al. 2016). In this case, it was found that the absence of the transcriptional activating activity of fur caused a decrease in iron-activated genes such as *vacJ* and *yrbE*, which control phospholipid transport. Phospholipid and fatty acid analysis of the OMVs and OM from wildtype and mutants of these genes in *H. influenzae* suggested that *vacJ*- and *yrbE*-dependent changes in envelope lipid composition could be the cause of the observed iron-regulated OMV formation. Together, these findings point to a link between iron availability and modulation of both vesicle production and cargo.

1.5.2 Biofilm versus planktonic lifestyle

Many studies highlight differences in both planktonic and biofilm OMV proteomes of *P. aeruginosa* (Toyofuku et al. 2012; Park et al. 2015). In particular, a proteomic analysis by Park et al. revealed differences in the amount of the antibiotic secondary metabolite and pigment, pyocyanin, in OMVs over time (Park et al. 2015). Vesicles from late biofilm cultures (96 hr) were found to contain higher levels of pyocyanin, in comparison to OMVs from early planktonic cultures (24 hr). Given that in early planktonic cultures, supernatants had low levels of pyocyanin as did later biofilm supernatants, the authors argue OMVs are serving as a reservoir for pyocyanin in the context of biofilms. Consistent with this finding is the enrichment for phenazine biosynthetic proteins in early biofilms in comparison to planktonic cultures (Park et al. 2015). Although the detection of pyocyanin in OMVs might point to a possible mechanism for the delivery of this toxin, it is yet to be determined whether pyocyanin within the vesicles can interact or inhibit growth of competing bacterial species.

In the case of *H. pylori* biofilms, OMVs seem to play more of a structural role. Extracellular DNA (eDNA) is a component of *H. pylori* biofilms, and using PicoGreen staining, Grande et al. observed increased levels of double stranded DNA (dsDNA) associated with biofilm OMVs in comparison to planktonic OMVs (Grande et al. 2015). It is argued that the association of eDNA with vesicle membranes explain the protection observed for *H. pylori* biofilms treated with DNase I (Grande et al. 2011). Thus, as

bacterial cells transition from a planktonic to a biofilm lifestyle, OMVs could not only have a role in toxin storage but also in protection of eDNA from degradation, maintaining the integrity of the extracellular matrix of the biofilm.

1.5.3 Oxygen availability and pH

Oxygen availability impacts bacterial physiology in biofilms as well as in liquid anaerobic conditions, and the ability of oxygen to modulate OMV production has been studied most extensively in *P. aeruginosa*. Most studies of OMV production in *P. aeruginosa* use aerobically grown cultures in which the Pseudomonas quinolone signal (PQS), which is identified to be involved in *P. aeruginosa* OMV production (Mashburn-Warren et al. 2008), is active. However, Toyofuku et al. focused on monitoring OMV production under denitrifying conditions (Toyofuku et al. 2013). *P. aeruginosa* undergo anaerobic respiration via denitrification, utilizing nitrates or oxidized forms of nitrogen (Arai 2011; Arat, Bullerjahn, and Laubenbacher 2015). This is particularly relevant during biofilm growth, due to the generation of anaerobic microenvironments because of inherent oxygen gradients within the biofilm (Xu et al. 1998; Werner, Roe, Bugnicourt, Franklin, Heydorn, et al. 2004).

Firstly, the authors determined that *P. aeruginosa* is able to produce OMVs in the absence of oxygen, conditions lacking PQS. They further observed marked differences in OMV production under anoxic conditions in different media. While anoxic cultures of *P. aeruginosa* produced very few vesicles in brain–heart infusion (BHI) medium, anoxic

Luria Bertani (LB) broth-grown cultures produced up to six-fold more vesicles in comparison to the aerobic cultures (Toyofuku et al. 2013), as measured by FM4-64 dye incorporation. This reduction in vesicle production is consistent with a previous study that revealed reduced vesicle production under anaerobic conditions in Brain-heart infusion (BHI) (Schertzer, Brown, and Whiteley 2010) despite the fact that the vesicle isolation and purification methods for these two studies were slightly different. When the same group examined the anaerobic OMV proteome, various pyocin-related proteins were found in the vesicles while pyocin structures were not observed. Pyocins are bacteriocins produced by *P. aeruginosa* that are toxic to other strains of this species. Additional experiments with mutants also uncovered a connection between OMVs and pyocin production under denitrifying conditions (Toyofuku et al. 2013). In the anaerobic conditions tested, nitric oxide (NO) was identified as an inducer of vesicle production given that a mutant for nitrite reductase (NIR) displayed a decrease in pyocin production as well as vesicle production. In accordance with these results, a microarray analysis by Chang et al. revealed oxidative stress induced pyocin genes in *P. aeruginosa* (Chang et al. 2005). Furthermore, treatment of *P. aeruginosa* with hydrogen peroxide (H_2O_2) has been shown to cause an increase in OMV production (Macdonald and Kuehn 2013). These results are all consistent with the idea that oxygen availability modulates OMV production; however, it is yet to be determined whether the enrichment of pyocin

synthesis proteins in OMVs provides *P. aeruginosa* vesicles with particular functions such as modulating stress resistance or pyocin production.

pH homeostasis is crucial for bacterial physiology and pathogenesis. Recent studies have shown that pH fluctuations can alter vesicle components. In *Francisella tularensis*, the causative agent of tularemia, changes in OMV protein cargo, as well as induction of OMV production was observed as a result of low pH (Klimentova et al. 2019). However, whether the change in pH had an impact on OMV function was not assessed. In contrast, a recent study on *Vibrio fischeri* showed that under acidic pH, which mimics the host environment, OmpU (an outer membrane protein) is upregulated, increasing the potency of OMVs to stimulate host development (Lynch et al. 2019). In this case, pH altered the packaging of *V. fischeri* OMVs resulting in a change in OMV-host interactions.

1.5.4 SOS response and antibiotic exposure

Bacteria encounter antibiotics in their native as well as human host environments, and antibiotics often result in activation of stress responses that can be tied to OMV production and function. A study by Maredia et al. revealed that the SOS response in *P. aeruginosa* increases OMV production (Maredia et al. 2012). A wildtype strain treated with ciprofloxacin to induce the SOS response experienced a 100-fold increase in OMVs, as measured by Bradford assay, in comparison to untreated cells. Tests with a LexA (SOS repressor) noncleavable strain indicated that both the SOS

response and the antibiotic itself contributed to the increase in OMV levels. To exclude the possibility of coprecipitated proteins in the OMV samples, Maredia et al. also performed a lipid analysis that revealed that ciprofloxacin-treated wildtype OMVs were heavier than those of the *lexAN* mutant strain (Maredia et al. 2012). Moreover, a proteomic analysis identified SOS-regulated proteins in OMVs of antibiotic-treated cells. The authors suggest therefore that in the presence of antibiotics, OMV production is enhanced and SOS plays a role in such a mechanism.

Whether ciprofloxacin-induced OMVs improve bacterial viability or resistance in the presence of the antibiotics was not studied by Mareida et al.; however, another study demonstrated that OMVs can improve survival by absorbing antibiotics in the environment (Manning, Kuehn, and C. 2011). A hypervesiculating mutant strain grew better than wildtype when treated with cyclic cationic antimicrobial peptides polymyxin B and colistin, but not when treated with antibiotics that target PG synthesis and protein synthesis. Furthermore, treatment of wildtype cultures with polymyxin B or colistin in the presence of purified OMVs resulted in increased survival in comparison to cultures without OMVs whereas the OMVs were not protective against ampicillin, ceftriaxone, or tetracycline. In the same study, purified OMVs from ETEC or from K-12 increased growth of ETEC in the presence of polymyxin B (Manning, Kuehn, and C. 2011). This is consistent with a model by which antibiotic exposure induces the production of vesicles

that interact with envelope-acting stressor molecules and confer protection, increasing survival, of OMV-producing as well as "bystander" bacteria.

In a subsequent set of studies, treatment of *S. maltophilia* with the β-lactam antibiotic imipenem was found to not only increase in OMV production, but also, analysis of the OMV proteome demonstrated that the vesicles contained β-lactamase (Devos et al. 2015; Devos et al. 2016). Whether the enzyme is selectively enriched in these OMVs or whether its increased abundance results from the bulk flow incorporation of an increased amount of enzyme in the periplasm due to stress is unknown.

The β-lactamase-containing OMVs observed by Devos et al. were further shown to be capable of improving bacterial survival during antibiotic exposure (Devos et al. 2016). Ampicillin-related vesicle functions have been studied for several other bacteria and are also consistent with their ability to confer protection to self or bystander bacteria. In the case of *Staphylococcus aureus*, addition of β-lactamase-containing vesicles from this Gram-positive bacterium mediated survival of ampicillin-susceptible *E. coli* DH5α and *S. aureus* strains in the presence of ampicillin. The same effect was observed for *S. enterica* serovar Enteridis, *E. coli* O157:H7, and *Staphylococcus epidermis* ATCC 12228 on LB supplemented with ampicillin (Lee, Lee, et al. 2013). Notably, vesicle-mediated resistance was genetically controlled. Only when OMV "donor" non-pathohogenic *E. coli* cells were transformed with a plasmid encoding β-lactamase were the OMVs able to

mediate the survival of an *E. coli* DH5α ampicillin-susceptible strain (Lee, Lee, et al. 2013).

The Devos group also treated bacterial cultures with penicillin G to induce the packaging of β-lactamase into *S. maltophilia* vesicles (Devos et al. 2016). OMVs from these stimulated cultures where then added to cultures of *P. aeruginosa*, and *Burkholderia cenocepacia*, bacterial species known to cohabitate with *S. maltophilia*. For both species, OMVs caused a 100-fold increase in the minimum inhibitory concentrations for other β-lactam antibiotics (imipenem, amoxicillin, and ticarcillin) (Devos et al. 2016). These results demonstrate that OMVs of resistant bacteria exposed to antibiotics can package active antibiotic-degrading enzymes and reduce the antibiotic susceptibility of bystander pathogens.

Another study showed that *A. baumannii* induced by ceftazidime produced bacterial membrane vesicles more toxic than those produced by imipenem-induced bacteria (Chiu et al. 2020). In their vesicle study, Chui et al. found that treating carbapenem-resistant *A. baumannii* with sub-inhibitory concentrations of ceftazidime not only induced vesicle production but treatment also changed the protein content of the vesicles, altering and increasing their virulence in comparison to imipenem-induced conditions (Chiu et al. 2020). This showed treatment with antibiotics at sub-inhibitory concentrations can greatly influence vesicle composition and virulence even on antibiotic-resistant strains. A subsequent study of *A. baumannii* showed that treatment

with eravacycline, a synthetic fluorocycline antibiotic designed to overcome resistance to tetracycline-specific efflux and ribosomal protection mechanisms (Sutcliffe et al. 2013), yielded OMVs with RNA expression profiles that were different compared to the whole-cell RNA expression profiles and enriched in survival proteins. This suggested OMVs might have a protective effect to the bacteria during antibiotic stress however the functional impact of the enrichment observed was not tested (Kesavan et al. 2020). In summary, there is ample evidence that OMVs play an important role in protecting bacteria during antibiotic exposure, mostly through extracellular enzymatic degradation of antibiotics.

1.5.5 Host factors

During invasion and colonization, bacteria encounter a variety of host factors that can potentially affect OMV production as well as content and cytotoxicity. One example is host-derived epoxides. Epoxides are toxic compounds secreted as by-products of eukaryotic metabolism with roles in cellular signaling. In the lung, a niche for *P. aeruginosa* during infection, leukocytes produce epoxides (Hayakawa et al. 1986; Gómez and Prince 2007) and, interestingly, OMVs produced by *P. aeruginosa* are known to contain the epoxide hydrolase enzyme Cif (CFTR inhibitory factor) (Bomberger et al. 2009). It has been previously established that Cif is regulated by direct binding and repression by CifR, an epoxide-responsive repressor (Ballok et al. 2014). Given that Cif is known to be packaged into OMVs of *P. aeruginosa*, Ballock et al. set to examine whether

epoxides mediate the packaging of Cif into vesicles. Treatment with a model epoxide, epibromohydrin induced changes in OMV shape and density; however, more interestingly, it altered the packaging of proteins into the vesicles, supporting the idea of selective sorting of cargo into OMVs. Furthermore, additional experiments revealed that vesicles formed in the presence of epibromohydrin had reduced epithelial cell cytotoxicity (Ballok et al. 2014). Therefore, during host invasion, exposure to human-derived epoxides could cause significant changes to bacterial vesicles that can influence host–pathogen interactions.

Besides the lungs, *P. aeruginosa* can colonize humans in other sites and is known to be the most common cause of corneal infection in contact-lens wearers (Stapleton and Dart 1995). However, the mechanism of *P. aeruginosa* infections outside of the lung has not yet been fully elucidated (Tam et al. 2010; Evans and Fleiszig 2013). Given differences in models of bacterial infection in the presence and absence of contact lenses, several studies have indicated that bacteria can release additional virulence factors in the eye-lens environment (Tam et al. 2010). In experiments with *P. aeruginosa* exposed to human tear fluid, Metruccio et al. revealed that OMV production is induced in the presence of both solutions in comparison to buffer only and epithelial cell lysates controls (Metruccio et al. 2016). As abundant components of human tear fluid, lysozyme and lactoferrin were tested, and lysozyme, specifically, was found to trigger OMV production to levels comparable to tear fluid. OMVs from the lysozyme-induced

conditions also had a similar protein-banding pattern as human tear-induced vesicles (Metruccio et al. 2016). In lactate dehydrogenase release assays to measure host cell lysis, these lysozyme-induced OMVs induced cytotoxicity of corneal epithelial cells to a greater degree than vesicles from uninduced conditions. These cytotoxicity results were consistent with in an in vivo model of mouse corneas. In the same *in vivo* study, recruitment of Ly6G/C myeloid cells was also observed as a result of the vesicle treatment. Furthermore, intact lysozyme-induced vesicles promoted association of *P. aeruginosa* to mouse corneas in an *ex vivo* model (Metruccio et al. 2016). These results suggest that the ocular environment can modulate the release of OMVs by *P. aeruginosa* during a corneal infection and affect cell adhesion as well as cytotoxicity towards host cells.

In *S. enterica* serovar Typhimurium following environmental shift to PhoP/Q- and PmrA/B-inducing conditions, which mimic effects of host cell infection and colonization (Bonnington and Kuehn 2016), a system was developed to track the native dynamics of lipid A changes. Growth conditions altering pH and Mg concentrations influenced OMV production, size, and lipid A content. Interestingly, lipid A content of OMVs did not fit with a stochastic model of content selection, revealing the significant OM retention as well as OMV enrichment of lipid A species in the different host-like conditions. The concept that OMV composition and production reflects changes occurring in the OM during host-induced OM remodeling was also studied by an

investigation of the effect of overexpression of PagL, a PhoP/Q controlled OM-localized lipid A deacylase in *S.* Typhimurium (Elhenawy et al. 2016). They found that deacylated lipid A was found exclusively in the OMVs, not the OM, of cells overexpressing PagL. This result suggests that PagL activity is extremely localized to small patches of the OM, or that PagL is active only after OMVs are formed, or both. The former possibility is supported by the fact that PagL overexpression also corresponded to increased levels of OMVs, and these data lead the authors to suggest that the deacylated LPS alters the OM geometry to promote budding.

1.5.6 Growth phase and media composition

Several studies have examined changes in OMV production and cargo under various growth conditions in addition to altering iron concentrations that were discussed in an earlier section. Whereas data from OMVs produced by the *P. putida* DOT-T1E strain in particular, revealed few changes to the OMV proteome under varying conditions (Baumgarten, Sperling, et al. 2012; Baumgarten, Vazquez, et al. 2012), studies of other strains and bacterial species have demonstrated media- and growth phase-dependent changes in OMV proteomes and production. For example, a study by Choi et al. on the proteome of *P. putida* KT2440 assessed OMV production of cells grown in different media: LB broth, Minimal medium with 10 mM succinate, or minimal medium with 5 mM benzoate. OMV production in LB media was found to be more than threefold increased than in the other two conditions. Interestingly, OMVs from cells

grown in benzoate-containing media contained proteins involved in benzoate degradation. However, it was not determined here whether the vesicles from the different conditions conferred some sort of protection against stress-inducing conditions (Choi et al. 2014). They did observe that OMVs derived from LB-rich media decreased cell viability of A549 carcinomic human alveolar basal epithelial cells, although it was not determined whether vesicles from the other two conditions are also able to confer cytotoxicity (Choi et al. 2014). In a study of *Gallibacterium anatis*, changes in medium composition also affected vesicle production. Addition of 1 mM EDTA to BHI medium or growth in RPMI 1640 HEPES medium (a mammalian cell culture medium) caused a reduction in OMV production in comparison to growth in BHI (Bager et al. 2013). Again, it remains unknown whether the reduction in OMV production is a functional advantage to cells grown in those specific conditions. In another study that focused on the effect of lignin rich media on the OMV proteome of *P. putida*, *R. jostii*, and *Amycolatopsis* sp. ATCC 49116, many enzymes known to degrade lignin-derived compounds were found enriched in OMVs derived from different bacterial growth stages (Salvachúa et al. 2020). In previous studies, Salvachúa et al. had shown that these three bacteria were efficient in depolymerizing lignin by employing extracellular enzymes and this was particularly relevant for industrial bioprocessing applications (Salvachúa et al. 2015). The discovery of lignin degrading enzymes in OMVs showed that vesicles could enhance this extracellular degradation (Salvachúa et al. 2020).

The impact of growth conditions on OMV production and function should also be thought of in a temporal context, as bacteria alter their composition throughout their cell cycle, and OMVs are likely to be similarly affected. While OMVs are produced at all stages of bacterial growth, the maximum rate of vesicle production has been known to occur at the end of log phase for various species of bacteria (Chatterjee and Das 1967; Gamazo and Moriyón 1987). Interestingly, *P. aeruginosa* vesicles from different growth phases also exhibit altered physical properties. For instance, vesicles from stationary phase cultures contained higher levels of PQS and were found to be more negatively charged in comparison to OMVs from the exponential phase (Tashiro et al. 2010). Also, based on the idea that vesicles may potentially play a role in cell to cell communication (Kadurugamuwa and Beveridge 1995), the same study employed FITC (fluorescein isothiocyanate)-labeled vesicles to test whether growth phase impacted association of vesicles with *P. aeruginosa* cells and observed that OMVs from stationary cells more readily associated with the bacterial cells. This could be explained by the fact that more negatively charged vesicles have an increased potential to form salt-bridges to the Ca^{2+} or Mg^{2+} surface of bacteria (Tashiro et al. 2010). Therefore, as bacteria transition between growth phase, vesicles can acquire inherently different properties that may influence their interactions with neighboring cells and this might be crucial for cell–cell communication.

1.5.7 Implications for OMV studies

There is a wide variety of studies, as highlighted above, addressing the impact of environmental conditions on OMV function, production and content. It is evident that shifts in environment conditions induce changes in OMV properties which are beneficial to the parent cell or the bacterial population in general. In some cases, it provides protection against antibiotics, while in others, it confers a fitness advantage. In order to understand the role of OMV secretion in bacterial fitness and survival during environmental shifts, it is important to study the content of the vesicles in relation to the bacterial OM to investigate whether preferential cargo packaging into OMVs results in changes to the parent cell membrane that are beneficial to the cell in the new environment.

1.6 OMVs and membrane remodeling

Whereas modifications to LPS and to the protein composition of the envelope are known to be critical for bacterial survival in particular conditions, there are very few-to-no known mechanisms for OM lipids or OMPs to be quickly degraded or recycled (Scandella and Kornberg 1971; Schindler, Osborn, and Koppel 1980; Rassam et al. 2015). Given what is known about OMV cargo selectivity, OMVs are thought to play a role in the quick remodeling of the bacterial envelope to enhance bacterial survival. OMV cargo selection suggests that the preferential retention in the OM or export of particular proteins or lipid species in OMVs can promote the generation of a remodeled

membrane, different from the one the bacterium had when first exposed to the environment that triggered the remodeling.

Results from several studies show that OMVs can, in fact, serve as a remodeling and maintenance mechanism for the Gram-negative OM during environmental changes or stress. Hypervesiculating mutants of *E. coli* were found to be less sensitive to stressors than hypovesiculating mutants suggesting the process of OMV production is an important mechanism for bacterial survival (McBroom and Kuehn 2007). In addition, OMV production is crucial for the cell to rid itself of a detrimental accumulation of proteins in the periplasm (Schwechheimer and Kuehn 2013). More recently, upon examination of OM LPS remodeling in *S. enterica* serovar Typhimurium after a shift to low pH and low Mg^{2+}, the lipid A content of OMVs was significantly different from that of the OM (Bonnington and Kuehn 2016). In these experiments, vesicles were observed to preferentially release unmodified LPS species, both during the shift and long after the shift, revealing a role for OMVs as a membrane remodeling mechanism to accommodate and maintain barrier properties during changes in environmental conditions.

1.7 Oxidative stress and OMVs

Studies have highlighted several links between oxidative stress and vesicle production. For example, oxygen availability in the bacterial environment has been shown to affect vesiculation levels in the context of *P. aeruginosa* biofilms where oxygen gradients are inherent to this type of community (Xu et al. 1998; Werner, Roe,

Bugnicourt, Franklin, A., et al. 2004). Anaerobic conditions were consistent with lower vesiculation levels as well as enrichment for pyocin synthesis proteins in the vesicles of *P. aeruginosa* (Toyofuku et al. 2013). Although it is still unknown whether this enrichment for pyocin synthesis proteins in OMVs predicts any functional role for these vesicles in conditions of oxygen depletion, there is evidence that oxidative stress can induce pyocin genes in *P. aeruginosa* (Chang et al. 2005). Additionally, studies have analyzed oxidative stress induction of OMV production: Van de Waterbeemd et al. found that oxidative stress caused by cysteine depletion triggered OMV release in *N. meningitidis* (van de Waterbeemd et al., 2013) and MacDonald et al. showed that in *P. aeruginosa*, OMV production increases after treatment with hydrogen peroxide (H_2O_2) (Macdonald and Kuehn 2013).

Additional evidence pointing to a connection between OMVs and oxidative stress comes from proteomic analysis of OMV content. Several studies have identified several proteins belonging to the oxidative stress response in OMVs (Toyofuku et al. 2012; Olofsson, Vallström, et al. 2010; Zielke et al. 2014; Oliveira et al. 2015; Lekmeechai et al. 2018). Authors indicate these proteins can help mediate oxidative stress extracellularly (Oliveira et al. 2015; Lekmeechai et al. 2018). Additionally, using a high-throughput screen designed to identify *E.* coli genes involved in vesiculation, Kulp et al. discovered that mutations in oxidative stress response pathways were highly enriched amongst mutants with hypo- and hypervesiculation phenotypes (McBroom and Kuehn

2007; Kulp et al. 2015). These studies on a variety of bacterial species demonstrate that understanding the relationship between oxidative stress and OMV biogenesis, content, and function, is an area worthy of further study.

1.7.1 Oxidative stress and the bacterial response

In general, oxidative stress is a common environmental threat to bacteria. When bacteria invade a human host, they are exposed to reactive oxygen species (ROS) produced by neutrophils and other immune cells which employ what is called an oxidative or respiratory burst to kill bacteria (Gwinn and Vallyathan 2006; Slauch 2011; Garin et al. 2001). Shifts from anaerobic to aerobic conditions can also induce oxidative stress in bacteria (Tamarit, Cabiscol, and Ros 1998), as well as exposure to UV radiation and molecules from competing microorganisms such as the redox active compounds pyocianin from *P. aeruginosa*, streptonigrin from *S. flocculus* and the plant-derived plumbagin (Hassett et al. 1992).

Exposure to antibiotics has also been shown to increase ROS in bacteria, mainly via alterations in the central metabolic pathway, NADPH depletion and the Fenton reaction (Dong et al. 2015; Dwyer et al. 2007; Kohanski et al. ; Dwyer, Collins, and Walker 2015) and although many studies have focused on disputing these findings, recent evidence points to a link between antibiotic exposure and ROS generation, with these species contributing to antibiotic-mediated bacterial killing (Liu et al. 2016).

During an oxidative stress event, bacteria can encounter ROS in many forms and it can affect the cell in different ways. Oxidative stress arises when the concentration of active oxygen increases to a level that exceeds the cell's defense capacity (Cabiscol, Tamarit, and Ros 2000). Major targets of oxidative stress in bacteria are DNA, RNA, proteins and lipids. Lipid peroxidation is a direct effect from attacks by free radicals. This decreases membrane fluidity and the effect is further amplified as polyunsaturated fatty acids are degraded to aldehydes which can damage proteins (Humphries and Szweda 1998). During oxidative stress, all four bases of DNA can be damaged and ROS can attack bases and sugars causing breaks in the DNA backbone, blocking replication (Dizdaroglu 1992; Sies and Menck 1992; Sies 1993; Cabiscol, Tamarit, and Ros 2000). According to Cabiscol et al., protein damage as a result of oxidative stress is not very well characterized but usually involve oxidation of sulfhydryl groups, reduction of disulfides, oxidative adduction of amino acid resides close to metal binding sites, reaction with aldehydes, modification of prosthetic groups or metal clusters, protein-protein cross-linking and peptide fragmentation (Cabiscol, Tamarit, and Ros 2000).

Given the great extent of damage cells can experience during an oxidative stress event, bacteria have specific regulons in charge of activating the appropriate protective response (Fig. 8).

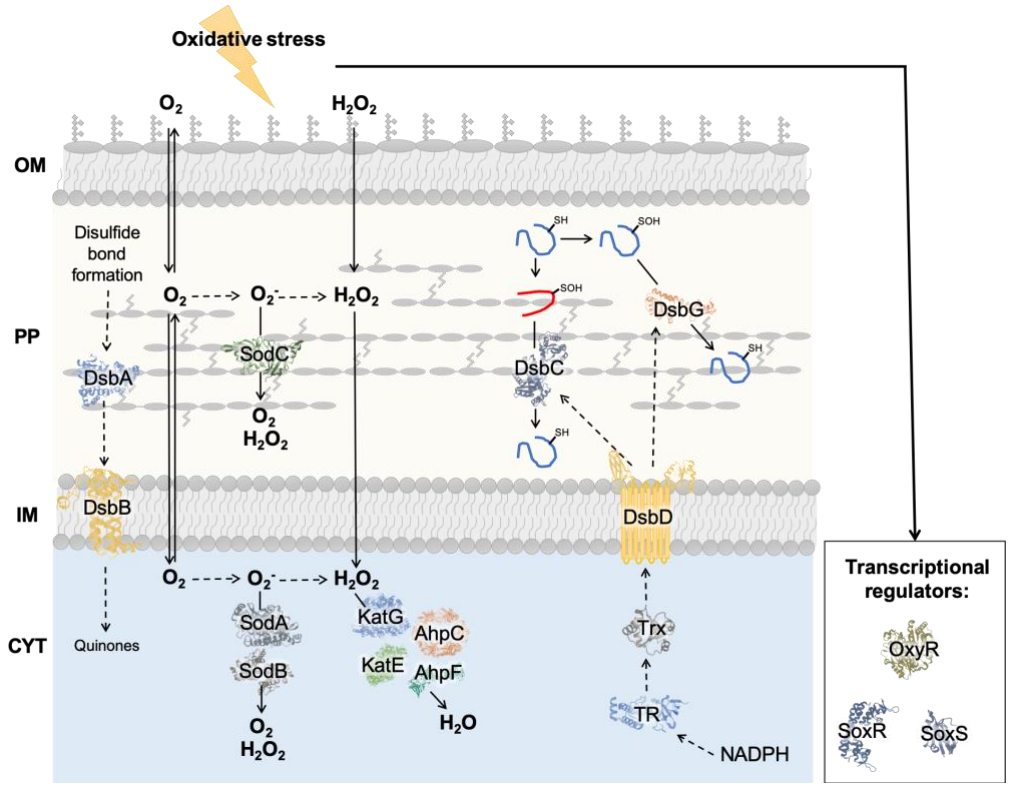

Figure 8: The oxidative stress response in Gram-negative bacteria.

Main transcriptional regulators of the oxidative stress response are the hydrogen peroxide-inducible genes activator OxyR (PDB: 3T22), the redox-sensitive transcriptional activator SoxR (PDB: 2ZHH) and the regulatory protein SoxS (PDB: 3DML). Disfulfide bonds are introduced into proteins by the DsbA (PDB: 1DSB) in the periplasm (PP). Electrons are transferred to the inner membrane (IM) by DsbB (PDB: 2K73) and then to quinones. The isomerase DsbC (PDB: 1JZO) corrects DsbA mistakes and is reduced by DsbD (PDB: 1L6P, 6DNL) an IM protein that receives electrons from the thioredoxin system (Trx, TR: thioredoxin reductase; PDB: 2PV9) in the cytoplasm (CYT). DsbD also transfters electrons to DsbC and DsgG (PDB: 1V57). DsbG repairs sulfenylated (SOH) proteins in the PP. Arts et al. suggest that DsbC interacts with partially unfolded sulfenylated proteins (in red). Superoxide (O_2^-, unable to cross membranes) is dismutated into H_2O_2 and O_2 by SodA (PDB: 1XRE) and SodB (PDB: 3TQJ) in the CYT and SodC (PDB: 2WWO) in the PP. H_2O_2 (which can cross membranes) is reduced by AhpCF (alkyl hydroperoxidase reductase, PDB: 1YF0, 4O5Q) in the CYT. KatG (PDB: 5L05) and KatE (PDB: 3TTT) are other catalases in the CYT. Arrows from the IM to O_2^- indicate the O_2^- formed from electron leakage from respiratory chain complexes. Dashed arrows show electron flows. Figure and caption adapted from (Arts, Gennaris, and Collet 2015).

Specifically, bacteria invoke one or both of the following stimulons: the peroxide stress and the superoxide stress response (Farr and Kogoma 1991). The peroxide stress response occurs in response to H_2O_2 and other organic peroxides and is under the control of the OxyR regulon; while the SoxR/S proteins positively control of genes in response to elevated levels of the superoxide radical anion, O_2^- or redox active compounds (Singh et al. 2013; Farr and Kogoma 1991). There are three types of superoxide dismutases in bacteria and each of them requires a different metal cofactor for proper function. All superoxide dismutases are known to convert O_2^- to H_2O_2 and SodA and B require iron and manganese respectively, while SodC is a copper and zinc superoxide dismutase. SodA and SodB detoxify the cytoplasmic from superoxide anion radical O_2^- the one-electron reduction product of oxygen that can be generated either spontaneously due to aerobic conditions or as a result of metabolic processes. The importance of SodC, which is periplasmic, is less known. However, it likely serves to detoxify superoxide anions released in the periplasm by respiratory complexes (Korshunov and Imlay 2006) or by host cell's macrophages during oxidative bursts (De Groote et al. 1997). In bacteria, H_2O_2 is reduced by peroxidases and catalases. The two component thiol-based alkyl hydroperoxide reductase AhpCF has been identified as the primary H_2O_2 scavenger, transferring electrons from NADH to H_2O_2, reducing it to water (Seaver and Imlay 2001a). Two other peroxidases such as Tpx, which handles bulkier hydroperoxides, and BCP (bacterioferritin comigratory protein), which reduces

various substrates at a lower efficiency (Jeong, Cha, and Kim 2000; Baker and Poole 2003). When higher concentrations of peroxides are present, the main catalases are the cytoplasmic KatG and KatE (Claiborne, Malinowski, and Fridovich 1979; Claiborne and Fridovich 1979; Seaver and Imlay 2001b).

Several proteins related to the oxidative stress response pathways were discovered to modulate OMV production in *E. coli* in a high-throughput screen (Kulp et al. 2015). Some of these proteins are directly involved in the oxidative stress response while others play roles related to iron homeostasis or electron transfer. Other proteins are known to be important for the oxidative stress response because mutants have been reported to be more sensitive than wildtype to oxidative stress. Mutants lacking the genes for the transcriptional regulator OxyR; the iron transporter MntH; the catalases KatG and KatE; and the dehydrogenase Lpd resulted in significantly lower OMV production than wildtype (Kulp et al. 2015). Other mutants showed higher OMV production levels such as the deletion mutant of the phosphoglycerate mutase gene *gpmM* (Kulp et al. 2015), which was reported to be more sensitive to H_2O_2 (Krisko et al. 2014). A mutant lacking the peroxidase component AhpC of AhpCF, and another lacking the flavin reductase Fre, which also acts as a ferric reductase (Fontecave, Eliasson, and Reichard 1987; Coves and Fontecave 1993; Fischer et al. 1990), were found to have significantly higher OMV production phenotypes than wildtype *E. coli* (Kulp et al. 2015). While a definitive justification for the up- or down-regulation of OMV

production in these mutants cannot be derived due to the heterogeneity of processes they belong to, Kulp et al. states these results suggest that an intact oxidative stress response is important for *E. coli* to maintain wildtype vesiculation levels (Kulp et al. 2015).

1.8 Summary and project aims

All Gram-negative bacteria produce OMVs derived from the envelop and contain OM-associated proteins, OM lipids, and proteins derived from the periplasm. While studies indicate that the incorporation of some OMV proteins is unregulated and occurs as "bulk flow", there is ample evidence that OMV cargo selectivity also occurs. Notably, several studies have found differences between the composition of the OMVs and the OM, indicating enrichment or exclusion of certain proteins over others. Selectivity in OMV protein incorporation can be beneficial to bacteria. OMVs can serve as vehicles for elimination of toxic or accumulated periplasmic material (McBroom and Kuehn 2007; Schwechheimer and Kuehn 2013) and have been reported to participate in membrane remodeling during environmental shifts (Bonnington and Kuehn 2016). Environmental conditions are known to influence OMV cargo selectivity and OMV function. However, a general mechanism driving OMV cargo incorporation in bacteria remains elusive.

Given the reported connections between OMV production and the oxidative stress response pathway, and based on the concept of environmental shifts modulating OMV cargo and function, I set out to investigate general principles of OMV cargo selectivity by identifying changes in OMV protein cargo after a shift to oxidative stress in *E. coli*. I hypothesized that a shift to oxidative stress conditions would trigger OMV-mediated remodeling, so I expected to observe differences in OMV cargo composition before and after stress. From studying these data, I was able to hypothesize a potential mechanism of cargo selectivity in *E. coli*. Thus, as my second aim, I investigated a potential selective cargo sorting mechanism using engineered model cargo.

2. Outer membrane associated proteins are differentially packaged into outer membrane vesicles by *Escherichia coli* during an environmental shift to oxidative stress conditions

2.1 Summary

Studies have shown that bacteria can modulate the composition of outer membrane vesicles (OMVs) when subjected to environmental shifts and that this modulation can influence their survival in a new environment. In this study, oxidative stress was chosen as a stressor and a proteomic analysis of outer membrane (OM) and OMV fractions from enterotoxigenic *E. coli* (ETEC) was performed. Results revealed significant differences in protein abundance in the OMV and OM fractions for cultures shifted to oxidative stress conditions. Our analysis showed a slight increase in periplasmic content that was independent of gene expression, and we followed up these findings to examine the extent to which the OMV was oxidized. To examine whether exported OM proteins were more oxidized, the amino acid sequences of proteins preferentially packaged into OMVs were also analyzed and the results showed that proteins with oxidizable residues were more packaged into OMVs in comparison with those retained in the membrane. Using a sensitive toxin activity assay, we further found that these changes correlated with a decrease in ETEC OMV cytotoxicity.

Quantitative proteomic analyses indicated two distinct classes of OM-associated proteins were differentially packaged into OMVs as a function of peroxide treatment.

Implementing a Bayesian hierarchical model, OM lipoproteins were determined to be preferentially exported during stress whereas integral OM proteins were preferentially retained in the cell. Selectivity was determined to be independent of transcriptional regulation of the proteins upon oxidative stress and was validated using randomly selected protein candidates from the different cargo classes.

Finally, we tested whether the differential sorting of proteins during stress contributed to the generation of a better suited bacterial membrane and found that shifted cells were more resistant to a secondary challenge of peroxide.

2.2 Introduction

Bacteria ubiquitously produce vesicles and the process of vesicle secretion is known to be genetically regulated (Bodero, Pilonieta, and Munson 2007; Kitagawa et al. 2010; Kulp et al. 2015; Nevermann et al. 2019; van der Westhuizen et al. 2019). Whereas some vesicle cargo can be incorporated by bulk flow, OMV cargo selectivity has been observed in multiple studies (Bonnington and Kuehn 2014; Schwechheimer and Kuehn 2015; Orench-Rivera and Kuehn 2016).

The regulated inclusion or exclusion of cargo into extracellular vesicles is crucial to their biological roles. Enriched packaging of cargo can lead to enhanced transport of particular proteins to a remote destination that can be beneficial to the cell, or can allow specific elimination of proteins that would have been toxic if they remained in the cell (Schwechheimer and Kuehn 2013). Exclusion of particular cargo from OMVs could also

be critical for the cell to preserve functionally important cellular processes. For example, our lab has previously investigated how both vesiculation levels and specific cargo selection into and exclusion from OMVs help bacteria to quickly remodel their envelope to accommodate shifts in the environment. We have also shown that hypervesiculating bacteria are less sensitive to stressors than hypovesiculating mutants of *E. coli* and that vesicle production is crucial for the cell to rid itself of a detrimental accumulation of proteins in the periplasm (McBroom and Kuehn 2007; Schwechheimer and Kuehn 2013). Upon examination of OM lipopolysaccharide (LPS) remodeling in *Salmonella enterica* serovar Typhimurium after a shift to and from PmrA/B-inducing conditions, it was observed that the lipid A content of OMVs significantly differed from that of the OM (Bonnington and Kuehn 2016). The preferential release of unmodified LPS species suggested a role for OMVs to accommodate changing environmental conditions that are similar to conditions of intracellular growth within mammalian host cells. There are very few-to-no known mechanisms for OM lipids or OM-associated proteins to be quickly degraded or recycled (Schindler, Osborn, and Koppel 1980; Rassam et al. 2015), therefore, these results show that OMVs can serve as a remodeling and maintenance mechanism for the Gram-negative OM during environmental changes or stress.

For this study we sought to investigate further aspects of OMV cargo selectivity by focusing on identifying differences in OMV protein cargo packaging in response to oxidative stress. We chose to examine a shift to oxidative conditions for several reasons.

Firstly, in a previous study we discovered that mutations in oxidative stress response pathways were highly enriched amongst *E. coli* mutants with hypo- and hypervesiculation phenotypes (McBroom and Kuehn 2007), and we wanted to better understand the relationship between oxidative stress and OMV production. Additionally, studies have highlighted the significant effect of oxidative stress on OMV production: Van de Waterbeemd et al. found that oxidative stress caused by cysteine depletion triggered OMV release in *N. meningitidis* (van de Waterbeemd et al. 2013) and MacDonald et al. showed that in *P. aeruginosa*, OMV production increases after treatment with hydrogen peroxide (H_2O_2) (Macdonald and Kuehn 2013). Furthermore, several studies on OMV composition have found proteins from the oxidative stress pathway in vesicles. For example, OMVs from *H. pylori* can mitigate extracellular oxidative stress due to the packaging of the catalase KatA in the OMVs (Lekmeechai et al. 2018).

In this study we used a quantitative proteomics approach to identify the protein composition of OMVs and OM fractions, and we found significant selective packaging of different classes of proteins upon oxidative stress that was unrelated to changes in gene expression. Our studies of OMV cargo also showed that proteins with oxidizable residues are preferentially packaged into OMVs.

2.3 Developing a protocol for monitoring changes in OMV packaging

In order to quantify changes to vesicular cargo during stress, we needed to develop a method that would allow us to isolate vesicles from the period of incubation where the cells are stressed. We also needed a bacterial strain with a constitutively high OMV yield. We chose enterotoxigenic *E. coli* (ETEC) H10407 which our lab has previously determined produces approximately 10-fold more vesicles than nonpathogenic K-12 *E. coli* strains (Horstman and Kuehn 2002). We also developed a treatment protocol that would cause oxidation of cellular contents, but would have negligible effects on bacterial membrane integrity and cell growth. No significant differences in Sytox Green accessibility was detected between cells isolated from treated cultures and untreated cultures when stationary phase ETEC cultures were incubated for 3 h at 37°C in the presence or absence of up to 20 mM H_2O_2 revealing intact membranes (Fig. 9A). Also, no significant differences in cell growth were observed after a 3 hr incubation in the presence or absence of 20 mM H_2O_2 (Fig. 9B).

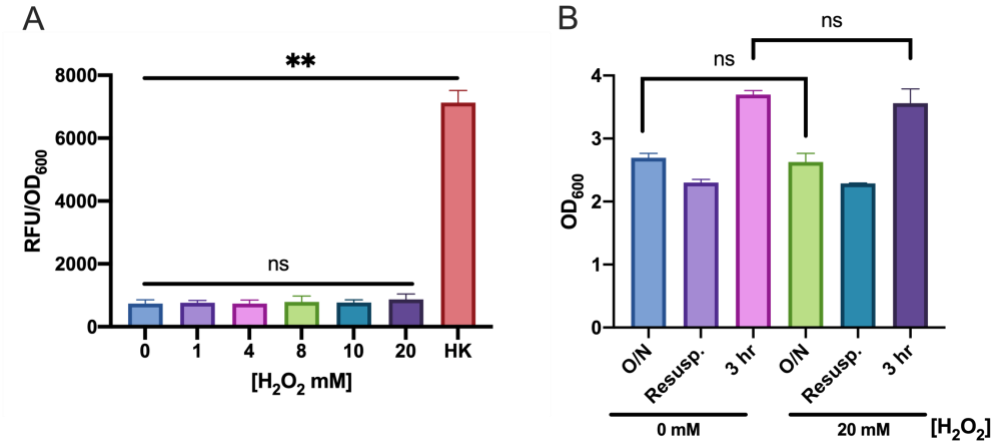

Figure 9: Shift conditions do not compromise membrane integrity or bacterial cell growth.

(A) Relative fluorescence (RFU) normalized by OD_{600} of ETEC cultures assayed with Sytox Green at 3 h after treatment with the indicated H_2O_2 concentrations. HK, heat-killed cell control. **(B)** OD_{600} of ETEC cultures was assayed after overnight growth (O/N), after resuspension in fresh media (Resusp.) and after 3 hr incubation (3 hr) with 0 mM or 20 mM H_2O_2. Error bars are SEM. P-values according to the Student's t test: ** $p \leq 0.01$; ns, not significant. (n=3).

We note that this concentration of H_2O_2 is higher than typically used in reports of oxidative stress in laboratory (K-12) strains of *E. coli*. However, higher concentrations (up to 50 mM) of H_2O_2 are usually necessary to induce stress in studies of pathogenic *E. coli* (Bearson, Lee, and Casey 2009; Felicio et al. 2009; Łoś et al. 2010; Mei et al. 2017). To validate that our treatment conditions did result in oxidation of ETEC proteins, we analyzed whole cell extracts and observed an increase in oxidative carbonyl modifications (Fig. 10).

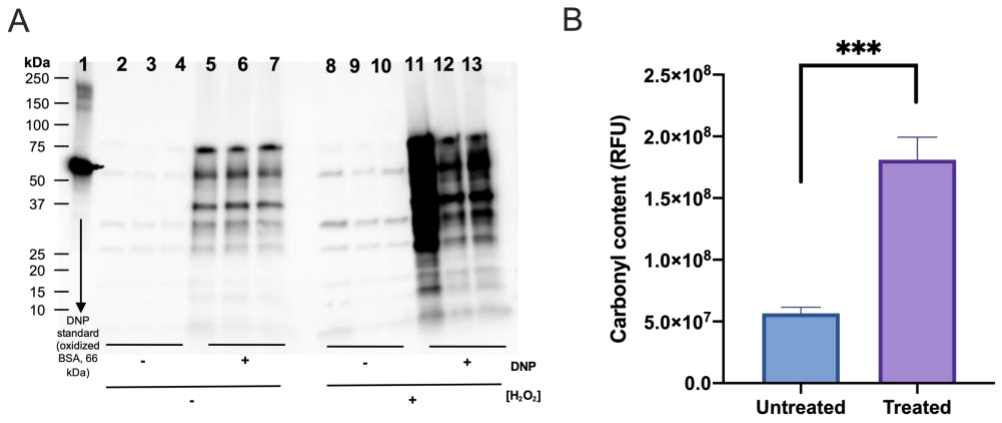

Figure 10: H_2O_2 treatment oxidizes protein in ETEC.

(A) Representative Oxyblot analysis of triplicate whole cells preparations from ETEC cultures treated for 3h with H_2O_2 (+) or mock treated (-). Derivatization with DNP is indicated (+) and underivatized samples are included as controls (-). DNP-derivatized oxidized bovine serum albumin (BSA) is included as a control in Lane 1. **(B)** Densitometric measurements of the Oxyblots of whole cell preparations from untreated and peroxide-treated cultures using FIJI software. Error bars are SEM. P-values according to the Student's t test: *** $p \leq 0.001$ (n=6).

Since the 3h shift to media containing 20 mM H_2O_2 caused cellular protein to be oxidized but did not perturb membrane integrity, we used these conditions in our further analyses. Unlike some other species examined in previous studies (Macdonald and Kuehn 2013; van de Waterbeemd et al. 2013), a comparison of OMV yield by protein and lipid assays in treated and untreated culture supernatants revealed that the oxidative treatment did not significantly alter OMV production by ETEC (Fig. 11). These data demonstrate that for ETEC a non-lethal shift with peroxide leads to the generation of oxidative species but not OMV induction.

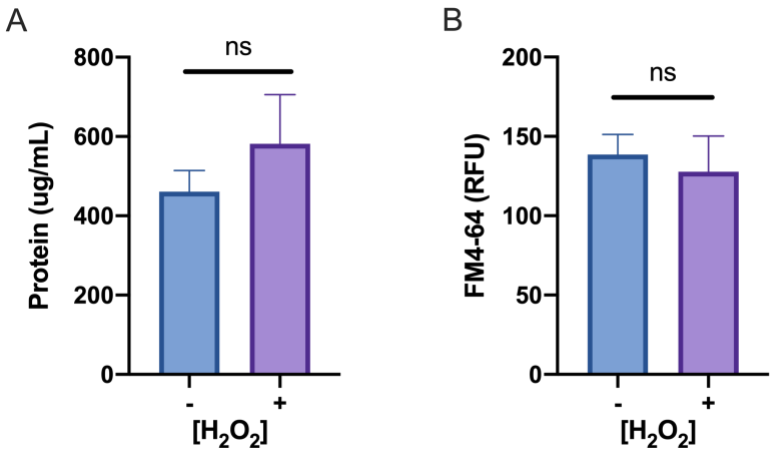

Figure 11: Oxidative stress does not alter vesicle production in ETEC.

(A) OMV production measured by Bradford (protein content) and **(B)** FM4-64 incorporation (lipid content) after a 3 h treatment with 20 mM H_2O_2 (+) or a mock shift (-) Values were normalized to the OD_{600} of the cultures at time of OMV harvest. (n=6). Error bars are SEM. ns, not significant.

In order to evaluate OMV packaging the ratio of cargo proteins in the OMVs compared with the OM it was critical to isolate and compare OMVs and OM from the same stationary phase culture. Stationary phase cultures of ETEC were centrifuged, the media replaced with fresh LB to exclude OMVs produced during earlier growth phases, and the cultures incubated for 3 h at 37°C during which time they generated OMVs. Once we obtained samples of OM and OMVs by this method we gradient-purified our samples and submitted them for proteomic analysis.

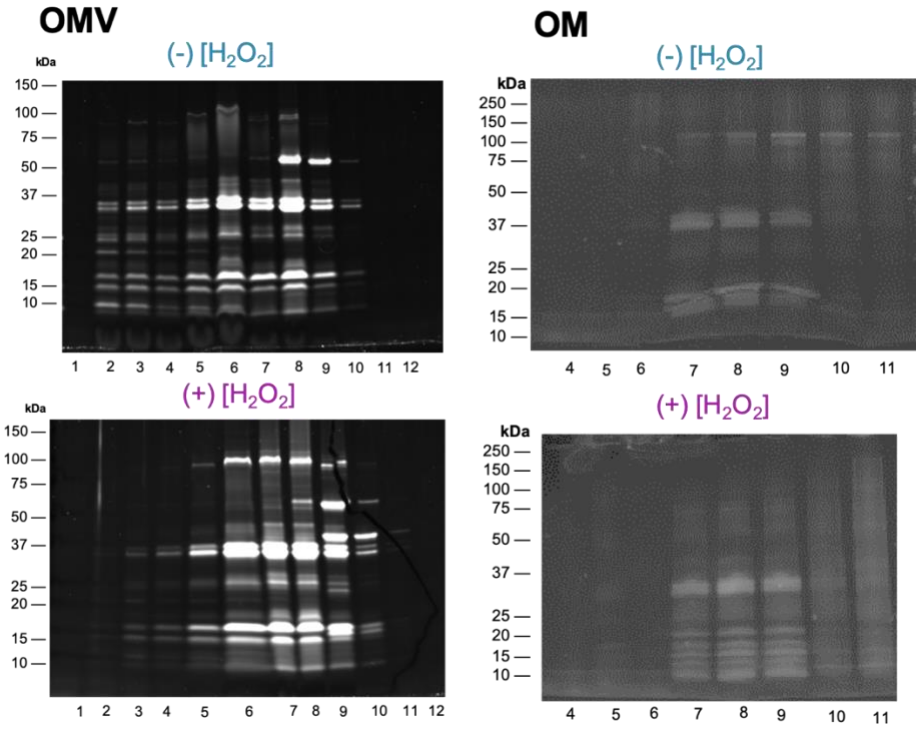

Figure 12: Representative SDS-PAGE gels of gradient purified OMV and OM fractions.

2.4 Proteomic analysis of ETEC OMVs produced under unstressed and oxidative stress conditions

We next used proteomic analyses to investigate ETEC OMV cargo under unstressed and upon oxidative stress conditions. After the cultures were shifted to oxidative conditions, the OM fraction of the cells and OMV preparations from the culture supernatants were then isolated and gradient-purified from three independent replicate cultures for quantitative proteomic mass spectroscopy (MS) analysis.

2.4.1 Proteomic data identification and annotation process

Proteins with at least two peptides present in the OM and OMV proteomic datasets were selected for further analysis. We noticed that the genome of ETEC strain O78:H11 found in UniProt contains a vast amount of unknown and/or uncharacterized proteins despite ETEC homology to nonpathogenic *E. coli*. Therefore, we had to "hand-annotate" proteins in our dataset to obtain more information about proteins in our study. First, the annotation of proteins was completed based on their homology with K-12 gene products, and proteins were annotated by cellular localization (Table 9). Then, OM-associated proteins were categorized as OM lipoproteins or integral OMPs and annotations individually cross-referenced using literature and database searches (Fig. 13).

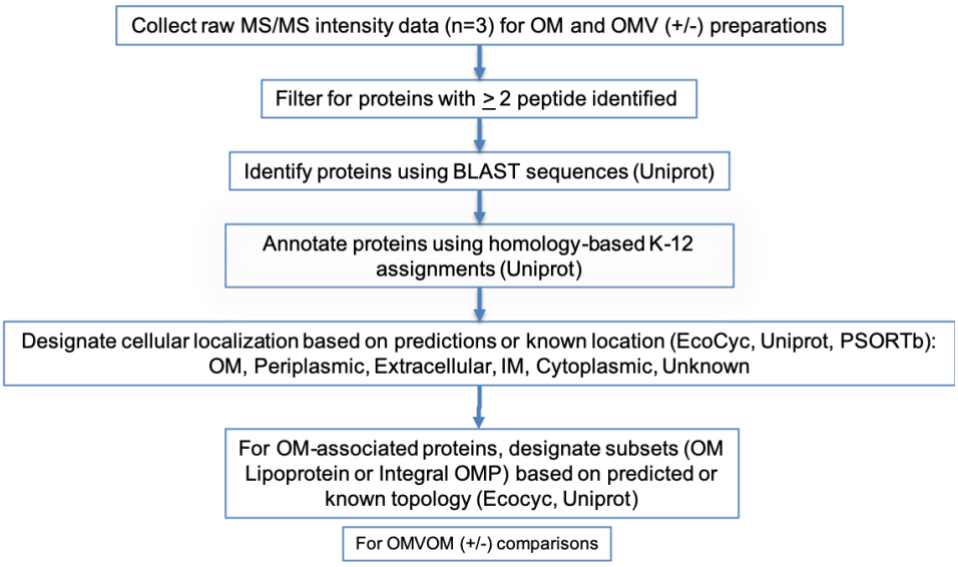

Figure 13: Proteomic data identification and annotation process.

Proteins in the preparations were categorized as extracellular (including pili, phage and flagellar), OM, periplasmic, inner membrane (IM), cytoplasmic, and unknown (if no information about localization was found in the databases) according to annotations individually cross-referenced using literature and database searches. Relative abundance within the preparations was determined based on the quantitative MS intensities, and, as expected, the data revealed that a majority (90.07%) of the proteins in the OMV preparation were designated to be located in the OM, periplasm, or extracellular milieu (Fig. 14).

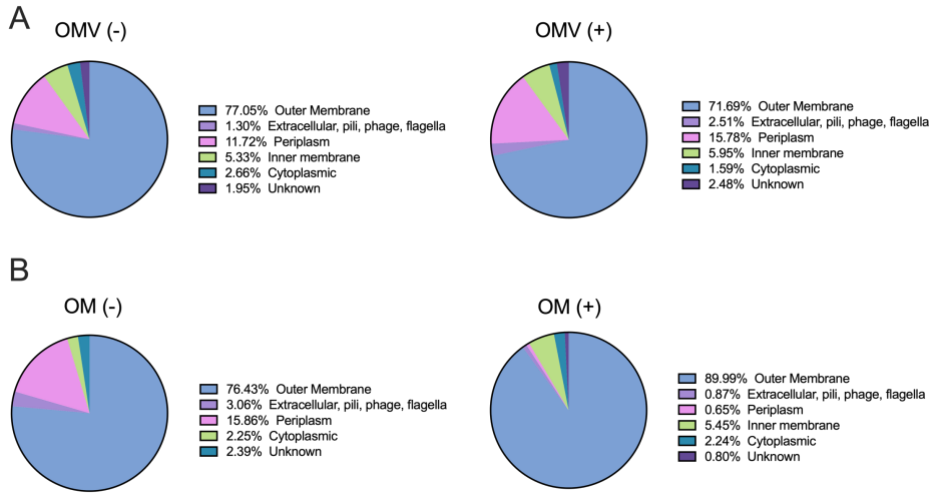

Figure 14: Subcellular localization of proteins in OM and OMV preparations from untreated and treated cultures.

The percentage of proteins annotated for each compartment was calculated from the average individual peptide intensities for those proteins which had 2 or more peptides identified by proteomics. Localization data obtained from UniProt and pSortB.

The sensitivity of the technique also yielded proteins from other subcellular locations, and while it is not known whether those are or are not specifically part of OMVs, previously published proteomic analyses of OMVs yielded similar results (Lee et al. 2007; Choi et al. 2011). After annotating the proteins, we proceeded to characterize packaging under unstressed and oxidative stress conditions.

2.4.2 Outer membrane proteins are selectively packaged in enterotoxigenic *Escherichia coli* OMVs under unstressed environmental conditions

To evaluate OMV cargo selectivity, the average intensity for each protein in the OMV and OM samples was calculated and a ratio determined based on the peptide abundance. We first determined the amount differentially packaged cargo from OMVs produced by ETEC grown in unshifted culture conditions. For these pseudo-stationary phase ETEC cultures, eleven OM-associated proteins were either enriched or excluded at least 2-fold as cargo in OMVs compared to their abundance in the cellular OM (highlighted in yellow and blue in Table 3, columns 1 and 3). These data revealed a basal level of OMV cargo selectivity for stationary phase ETEC in unstressed conditions.

2.4.3 Oxidative stress alters the packaging of outer membrane-associated OMV cargo in enterotoxigenic *Escherichia coli*

Oxidative treatment of the ETEC cultures yielded significantly different cargo packaging results. Specifically, a cursory inspection of the types of OM-associated proteins in the differentially packaged groups suggested a substantial difference between the localization of OM lipoproteins and integral OM proteins (Table 3).

Table 3: Selective OM retention and OMV packaging with and without stress, and change in selectivity after oxidative stress for OM-associated proteins

Column #:	1	2	3	4	5	6	7	8			
OM-associated protein (Bolded=lipoprotein; Non-Bolded=integral; Italics=unknown)	**>2-fold excluded from OMVs without stress**	**>2-fold excluded from OMVs after stress**	**> 2-fold enriched in OMVs without stress**	**>2-fold enriched in OMVs after stress**	**Selectivity in OMVs changed >2-fold with stress**	**Amount in OM changed > 2-fold with stress**	**OM lipoprotein**	**Integral OM protein**	**Part of multiprotein complex**	**IM tethered**	**Function**
E3PIP9	X				up	down	X				Uncharacterized
YglB	X				up	down	X				Biofilm formation
ChiQ				X	up	down	X				Sugar-induced
LpoB				X	up	down	X				Peptidoglycan modification
MliC				X	up	down	X				LPS assembly
RcsF				X	up	down	X				Role in stress conditions
YajI				X	up	down	X				Uncharacterized
YfeY				X	up	down	X				Role in stress conditions
YgdI				X	up	down	X				Uncharacterized
YgdR				X	up	down	X				Uncharacterized
YraP				X	up	down	X				Role in stress conditions
LoiP				X	up	down	X				Metalloprotease / Role in stress conditions / Heat shock
LolB/LolP					up	down	X				Lipoprotein biogenesis
NlpD					up	down	X				Peptidoglycan modifying
OsmE					up	down	X				Osmotic regulation
BamD		X			down	up	X		x		OM protein assembly

MlaA		X			down	up	X				OM maintenance
Sip	X	X					X				Role in stress conditions
RlpA				X	up		X				Peptidoglycan modifying
YajG				X	up		X				Uncharacterized
NlpE				X			X				Copper homeostasis
YbaY				X			X				Uncharacterized
LpoA					up		X				Peptidoglycan modification
YifL					up		X				Uncharacterized
GfcD		X			down		X				LPS assembly
Lpp		X			down		X				Petidoglycan anchoring
Wza		X			down		X				LPS assembly
YeaY		X			down		X				Role in stress conditions
SilC		X			down		X				Silver resistance
LptE					down		X		x	x	LPS assembly
NlpI		X					X				Peptidoglycan modifying
OmpW	X	X			up	down		X			Colicin binding / Transport / Role in stress conditions
TibA	X				up	down		X			Adhesion and invasion
Flu_2 (isoform)			X		down	down		X			Adhesion and invasion
BamA		X			down	up		X	x		OM protein assembly
BtuB		X			down	up		X	x	x	Iron homeostasis
FadL		X			down	up		X			Fatty acid transport
LptD		X			down	up		X	x	x	LPS assembly
OmpA		X			down	up		X			Role in stress conditions / Peptidoglycan anchoring
OmpE/Pho E		X	X		down	up		X			Transport

OmpF		X			down	up		X			Colicin binding / Transport / Role in stress conditions
OmpX		X			down	up		X			Role in stress conditions
PagP		X			down	up		X			LPS assembly
PldA		X			down	up		X			OM maintenance
TamA		X			down	up		X	x	x	OM protein assembly
TolC		X			down	up		X	x	x	Drug efflux
BcsC		X			down	up		X	x	x	Cellulose synthesis
FhuE		X			down	up		X	x	x	Iron homeostasis
CirA					down	up		X	x	x	Iron homeostasis / Colicin binding
FecA			X		down	up		X	x	x	Iron homeostasis
FepA					down	up		X	x	x	Iron homeostasis / Colicin binding
FhuA					down	up		X	x	x	Iron homeostasis
Fiu			X		down	up		X	x	x	Iron homeostasis
YfaZ					down	up		X			Transport
YncD					down	up		X	x	x	Iron homeostasis
YnfB		X			down	up					Uncharacterized
LamB	X	X						X			Sugar transport
LomR	X	X						X			Role in virulence
Flu		X			down			X			Adhesion and invasion
NmpC		X						X			Peptidoglycan anchoring / Transport
OmpC		X						X			Transport

OM lipoproteins appeared to be selectively exported (14/44, highlighted in gray in Table 3, column 4) with fewer being selectively retained (9/44, highlighted in pink in Table 3, column 2), whereas integral OM proteins appeared to be selectively retained upon stress (20/44, highlighted in green in Table 3, column 2) and none exhibited selective OMV packaging (0/44). When we further interrogated the dataset regarding whether the cargo exhibited a >2-fold change in packaging upon oxidative stress, we found that a substantial majority (23/32, highlighted in blue in Table 3, column 5) of the OM-associated cargo that decreased in the amount packaged into OMVs with stress, were integral OM proteins. Conversely, a substantial majority (19/21, highlighted in orange in Table 3, column 5) of the OM-associated cargo that increased in the amount packaged into OMVs with stress were OM lipoproteins. These data suggested a stress-induced selectivity of OMV cargo based on the topological class of the OM-associated protein.

We next examined whether the decrease or increase in packaging of OM-associated proteins into OMVs corresponded to respectively higher or lower amounts of those proteins in the OM fractions of treated cells compared with untreated cells (Table 3). Indeed, nearly all of OM-associated proteins exhibiting reduced OMV packaging upon oxidative stress were at higher levels in the OM of treated cells (highlighted in blue, Table 3, column 6). The exception was the polypeptide identified as Flu, which is known to be highly down-regulated during oxidative conditions (Wallecha et al. 2003).

Also, nearly all OM-associated proteins exhibiting increased OMV packaging upon oxidative stress were at reduced levels in the OM of treated cells (highlighted in orange, Table 3, column 6). Therefore, oxidative stress-induced differential packaging of OM-associated proteins into OMVs correlates with a corresponding difference in the composition of the ETEC OM. These results suggest ETEC may selectively modulate OMV content upon oxidative stress in order to yield a cellular OM barrier with a particular composition.

2.5 Statistical model reveals differential sorting of lipoproteins and integral proteins during stress conditions

Our proteomic dataset was only based on a triplicate sample size contained high variance in average intensities. This is not atypical for proteomic data; however, we were unable to evaluate the results statistically for individual proteins. Instead, we examined the data by applying a Bayesian hierarchical linear model. This analysis is specifically suited for analysis of data with small n, high variance, and containing natural groupings (in this case, the proteins were topologically either OM lipoproteins or integral OM proteins).

2.5.1 Bayesian Hierarchical models

Bayesian analyses are frequently used in the clinical setting to estimate the size of a treatment effect in a population (Quintana, Viele, and Lewis 2017). In these analyses the data are assumed to arise from a process characterized by parameters, numerical quantities that characterize a population. Thus, testing the impact of a treatment can be

evaluated in terms of the parameters related to the treatment. Bayesian hierarchical models require that first, the data have a natural grouping, in our case the specific protein. By assuming that these proteins come from an underlying population they can "share" information between the proteins to obtain better estimates of the baseline levels. Secondly, prior information about the parameters, is incorporated into the model (Quintana, Viele, and Lewis 2017). This information is incorporated as a probability distribution on the parameters before observing data, known as a prior (van de Schoot et al. 2014). Given a prior and a likelihood (the data generation process), we can update our knowledge of the parameters through Bayes rule yielding a posterior distribution. From this posterior we can evaluate the probability that the parameter lies in a particular interval. Because we are testing the hypothesis that the treatment has no effect, this becomes equivalent to determining if 0 falls in a high-probability region of the posterior for the parameter of interest, known as a credible interval.

Estimating the posterior for many models involves intractable high-dimensional integrals to represent the denominator in Bayes rule. To circumvent these difficulties, we instead draw samples from our posterior distribution using Markov chain Monte Carlo (MCMC). We can construct empirical credible intervals using the samples, generally the highest density region containing 95% of the posterior probability.

Thus, in our analysis, we characterized the OMV packaging ratio as a function of a protein-specific level with an effect and the treatment impact. We split the proteins

into two groups, integral proteins and lipoproteins and estimated a treatment effect for each group separately. By examining the credible interval on the parameter associated with the treatment we could determine the sign of the impact as well as statistical significance.

Here is our full model specification including our likelihood and prior distribution for reproducibility purposes:

$$Y_{ij} \sim N(\alpha + \alpha_i + \beta\chi_i, \tau^2) \quad [1]$$

$$P(\beta) \propto 1 \quad [2]$$

$$P(\alpha_i) = N(0, \sigma^2) \quad [3]$$

$$P(\sigma^2) = t_3(0,10) \quad [4]$$

In [1], Y_{ij} is our $\log_2$ ratio of OMV packaging for protein *i*, for sample *j*. Y_{ij} is a function of α which is our general protein offset or baseline OMV packaging for each protein; α_i which is the impact of a particular protein, or deviation from baseline packaging (specific protein deviation from the general mean α); β, the treatment effect size (our goal is to estimate this, the impact the treatment has on the $\log_2$ fold of a given protein); χ_i which is 1 for treated and 0 for untreated samples; and τ^2 which is the variance of the data. [2], [3], and [4] are our prior distributions of the parameters. Formula [2] is an improper distribution that does not integrate to 1 but once we observe a single observation, the posterior is a proper posterior distribution. This means we have no prior beliefs on the size of the treatment. [3] indicates our offset comes from one

population. This is what allows us to share information between the proteins to better estimate offsets of proteins. [4] is a truncated t distribution with 3 degrees of freedom and it states that our variance has to be positive.

We applied this model and observed that the packaging of the two groups, OM lipoproteins and OM integral proteins, indeed changed upon treatment (Fig. 15). The results indicated that OM lipoproteins were significantly preferentially packaged (with treatment decreasing the fold packaging value and a p-value of ≤0.05) in comparison to OM integral proteins (with fold values increased as a result of treatment and a p-value of ≤0.0001) (Fig. 16). Thus, the initial observation of differential packaging based on the average values calculated for each protein was confirmed by the hierarchical model analysis of the data.

Integral proteins

	Estimate	Est. Error	l-95% CI	u-95% CI	Eff. Sample	Rhat
Group-Level Effects						
sd (Intercept)	0.24	0.16	0.01	0.60	1398	1.00
Population-Level Effects						
Intercept	0.03	0.16	-0.29	0.34	4000	1.00
Treatment	-1.45	0.22	-1.86	-1.02	4000	1.00
Family Specific Parameters						
sigma	1.53	0.08	1.38	1.69	4000	1.00

Lipoproteins

	Estimate	Est. Error	l-95% CI	u-95% CI	Eff. Sample	Rhat
Group-Level Effects						
sd (Intercept)	0.12	0.09	0.00	0.33	2313	1.00
Population-Level Effects						
Intercept	-0.16	0.12	0.00	0.33	4000	1.00
Treatment	0.34	0.17	0.01	0.67	4000	1.00
Family Specific Parameters						
sigma	1.60	0.06	1.49	1.72	4000	1.00

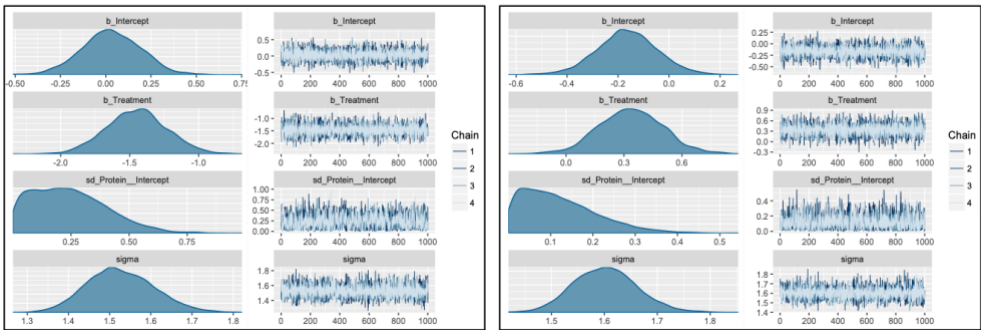

Figure 15: Bayesian estimates and posterior distributions for treatment effect on OMV packaging of protein groups.

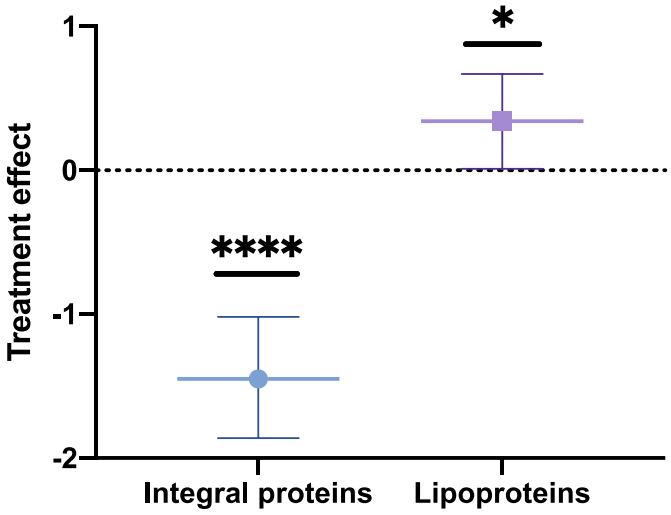

Figure 16: Oxidative stress causes a preferential export of lipoproteins into OMVs and a preferential retention of integral proteins in the OM of enterotoxigenic *Escherichia coli*.

Parameter values for the treatment effect on OMV packaging ratios were calculated for OMV(+):OM(+), and OMV(-):OM(-) to obtain the increase or decrease in protein packaging in OMVs due to treatment stress. P-values calculated from confidence intervals (treatment effect): * $p \leq 0.05$, **** $p \leq 0.0001$.

2.6 No correlation is observed between packaging of proteins into OMVs and gene expression under stress conditions

Because it is known that increases of envelope proteins incorporated into vesicles can occur by overexpression of those proteins (McBroom and Kuehn 2007), we wondered whether the observed preferential incorporation of OM lipoproteins compared with integral proteins upon oxidative stress was due to oxidation-induced differences in expression of the sets of genes encoding these proteins. To address this question, we mined the GEO profiles dataset of the NCBI (Edgar, Domrachev, and Lash

2002; Barrett et al. 2013), specifically GSE4735 (Partridge et al. 2006). This dataset reports on the dynamics of oxidative stress-induced gene expression and was useful for our analysis since the transition from anaerobic to aerobic conditions has been noted to be comparable to oxidative stress (Cabiscol, Tamarit, and Ros 2000). The gene expression profiles for OM integral proteins and lipoproteins in this dataset were classified by their gene expression profiles according to their packaging into OMVs. Only 2% of the OM lipoproteins identified in our study showed increased gene expression under the stress conditions shown in the GEO dataset using a 2-fold threshold (Fig. 17A). As for the OM integral proteins, only 6.4% showed decreased expression (Fig. 17B). Although this analysis is based on data using other *E. coli* strains, it is relevant since genetic regulatory elements such as the response to oxidative stress are typically well-conserved within a bacterial species (with ETEC having an 88% symmetrical identity with *E. coli* strain K-12 substr. MG1655 (Crossman et al. 2010)). Therefore, it appeared that the selective packaging of OM lipoproteins over integral proteins into OMVs that we observed for H_2O_2 stressed ETEC is likely not simply due to an oxidation-induced increase in their gene expression.

In order to validate that levels of gene expression were not the direct cause of oxidation-induced cargo selection in our ETEC strain, two lipoprotein genes, two integral protein genes and two periplasmic genes were chosen at random out of our OMV cargo datasets. We isolated RNA from unshifted and oxidatively stressed ETEC

cultures and used qRT-PCR to evaluate whether increases or decreases in gene expression directly correlated with packaging patterns of these classes of proteins. Our results showed that this group of lipoproteins was not expressed more than the integral OM or periplasmic protein groups after a shift to oxidative stress (Fig 13C), supporting the conclusion that there is not a correlation between the observed selective packaging of different classes of proteins and gene expression.

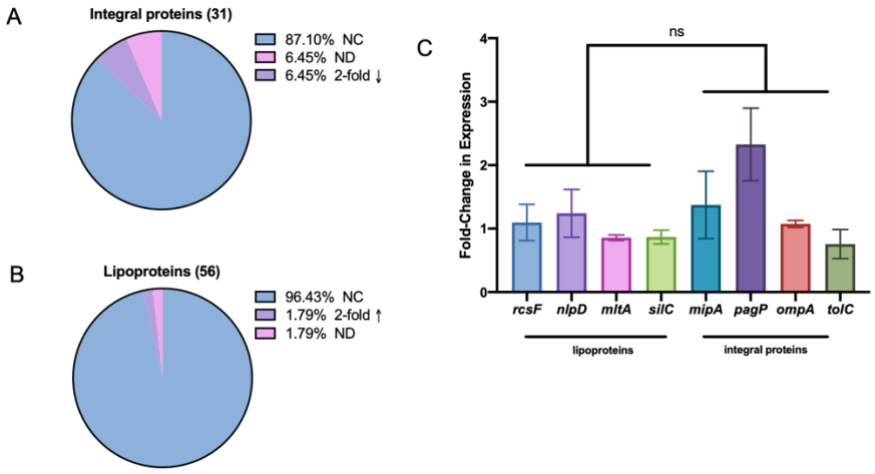

Figure 17: Results from mining GEO profile GSE4735 and validation in ETEC of selected genes.

(A and B) Changes of a 2-fold increase or decrease from database mining of GEO profile GSE4735 for gene expression after shift from anaerobic to aerobic conditions. NC, no change; 2-fold ↑, > two-fold increased expression; 2-fold ↓, < two-fold decreased expression; ND, not in database. **(C)** Fold change in expression was measured by qRT-PCR after 3h H_2O_2 treatment compared to untreated controls for randomly selected genes encoding OM lipoproteins or integral OM proteins in ETEC. Error bars are SEM; ns, not significant.

2.7 K-12 E. coli knockout mutants of lipoproteins and integral proteins do not show patterns of differential sensitivity to H_2O_2

The selective preferential retention of integral OMPs in the cellular OM, suggested that the bacteria may benefit from retaining these OMPs when growing in an oxidizing environment. Thus, we initially predicted that mutants lacking these integral OMPs might be more sensitive to H_2O_2 stress. When we tested mutants of K-12 E. coli for H_2O_2 sensitivity all mutants tested were more sensitive than wildtype (WT) to treatment (Fig. 18A). This was consistent with our hypothesis.

Further, we wondered if the fact that lipoproteins were preferentially being exported upon oxidative stress meant that the bacteria either did not need them or they were detrimental for the cells in the new environment. We hypothesized that, if this was true, mutants lacking lipoproteins would not be more sensitive to H_2O_2. When we tested the sensitivity of several lipoprotein mutants using the non-pathogenic K-12 strain BW2511, we found that all the mutants showed increased sensitivity in comparison to the WT (Fig. 18B). Therefore, this data did not support the model that the absence of these proteins in the OM was beneficial to cells in oxidative stress conditions. While integral protein mutants were more sensitive to oxidative stress like we predicted, lipoproteins were also more sensitive than WT. Together these data show that the deletion of any OM-associated protein, whether integral or lipid anchored, is detrimental to the ability of cells to withstand oxidative stress. The evaluation of a more nuanced depletion or enrichment of proteins in the cell OM, rather than analysis of the

complete deletion phenotypes, is likely to give a more physiological answer to testing these hypotheses.

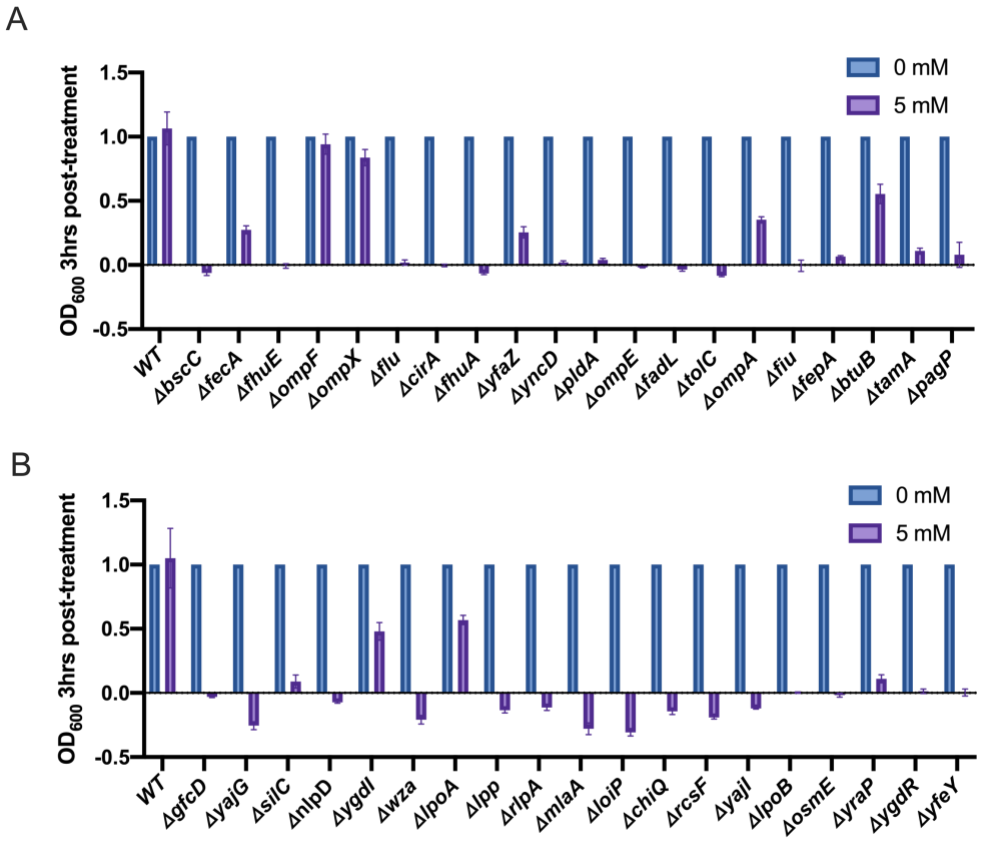

Figure 18: Sensitivity of *E. coli* K-12 OM lipoprotein and integral protein mutants to H_2O_2.

(A) Sensitivity of K-12 E. coli OM integral protein and **(B)** lipoprotein mutants to 5mM. of H_2O_2. Cultures were resuspended in new media with different concentrations of H_2O_2 and OD_{630} was monitored for 4 hours. Figure shows difference in OD_{630} from time 0 and all values are normalized to the average value of their respective untreated sample (0 mM).

2.8 Validation of differential OM-associated protein class sorting upon oxidative stress

To test our hypothesis that differential export and retention of classes of OM-associated proteins occurs as a result of oxidative stress, we quantified the incorporation into OMVs of OM lipoprotein and integral OM protein cargo in a standard laboratory *E. coli* strain. Lipoproteins YfeY and YgdI and integral proteins PhoE and TamA were chosen for evaluation as OMV cargo since they had previously been tagged with His_6 at their C-terminus without interfering with their localization or stability (Van Gelder et al. 1996; Shen et al. 2014). Non-pathogenic *E. coli* strain BL21 cells were transformed with expression plasmids encoding the tagged proteins (Fig. 30 and 31) and the constructs expressed without using a transcriptional inducer.

The expected OM localization of all four tagged proteins was confirmed by immunoblotting of subcellular fractions (Fig. 19A). Oxidative stress conditions were also optimized for the BL21 strains. A lower concentration of peroxide (1 mM) was used compared with the conditions used for ETEC cultures, given the lower tolerance to oxidative stress in non-pathogenic strains (Fig. 19B). Membrane integrity was confirmed to be uncompromised for all the BL21 constructs treated with 1 mM H_2O_2 (Fig. 19C).

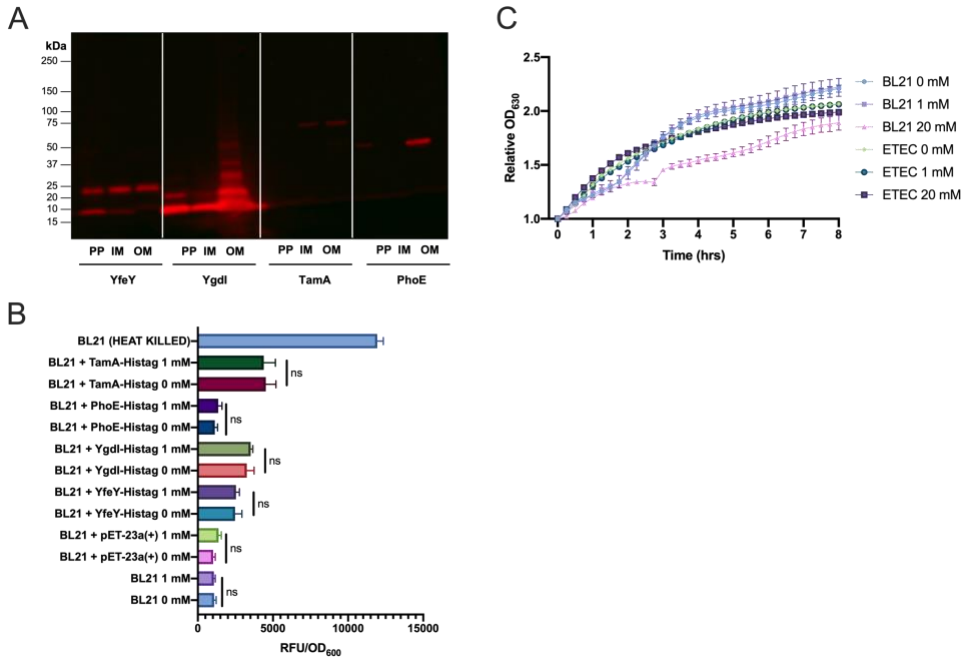

Figure 19: OM localization, and treatment and membrane integrity assays for lipoprotein and integral proteins used in this study.

(A) OM localization of tagged constructs. Subcellular fractions (equal concentrations of protein) were separated by SDS-PAGE and detected by immunoblotting. PP, periplasm; IM, inner membrane; OM, outer membrane. **(B)** *E. coli* strain BL21 is more sensitive to H_2O_2 than ETEC. Cells were inoculated onto 96-well plate from a 5 mL overnight culture at a dilution of 1:5000 in media and the indicated concentration of H_2O_2. Cultures were incubated for 8 h at 37°C, and OD_{630} was recorded every 15 min. OD_{630} values were normalized to starting OD_{630} values at time 0. **(C)** Oxidative stress does not compromise membrane integrity relative to untreated cultures. Relative fluorescence (RFU) normalized to OD_{600} of the indicated BL21 construct cultures assayed with Sytox Green at 3h after treatment with 1 mM H_2O_2 or mock treated. Heat-killed cell control is shown. (n=4). Error bars are SEM; ns, not significant.

OMVs and OM from untreated and hydrogen peroxide-treated uninduced cultures of the transformed constructs were purified as described earlier for the ETEC preparations. The OMV:OM packaging ratio for each cargo protein was calculated based

on quantitative immunoblotting of purified OMV and OM preparations from untreated and treated cultures. Upon oxidative treatment, OM lipoproteins YfeY and YgdI both showed an increase in packaging into OMVs, and integral OM protein PhoE showed a decrease in OMV packaging (Fig. 20). The integral OM protein TamA did not show a significant difference in packaging. The results observed for 3 out of 4 of these randomly selected proteins are consistent with our hypothesis that generally, but not in all cases, oxidative stress leads to differential OMV packaging of OM lipoprotein and integral OM proteins in *E. coli*.

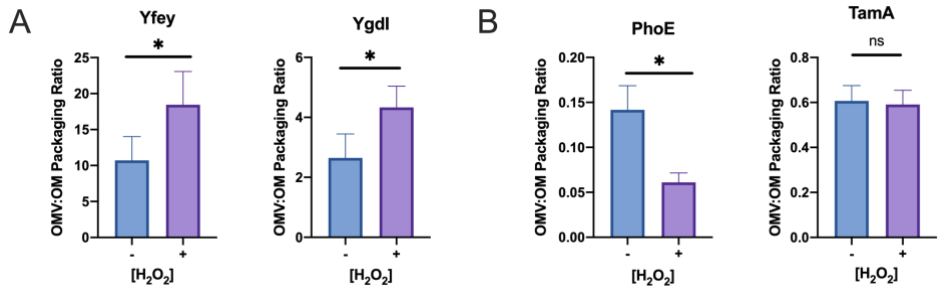

Figure 20: Validation of preferential packaging of lipoproteins into OMVs upon oxidative stress.

Packaging ratios (OMV:OM) were calculated from the detection of tagged OM lipoproteins **(A)** or integral OM proteins **(B)** by quantitative immunoblotting of OM and OMV preparations from untreated (-) and 3h H_2O_2-treated (+) BL21 constructs. YfeY (n=8), YgdI (n=4), PhoE (n=6), TamA (n=6). Error bars are SEM. P-values according to the Student's t test: * $p \leq 0.05$.

2.9 OMVs carry oxidized, functionally altered cargo and slightly increased periplasmic content, possibly dependent on gene expression

While a majority (89.98%) of the proteins in the OMVs from treated cultures were proteins localized to OM, we also observed periplasmic and extracellular proteins (Fig. 14). We noticed that a slightly higher proportion of periplasmic proteins appeared to be present in the OMVs isolated from treated cultures compared to the OMVs from untreated cultures and followed up on this with statistical analysis.

2.9.1 Oxidative stress causes a slight increase in OMV periplasmic cargo and this is possibly correlated with gene expression

Results indicated that in comparison to OMVS from mock-treated cultures, OMVs produced in response to treatment with H_2O_2 contained a significantly higher abundance of periplasmic protein (Fig. 21A). Extracellular proteins such as flagella, phage and pili were also significantly increased in abundance. This was not surprising since several studies have reported upregulation of these genes by stress conditions in *E. coli* and other strains (Raivio 2005; Licznerska et al. 2016; Wang et al. 2010; Lin et al. 2016).

We further investigated whether there was a subclass or functional preference for preferentially included or excluded periplasmic cargo upon oxidative stress but could not find a statistically significant change associated with a functional group. These results demonstrated that while oxidative stress causes differences in abundance of

soluble cargo in ETEC OMVs, there is no obvious functional enrichment for the soluble vesicle cargo.

To investigate whether the overall increase of periplasmic protein cargo in our OMV samples after treatment, was due to periplasmic protein overexpression, we mined the database mentioned above for periplasmic gene expression data. If periplasmic proteins were generally upregulated in stress conditions, it would explain why stress increased their levels in the samples. From an analysis of the gene expression data, none of the genes encoding the periplasmic proteins in our study were found to increase at least 2-fold, and 2% showed a 2-fold decrease (Fig. 22A). Again, with the acknowledged limitations of this analysis, these data suggest that the increased presence of periplasmic proteins in the OMVs from treated ETEC cultures is not a result of their increased expression upon peroxide stress. In contrast, when we sought to validate this gene expression data from the databases using qRT-PCR, our results showed that periplasmic proteins were not expressed more than integral proteins, but were expressed more than lipoprotein groups after a shift to oxidative stress, (Fig. 22B). This demonstrated a slight correlation between the increase in OMV cargo and gene expression for periplasmic proteins.

Based on the higher periplasmic content in OMVs from treated cultures we hypothesized that these OMVs would be denser than OMVs from untreated cultures. To test this, we evaluated the density of the OMVs using equilibrium gradient

centrifugation. If OMVs from a treated culture were denser than OMVs from untreated ETEC, we would expect a shift in the peak of OMV-associated protein to denser fractions. Indeed, the gradient analysis showed that OMV (+) proteins were present in slightly more dense fractions compared with OMV (-) proteins (Fig 21B). That this observed change in OMV density is modest is not surprising, since periplasmic proteins are only a small fraction of the overall OMV content. We wondered if the higher periplasmic content in OMVs reflected a corresponding increase in the concentration of periplasmic protein in cells upon oxidation stress. Periplasm preparations isolated from ETEC cultures after the 3h shift to oxidative conditions and from untreated ETEC were quantified for protein content by densitometry after SDS-PAGE. The results showed that there was not a significant difference in periplasmic protein content for untreated and treated cells (Fig. 21C). Together the data indicate that a selective increase in periplasmic protein packaging into OMVs occurs upon oxidative stress and it seems to be related to an increase in gene expression. More periplasmic gene candidates should be tested by qRT-PCR to strengthen this conclusion.

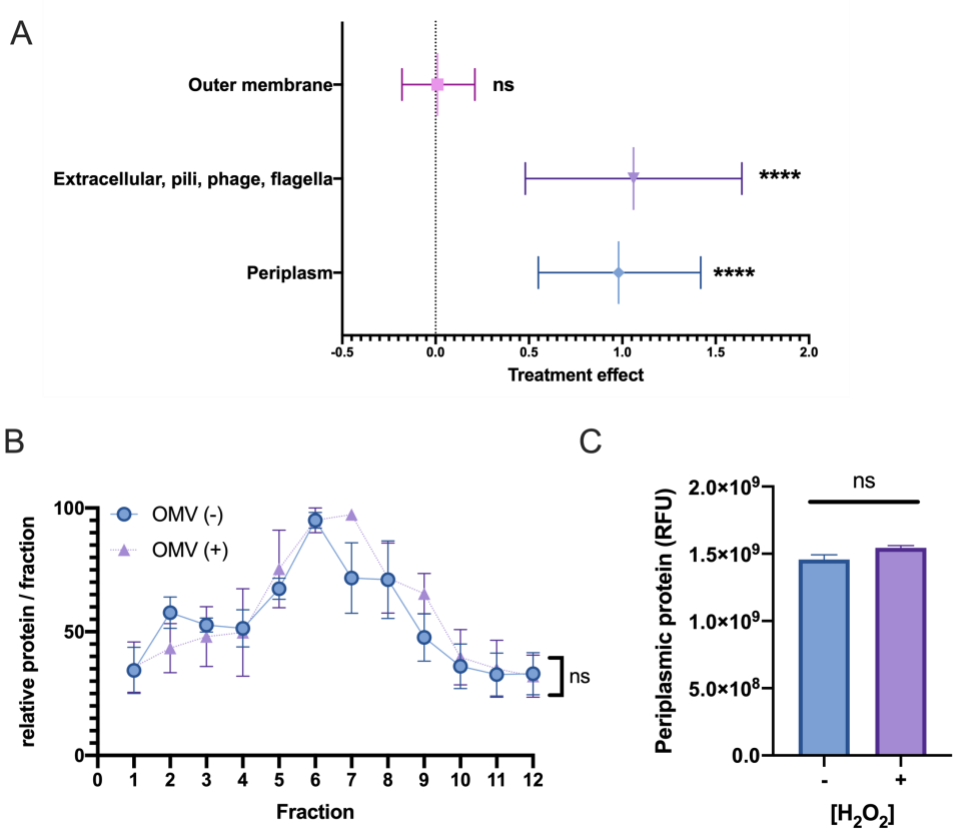

Figure 21: Oxidative stress increases the periplasmic content of OMVs.

(A) Parameter values for treatment effect on protein abundance in each cellular compartment. Parameters calculated for the OMV (+), OMV(-) to obtain the increase or decrease in protein abundance in OMVs due to treatment stress. **(B)** Relative protein in fractions of OMV (+) and OMV (-) samples separated using an equilibrium density gradient. Protein quantitation from densitometry was obtained using FIJI software and normalized to the fraction containing the maximum protein content in each gel (n=3). Arrow indicates a shift to heavier fractions in the OMV (+) sample. **(C)** Cellular periplasmic protein concentrations from untreated and H_2O_2- treated cultures normalized to cell concentration. Periplasmic preparations were separated by SDS-PAGE, stained for protein, quantitated by densitometry and analyzed using FIJI (n=3).

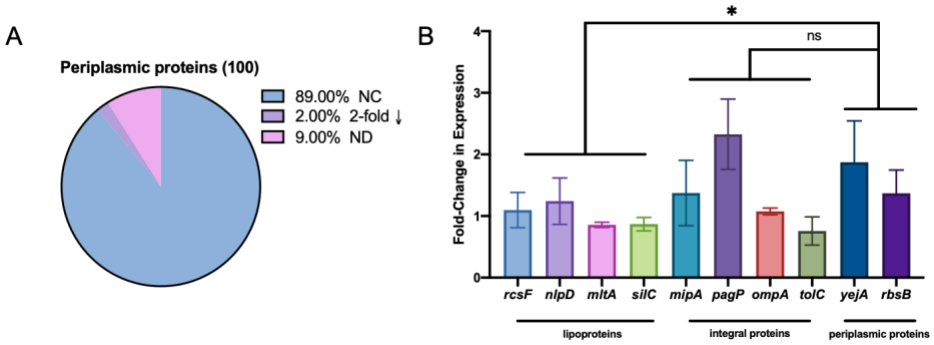

Figure 22: Results from mining GEO profile GSE4735 and validation in ETEC of selected periplasmic genes.

(A) Changes of a 2-fold increase or decrease from database mining of GEO profile GSE4735 for gene expression after shift from anaerobic to aerobic conditions. NC, no change; 2-fold ↑, ≥ two-fold increased expression; 2-fold ↓, ≤ two-fold decreased expression; ND, not in database. **(B)** Fold change in expression was measured by qRT-PCR after 3h H_2O_2 treatment compared to untreated controls for randomly selected genes encoding OM lipoproteins, integral OM proteins or periplasmic proteins in ETEC. Error bars are SEM; ns, not significant.

2.9.2 OMV cargo is more oxidatively modified in response to stress

As our prior research indicated that misfolded protein is selectively packaged into OMVs (Schwechheimer and Kuehn 2013), we also wondered whether proteins that are more prone to be oxidized due to stress are more likely to be exported in OMVs after a shift to H_2O_2-containing media. We mined the UNIPROT database for proteins that were either preferentially exported in OMVs or retained in the OM in our analysis and calculated percentage of methionine (Met) and cysteine (Cys) residues in each protein (disregarding the initial Met). The results revealed that, compared to retained proteins, exported proteins had significantly more Met or Cys residues (Fig. 23A). We also observed an increase in carbonyl modifications present in our OMV samples from treated cultures compared to untreated cultures (Fig. 23B) Together these data revealed that, in addition to lipoproteins, proteins more prone to oxidation are more likely to be packaged in OMVs.

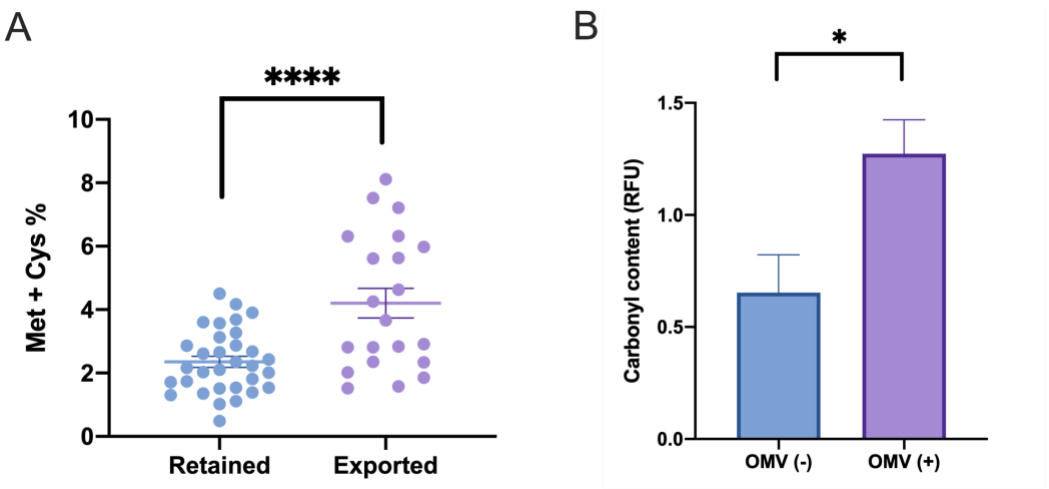

Figure 23: Cargo contains a higher amount of oxidizable residues and it is more oxidatively modified in response to stress.

(A) Methionine and Cysteine percentage (Met and Cys residues per total amino acids in protein without initial Met) in preferentially exported vs preferentially retained proteins in oxidized samples **(B)** Densitometric Oxyblot analysis of OMV proteins from 3h H2O2 treated (+) or untreated (-) ETEC cultures using FIJI software and normalized to non-derivatized samples (n=6). Error bars are SEM. P-values according to the Student's t test: * $p \leq 0.05$, **** $p \leq 0.0001$.

2.9.3 Oxidative stress reduces OMV cytotoxicity

To test whether oxidative stress not only affected the OMV content but also their function, we assayed the toxicity of ETEC vesicles. We used an established assay in which the degree of Y-1 adrenal cell rounding quantitatively reflects the toxicity of heat-labile enterotoxin-carrying ETEC OMVs (Horstman and Kuehn 2000; Donta, Moon, and Whipp 1974). Y-1 cell morphology was scored after incubation with equivalent amounts purified OMVs (by protein) from ETEC cultures that had been either treated with

hydrogen peroxide or left untreated. Y-1 cells incubated with OMVs derived from untreated cultures were significantly more rounded than those incubated with OMVs produced in oxidized cultures (Fig. 24). These results show that the toxicity of ETEC vesicles from oxidized cultures is reduced, suggesting OMV packaged proteins may be oxidatively modified or altered in function.

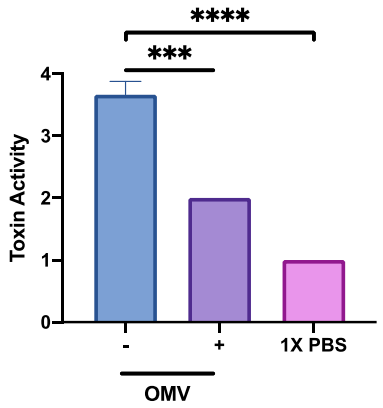

Figure 24: Oxidative stress reduces OMV cytotoxicity.

OMV (-): vesicles from untreated ETEC cultures. OMV (+): vesicles from H_2O_2-treated ETEC cultures. Buffer control: PBS. Y1 cells (4×10^5) were plated in gelatin-coated 24-well polystyrene plates and allowed to adhere overnight. The growth medium was replaced with 1 ug of vesicle sample, or an equivalent volume of PBS, diluted in F-12K media (250 µl). Morphology was scored 18 h later. Toxin activity scores: 1 = <25% rounding, 2 = 26–50% rounding, 3 = 51–75% rounding, 4= >76% rounding. P-values according to the Student's t test: *** $p \leq 0.001$, **** $p \leq 0.0001$ (n=6).

2.10 Remodeled membrane confers fitness advantage to the bacteria upon secondary challenge

Given the observed OM composition changes that arose as a result of oxidative stress, we hypothesized that these changes might confer a fitness advantage to the bacterial cell upon a secondary challenge of H_2O_2. We inoculated cells from cultures incubated for 3 hours in the presence of H_2O_2 (shifted) or absence (mock-shifted) and we challenged for a second time and monitored growth (OD) for 8 hours (Fig. 25). The results showed that shifted cells had increased resistance H_2O_2. This suggested the oxidative stress-induced remodeling of the bacterial cell membrane provided a fitness advantage upon a secondary challenge of oxidative stress.

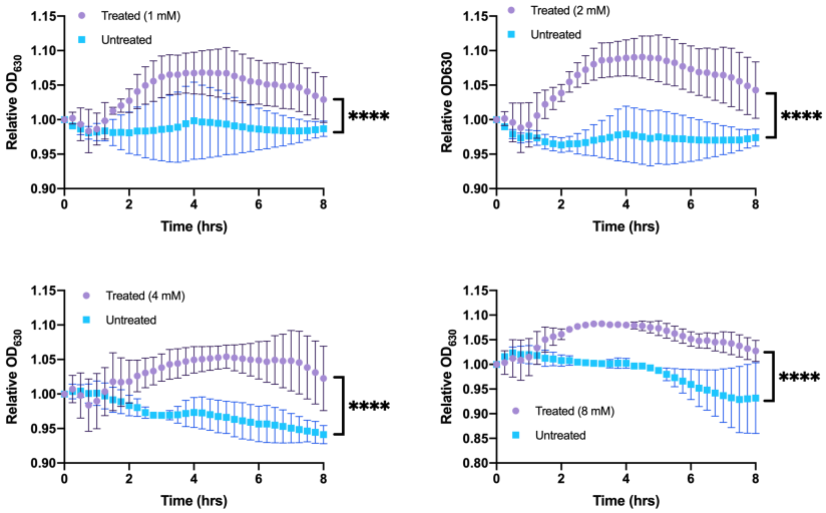

Figure 25: Remodeled membrane confers fitness advantage to the bacteria upon secondary challenge.

Growth curves from 3h shifted or mock-shifted ETEC cultures subjected to indicated concentrations of H_2O_2. P-values according to the Student's t tests performed for Area Under the Curve parameters (Mock Shift vs Shift curves). : * $p \leq 0.05$, ** $p \leq 0.01$, **** $p \leq 0.0001$.

2.11 Discussion

By quantitatively comparing the protein composition of *E. coli* OMVs and cellular OM produced during unstressed and oxidatively stressed conditions, this study revealed the unanticipated differential sorting of two classes of OM embedded proteins into the secreted OMVs. After annotating and examining differences in retained and exported ratios of the various polypeptides, we were able to detect trends in the selective packaging of specific classes of OM-localized proteins. Based on a low sample size (n=3) and high variance in the content for the OM and OMV preparations, not uncommon for bacterial subcellular fractionation (Baik et al. 2004; Ebanks et al. 2005; Sezonov, Joseleau-Petit, and D'Ari 2007; Liu et al. 2008; Nikaido 2009; Sridhar and Steele-Mortimer 2016), statistically significant differences were not found for the differential packaging of individual proteins in treated or untreated conditions. Instead, we implemented a statistical model to analyze the changes in fold values of the two protein classes found in our study: lipoproteins and integral proteins (Efron et al. 2001; Gottardo et al. 2006; Manda, Walls, and Gilthorpe 2007; Walker et al. 2008). The results showed a significant preferential export of OM lipoproteins in comparison to integral OM proteins.

We considered several explanations for the observed differential packaging of the lipoprotein and integral classes of OM cargo. First, our experimental methodology

could have resulted in the biased enrichment of different classes of proteins in the preparations. However, we note that by using lysozyme and French press methods to obtain OM for analysis, we avoided the issue that detergent can reduce the abundance of lipoproteins in OM samples (Zhang et al. 2018).

Next, we hypothesized that the increase in lipoprotein export reflected the need for the cell to rid itself of unneeded lipoproteins during stress and that lipoprotein mutants would be more resistant to oxidative stress than WT. We also considered that integral proteins were being retained because they were needed in the cell during oxidative stress. While our results for integral protein mutants were indeed more sensitive than WT as we predicted, lipoprotein mutants were also more sensitive. This leads us to consider that mutations in OMV components tend to generally cause peroxide sensitivity and does not explain the packaging tendencies observed.

We further wondered if the selectivity we observed was related to the observed enrichment of lipoprotein cargo into OMVs discovered in a study of *B. thetaiotaomicron* (*Bt*) (Valguarnera et al. 2018). In addition to the fact that *Bt* contains surface-exposed lipoproteins, a feature not found in *E.* coli, the lipoprotein sorting mechanism in *Bt* is further distinct from that found in this study. Notably, the preferential OMV packaging of lipoproteins in *Bt* depends on a canonical signal sequence that is not found in the ETEC lipoproteins. Further, lipoprotein sorting into OMVs was not compared for unstressed and stressed cultures of *Bt*, thus it is not known if the selectivity is

environmentally-regulated. Therefore, the differential cargo sorting into OMVs that we observed appears distinct and mediated by a previously unknown mechanism.

We also analyzed whether the sorting trends for lipoproteins, integral proteins we observed were due to corresponding changes in gene expression, but found no direct correlation between the differential incorporation of lipoproteins and integral proteins and gene expression during oxidative stress conditions in *E. coli* databases. Expression results for several randomly selected gene candidates also did not reveal any correlation between packaging patterns and gene expression of these protein classes.

An additional statistical analysis on protein abundances in different cellular compartments reflected an increase in OMV periplasmic protein cargo during oxidative stress. Our assays to determine periplasmic density and changes in OMV density detected only a subtle increase in OMV density, and we believe that these methods were likely not sufficiently sensitive to find significant differences. We did find that this increase was independent of gene expression by testing two periplasmic protein candidates. A proteomic study focusing solely on periplasmic cargo could help elucidate the reason for the slight increase in periplasmic content reflected in the proteomic data.

As a follow up to the periplasmic data, we studied another aspect of post-treatment OMV cargo, its impact on OMV function. For this, we explored changes in OMV production as a result of stress and the oxidation state of OMV cargo. Previous studies have shown that upon stress, bacteria either increase OMV production, or

increase the selectivity of damaged or immature cargo into OMVs, or both (Orench-Rivera and Kuehn 2016). In this study, we did not observe a significant increase in ETEC OMV production after oxidative stress. It is possible that any benefit mediated by increased levels OMV production during oxidative conditions, for example to remove damaged or misfolded envelope proteins, are already met by the high constitutive level of OMV production by ETEC. Indeed, we observed an increase in oxidative stress-induced modifications to OMV proteins. While this was not surprising, since vesicles were derived from oxidized cultures, a closer look at the composition of the proteins preferentially exported (after calculating difference of at least 2-fold between treated and untreated samples) in comparison to the ones preferentially retained in the membrane, revealed a higher amount of oxidizable resides. These data show that proteins more likely to have been oxidized were enriched for export upon stress. Additionally, we found that OMVs from oxidized ETEC cultures were less cytotoxic than control OMVs, consistent with the enhanced packaging of oxidized and/or damaged cargo or host targeting and trafficking receptors. The enrichment of proteins with oxidizable residues as well as the associated decrease in OMV cytotoxicity are consistent with a model in which OMVs help rid the cell of oxidatively modified proteins in response to oxidative stress. However simply packaging damaged protein did not appear to explain the proteomic analysis regarding the observed differential packaging of classes of OM proteins.

Results from our lab suggest that OMVs can contribute to OM remodeling during a shift in environmental conditions (Bonnington and Kuehn 2016). Based on the differential protein sorting observed during our oxidative stress conditions we sought to investigated whether this stress-induced, OMV-facilitated remodeling of the OM composition conferred bacterial cells with a fitness advantage. To test this, we employed a secondary-challenge assay. Results showed that shifted cells showed increase resistance to a secondary challenge of H_2O_2. Although increased resistance to a secondary challenge has been previously observed to reflect transcriptional changes and the emergence of persister cells (Fisher, Gollan, and Helaine 2017; Chung, Bang, and Drake 2006), we hypothesize that this OMV-mediated modification of membrane architecture has a significant impact on bacterial cell survival during stress.

In sum, the data demonstrate that changes in environmental conditions, notably a shift to oxidative stress, cause differences in OMV cargo composition in *E. coli* and that these changes can be quantified and validated using tagged protein constructs. Results also show changes in OMV cargo selectivity were shown to contribute to OMV membrane remodeling by providing bacteria with a fitness advantage in the face of stress.

3. Uncovering a mechanism for OMV cargo selection based on physical tethering to the bacterial cell wall

3.1 Summary

In our study, proteomic analysis of outer membrane (OM) and OM vesicle (OMV) fractions from enterotoxigenic *Escherichia coli* revealed significant differences in protein abundance in the OMV and OM fractions for cultures shifted to oxidative stress conditions. Analysis of sequences of proteins preferentially packaged into OMVs showed that proteins with oxidizable residues were more packaged into OMVs in comparison with those retained in the membrane. In addition, the results indicated two distinct classes of OM-associated proteins were differentially packaged into OMVs as a function of H_2O_2 treatment. Implementing a Bayesian hierarchical model, OM lipoproteins were determined to be preferentially exported during stress whereas integral OM proteins were preferentially retained in the cell. Based on these data, we tested a hypothetical functional and mechanistic basis for OMV cargo selectivity during oxidative stress using OmpA constructs. Results from this study revealed a potential mechanism for cargo selectivity into OMVs.

3.2 Introduction

OMV cargo selectivity has been observed in bacteria under standard growth conditions (Zavan et al. 2019; McMahon et al. 2012) and studies have shown that packaging of specific protein content in vesicles can be beneficial to bacteria (Veith et al. 2014; Liu et al. 2019; Horstman and Kuehn 2000; Glowczyk et al. 2017), especially in the

context of environmental shifts (Ballok et al. 2014). Preferential incorporation or exclusion of proteins into and from OMVs plays an important role for bacterial physiology and influences OMV function; however, the mechanism of cargo selection remains understudied.

Mechanisms of cargo incorporation are well-studied for eukaryotic intracellular transport vesicles (Aridor et al. 1998; Kaiser 2000), as well as eukaryotic extracellular vesicles that derive from multivesicular bodies (Colombo et al. 2013; Li et al. 2018; Anand et al. 2019), and from the plasma membrane (Cocucci, Racchetti, and Meldolesi 2009; Tricarico, Clancy, and D'Souza-Schorey 2017). However, only very few studies have addressed the mechanism behind specific cargo selection in bacteria. For instance, our previous work showed that a mimic of a misfolded OMP intermediate recognized by the cell as a σ^E-activating stress signal, was preferentially incorporated into OMVs, indicating OMV incorporation can be determined by the protein's folding state, although the physical mechanism underlying the selective incorporation into the budding OMVs of cargo that contained the σ^E-activating signal was not determined (McBroom and Kuehn 2007). Haurat et al. revealed a mechanism in *Porphyromonas gingivalis* by which gingipains are preferentially associated with OMVs by associating with particular forms of LPS while excluding other abundant OM proteins (Haurat et al. 2011). In *Bacteroides thetaiotaomicron*, Valguarnera et al. found that enrichment of lipoproteins in OMVs was explained by the presence of a lipoprotein export sequence

that determined sorting in that system (Valguarnera et al. 2018). Interestingly, while some studies have addressed the mechanism of cargo selection in bacteria, studies indicating environmental change-induced OMV cargo selectivity do not provide a molecular rationale. For example, Ballock et al. noted that the proteins Cif and OprF were preferentially packaged in OMVs from *Pseudomonas aeruginosa* when cells were exposed to the epoxide epibromohydrin compared to their packaging in OMVs from untreated cells (Ballok et al. 2014) but the mechanism behind this enrichment remained elusive. Further, for *Serratia marcescens*, McMahon et al. found that, when compared to the OM, OMVs were enriched in several OM proteins (OmpA, OmpW, OmpX, MipA) when cells were grown at 30°C (McMahon et al. 2012), but the mechanism behind this selectivity also remained unexplored.

As a follow-up to our proteomic findings, we sought to investigate the mechanism behind the differential incorporation of lipoproteins vs integral proteins in *E. coli* after a shift to oxidative stress conditions. Our previous results showed that during oxidative stress conditions, OMVs preferentially packaged lipoproteins while integral proteins were more likely to be retained in the OM, and that this differential sorting was independent of gene expression patterns. Since the integral proteins found to be preferentially retained in the OM are known to have more physical ties to other ell envelope components in comparison to OM-associated lipoproteins, we hypothesized that ties to the cell envelope modulated incorporation of proteins into vesicles.

To test our hypothesis, we investigated a potential mechanism for the preferential OM retention or packaging of proteins into OMVs based on cell wall anchoring using OmpA as a model protein. Overall, this study provides insight into vesicle-mediated mechanisms of membrane remodeling in bacteria experiencing environmental shifts, as well as a general mechanistic basis for OMV protein cargo selectivity in unstressed conditions.

3.3 Gene Ontology analysis reveals preferentially retained OM proteins during oxidative stress are enriched in categories related to transport and iron homeostasis

To investigate the differential sorting observed in our proteomic study, we considered how the distinctive general functions and features of lipoproteins and integral OM proteins could govern cargo selectivity. Gene Ontology analysis revealed that, amongst all the OM proteins we detected, the proteins that were at least 2-fold more retained upon oxidative stress were enriched for those related to transport and iron homeostasis (Table 4 and Table 11). In contrast, those proteins that showed increased packaging into OMVs upon stress revealed no significant enrichment in any GO biological process category (Table 4).

Table 4: Preferentially retained OM-associated proteins are enriched in transport and iron homeostasis GO categories

GO biological process	Preferentially retained proteins		Preferentially exported proteins	
	Fold Enrichment	P-value	Fold Enrichment	P-value
Siderophore transmembrane transport	90.9	3.52E-10	<0.01	1.00E00
• **iron ion transmembrane transport**	70.7	3.83E-11	<0.01	1.00E00
• **siderophore transport**	60.6	3.41E-12	<0.01	1.00E00
Gram-negative-bacterium-type cell outer membrane assembly	45.6	3.36E-06	<0.01	1.00E00
Bacteriocin transport	45.4	6.95E-05	<0.01	1.00E00
Protein localization to membrane	21.6	4.69E-04	11.0	9.08E-02
Iron ion homeostasis	19.4	7.70E-06	<0.01	1.00E00
Lipid transport	18.9	8.63E-06	<0.01	1.00E00

One characteristic in common for this preferentially retained set of proteins is their interaction with cell envelope components such as peptidoglycan (PG) and/or IM components such as the TonB/ExbBD and AcrAB systems (Zgurskaya and Nikaido 1999; Husain, Humbard, and Misra 2004; Pawelek et al. 2006; Shultis et al. 2006) (Fig. 1). This discovery suggested a mechanistic basis for cargo retention: protein connections with other cell envelope components reduce entry into OMVs, and oxidative stress exacerbates such mechanistic differences in cargo availability.

3.4 Implementing OmpA as a model protein for testing tethering as a mechanism for OMV incorporation or exclusion of proteins during stress

In order to test our mechanistic hypothesis of cargo selectivity, we used two versions of the integral protein OmpA to model envelope-tethered and untethered OM proteins, for several reasons. OmpA is one of the most abundant OM proteins in *E. coli* with an eight-stranded β-barrel N-terminal domain and a soluble C-terminal domain located in the periplasm (Ortiz-Suarez et al. 2016) which can non-covalently bind to PG (Park 2011). Both domains are connected by a flexible 15-amino acid linker (Ortiz-Suarez et al. 2016). OmpA has been shown to influence vesicle production by modulation of cell envelope connectivity and a deletion of this protein resulted in increased vesiculation in *E. coli* (Schwechheimer, Kulp, and Kuehn 2014), *Vibrio cholerae* (Valeru et al. 2014) and *Salmonella enterica* (Deatherage et al. 2009) (Fig. 26). OmpA has also been previously employed to isolate OMVs (Alves et al. 2017) and to direct loading into OMVs through protein fusions (Alves et al. 2015; Alves, Turner, and Walper 2016; Alves et al. 2016) due to its abundance in the OM and OMVs.

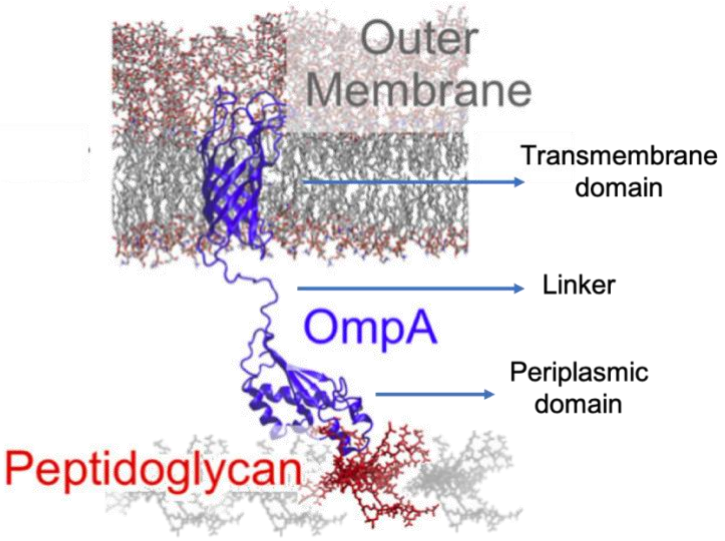

Figure 26: Overview of OmpA structure.

The N-terminal domain of OmpA is an eight-stranded β-barrel embedded in the OM. A 15-amino acid linker joins the N-terminal domain to the C-terminal periplasmic domain which interacts with PG. Image adapted from: (Samsudin, et al. 2016).

Notably, both the epitope-tagged constructs we used of full-length OmpA (encoded by pGI10) and truncated OmpA lacking the PG-binding domain (encoded by pGV30) have been previously determined to be stable and folded properly in the membrane (Verhoeven, Dogterom, and den Blaauwen 2013). We confirmed that this was also the case in our assay conditions (Fig. 27). Critically, these features allowed us to avoid issues of membrane and cargo instability commonly complicating the accurate evaluation of packaging of nonnative OMV cargo independent of folded state. Further, in *S. enterica* the periplasmic domain of OmpA has also been implicated in the modulation of the open/closed states of OmpA during oxidative stress to regulate

membrane permeability (van der Heijden et al. 2016), thus its behavior upon oxidative stress is of physiological interest.

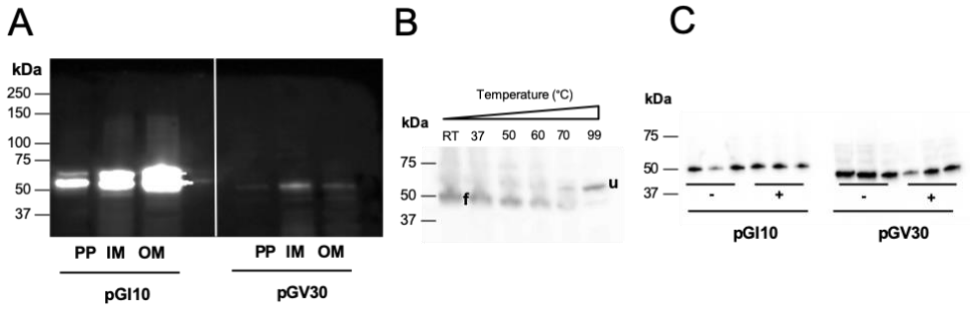

Figure 27: Proper localization and folding of tagged OmpA constructs in the OM and OMVs.

(A) Subcellular fractions (equal concentrations of protein) were separated by SDS-PAGE and detected by immunoblotting. PP, periplasm; IM, inner membrane; OM, outer membrane. **(B)** OM fractions from the pGV30 strain were resuspended in 5X SDS-PAGE sample buffer and either not heated (RT), or heated at 37°C for 5 min, at 50°C, 60°C and 70°C for 15 min, or at 99°C for 10 min. and detected by immunoblotting. Folded and unfolded versions of the protein are indicated by f- and u- next to the bands, respectively. **(C)** OMVs purified from the indicated mock-treated (-) and 1 mM H_2O_2-treated (+) BL21 cultures expressing the OmpA constructs were analyzed in triplicate by SDS-PAGE without boiling and detected by immunoblotting. The location of the OmpA construct bands at ~50 kDa indicates they were in a folded state in the OMVs.

3.5 Selective packaging of truncated OmpA compared to full-length OmpA into OMVs is exacerbated with oxidative stress

We first tested whether protein interaction with the cell wall was a potential mechanism for OM protein sorting into OMVs. The data showed a significant preferential packaging of the truncated version of OmpA into OMVs in comparison with the full-length version of the protein (Fig. 28B). Using treatment conditions verified to

maintain membrane integrity (Fig. 28A), we further noted a significant increase truncated OmpA selectivity into OMVs under oxidative stress (Fig. 28C). These data suggest that protein packaging into OMVs is controlled by physical tethering of the proteins to cell envelope components and that oxidative stress exacerbates this effect.

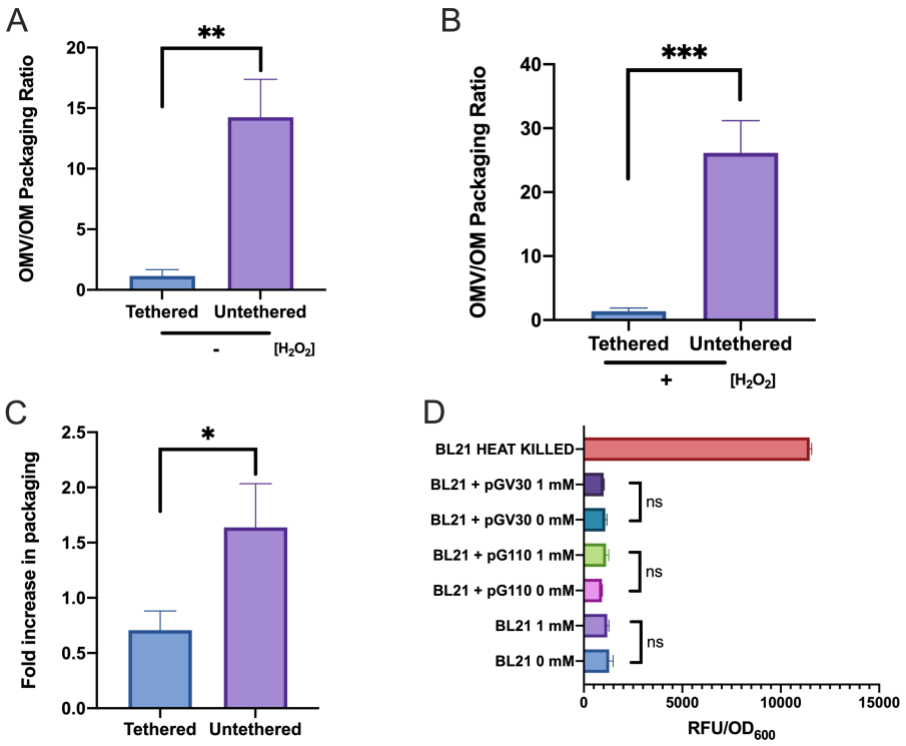

Figure 28: Selective packaging of truncated OmpA compared to full-length OmpA into OMVs is exacerbated with oxidative stress.

Packaging ratios (OMV:OM) for full-length OmpA and truncated OmpA were determined by immunoblotting for untreated BL21/pGI10 and BL21/pGV30 cultures, respectively for **(A)** unstressed cultures and **(B)** stressed cultures. **(C)** OMV:OM packaging ratios for the full-length and truncated OmpA constructs in unstressed cultures from part A was compared to that for 3h H_2O_2-treated cultures and fold-change calculated. (n=6 for pGI10, n=5 for pGV30). **(D)** Relative fluorescence (RFU) normalized by OD_{600} of cultures assayed with Sytox Green at 3 h after treatment with the indicated H_2O_2 concentrations. HK, heat-killed cell control (n=3). Error bars are SEM. P-values according to the Student's t test: * $p \leq 0.05$, ** $p \leq 0.01$, *** $p \leq 0.001$; ns, not significant.

3.6 Discussion

The observed significant preferential retention of OM integral proteins over lipoproteins under oxidized conditions led us to hypothesize that distinct protein topology within the envelope might be a general determinant for retention or export. Specifically, most OM lipoproteins that were unlikely to be engaged with other envelope components were significantly enriched in the exported fraction whereas the integral OM proteins discovered to be more significantly retained in the cells in our study were mostly iron transporters that are known to associate with cell wall and IM components (Tables 3, 4 and 11). By using the two OmpA constructs that differ in their ability to bind the cell wall, we were able to test this theory.

The data showed that truncated version of OmpA was significantly more packaged than the full-length version under unstressed conditions (Fig. 29A). We acknowledge the limitations of this evaluation, as we grossly simplified the OM cargo into two topological classifications, "tethered vs untethered," to model the difference between OM lipoproteins and integral OM proteins. Nevertheless, these data support a mechanism wherein OMV budding events occur within sites of low membrane anchoring, causing proteins in these sites to be incorporated as OMV cargo, whereas integral proteins that are engaged with components of the envelope are retained (Fig. 29B). Our experimental results also support two exclusively proteomic studies. Lappann et al. found that constitutively-produced *Neisseria meningitidis* contained a relatively low

abundance of membrane-anchoring proteins compared to the OM (Lappann et al. 2013). Additionally, a study on *Porphyromonas gingivalis* OMVs showed that proteins with an OmpA peptidoglycan-binding motif and TonB-dependent receptors were preferentially retained in the OM (Veith et al. 2014). Notably, for some OM-associated proteins, there are changes in tethering during stress, and thus this selective export/retention mechanism can be exacerbated upon environmental changes (Fig. 29C).

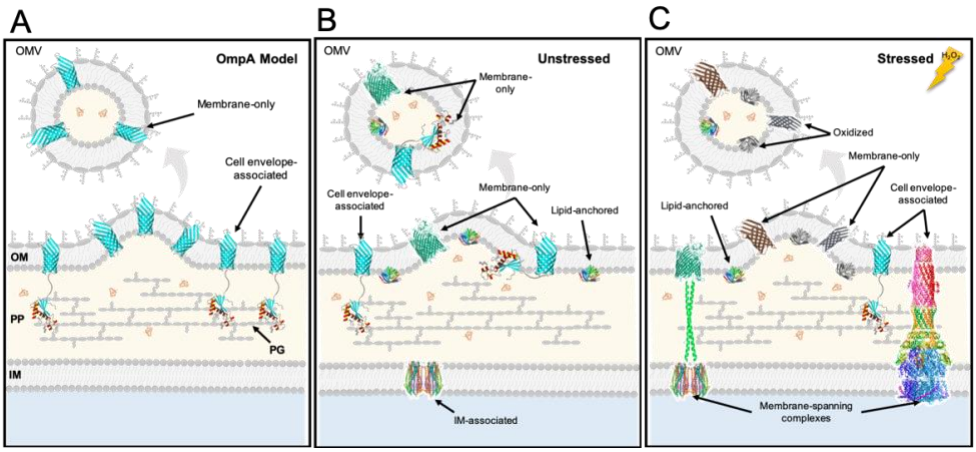

Figure 29: Summary for the selective OMV packaging of untethered cargo into OMVs in unstressed and stressed conditions.

(A) Results from studying the packaging of OmpA constructs revealed that cell envelope-associated (full-length) cargo tend to be retained whereas membrane only (truncated) cargo tend to enter OMVs. Results from studying selective native cargo OMV packaging during unstressed **(B)** and stressed **(C)** conditions revealed that the ability of proteins to tether to the cell envelope is a determinant for incorporation as OMV cargo. Integral OM proteins engaged in cell envelope complexes which increase cellular efflux and nutrient import are preferentially retained in the membrane after stress, maybe whereas oxidized proteins as well as untethered OM proteins will be preferentially exported into OMVs. OM, outer membrane; IM, inner membrane; PP, periplasm; PG, peptidoglycan. OmpA structure from (Ishida, Garcia-Herrero, and Vogel 2014); AcrAB-TolC by (Wang et al. 2017); LolB (lipoprotein), PDB 1IWM; TonB extensions modeled from PDB 1JCD; ExbB/ExbD from PDB 5ZFV; FhuA from PDB 2GRX; OmpX from PDB 1QJ8.

4. Materials and methods

4.1 Culture conditions

Luria Bertani (LB) broth cultures (750 mL) of ETEC strain H10407 (ATCC 35401) were inoculated with 3 mL of overnight culture and grown to stationary phase (37ºC, 200 rpm, ~16 h). Cells were pelleted (3,500 x g, 8 min, 20°C), resuspended in 750 mL fresh LB, either with or without hydrogen peroxide (H_2O_2, 20 mM), and cultures incubated for another 3 h (37ºC, 200 rpm). This procedure leads to cultures considered to be in "pseudo-stationary phase" since stationary phase cells resuspended in fresh media is acknowledged to be slightly different from stationary cultures in their original spent media but is necessary to rid the media of OMVs produced in earlier phases of growth. LB broth cultures (250 mL) of BL21 constructs were inoculated with 1 mL of overnight culture and grown to stationary phase overnight at 37°C. Cells were pelleted (3,500 x g, 8 min, 20°C), resuspended in 250 mL fresh LB, either with or without H_2O_2 (1 mM), and cultures incubated for another 3 h (37ºC, 200 rpm).

4.2 Sytox Green sensitivity assay

Untreated and peroxide-treated ETEC or BL21 construct cultures were centrifuged and resuspended in 10 mM Tris-HCl buffer, pH 8. Sytox Green (Thermofisher) (18 μL of a 0.1 mM solution) was added to 1 ml of the bacterial suspensions and fluorescence assessed at 500nm excitation/550nm emission. Heat killed

bacteria (100°C, 10-60 min) from untreated ETEC or BL21 cultures were used as a positive control.

4.3 OMV isolation

OMVs were isolated from the untreated and peroxide-treated cultures as previously described (Horstman and Kuehn 2000). Briefly, cells were centrifuged (10,000 x g, for 10 min, 4°C) and supernatants were saved. Supernatants were filtered using 0.45 μm membrane filters (Millipore) and OMVs in the sterile supernatants were pelleted (38,400 x g, 3 h, 4°C). The OMV-containing pellets were washed by resuspending in Phosphate Buffered Saline (PBS) (10 mM dibasic phosphate, 137 mM NaCl, 2.7 mM KCl pH 8.0) and re-pelleted (91,149 x g, 1 h, 4°C).

4.4 OM isolation

Untreated and peroxide-treated ETEC cultures were pelleted (10,000 x g, 4°C, 10 min) and cells resuspended in PBS containing 1 mg/mL of freshly prepared lysozyme from a stock solution of 10 mg/mL in 10 mM Tris-HCl, pH 8.0. Bacteria were then lysed by French press twice at 10,000 psi, and saved for further purification.

Untreated and treated BL21 construct cultures were pelleted (4575 x g, 20°C, 10 min) and cells resuspended in 20 mM Tris-Cl, 20% sucrose, 5 mM EDTA, pH 8.0. 100 uL of Lysozyme (15 mg/mL) was added, and the cells were incubated on ice for 40 min. After the incubation, 150 mM $MgCl_2$ was added, and the cells were pelleted (4575 x g, 20°C, 10 min). The cell pellet was then resuspended in 10 mM Tris, pH 8.0 and sonicated

(7 rounds of 15s pulses at 80% amplitude followed by 15s of cooling). Cell fragments were pelleted by centrifugation (4575 x g, 15 min, 4°C) and the supernatant was removed. Membranes were pelleted from the supernatant by centrifugation (40,000 x g, 1 h 4°C). The membrane pellet was washed with 10 mM Tris, pH 8.0, resuspended in dH_2O, and membranes fractured by freezing at -80°C and thawing at room temperature. The membrane suspension was then mixed 4:5 with Sarkosyl solution (1.67% Sarkosyl and 11.1 mM Tris, pH 8.0) and incubated at room temperature for 20 min. The OM fraction was pelleted by centrifugation (40,000 x g, 90 min, 27°C), washed in 10 mM Tris, pH 8.0, and resuspended in PBS.

4.5 Periplasm isolation

For quantification of periplasmic protein content after SDS-PAGE, cultures of ETEC cells were grown overnight, cells were pelleted (4575 x g, 20°C, 10 min), resuspended in fresh LB, either with or without H_2O_2 (20 mM), and cultures incubated for another 3 h (37ºC, 200 rpm). Untreated and treated cultures were spun down (4575 x g, 20°C, 10 min) to pellet cells. Cells were diluted to the same OD_{600} and resuspended in half of the original culture volume with 2 mg/mL of polymyxin B in PBS (pH 8.0). Cultures were shaken gently (50 rpm) at 37°C for 1 hour. Spheroplasts were pelleted by centrifugation (4575 x g, 20°C, 10 min) and the supernatant was collected as the periplasmic fraction.

4.6 OMV quantification

For protein-based quantitation, 10 μL of each OMV sample in PBS was incubated for 10 min with 300 μL of Bradford reagent (Thermo Scientific) and then absorbance at 595 nm was measured. For lipid-based quantitation, 20 μL of each OMV sample was incubated with 20 μL of 100μg/ml FM4-64 (Molecular Probes) and incubated at 37°C for 10 min. PBS alone was used a negative control. Protein and lipid measurements were normalized to OD_{600}.

4.7 OMV and OM sample purification and preparation for proteomics

Pelleted OMVs and OM fractions were adjusted to 45 and 36% (v/v) iodixanol (Optiprep, Greiner) by the addition of Optiprep in HS buffer (10 mM HEPES, pH 7.4; 150 mM NaCl) in a total of 0.5 mL, loaded in the bottom of a 12.5 mL ultracentrifuge tube (Beckman) and layered with decreasing percentages of OptiPrep/HS (1 mL of a 40% concentration, 1 mL 35%, 3 mL 30%, 3 mL 25%, and 2 mL 20%). Samples were centrifuged (280,755 x g, 18h, 4°C), and fractions were removed sequentially from the top of the gradient. The iodixanol was removed by dilution in PBS followed by two rounds of high-speed centrifugation (91,149 x g, 1 h, 4°C), and the pellets were resuspended in PBS. Fractions were separated by SDS-PAGE and proteins detected using Ruby Stain. Fractions enriched in outer membrane proteins (OmpF/C and OmpA) were selected for proteomic analysis.

4.8 Proteomic analysis

See supplementary materials for sample preparation, data collection and analysis performed by Duke Core proteomics facility. For annotation of proteomic data, all protein sequences were blasted using the UniProt server (UniProt Consortium 2018) and matched to *E. coli* K12 strain homologues based on 90-100% homology. Subcellular localizations and information on topology and function were obtained from EcoGene (Zhou and Rudd 2013), EcoCyc (Keseler et al. 2017), MetaCyc (Caspi et al. 2018), and PSORTb (Yu et al. 2010) (Tables 9 and 10).

From the quantitative proteomic data, we determined for which proteins there was at least a 2-fold decrease or increase in packaging (OMV/OM ratio) in H_2O_2 untreated (-) and treated (+) conditions (Table 3, columns 2 and 4, respectively). We also determined which OM-associated proteins displayed a difference in packaging of at least 2-fold between the treated and untreated conditions, |OMV(+):OM(+) - OMV(-):OM(-)| > 1 (Table 3, Column 5) and gene ontology (GO) analysis was performed on these increased ("up") and decreased ("down") groups to identify significant enrichment of particular biological processes (Ashburner et al. 2000); (Table 11). The OM-associated proteins that changed in concentration at least 2-fold in the OM samples for treated (+) compared with untreated (-) conditions was also determined (Table 3, column 6).

4.9 Statistical analysis and model for protein sorting from proteomic dataset

To estimate the effect of the treatment on the protein packaging ratio (OMV:OM) and whether the effect is associated with protein type (lipoprotein vs integral protein), we implemented a Bayesian hierarchical model. Our statistical model contains parameter β that describes how the global protein packaging ratio (y) changes with treatment (x), namely, the impact the treatment has on the $\log_2$ of the ratio. We also have a random effect, α, for each individual protein (accounting for the different base levels of protein expression). In Bayesian statistics we represent our prior beliefs about a parameter in terms of a probability distribution on that parameter, called a prior. After observing data, we can update our beliefs and obtain a new probability distribution, called a posterior that represents a combination of our prior beliefs and the observed data. In this case our prior for the variance of our random effect is a t-distribution and we use an improper uniform prior for β (prior does not integrate to 1 but gives a proper distribution for the posterior). While the posterior has no analytic form (a simple equation), we can draw samples from the posterior using Markov Chain Monte Carlo. From these samples we can infer properties such as mean, median, credible intervals etc., about our posterior distribution. We implement this using the brms R package (Bayesian Regression Models using Stan) (Bürkner 2017, 2018). The exact sampling method they use to obtain these posterior samples is provided in their documentation. The same statistical analysis approach was used on the localization dataset to compare

abundances of proteins from different cellular compartments in OMVs from treated (+) vs untreated (-) cultures and to determine functional enrichment of periplasmic proteins (with classifiers: cell wall metabolism, chaperone, hydrolase, part of ABC transporter, redox, or other) in OMVs from treated (+) vs untreated (-) cultures.

4.10 Statistics for non-proteomic data

For direct sample size comparison, the paired t-test was used, and for fold comparison, the unpaired, all using Prism 8 software. The T-test value of ≤0.05 was considered statistically significant. The number of times each experiment was repeated (n) is indicated in the figure captions.

4.11 Gene expression data from the GEO database

We mined the GEO database (Edgar, Domrachev, and Lash 2002; Barrett et al. 2013; Clough and Barrett 2016) to obtain gene expression profiles under stress for the OM proteins, lipoproteins and periplasmic proteins in our study. Gene expression 60 min after transition from anaerobic to aerobic conditions was used from the GSE4735 dataset (Partridge et al. 2006).

4.12 Detection of carbonyl-modified proteins

The Protein Carbonyl Assay Kit (ab178020, Abcam) was used to detect oxidized proteins in OMV and pelleted whole cell (4575 x g, 20°C, 10 min) samples. Total protein was extracted from the samples from untreated and treated cultures and oxidized proteins were derived according to manufacturer instructions. Derived samples were

separated using SDS-PAGE and immunoblotted using the anti-DNP antibody provided. SuperSignal West Pico PLUS Chemiluminescent Substrate (Thermo Fisher Scientific 34577) was used to detect the derivatized oxidized proteins. FIJI (ImageJ) software was used to calculate lane densities.

4.13 qRT-PCR

Cultures of ETEC cells (25 mL) were grown overnight, cells were pelleted (4575 x g, 20°C, 10 min), resuspended in fresh LB, either with or without H_2O_2 (20 mM), and cultures incubated for another 3 h (37ºC, 200 rpm). After 3h, cells were pelleted by centrifugation (4575 x g, 20°C, 10 min) and RNA was extracted using RNeasy kit (QIAGEN) according to the manufacturer's instructions. cDNA was synthesized with High-Capacity cDNA Reverse Transcription Kit (Applied Biosystems 4368813) and quantitative real-time PCR reactions of the listed genes were performed using SYBR Select Master Mix (Applied Biosystems 4472908) in the Applied Biosystems StepOne-plus or QuantStudio 3 Real-time PCR System, following the manufacturer's instructions. See Table 5 for primers synthesized (Eurofins) and used for analysis. Each sample was assayed in triplicate with wells with no cDNA used as negative control. Relative gene expression quantifications were calculated using the comparative Ct method with 16S as endogenous control using primers as described (Chakravorty et al., 2007). Fold expression changes were determined using the formula 2-ΔΔCt.

Table 5: qRT-PCR primers used in this study

Seq Name	Seq 5' to 3'	Reference
LEFT_1_PAGP	CTGTCGCGTTGGGATGAAAA	this study
RIGHT_1_PAGP	AATTCCAGTTATCGCGTGCC	this study
LEFT_1_MIPA	CTTACTGGTCGCCGCTTTAC	this study
RIGHT_1_MIPA	AGGCCATATCCCAGACGATG	this study
LEFT_1_RCSF	GACTCTTGCCAGGCCTCTAA	this study
RIGHT_1_ RCSF	GCCGTAATGTTAAGCGCAGA	this study
LEFT_1_NLPD	GGAAGCCCAAAATTCACCGT	this study
RIGHT_1_ NLPD	TTTGCGGTTGTTGAGTAGCC	this study
LEFT_1_RBSB	GAACCTGTTGACCGCTCATC	this study
RIGHT_1_ RBSB	CGCTGCTAGTTTGCCATCAT	this study
LEFT_1_YEJA	CGCTGGAATTTCGACACCAT	this study
RIGHT_1_ YEJA	TCCTGGGCTGATTCGTTCTT	this study
LEFT_OMPA	GGCCACTCCGAAAGATAACA	this study
RIGHT_OMPA	ACGGCATACGACCTAACCAG	this study
LEFT_TOLC	TTTTAACGTGGGCCTGGTAG	this study
RIGHT_TOLC	CGTTTTTCGGCTTCTTTCAG	this study
LEFT_SILC	GGGTCTGGAGCTCAGCTATG	this study
RIGHT_SILC	GGAGTTGTTCGTACGCCAGT	this study
LEFT_MLTA	GGGTCTGGAGCTCAGCTATG	this study
RIGHT_MLTA	GGAGTTGTTCGTACGCCAGT	this study
16s1_F_V3	CCAGACTCCTACGGGAGGCAG	(Chakravorty et al. 2007)
16s1_R_V3	CGTATTACCGCGGCTGCTG	(Chakravorty et al. 2007)

4.14 Plasmid constructs

His-tagged versions of YfeY, YgdI, PhoE, and TamA were synthesized with codon-optimization for expression in *E. coli* and cloned into the Multiple Cloning Site in the vector pET-23a(+) (Genscript USA Inc.). We relied on the background expression

(inherent leakiness) of the T7 promoter in the pET-23a(+) vector for expression of these constructs. OmpA constructs pGI10 (full length OmpA fused to mCherry) and pGV30 (truncated OmpA fused to mCherry) were generously provided by Dr den Blaauwen from the University of Amsterdam (Verhoeven, Dogterom, and den Blaauwen 2013) (See Fig. 30 and 31, and Table 6 for sequences and references). BL21-AI™ One Shot™ Chemically Competent *E. coli* (Invitrogen C607003) cells were transformed with constructs, and ampicillin was used as marker for plasmid selection. For OmpA constructs, cultures were grown to stationary phase (37ºC, 200 rpm, ~16 h) in the presence of 0.1 mM IPTG added at the start of the culture.

Table 6: Protein constructs used in this study

Construct	Sequence	Details	Plasmid-encoded antibiotic resistance	Reference
pYfeY-His	MKSLRLMLCAMPLMLTGCSTMSSVNWSAANPWNWFGSSTKVSEQGVGELTASTPLQEQAIADALDGDYRLRSGMKTANGNVVRFFEVMKGDNVAMVINGDQGTISRIDVLDSDIPADTGVKIGTPFSDLYSKAFGNCQKADGDDNRAVECKAEGSQHISYQFSGEWRGPEGLMPSDDTLKNWKVSKIIWRRLVPR/GS**HHHHHH**	**Vector:** pET23a(+), in frame with the C-terminal His tag in the plasmid and a thrombin cleavage site (LVPR/GS) added.	Amp	This study
pYgdI-His	MKKTAAIISACMLTFALSACSGSNYVMHTNDGRTIVSDGKPQTDNDTGMISYKDANGNKQQINRTDVKEMVELDQLVPR/GS**HHHHHH**	**Vector:** pET23a(+), in frame with the C-terminal His tag in the plasmid and a thrombin cleavage site (LVPR/GS) added.	Amp	This study
pPhoE-His	MKKSTLALVVMGIVASASVQAA**HHHHHH**V**IEGRV**AEIYNKDGNKLDVYGKVKAMHYMSDNASKD	**Vector:** pET23a(+), in frame with an internal His tag and a Factor	Amp	This study

	GDQSYIRFGFKGETQINDQLTGY GRWEAEFAGNKAESDTAQQKTR LAFAGLKYKDLGSFDYGRNLGA LYDVEAWTDMFPEFGGDSSAQT DNFMTKRASGLATYRNTDFFGVI DGLNLTLQYQGKNENRDVKKQ NGDGFGTSLTYDFGGSDFAISGA YTNSDRTNEQNLQSRGTGKRAE AWATGLKYDANNIYLATFYSETR KMTPITGGFANKTQNFEAVAQY QFDFGLRPSLGYVLSKGKDIEGIG DEDLVNYIDVGATYYFNKNMSA FVDYKINQLDSDNKLNINNDDIV AVGMTYQF	Xa cleavage site added based on the construct from (Van Gelder et al. 1996).		
pTamA-His	MRYIRQLCCVSLLCLSGSAVAAN VRLQVEGLSGQLEKNVRAQLSTI ESDEVTPDRRFRARVDDAIREGL KALGYYQPTIEFDLRPPPKKGRQ VLIAKVTPGVPVLIGGTDVVLRG GARTDKDYLKLLDTRPAIGTVLN QGDYENFKKSLTSIALRKGYFDSE FTKAQLGIALGLHKAFWDIDYNS GERYRFGHVTFEGSQIRDEYLQN LVPFKEGDEYESKDLAELNRRLS ATGWFNSVVVAPQFDKARETKV LPLTGVVSPRTENTIETGVGYSTD VGPRVKATWKKPWMNSYGHSL TTSTSISAPEQTLDFSYKMPLLKN PLEQYYLVQGGFKRTDLNDTESD STTLVASRYWDLSSGWQRAINLR WSLDHFTQGEITNTTMLFYPGV MISRTRSRGGLMPTWGDSQRYSI DYSNTAWGSDVDFSVFQAQNV WIRTLYDRHRFVTRGTLGWIETG DFDKVPPDLRFFAGGDRSIRGYK YKSIAPKYANGDLKGASKLITGSL EYQYNVTGKWWGAVFVDSGEA VSDIRRSDFKTGTGVGVRWESPV GPIKLDFAVPVADKDE**HHHHHH** HHGLQFYIGLGPEL	**Vector:** pET23a(+), in frame with a His-tag on an external loop based on the construct from (Shen et al. 2014).	Amp	This study
pGI10	Full-length OmpA	pTHV037 OmpA-LEDPPAEF-mCherry	Amp	(Verhoeven, Dogterom, and den Blaauwen 2013),
pGV30	Truncated OmpA	pTHV037 OmpA-177-(SA-1)-LEDPPAEF-mCherry	Amp	(Verhoeven, Dogterom, and den Blaauwen 2013)

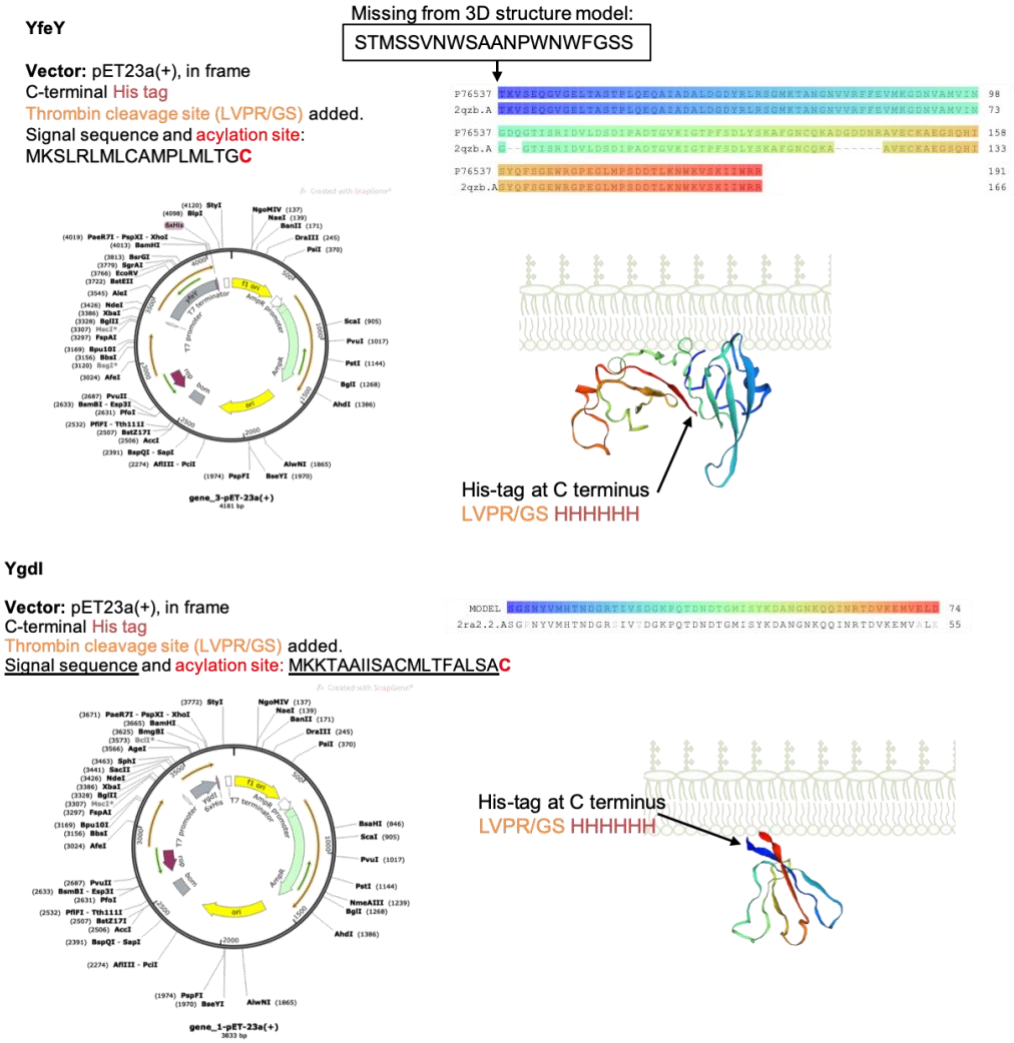

Figure 30: Lipoprotein constructs used in this study.

Features of the construct encoding the C-terminally His_6-tagged lipoproteins are summarized as well as a graphical model of their 3-dimensional structure relative to a membrane, color coded from blue to red, N- to C-terminus, respectively (Bienert et al. 2017).

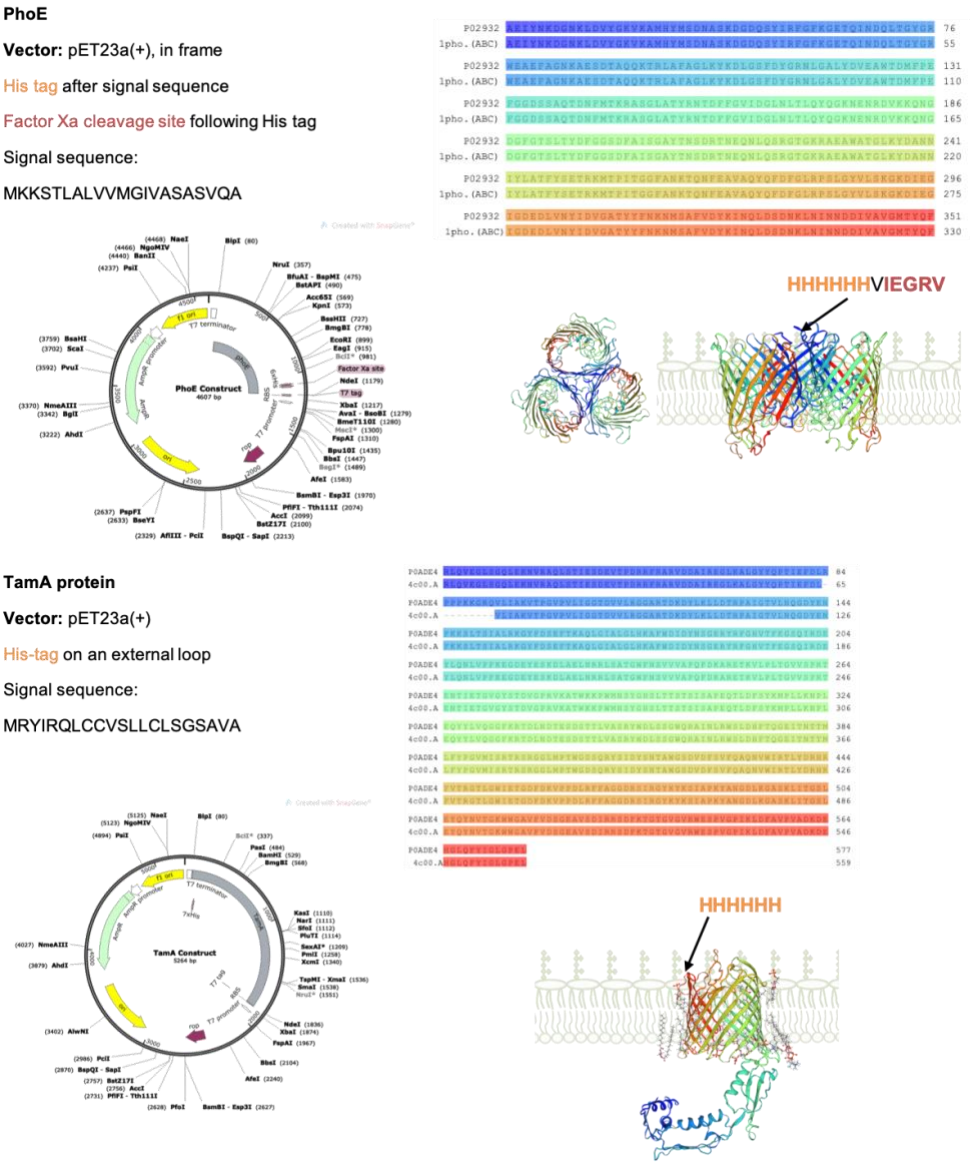

Figure 31: Integral protein constructs used in this study.

Features of the construct encoding the His$_6$-tagged OM proteins are summarized as well as a graphical model of their 3-dimensional structure relative to a membrane, color coded from blue to red, N- to C-terminus, respectively (Bienert et al. 2017).

4.15 Immunoblot for validation of protein packaging into OMVs

OMV and OM samples were separated using Mini-PROTEAN TGX (Tris-Glycine eXtended) Stain-Free Precast Gels (BIORAD) (for detecting YfeY (Fig. 32A), PhoE (Fig. 32C), TamA (Fig. 32D) constructs) or Mini-PROTEAN Tris-Tricine Stain-Free Precast Gels (BIORAD) (for detecting YgdI (Fig. 32B) constructs). Proteins were transferred onto nitrocellulose using Semidry electroblotting OWL System (Thermo Scientific) for 45 min at 200 mA. The nitrocellulose was blocked (5% milk, in TBS-T (Tris-buffered saline with 1% Tween 20), then incubated overnight with primary 6x-His Tag mouse Monoclonal Antibody (Thermo Fisher Scientific MA1-135), followed by three 5 min washes with TBS-T and a 5 min wash of TBS (TBS-T without the Tween). After incubation washes were repeated and membrane was incubated for an hour with IRDye 680RD Goat Anti-Mouse IgG (H+L) (LI-COR 925-68070) (to detect YfeY, YgdI, and PhoE) or Goat Anti-Mouse IgG H&L (Alexa Fluor 680) (ab175775, Abcam) (to detect TamA). The blot was imaged using an Odyssey Imaging System. The fluorescence (RFU) of the protein band was quantified by densitometry using FIJI and normalized using the FM4-64 measurements of the OMV and OM samples. For OmpA constructs, western blotting was performed as described using anti-RFP-HRP conjugated antibody (ab34767). After incubation washes were performed as described, and the nitrocellulose blot was incubated for 5 min with SuperSignal™ West Pico PLUS Chemiluminescent Substrate (Thermo Fisher Scientific 34577). When necessary, samples were diluted so that the

immunoreactive signals would be in the linear range of detection and the RFU values multiplied to account for differences in dilution. The blot was imaged using a c300 Azure biosystems Gel Imaging System.

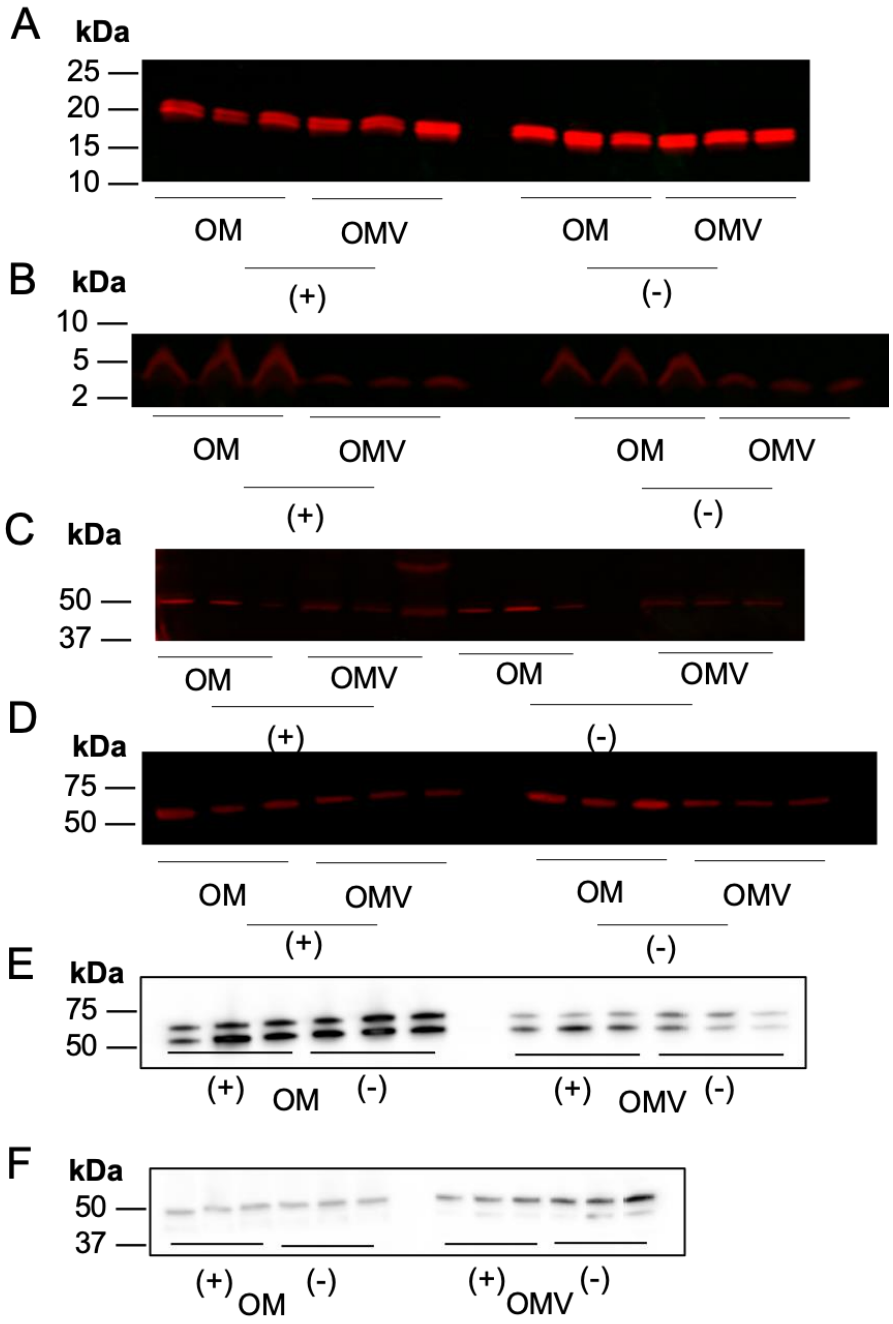

Figure 32: Representative blot for OMV packaging of tagged constructs.

Western blots of **(A)**YfeY, **(B)** YgdI, **(C)** PhoE, **(D)** TamA, **(E)** pGI10, and **(F)** pGV30, in the absence (-), 0 mM or presence (+) of 1 mM of H_2O_2. constructs. in the absence (-) or presence (+) of 1 mM of H_2O_2.

5. Conclusions

The process of OMV secretion has been shown to be beneficial to bacteria. Moreover, studies have shown that OMV cargo selectivity modulate OMV function and contributes to bacterial virulence and survival during stress.

In this dissertation, I sought to investigate changes in *E. coli* OMV cargo during oxidative stress and found that stress induced a differential sorting among OM-associated proteins. Lipoproteins were preferentially exported into OMVs while integral proteins remained the membrane. These changes in protein sorting were independent of gene expression. We validated these initial ETEC findings in an BL21 *E. coli* strain and subsequently tested a mechanism based on physical protein tethering to the cell wall using OmpA as a model protein. Our results showed that physical tethering to the cell wall modulated cargo selection in unstressed conditions and that this effect is exacerbated during stress.

Envelope structure has been found to impact levels OMV production, and the current study contributes to this model that changes in envelope structure also affect OMV cargo packaging. Gram-negative bacteria can modulate vesiculation by altering PG-OM cross-linking via localized modulation of PG degradation and synthesis (Schwechheimer, Rodriguez, and Kuehn 2015). Accumulation of PG or LPS fragments led to an increase in vesiculation by pushing the OM outwards causing cargo to be incorporated in sites where the OM had decreased levels of cell wall-bound Lpp

(Braun's lipoprotein) (Schwechheimer, Kulp, and Kuehn 2014). Whether these effects are coordinated with cargo selectivity remains to be explored.

There is likely to be a direct, evolved relationship between the functional cellular benefits and the envelope tethering-dependent differential packaging classes of OM-associated components into OMVs. As mentioned earlier, OMVs benefit cells as a stress response by enabling the elimination of toxic, damaged envelope components (McBroom and Kuehn 2007; Schwechheimer and Kuehn 2013), and this was further corroborated by findings here that proteins containing residues more susceptible to oxidative damage material were the enriched in the OMVs. However, we considered whether the cell also benefited from the inverse situation - increased retention of cargo important to the cell with reduced levels of export via OMVs. Several results support this potentially functional benefit of cargo selectivity. We found the packaging differential between the full-length and truncated OmpA further increased upon stress, and we note that OmpA plays a role in oxidative response and that beneficial role coincides with PG association (van der Heijden et al. 2016). In addition, of the 23 integral OM proteins whose exclusion as OMV cargo increased after oxidative stress, nearly all were also measured in higher abundance in the OM after the stress (highlighted in blue, Table 3, columns 5 and 6). Therefore, the cell preferentially retained the subclass of OM proteins that are transporters and these are important in nutrient acquisition and export which may be needed to maintain cellular homeostasis during or after oxidative stress.

The cargo that shifted to become more released as OMV cargo upon oxidative stress were mainly OM lipoproteins that also became less abundant in the OM after the stress (15/21, highlighted in orange, Table 3, columns 5 and 6). Whether increased OM lipoprotein content would be harmful to the cells following oxidative stress, or whether this shift in OM abundance was a repercussion of spatial constraints from having an increased retention of the integral OM proteins remains unclear. In sum, the results support our model that selective cargo retention *vs*. release in OMVs resulting from differences in envelope tethering can generate changes in the OM composition which could be beneficial to the cell, particularly in response to an environmental stress. This is consistent with data from our secondary challenge assay which showed that oxidative stress conferred a fitness advantage to cells to a second challenge of H_2O_2.

Sudden stresses, such as changes in environmental conditions are a common occurrence for bacteria. ETEC, for instance, is known to colonize the surface of fruits and vegetables and is present in environmental water; however, once in a mammalian host, it is suddenly exposed to acidic and alkaline shifts in the gastrointestinal tract, shifts in carbon sources, and attack by competing bacteria as well as the host immune response (Gonzales-Siles and Sjöling 2016). The outermost barrier against stress is the cell envelope, and during changing conditions bacteria are forced to not only metabolically adapt, but also change this barrier to survive. While transcriptional responses play a role, we now add that the cell envelope connectivity can contribute to the ability of

bacteria to adjust to drastic or rapid changes in the environment by influencing cellular retention and OMV-mediated protein export. Insight into general biological principles gained in studies like this can likely be useful in optimizing the engineering of biologically active nanoparticles and membrane vesicles and OMV-based vaccines for a variety of applications pertinent to ecology and human health.

5.1 Future directions and impact on the field

While we uncovered one potential mechanism driving OMV cargo incorporation during stress, we recognize it might not be the only mechanism determining OMV cargo selection. Further studies are necessary to unravel more aspects of OMV cargo selection during oxidative stress. Future directions for this study can focus on exploring differences in cargo selection for periplasmic content. Establishing a comparison to whole cell periplasmic content to determine cargo enrichment might pose a challenge. However, tagged protein constructs have previously been employed to test packaging of periplasmic cargo (Schwechheimer and Kuehn 2013; McBroom and Kuehn 2007). Interestingly, a similar mechanism for cargo selection based on physical tethering to cell wall components has been hypothesized for *N. menigitidis* (Lappann et al. 2013) and *P. gingivalis* (Veith et al. 2014). Therefore, we can also expand this study by investigating whether this mechanism is ubiquitous across bacterial strains and stressors.

Overall, this dissertation examines the impact a shift to oxidative stress conditions have on OMV composition and protein selectivity and broadens the

knowledge on how *E. coli* modulates its OM composition during stress. While many studies have observed OMV protein selectivity under steady state conditions, this study is the first to show that a differential OM-associated protein sorting based on protein classes occurs during a shift in environmental conditions. Furthermore, this dissertation describes the first study to not only describe, but test a mechanism for OMV protein sorting using a model protein. I also believe this study significantly contributes to the field of bacterial vaccine bioengineering by providing important insight into the process by which proteins can be selected into vesicles.

5.2 Moving the OMV field forward

Despite the many studies highlighting the importance of bacterial vesicles in bacterial physiology and in the host-pathogen interaction, many questions still remain. For instance, what other mechanisms govern OMV production? What type of energy is used to generate vesicle scission? Is a specific, conserved (set of) protein(s) responsible and needed for this process? Does lipid transport and biogenesis play a role in OMV secretion? For the OMV field to move forward and answer these pressing questions, I propose several research routes. Firstly, more high-throughput vesicle assays need to be performed. Assaying mutant libraries for vesicle production in a variety of bacterial strains can allow for identification of genes involved in vesiculation and metabolic pathways related to vesicle secretion. This has already been done in *E. coli* and *S. enterica* (Kulp et al. 2015; Nevermann et al. 2019), however these genetic screens were performed

differently. Therefore, secondly, I believe it is also important that the field establishes universal protocols including OMV isolation and packaging characterization methods. Because environmental conditions greatly influence vesicle cargo, function, and quantity in bacteria, without standardization of protocols, results from different research groups are difficult to compare. Ideally, for any vesicle-producing bacterium, we would need: baseline OMV production, and OMV properties characterized under standard growth conditions as well as under varying environmental conditions. These results coupled with genome-wide assessments of vesicle production would greatly inform OMV studies and provide insights into the mechanistic nuances of OMV secretion.

Appendix A

Abbreviations used in this text

CFU: colony forming units

CYT: cytoplasm

ETEC: enterotoxigenic E. coli

IM: inner membrane

LB: Luria-Bertani broth

LPS: lipopolysaccharide

OM: outer membrane

OMP: outer membrane protein

OMV: outer membrane vesicle

PBS: phosphate-buffered saline

PG: peptidoglycan

PP: periplasm

RFU: relative fluorescence unit

ROS: reactive oxygen species

SDS-PAGE: sodium dodecyl sulfate-polyacrylamide gel electrophoresis

TBS: tris-buffered saline

WT: wildtype

Appendix B

Supplementary tables

Table 7: Summary of recent proteomic analyses of OMV composition[1]

Species	Size (nm)[2]	Growth Phase[3]	Medium	Proteome[4]	Functional Analysis[5]	Immunological Activity Analysis[6]	Reference
Aeromonas hydrophila ATCC 7966	90 - 100	stationary	Tryptic soy agar	211	✓	✓	(Avila-Calderón et al. 2018)
Acinetobacter baumanii Clinical isolate A38	30 - 140	early stationary	LB broth	148	✓	✓	(Li et al. 2015)
A. baumanii Clinical isolate 5806				138	✓	✓	
A. baumanii ATCC 19606	40 - 70	log	LB broth	ND		✓	(Jun et al. 2013)
A. baumanii ATCC 17978	ND	in host	Mouse pneumonia model	112		✓	(Jin et al. 2011)
A .baumanii Clinical isolate DU202	20 - 160	early stationary	LB broth	132	✓		(Kwon So 2009)
A. radioresistens Clinical isolate MMC5	10 - 150	early stationary	LB broth	71	✓		(Fulsundar et al. 2015)
Bacteroides fragilis NCTC 9343	30 - 80	stationary	Supplemented BHI, or supplemented basal medium	115	✓		(Elhenawy, Debelyy, and Feldman 2014)
B. thetaiotaomicron VPI-5482	ND	stationary		21			
Toxigenic *B. fragilis* (ETBF)	30 - >90	log	Blood agar plates	140			(Zakharzhevskaya et al. 2017)
Nontoxigenic *B. fragilis* (NTBF)				39			
638R *B. fragilis*	ND	late-exponential	MDM broth	23			(Ferreira et al. 2018)

Bortedella pertussis Tomaha I-derivative BP536	70 – 230	stationary	Supplemented Stainer-Scholte medium	ND	✓	✓	(Gasperini et al. 2018)
B. pertussis Tomaha I-derivative BP537							
Campylobacter jejuni ATCC 700819	50	mid log	BHI	134			(Jang et al. 2013)
Escherichia coli MG1655	80 - 100	stationary	LB broth	316	✓		(Kulkarni, Nagaraj, and Jagannadham 2015)
E. coli Nissle 1917	20 - 60	early log	LB broth	192			(Aguilera et al. 2014)
E. coli DH5α	20 - 40	stationary	LB broth	141			(Lee et al. 2007)
EHEC O157:H7 5791/99	125.3 – 180.8	stationary	LB broth	59	✓		(Bielaszewska et al. 2017)
EHEC O157:H- 493/89	92.1 – 159.3	stationary	LB broth	66	✓		
Delftia sp. Cs1-4*	ND	biofilm	Defined mineral salts medium	19			(Shetty et al. 2011)
Francisella novicida ATCC 15482	43 - 125	stationary	0.1% l-cysteine HCl BHI broth	416	✓		(Pierson et al. 2011)
F. philomiragia ATCC 25015		stationary	Chamberlain's medium	238	✓		
F. noatunensis subsp. *orientalis*	60 - 80	late-stationary	Supplemented Eugon broth		✓	✓	(Lagos et al. 2017)
F. novicida ATCC 15482	50 - 300, OM tubes: 0.3-1.5 μm	log, early stationary	BHI	99, 286	✓	✓	(McCaig, Koller, and Thanassi 2013)
Fusobacterium nucleatum	40 - 110	early stationary	Fastidious Anaerobe Agar or	98			(Liu et al. 2019)

			tryptic soy broth				
Haemophilus influenza Clinical isolate 86-028NP	20 - 200	stationary	BHI	142		✓	(Sharpe, Kuehn, and Mason 2011)
H. parasuis Nagasaki	50 - 200	early stationary	Supplemented BHI (liquid and plate grown)	86 (liquid), 250 (plate grown)		✓	(McCaig et al. 2016)
H. parasuis D74				93 (liquid), 251 (plate grown)			
Helicobacter pylori	50 - 110	early stationary	Blood agar plates of Brucella agar, Brucella broth	306	✓		(Olofsson, Vallstrom, et al. 2010)
H. pylori							
Klebsiella pneumoniae ATCC 13883	20 - 200	early stationary	LB broth	159	✓	✓	(Lee et al. 2012)
K. pneumoniae ATCC 10031	86.54	stationary	LB broth	5		✓	(Martora et al. 2019)
Mannheimia haemolytica serotype S1 strain 89010807N	10 - 20	early stationary	BHI	226		✓	(Ayalew et al. 2013)
Moraxella catarrhalis	50 - 150	stationary	BHI	57	✓		(Schaar, Nordstrom, et al. 2011)
Mycobacterium tuberculosis H37Rv	20 - 250	early stationary	Minimal media	287			(Lee et al. 2015)
M. bovis BCG	40 - 250	10 days	Defined minimal media+	66	✓	✓	(Prados-Rosales et al. 2011)
M. smegmatis				64	✓	✓	
Myxococcus xanthus DK1622 WT	30 - 100	18 hrs in plates Vegetative / developmental cells	CTT medium	107/124			(Kahnt et al. 2010)
M. xanthus	ND	late log	DCY-rich medium	75			(Whitworth, Slade, and Mironas 2015)

Neisseria gonorrhoeae[§]	ND	late log	GCBL Medium[+]	168			(Zielke et al. 2014)
Novosphingobium pentaromativorans	25 -70	exponential	Marine broth	187			(Yun et al. 2017)
Novosphingobium sp. PP1Y	100 – 200	mid- and late-exponential	PPMM or LB broth	17	✓		(De Lise et al. 2019)
Piscirickettsia salmonis	ND	log	AUSTRAL-salmonid rickettsial septicemia broth	452	✓		(Oliver et al. 2017)
Porphyromonas gingivalis W50	60 - 120	log	Supplemented Tryptic soy-enriched BHI broth	151			(Veith et al. 2014)
P. gingivalis ATCC 53978							
P. gingivalis 33277	ND	log	Tryptic soy broth	67			(Mantri et al. 2015)
P. gingivalis W83				70			
P. gingivalis W50	ND	Stationary	Heme Limited / Heme Excess Media	1211			(Veith et al. 2018)
Prochlorococcus MIT9313	70 - 100	mid/late log	Constant light flux conditions, Pro99 media	27			(Biller et al. 2014)
Prochlorococcus MED4	ND			40	✓		
Pseudomonas aeruginosa	~<200 nm	in biofilm	LB broth	76			(Toyofuku et al. 2012)
		stationary		194			
P. aeruginosa PAO1	ND	biofilm (24, 48, and 96 hrs)	Tryptic soy broth	18, 78, 98	✓		(Park et al. 2015)

P. aeruginosa PAO1	50 - 250	early log	Lysogeny broth	338			(Choi et al. 2011)
P. putida KT2440	25 - 75	log	LB broth	243	✓		(Choi et al. 2014)
P. putida KT2440			Minimal medium + 10 mM succinate	359			
P. putida KT2440			Minimal medium + 5 mM benzoate	456			
P. syringae Lz4W	60 - 100	stationary	Antarctic bacterial medium	429	✓		(Kulkarni, Swamy Ch, and Jagannadham 2014)
P. syringae pv. Tomato T1	120 - 125	early stationary	King's broth medium	139			(Chowdhury and Jagannadham 2013)
Rhizobium etli CE3	40 – 100	log and stationary	Succinate - ammonium minimal medium	164			(Taboada et al. 2019)
Salmonella enterica serovar Choleraesuis strain χ3545	100 - 200	Stationary	LB broth	192		✓	(Liu et al. 2017)
Shewanella vesiculosa	25 - 250	late log	Tryptic soy agar	46			(Pérez-Cruz et al. 2013)
Shigella flexneri 2a str	50 - 200	log	Tryptic soy broth	148			(Chen et al. 2014)
Strenotrophomonas maltophilia ATCC13637	ND	early stationary	LB broth	274			(Ferrer-Navarro et al. 2016)
S. maltophilia M30	ND	early stationary		133			
S. maltophilia 44/98 (LMG 26824)	NS	early stationary	LB broth	234			(Devos et al. 2015)
Treponema denticola	ND	late-log	Oral bacteria	942			(Veith et al. 2019)

			growth media				
V. fischeri	>200	stationary	LBS medium				(Lynch et al. 2019)
Xylella fastidiosa strains Temecula1, 9a5c and Fb7	100	stationary	Periwinkle wilt glucose broth	26, 31, 12			(Feitosa-Junior et al. 2019)

[1] From publications in 2010-2020.
[2] Diameter range or average.
[3] Growth phase when OMVs were isolated for analysis.
[4] Total proteins identified in sample, studies where only most abundant were identified are not included in this table.
[5] One or more of the following: OMVs were found to have some activity via supplementation of OMVs to another culture; OMVs conferred some sort of protection (e.g. antibiotic tolerance); OMVs were tested for cytotoxicity.
[6] OMVs elicited immune response (e.g. cytokine secretion) when incubated with mammalian cells.
*Strain is flagella production mutant
[+]See reference for details
[§]Many OMV studies on this bacterium are focused on detergent-derived vesicles and not included in this table.

Table 8: Recent studies were lipid analysis was performed on OMVs and/or DNA presence was detected in vesicle samples.

Species	Lipid Analysis	DNA Presence	Reference
Acinetobacter radioresistens MMC5 strain	✓*		(Fulsundar et al. 2015)
A. baylyi		✓	(Fulsundar et al. 2014)
Ahrensia kielensis		✓	(Hagemann and J. 2013)
Bacteroides fragilis	✓		(Elhenawy, Debelyy, and Feldman 2014)
B. thetaiotaomicron	✓		
Delftia sp. Cs1-4	✓		(Shetty and Hickey 2014; Shetty et al. 2011)
Francisella novicida ATCC 15482		✓	(Pierson et al. 2011)
F. philomiragia ATCC 25015		✓	
Haemophilus influenzae		✓	(Sharpe, Kuehn, and Mason 2011)
Helicobacter pylori	✓		(Olofsson, Vallstrom, et al. 2010)
Kingella knigae		✓	(Maldonado et al. 2011)
Moraxella catarrhalis		✓	(Schaar, Nordstrom, et al. 2011)
Mycobacterium bovis BCG	✓	✓	(Prados-Rosales et al. 2011)
M. smegmatis	✓	✓	
Novosphingobium sp. PP1Y	✓*		(De Lise et al. 2019)
Prochlorococcus sp.	✓	✓	(Biller et al. 2014)
Pseudoalteromonas marina		✓	(Hagemann and J. 2013)
Pseudomonas syringae Lz4W	✓		(Kulkarni, Swamy Ch, and Jagannadham 2014)
Pseudomonas syringae pv. Tomato T1	✓		(Chowdhury and Jagannadham 2013)
Shewanella vesiculosa		✓	(Frias et al. 2010; Pérez-Cruz et al. 2013)
Shigella flexneri 2a str			(Chen et al. 2014)
Vibrio cholerae		✓	(Langlete, Krabberød, and Winther-Larsen 2019)

Table 9: Localization of proteins with 2 or more peptides

Primary Protein Name	Protein Description	Localization
D0Z6S1_ECOH1	Plasmid stable inheritance protein (ParA homolog)	CYT
E3PAF3_ECOH1	KHG/KDPG aldolase [includes: 4-hydroxy-2-oxoglutarate aldolase 2 dehydro-3-deoxy-phosphogluconate aldolase]	CYT
E3PAF5_ECOH1	Glucose-6-phosphate 1 -dehydrogenase	CYT
E3PAF7_ECOH1	Pyruvate kinase	CYT
E3PAG9_ECOH1	Aspartyl-tRNA synthetase - tRNA ligase	CYT
E3PAJ7_ECOH1	Alpha-trehalose-phosphate synthase (UDP-forming)	CYT
E3PAK5_ECOH1	Bacterial non-heme ferritin	CYT
E3PAX1_ECOH1	Uridine phosphorylase	CYT
E3PAX3_ECOH1	Ubiquinone/menaquinone biosynthesis C-methyltransferase	CYT
E3PAY1_ECOH1	3-octaprenyl-4-hydroxybenzoate carboxy-lyase	CYT
E3PAY8_ECOH1	Protoporphyrinogen oxidase - Menaquinone	CYT
E3PB02_ECOH1	Glutamine synthetase	CYT
E3PB03_ECOH1	Putative lipopolysaccharide core biosynthesis GTP-binding protein - TypA/BipA	CYT
E3PB41_ECOH1	Superoxide dismutase	CYT
E3PB48_ECOH1	ATP-dependent 6-phosphofructokinase	CYT
E3PB51_ECOH1	Triosephosphate isomerase	CYT
E3PB55_ECOH1	Universal stress protein	CYT
E3PB58_ECOH1	Glycerol kinase	CYT
E3PB60_ECOH1	Cell division protein	CYT
E3PB61_ECOH1	Regulator of ribonuclease activity A	CYT
E3PB63_ECOH1	ATP-dependent protease ATPase subunit	CYT
E3PB68_ECOH1	50S ribosomal protein L31	CYT
E3PB74_ECOH1	Catalase-peroxidase	CYT
E3PB87_ECOH1	Phosphoenolpyruvate carboxylase	CYT
E3PB98_ECOH1	Transaldolase	CYT
E3PBA3_ECOH1	Chaperone protein	CYT
E3PBB3_ECOH1	30S ribosomal protein S20	CYT
E3PBB6_ECOH1	Isoleucine - tRNA ligase	CYT
E3PBH3_ECOH1	IS2 transposase (InsD7) nucleic acid binding	CYT
E3PBH8_ECOH1	AMP nucleosidase	CYT
E3PBN1_ECOH1	UPF0265 protein	CYT

E3PBQ6_ECOH1	6-phosphogluconate dehydrogenase, decarboxylating	CYT
E3PBQ8_ECOH1	Putative capsular polysaccharide	CYT
E3PBQ9_ECOH1	Capsular polysaccharide	CYT
E3PBR2_ECOH1	Putative UDP-D-galactose:(Glucosyl)lipopolysaccharide-1, 6-D-galactosyltransferase	CYT
E3PBR3_ECOH1	Uncharacterized protein (LPS synthesis)	CYT
E3PBR5_ECOH1	Mannose-1-phosphate guanyltransferase	CYT
E3PBR7_ECOH1	Uncharacterized protein	CYT
E3PBU8_ECOH1	Elongation factor Tu	CYT
E3PBV0_ECOH1	Transcription termination/antitermination protein	CYT
E3PBV1_ECOH1	50S ribosomal protein L11	CYT
E3PBV2_ECOH1	50S ribosomal protein L1	CYT
E3PBV3_ECOH1	50S ribosomal protein L10	CYT
E3PBV4_ECOH1	50S ribosomal protein L7/L12	CYT
E3PBV5_ECOH1	DNA-directed RNA polymerase subunit beta	CYT
E3PBV6_ECOH1	DNA-directed RNA polymerase subunit beta	CYT
E3PBW9_ECOH1	DNA-binding protein HU-alpha	CYT
E3PBY0_ECOH1	Isocitrate lyase	CYT
E3PBZ0_ECOH1	Glucose-6-phosphate isomerase	CYT
E3PC00_ECOH1	Maltose/maltodextrin import ATP-binding protein	CYT
E3PC10_ECOH1	Putative general stress response protein	CYT
E3PC71_ECOH1	Quinone oxidoreductase	CYT
E3PC77_ECOH1	UvrABC system protein A	CYT
E3PC79_ECOH1	Single-stranded DNA-binding protein	CYT
E3PCD2_ECOH1	Fructose repressor	CYT
E3PCD3_ECOH1	Transcriptional regulator	CYT
E3PCD4_ECOH1	Ribosomal RNA small subunit methyltransferase H	CYT
E3PCE7_ECOH1	Cell division protein	CYT
E3PCG4_ECOH1	Pyruvate dehydrogenase E1 component	CYT
E3PCG5_ECOH1	Acetyltransferase component of pyruvate dehydrogenase complex - Dihydrolipoyllysine-residue acetyltransferase component of pyruvate dehydrogenase complex	CYT
E3PCG8_ECOH1	Aconitate hydratase B	CYT
E3PCH5_ECOH1	Hypoxanthine phosphoribosyltransferase	CYT
E3PCH6_ECOH1	Carbonic anhydrase	CYT
E3PCH7_ECOH1	ABC transporter - ATP-binding protein	CYT
E3PCI3_ECOH1	Pantothenate synthetase	CYT
E3PCI4_ECOH1	3-methyl-2-oxobutanoate hydroxymethyltransferase	CYT

E3PCJ3_ECOH1	Poly(A) polymerase I	CYT
E3PCK4_ECOH1	Glutamate-1-semialdehyde 2,1-aminomutase	CYT
E3PCN4_ECOH1	Xylulose kinase	CYT
E3PCN5_ECOH1	D-mannonate oxidoreductase, NAD-binding	CYT
E3PCP1_ECOH1	Fructose-bisphosphate aldolase class 1	CYT
E3PCQ8_ECOH1	Methionine - tRNA ligase	CYT
E3PCV7_ECOH1	Fructose-specific PTS system EIIBC component	CYT
E3PCV9_ECOH1	Putative multiphosphoryl transfer protein	CYT
E3PCX7_ECOH1	50S ribosomal protein L25	CYT
E3PD51_ECOH1	Lysine--tRNA ligase	CYT
E3PD89_ECOH1	Putative type II restriction enzyme Type IIS restriction enzyme Eco57I	CYT
E3PD97_ECOH1	Aspartate ammonia-lyase	CYT
E3PDA0_ECOH1	10 kDa chaperonin	CYT
E3PDA1_ECOH1	60 kDa chaperonin	CYT
E3PDA5_ECOH1	Elongation factor P	CYT
E3PDB2_ECOH1	5'-methylthioadenosine/S-adenosylhomocysteine nucleosidase	CYT
E3PDB6_ECOH1	UPF0325 protein	CYT
E3PDB8_ECOH1	2,3,4,5-tetrahydropyridine-2,6-dicarboxylate N-succinyltransferase	CYT
E3PDC1_ECOH1	30S ribosomal protein S2	CYT
E3PDC2_ECOH1	Elongation factor Ts	CYT
E3PDC4_ECOH1	Ribosome-recycling factor	CYT
E3PDD2_ECOH1	3-hydroxyacyl-[acyl-carrier-protein] dehydratase	CYT
E3PDD3_ECOH1	Acyl-[acyl-carrier-protein]--UDP-N-acetylglucosamine O-acyltransferase (LPS synthesis)	CYT
E3PDD7_ECOH1	Acetyl-coenzyme A carboxylase carboxyl transferase subunit alpha	CYT
E3PDE7_ECOH1	Proline--tRNA ligase	CYT
E3PDL3_ECOH1	Putative acetyltransferase	CYT
E3PDL5_ECOH1	Aminoacyl-histidine dipeptidase - Cytosol non-specific dipeptidase	CYT
E3PDL7_ECOH1	Esterase	CYT
E3PDT2_ECOH1	DNA gyrase subunit A	CYT
E3PDT5_ECOH1	Ribonucleoside-diphosphate reductase	CYT
E3PDW5_ECOH1	1,4-dihydroxy-2-naphthoyl-CoA synthase	CYT
E3PDY2_ECOH1	NADH-quinone oxidoreductase chain L	CYT
E3PDY5_ECOH1	NADH-quinone oxidoreductase subunit I	CYT
E3PDY7_ECOH1	NADH-quinone oxidoreductase	CYT
E3PDY8_ECOH1	NADH-quinone oxidoreductase subunit F	CYT
E3PDY9_ECOH1	NADH-quinone oxidoreductase subunit E	CYT

E3PDZ0_ECOH1	NADH-quinone oxidoreductase subunit C/D	CYT
E3PDZ1_ECOH1	NADH-quinone oxidoreductase subunit B	CYT
E3PDZ2_ECOH1	NADH-quinone oxidoreductase subunit A	CYT
E3PDZ8_ECOH1	UPF0304 protein	CYT
E3PE00_ECOH1	Acetate kinase	CYT
E3PE01_ECOH1	Phosphate acetyltransferase	CYT
E3PE08_ECOH1	Epimerase family protein	CYT
E3PE21_ECOH1	Acetyl-coenzyme A carboxylase carboxyl transferase subunit beta	CYT
E3PE40_ECOH1	RNA-binding protein	CYT
E3PE43_ECOH1	Modulator of FtsH protease	CYT
E3PE45_ECOH1	Adenylosuccinate synthetase	CYT
E3PE46_ECOH1	HTH-type transcriptional repressor	CYT
E3PE47_ECOH1	Ribonuclease R	CYT
E3PE68_ECOH1	30S ribosomal protein S6	CYT
E3PE70_ECOH1	30S ribosomal protein S18	CYT
E3PE71_ECOH1	50S ribosomal protein L9	CYT
E3PE82_ECOH1	FKBP - Type 22 kDa - Peptidyl-prolyl cis-trans isomerase	CYT
E3PE88_ECOH1	2',3'-cyclic-nucleotide 2'-phosphodiesterase	CYT
E3PE89_ECOH1	CysQ protein	CYT
E3PE97_ECOH1	Inorganic pyrophosphatase	CYT
E3PEA2_ECOH1	Fructose-1,6-bisphosphatase class 1	CYT
E3PEA4_ECOH1	UPF0307 protein	CYT
E3PEA6_ECOH1	Putative modulator of DNA gyrase - Metalloprotease	CYT
E3PEB3_ECOH1	Putative endoribonuclease	CYT
E3PEC8_ECOH1	Probable cytosol aminopeptidase	CYT
E3PEN9_ECOH1	NAD/NADP-dependent betaine aldehyde dehydrogenase	CYT
E3PEQ3_ECOH1	Putative zinc-binding dehydrogenase - Aldehyde reductase	CYT
E3PEU4_ECOH1	Putative semialdehyde dehydrogenase	CYT
E3PEU8_ECOH1	3-oxoacyl-[acyl-carrier-protein] synthase I	CYT
E3PEW4_ECOH1	Fatty acid oxidation complex subunit alpha	CYT
E3PEW5_ECOH1	3-ketoacyl-CoA thiolase	CYT
E3PEX6_ECOH1	DNA-binding response regulator in two-component regulatory system with EvgS 2488	CYT
E3PEZ5_ECOH1	Glucokinase	CYT
E3PF04_ECOH1	Glutamate - tRNA ligase	CYT
E3PF15_ECOH1	Cysteine synthase	CYT
E3PF16_ECOH1	Phosphocarrier protein	CYT

E3PF17_ECOH1	Phosphoenolpyruvate-protein phosphotransferase	CYT
E3PF18_ECOH1	Glucose-specific PTS system EIIA component	CYT
E3PF55_ECOH1	NADP-dependent malic enzyme	CYT
E3PF56_ECOH1	Transaldolase	CYT
E3PF57_ECOH1	Transketolase	CYT
E3PFF5_ECOH1	Putative colanic acid biosynthesis acetyltransferase	CYT
E3PFG4_ECOH1	Deoxyribose-phosphate aldolase	CYT
E3PFG6_ECOH1	Phosphopentomutase	CYT
E3PFG7_ECOH1	Purine nucleoside phosphorylase DeoD-type	CYT
E3PFH3_ECOH1	ABC transporter - ATP-binding protein	CYT
E3PFH8_ECOH1	Right origin-binding protein	CYT
E3PFI3_ECOH1	Aerobic respiration control protein	CYT
E3PFN2_ECOH1	6,7-dimethyl-8-ribityllumazine synthase	CYT
E3PFN8_ECOH1	Geranyltranstransferase - Farnesyl diphosphate synthase	CYT
E3PFP0_ECOH1	tRNA sulfurtransferase	CYT
E3PFP3_ECOH1	UPF0234 protein	CYT
E3PFQ2_ECOH1	Trigger factor	CYT
E3PFQ3_ECOH1	ATP-dependent Clp protease proteolytic subunit	CYT
E3PFQ5_ECOH1	Lon protease	CYT
E3PFQ6_ECOH1	DNA-binding protein HU-beta	CYT
E3PFS4_ECOH1	Maltose O-acetyltransferase	CYT
E3PFT6_ECOH1	Nucleoid-associated protein	CYT
E3PFT8_ECOH1	Chaperone protein	CYT
E3PFT9_ECOH1	Adenylate kinase	CYT
E3PFU0_ECOH1	Ferrochelatase	CYT
E3PFV7_ECOH1	Thioredoxin-like protein	CYT
E3PFV8_ECOH1	Putative short chain dehydrogenase	CYT
E3PFW8_ECOH1	4-hydroxy-tetrahydrodipicolinate synthase	CYT
E3PFX0_ECOH1	Putative peroxiredoxin - Bacterioferritin comigratory protein	CYT
E3PFY8_ECOH1	Uracil phosphoribosyltransferase	CYT
E3PG51_ECOH1	GMP synthase [glutamine-hydrolyzing]	CYT
E3PG52_ECOH1	Inosine-5'-monophosphate dehydrogenase	CYT
E3PG55_ECOH1	GTPase Der	CYT
E3PG58_ECOH1	Histidine - tRNA ligase	CYT
E3PG62_ECOH1	Nucleoside diphosphate kinase	CYT
E3PG65_ECOH1	Sulfurtransferase - 3-mercaptopyruvate sulfurtransferase	CYT

E3PG67_ECOH1	Peptidase B	CYT
E3PG74_ECOH1	Cysteine desulfurase	CYT
E3PG77_ECOH1	Inositol-1-monophosphatase	CYT
E3PG95_ECOH1	Serine hydroxymethyltransferase	CYT
E3PG96_ECOH1	Flavohemoprotein	CYT
E3PGF6_ECOH1	UDP-2,3-diacylglucosamine hydrolase	CYT
E3PGF7_ECOH1	Peptidyl-prolyl cis-trans isomerase	CYT
E3PGL5_ECOH1	Alkyl hydroperoxide reductase subunit C	CYT
E3PGL6_ECOH1	Alkyl hydroperoxide reductase subunit F	CYT
E3PGL7_ECOH1	Universal stress protein G	CYT
E3PGN2_ECOH1	Cold shock-like protein	CYT
E3PGP8_ECOH1	DNA polymerase III, delta subunit	CYT
E3PGQ0_ECOH1	Leucine - tRNA ligase	CYT
E3PGV9_ECOH1	Elongation factor 4	CYT
E3PGW6_ECOH1	ATP-dependent RNA helicase	CYT
E3PGW9_ECOH1	Autonomous glycyl radical cofactor - Acts as a radical domain for damaged PFL and possibly other radical proteins	CYT
E3PGX8_ECOH1	Chaperone protein	CYT
E3PGZ0_ECOH1	50S ribosomal protein L19	CYT
E3PGZ3_ECOH1	30S ribosomal protein S16	CYT
E3PGZ4_ECOH1	Signal recognition particle protein	CYT
E3PGZ6_ECOH1	Putative magnesium transport protein	CYT
E3PH03_ECOH1	SsrA-binding protein	CYT
E3PH30_ECOH1	L-2-hydroxyglutarate oxidase	CYT
E3PH32_ECOH1	4-aminobutyrate aminotransferase	CYT
E3PH39_ECOH1	DNA-binding protein	CYT
E3PH56_ECOH1	S-ribosylhomocysteine lyase	CYT
E3PH60_ECOH1	Carbon storage regulator	CYT
E3PH61_ECOH1	Alanine - tRNA ligase	CYT
E3PH62_ECOH1	Protein RecA	CYT
E3PH71_ECOH1	N-acetylglucosamine-6-phosphate deacetylase	CYT
E3PH74_ECOH1	Glutamine - tRNA ligase	CYT
E3PH78_ECOH1	Flavodoxin 1	CYT
E3PH81_ECOH1	Negative modulator of initiation of replication	CYT
E3PH82_ECOH1	Phosphoglucomutase	CYT
E3PHA9_ECOH1	Citrate synthase	CYT
E3PHB4_ECOH1	2-oxoglutarate dehydrogenase E1 component	CYT

E3PHB5_ECOH1	Dihydrolipoyllysine-residue succinyltransferase component of 2-oxoglutarate dehydrogenase complex	CYT
E3PHB6_ECOH1	Succinyl-CoA ligase [ADP-forming] subunit beta	CYT
E3PHB7_ECOH1	Succinyl-CoA ligase [ADP-forming] subunit alpha	CYT
E3PHD7_ECOH1	2,3-bisphosphoglycerate-dependent phosphoglycerate mutase	CYT
E3PHE9_ECOH1	6-phosphogluconolactonase	CYT
E3PHL2_ECOH1	Sorbitol-6-phosphate 2-dehydrogenase (Glucitol-6-phosphate dehydrogenase)	CYT
E3PHQ2_ECOH1	tRNA pseudouridine synthase D	CYT
E3PHT5_ECOH1	7-carboxy-7-deazaguanine synthase	CYT
E3PHT6_ECOH1	Enolase	CYT
E3PHT7_ECOH1	CTP synthase	CYT
E3PHU1_ECOH1	GTP pyrophosphokinase	CYT
E3PI01_ECOH1	Putative phosphatidylethanolamine-binding protein	CYT
E3PI10_ECOH1	Molybdenum cofactor biosynthesis protein B	CYT
E3PI27_ECOH1	ATP-dependent RNA helicase	CYT
E3PI30_ECOH1	Putative glycosyl transferase	CYT
E3PI42_ECOH1	DNA protection during starvation protein	CYT
E3PI57_ECOH1	Molybdopterin biosynthesis protein	CYT
E3PI70_ECOH1	Deoxyribose operon repressor	CYT
E3PI94_ECOH1	Arginine ABC transporter - ATP-binding protein	CYT
E3PIA6_ECOH1	Uncharacterized protein	CYT
E3PIG6_ECOH1	Lysine--tRNA ligase	CYT
E3PIH4_ECOH1	RNA-modifying protein	CYT
E3PIH9_ECOH1	Glycine dehydrogenase (decarboxylating)	CYT
E3PII1_ECOH1	Aminomethyltransferase	CYT
E3PII9_ECOH1	Ribose-5-phosphate isomerase A	CYT
E3PIK0_ECOH1	Fructose-bisphosphate aldolase class 2	CYT
E3PIK1_ECOH1	Phosphoglycerate kinase	CYT
E3PIK9_ECOH1	Transketolase	CYT
E3PIM3_ECOH1	Putative amino acid racemase	CYT
E3PIN1_ECOH1	Uncharacterized protein	CYT
E3PIQ4_ECOH1	ATP-dependent Clp protease ATP-binding subunit	CYT
E3PIQ7_ECOH1	ABC transporter - ATP-binding/permease protein	CYT
E3PIQ8_ECOH1	ABC transporter - ATP-binding/permease protein	CYT
E3PIR0_ECOH1	Leucine-responsive regulatory protein	CYT
E3PIR4_ECOH1	Serine - tRNA ligase	CYT

E3PIR6_ECOH1	Anaerobic dimethyl sulfoxide reductase chain B	CYT
E3PIS4_ECOH1	Formate acetyltransferase 1	CYT
E3PIS6_ECOH1	Putative fatty acid binding protein or Ribosomal protein S12 methylthiotransferase accesory factor	CYT
E3PIS8_ECOH1	Phosphoserine aminotransferase	CYT
E3PIT2_ECOH1	30S ribosomal protein S1	CYT
E3PIT3_ECOH1	Integration host factor subunit beta	CYT
E3PIT8_ECOH1	UPF0434 protein	CYT
E3PIU5_ECOH1	Chromosome partition protein	CYT
E3PIU9_ECOH1	Aspartate aminotransferase	CYT
E3PIV1_ECOH1	Asparagine - tRNA ligase	CYT
E3PIX2_ECOH1	Ribosomal RNA large subunit methyltransferase K/L	CYT
E3PIX9_ECOH1	Putative Lon Portease Homolog	CYT
E3PJ12_ECOH1	Cold shock-like protein	CYT
E3PJ22_ECOH1	Acyl carrier protein	CYT
E3PJ30_ECOH1	Putative lipoprotein	CYT
E3PJ92_ECOH1	Malate synthase G	CYT
E3PJD3_ECOH1	2,5-diketo-D-gluconic acid reductase A	CYT
E3PJG3_ECOH1	Uncharacterized protein	CYT
E3PJG9_ECOH1	Curved DNA-binding protein	CYT
E3PJH2_ECOH1	Uncharacterized protein	CYT
E3PJH3_ECOH1	NAD(P)H dehydrogenase - Quinone	CYT
E3PJL4_ECOH1	Acidic protein	CYT
E3PJM3_ECOH1	N-methyl-L-tryptophan oxidase	CYT
E3PJM8_ECOH1	Glutaredoxin 2	CYT
E3PJQ3_ECOH1	50S ribosomal protein L32	CYT
E3PJQ4_ECOH1	Phosphate acyltransferase	CYT
E3PJQ5_ECOH1	3-oxoacyl-[acyl-carrier-protein] synthase 3	CYT
E3PJQ7_ECOH1	3-oxoacyl-[acyl-carrier protein] reductase	CYT
E3PJQ8_ECOH1	Acyl carrier protein	CYT
E3PJQ9_ECOH1	3-oxoacyl-[acyl-carrier-protein] synthase 2	CYT
E3PJR1_ECOH1	Putative aminodeoxychorismate lyase (YceG-like family), binds nucleic acid	CYT
E3PJR7_ECOH1	Putative nucleotide-binding protein - Purine nucleoside phosphoramidase	CYT
E3PJS1_ECOH1	UPF0227 protein	CYT
E3PJS2_ECOH1	NADH dehydrogenase	CYT
E3PJW7_ECOH1	Bifunctional protein	CYT
E3PJY0_ECOH1	30S ribosomal protein S21	CYT

E3PJY2_ECOH1	RNA polymerase sigma factor	CYT
E3PK14_ECOH1	Uncharacterized protein	CYT
E3PK16_ECOH1	Putative glutathione S-transferase - Glutathionyl-hydroquinone reductase	CYT
E3PK64_ECOH1	Uncharacterized protein	CYT
E3PK65_ECOH1	Putative general stress protein - Protein deglycase 2	CYT
E3PK74_ECOH1	ATP-dependent RNA helicase	CYT
E3PK76_ECOH1	Polyribonucleotide nucleotidyltransferase	CYT
E3PK77_ECOH1	30S ribosomal protein S15	CYT
E3PK80_ECOH1	Translation initiation factor IF-2	CYT
E3PK81_ECOH1	Transcription termination/antitermination protein	CYT
E3PK89_ECOH1	Ribosomal RNA large subunit methyltransferase E	CYT
E3PK91_ECOH1	Transcription elongation factor	CYT
E3PK95_ECOH1	50S ribosomal protein L27	CYT
E3PK96_ECOH1	50S ribosomal protein L21	CYT
E3PK99_ECOH1	UDP-N-acetylglucosamine 1-carboxyvinyltransferase	CYT
E3PKA2_ECOH1	Putative organic solvent tolerance protein - Toulene-resistance protein	CYT
E3PKD7_ECOH1	Peptidase T	CYT
E3PKE0_ECOH1	Two-component response regulator	CYT
E3PKE1_ECOH1	Adenylosuccinate lyase	CYT
E3PKE6_ECOH1	Isocitrate dehydrogenase [NADP]	CYT
E3PKG2_ECOH1	Cell division topological specificity factor	CYT
E3PKJ0_ECOH1	Ribosome-binding ATPase	CYT
E3PKJ4_ECOH1	Ribose-phosphate pyrophosphokinase	CYT
E3PKK2_ECOH1	2-dehydro-3-deoxyphosphooctonate aldolase	CYT
E3PKL9_ECOH1	Formyltetrahydrofolate deformylase	CYT
E3PKM3_ECOH1	UTP-glucose-1-phosphate uridylyltransferase	CYT
E3PKM4_ECOH1	DNA-binding protein	CYT
E3PKM6_ECOH1	Aldehyde-alcohol dehydrogenase	CYT
E3PKQ3_ECOH1	RNase adapter protein	CYT
E3PKQ7_ECOH1	Glyoxalase - Enhancing lycopene biosynthesis protein 2 (Sigma cross-reacting protein 27A)	CYT
E3PKR8_ECOH1	N-acetylneuraminate lyase	CYT
E3PKS2_ECOH1	Stringent starvation protein A	CYT
E3PKS3_ECOH1	30S ribosomal protein S9	CYT
E3PKS4_ECOH1	50S ribosomal protein L13	CYT
E3PKS9_ECOH1	Malate dehydrogenase	CYT
E3PKT9_ECOH1	Ribonuclease g	CYT

E3PKU3_ECOH1	Rod shape-determining protein	CYT
E3PKU5_ECOH1	Putative zinc-binding dehydrogenase	CYT
E3PKU6_ECOH1	Biotin carboxyl carrier protein of acetyl-CoA carboxylase	CYT
E3PKU7_ECOH1	Biotin carboxylase - Acetyl-CoA carboxylase subunit A	CYT
E3PKX0_ECOH1	Peptide deformylase	CYT
E3PKX8_ECOH1	50S ribosomal protein L17	CYT
E3PKX9_ECOH1	DNA-directed RNA polymerase subunit alpha	CYT
E3PKY0_ECOH1	30S ribosomal protein S4	CYT
E3PKY1_ECOH1	30S ribosomal protein S11	CYT
E3PKY2_ECOH1	30S ribosomal protein S13	CYT
E3PKY5_ECOH1	50S ribosomal protein L15	CYT
E3PKY6_ECOH1	50S ribosomal protein L30	CYT
E3PKY7_ECOH1	30S ribosomal protein S5	CYT
E3PKY8_ECOH1	50S ribosomal protein L18	CYT
E3PKY9_ECOH1	50S ribosomal protein L6	CYT
E3PKZ0_ECOH1	30S ribosomal protein S8	CYT
E3PKZ1_ECOH1	30S ribosomal protein S14	CYT
E3PKZ2_ECOH1	50S ribosomal protein L5	CYT
E3PKZ3_ECOH1	50S ribosomal protein L24	CYT
E3PKZ4_ECOH1	50S ribosomal protein L14	CYT
E3PKZ5_ECOH1	30S ribosomal protein S17	CYT
E3PKZ6_ECOH1	50S ribosomal protein L29	CYT
E3PKZ7_ECOH1	50S ribosomal protein L16	CYT
E3PKZ8_ECOH1	30S ribosomal protein S3	CYT
E3PKZ9_ECOH1	50S ribosomal protein L22	CYT
E3PL00_ECOH1	30S ribosomal protein S19	CYT
E3PL01_ECOH1	50S ribosomal protein L2	CYT
E3PL02_ECOH1	50S ribosomal protein L23	CYT
E3PL03_ECOH1	50S ribosomal protein L4	CYT
E3PL04_ECOH1	50S ribosomal protein L3	CYT
E3PL05_ECOH1	30S ribosomal protein S10	CYT
E3PL15_ECOH1	Uncharacterized protein	CYT
E3PL16_ECOH1	Uncharacterized protein	CYT
E3PL25_ECOH1	Uncharacterized protein	CYT
E3PL27_ECOH1	Pseudouridine synthase	CYT
E3PL36_ECOH1	Aconitate hydratase	CYT

E3PL48_ECOH1	Enoyl-[acyl-carrier-protein] reductase [NADH]	CYT
E3PL50_ECOH1	Peptide ABC transporter, ATP-binding protein	CYT
E3PL51_ECOH1	Peptide ABC transporter, ATP-binding protein	CYT
E3PL93_ECOH1	Universal stress protein E	CYT
E3PLA3_ECOH1	Zinc transport protein	CYT
E3PLA6_ECOH1	Putative universal stress protein	CYT
E3PLB4_ECOH1	Putative exported protein - Methionine aminotransferase	CYT
E3PLE4_ECOH1	Bacterioferritin	CYT
E3PLE8_ECOH1	Elongation factor G	CYT
E3PLE9_ECOH1	30S ribosomal protein S7	CYT
E3PLF0_ECOH1	30S ribosomal protein S12	CYT
E3PLF6_ECOH1	Peptidyl-prolyl cis-trans isomerase	CYT
E3PLG5_ECOH1	Cyclic AMP receptor protein - Catabolite gene activator	CYT
E3PLJ1_ECOH1	Tryptophan - tRNA ligase	CYT
E3PLJ6_ECOH1	3-dehydroquinate synthase	CYT
E3PLL0_ECOH1	Phosphoenolpyruvate carboxykinase [ATP]	CYT
E3PLM3_ECOH1	Alpha-1,4 glucan phosphorylase	CYT
E3PLN1_ECOH1	Glycerol-3-phosphate dehydrogenase	CYT
E3PLN3_ECOH1	Alpha-1,4 glucan phosphorylase	CYT
E3PLN4_ECOH1	Glycogen synthase	CYT
E3PLN8_ECOH1	Aspartate-semialdehyde dehydrogenase	CYT
E3PLR4_ECOH1	ATP-dependent helicase	CYT
E3PLR7_ECOH1	Glyceraldehyde-3-phosphate dehydrogenase	CYT
E3PLX9_ECOH1	NAD-dependent malic enzyme	CYT
E3PLY0_ECOH1	Stationary phase induced ribosome associated protein	CYT
E3PLY2_ECOH1	Peroxiredoxin	CYT
E3PLZ3_ECOH1	Glutamate decarboxylase	CYT
E3PM40_ECOH1	NADP-dependent L-serine/L-allo-threonine dehydrogenase	CYT
E3PM42_ECOH1	Uncharacterized protein - Putative selenoprotein	CYT
E3PM89_ECOH1	Oligopeptidase A	CYT
E3PME8_ECOH1	Glycine - tRNA ligase beta subunit	CYT
E3PMH7_ECOH1	NAD(P) transhydrogenase subunit beta	CYT
E3PMH8_ECOH1	NAD(P) transhydrogenase subunit alpha	CYT
E3PMI8_ECOH1	Mannose-6-phosphate isomerase	CYT
E3PMJ4_ECOH1	7-alpha-hydroxysteroid dehydrogenase	CYT
E3PMJ8_ECOH1	Adenosine deaminase	CYT

E3PML5_ECOH1	Pyridoxine/pyridoxamine 5'-phosphate oxidase	CYT
E3PMN1_ECOH1	Glutaredoxin	CYT
E3PMN3_ECOH1	Superoxide dismutase	CYT
E3PMP2_ECOH1	Putative monooxygenase	CYT
E3PMQ1_ECOH1	Pyruvate kinase I	CYT
E3PMR2_ECOH1	Putative FAD-binding oxidase	CYT
E3PMS7_ECOH1	Phosphoenolpyruvate synthase	CYT
E3PMX2_ECOH1	Glycerol-3-phosphate dehydrogenase [NAD(P)+]	CYT
E3PMX3_ECOH1	Protein-export protein	CYT
E3PMX4_ECOH1	Glutaredoxin 3	CYT
E3PMX5_ECOH1	Putative rhodanase-like exported protein	CYT
E3PMX6_ECOH1	2,3-bisphosphoglycerate-independent phosphoglycerate mutase	CYT
E3PMY0_ECOH1	L-threonine 3-dehydrogenase	CYT
E3PMY3_ECOH1	ADP-L-glycero-D-manno-heptose-6-epimerase	CYT
E3PMY9_ECOH1	Lipopolysaccharide core biosynthesis protein - LPS cores heptose (II) kinase (LPS synthesis)	CYT
E3PMZ3_ECOH1	UDP-glucose:(Heptosyl) LPS alpha-1,3-glucosyltransferase - LPS core biosynthesis protein	CYT
E3PMZ4_ECOH1	Heptosyl-III-transferase - Lipopolysaccharide core heptosyltransferase	CYT
E3PMZ9_ECOH1	50S ribosomal protein L28	CYT
E3PN17_ECOH1	Putative exported protein	CYT
E3PN97_ECOH1	Integration host factor subunit alpha	CYT
E3PN98_ECOH1	Phenylalanine--tRNA ligase beta subunit	CYT
E3PN99_ECOH1	Phenylalanine--tRNA ligase alpha subunit	CYT
E3PNA0_ECOH1	50S ribosomal protein L20	CYT
E3PNA2_ECOH1	Translation initiation factor IF-3	CYT
E3PNA3_ECOH1	Threonine - tRNA ligase	CYT
E3PNA7_ECOH1	Phosphofructokinase	CYT
E3PNB6_ECOH1	Catalase HPII	CYT
E3PND2_ECOH1	Succinylornithine transaminase	CYT
E3PNE9_ECOH1	Putative nitroreductase	CYT
E3PNG3_ECOH1	Glyceraldehyde-3-phosphate dehydrogenase A	CYT
E3PNG7_ECOH1	Putative serine protein kinase	CYT
E3PNK8_ECOH1	Cold shock-like protein	CYT
E3PNL2_ECOH1	Putative exported protein (DNA repair?)	CYT
E3PNL7_ECOH1	RNA chaperone	CYT
E3PNM5_ECOH1	Putative exported protein	CYT

E3PNQ2_ECOH1	Ribonuclease P protein component	CYT
E3PNQ7_ECOH1	Tryptophanase	CYT
E3PNS3_ECOH1	Phosphate-specific transport system accessory protein	CYT
E3PNS8_ECOH1	Glutamine - fructose-6-phosphate aminotransferase [isomerizing]	CYT
E3PNX0_ECOH1	ATP-dependent RNA helicase	CYT
E3PNX1_ECOH1	Thioredoxin	CYT
E3PNX3_ECOH1	Transcription termination factor	CYT
E3PNZ2_ECOH1	Porphobilinogen deaminase	CYT
E3PNZ3_ECOH1	Adenylate cyclase	CYT
E3PLE6_ECOH1	Putative glycosyl hydrolase, possible endochitinase	EC
E3PLV3_ECOH1	Possible exported protein	EC
ELAH_ECOH1	Heat-labile Enterotoxin A	EC
ELBH_ECOH1	Heat-labile Enterotoxin B	EC
E3PAU9_ECOH1	Flagellin	EC-FLA
E3PBC4_ECOH1	Flagellar M-ring protein	EC-FLA
E3PBC5_ECOH1	Flagellar motor switch protein	EC-FLA
E3PBD0_ECOH1	Flagellar protein	EC-FLA
E3PBD3_ECOH1	Flagellar protein	EC-FLA
E3PJP0_ECOH1	Flagellar hook protein	EC-FLA
E3PJP2_ECOH1	Flagellar basal-body rod protein	EC-FLA
E3PJP3_ECOH1	Flagellar L-ring protein	EC-FLA
E3PJP6_ECOH1	Flagellar hook-associated protein 1	EC-FLA
E3PAP0_ECOH1	Putative phage protein	EC-PHAGE
E3PC23_ECOH1	Uncharacterized protein (likely phage protein)	EC-PHAGE
E3PC42_ECOH1	Hypothetical phage protein	EC-PHAGE
E3PC57_ECOH1	Hypothetical phage protein	EC-PHAGE
E3PFZ9_ECOH1	Prophage holin	EC-PHAGE
E3PG21_ECOH1	Hypothetical phage protein	EC-PHAGE
E3PG22_ECOH1	Hypothetical phage protein	EC-PHAGE
E3PG24_ECOH1	Putative phage protein - bbp21	EC-PHAGE
E3PG26_ECOH1	Hypothetical phage protein	EC-PHAGE
E3PGH0_ECOH1	Bacteriophage N4 adsorption protein A	EC-PHAGE
E3PGU8_ECOH1	Putative phage protein	EC-PHAGE
E3PKG5_ECOH1	Uncharacterized protein (Fels-1 Prophage Protein-like family protein)	EC-PHAGE
D0Z6Y2_ECOH1	Conjugal transfer protein	EC-PILI
D0Z6Y7_ECOH1	Conjugal transfer protein	EC-PILI

E3PEE8_ECOH1	FimA Pilin	EC-PILI
E3PEF0_ECOH1	FimC Chaperone	EC-PILI
E3PEF1_ECOH1	FimD Usher	EC-PILI
E3PEF4_ECOH1	FimH Pilin adhesin	EC-PILI
E3PPC3_ECOH1	CfA/I fimbrial subunit A - Colonization factor antigen subunit A - Putative chaperone	EC-PILI
E3PPC5_ECOH1	Cfa/I fimbrial subunit C - Colonization factor antigen subunit C - Outer membrane usher protein	EC-PILI
E3PPC6_ECOH1	Cfa/I fimbrial subunit E - Colonization factor antigen I subunit E - Pilin subunit	EC-PILI
FMC1_ECOH1	CFA/I fimbrial subunit B	EC-PILI
D0Z6U9_ECOH1	Integral membrane sensor signal transduction histidine kinase	IM
E3PAF8_ECOH1	Lipid A biosynthesis myristolytransferase (LPS synthesis)	IM
E3PAI9_ECOH1	Methyl-accepting chemotaxis protein II - Aspartate chemoreceptor protein)	IM
E3PAU2_ECOH1	L-cysteine transporter, ATP-binding protein	IM
E3PAU3_ECOH1	L- cystine ABC transporter, permease protein	IM
E3PAV4_ECOH1	Putative membrane protein (YeeE/YedE family protein)	IM
E3PAV6_ECOH1	Magnesium transport protein	IM
E3PAX5_ECOH1	Probable protein kinase - Quinone biosynthesis	IM
E3PAX6_ECOH1	Sec-independent protein translocase protein	IM
E3PAX7_ECOH1	Sec-independent protein translocase protein	IM
E3PAX8_ECOH1	Sec-independent protein translocase protein	IM
E3PB26_ECOH1	Formate dehydrogenase-O, iron-sulfur subunit	IM
E3PB44_ECOH1	Two-component sensor kinase	IM
E3PB50_ECOH1	CDP-diacylglycerol pyrophosphatase	IM
E3PB62_ECOH1	1,4-dihydroxy-2-naphthoate octaprenyltransferase	IM
E3PB65_ECOH1	Cell division protein	IM
E3PB86_ECOH1	Putative membrane protein	IM
E3PB92_ECOH1	Bifunctional aspartokinase I/homoserine dehydrogenase I	IM
E3PBE1_ECOH1	Cellulose synthesis regulatory protein (Signal transduction protein)	IM
E3PBE3_ECOH1	Putative membrane protein	IM
E3PBI5_ECOH1	Adenosylcobinamide-GDP ribazoletransferase	IM
E3PBP0_ECOH1	Required for Type I pili	IM
E3PBQ4_ECOH1	Chain length determinant protein (LPS synthesis)	IM
E3PBY5_ECOH1	Putative transporter (YqeW-like)	IM
E3PC06_ECOH1	Glycerol-3-phosphate acyltransferase	IM
E3PC07_ECOH1	Diacylglycerol kinase	IM
E3PC09_ECOH1	DinF - MATE efflux faily protein	IM

E3PCA1_ECOH1	Glutathione-regulated potassium-efflux system protein	IM
E3PCA9_ECOH1	Co-chaperone protein	IM
E3PCD6_ECOH1	Penicilllin-binding protein 3	IM
E3PCD9_ECOH1	Phospho-N-acetylmuramoyl-pentapeptide-transferase	IM
E3PCE1_ECOH1	Putative lipid II flippase	IM
E3PCE2_ECOH1	UDP-N-acetylglucosamine--N-acetylmuramyl-(pentapeptide) pyrophosphoryl-undecaprenol N-acetylglucosamine transferase (MurG)	IM
E3PCF0_ECOH1	Protein translocase subunit	IM
E3PCG1_ECOH1	AmpE protein	IM
E3PCH4_ECOH1	Quinoprotein glucose dehydrogenase	IM
E3PCJ9_ECOH1	Penicillin-binding protein 1B	IM
E3PCK1_ECOH1	Ferrichrome transport ATP-binding protein	IM
E3PCK5_ECOH1	H(+)/Cl(-) exchange transporter	IM
E3PCL1_ECOH1	Putative transport protein	IM
E3PCL2_ECOH1	Putative exported protein_Outer membrane Porin	IM
E3PCM2_ECOH1	Multidrug resistance protein	IM
E3PCM6_ECOH1	Two-component sensor kinase	IM
E3PCS4_ECOH1	D-lactate dehydrogenase (Dld)	IM
E3PCT4_ECOH1	Putative exported protein	IM
E3PCW6_ECOH1	Lipid A 1-diphosphate synthase	IM
E3PCW8_ECOH1	Putative signal transduction protein	IM
E3PCX2_ECOH1	ABC-transporter, ATP-binding protein	IM
E3PCY0_ECOH1	Putative sulphatase	IM
E3PCY4_ECOH1	Putative sodium/hydrogen exchanger	IM
E3PD30_ECOH1	Proline/betaine transporter	IM
E3PD33_ECOH1	Putative membrane protein	IM
E3PD44_ECOH1	Anaerobic C4-dicarboxylate transporter	IM
E3PD58_ECOH1	Inner membrane protein	IM
E3PD94_ECOH1	Thiol:disulfide interchange protein	IM
E3PD96_ECOH1	Anaerobic C4-dicarboxylate transporter	IM
E3PDA6_ECOH1	Putative entericidin A	IM
E3PDA7_ECOH1	Putative entericidin b	IM
E3PDC8_ECOH1	Zinc metalloprotease, regulator of sigma E protease	IM
E3PDF0_ECOH1	Lipoprotein	IM
E3PDH7_ECOH1	Copper/silver efflux system, membrane component	IM
E3PDH9_ECOH1	Putative cation-transporting P-type ATPase	IM
E3PDK1_ECOH1	Acyl-CoA dehydrogenase	IM

E3PDL6_ECOH1	Xanthine phosphoribosyltransferase	IM
E3PDP8_ECOH1	Cytochrome C-type biogenesis protein	IM
E3PDR8_ECOH1	Phosphotransferase	IM
E3PDS0_ECOH1	Sensor histidine kinase	IM
E3PDU1_ECOH1	Glycerol-3-phosphate transporter	IM
E3PDV6_ECOH1	ArnC LPS synthesis	IM
E3PDV9_ECOH1	Undecaprenyl phosphate-alpha-4-amino-4-deoxy-L-arabinose arabinosyl transferase	IM
E3PE23_ECOH1	Fumarate reductase subunit C	IM
E3PE24_ECOH1	Succinate dehydrogenase iron-sulfur subunit	IM
E3PE25_ECOH1	Fumarate reductase flavoprotein subunit	IM
E3PE30_ECOH1	Miniconductance mechanosensitive channel	IM
E3PE31_ECOH1	Phosphatidylserine decarboxylase proenzyme	IM
E3PE42_ECOH1	Modulator of FtsH protease	IM
E3PE81_ECOH1	Putative exported protein	IM
E3PE83_ECOH1	D-serine/D-alanine/glycine transporter	IM
E3PE90_ECOH1	Putative exported protein - Transcriptional regulator	IM
E3PE92_ECOH1	UPF0053 inner membrane protein	IM
E3PE95_ECOH1	Putative exported protein - Translocation and assembly module	IM
E3PEB0_ECOH1	Trehalose-specific PTS system EIIBC component	IM
E3PEB2_ECOH1	Mg(2+) transport ATPase, P-type	IM
E3PEC9_ECOH1	Putative permease - LPS export system permease protein	IM
E3PED0_ECOH1	Putative permease - LPS export sstem permease protein	IM
E3PEU7_ECOH1	UPF0226 membrane protein	IM
E3PEX7_ECOH1	Putative hybrid sensory histidine kinase in two-component regulatory system - Sensor protein	IM
E3PEZ9_ECOH1	Nucleoside permease	IM
E3PF01_ECOH1	Putative signal transduction protein	IM
E3PF13_ECOH1	Cell division protein	IM
E3PF14_ECOH1	Sulfate transporter	IM
E3PF79_ECOH1	Putative membrane protein	IM
E3PF86_ECOH1	Putative carbon starvation protein	IM
E3PF87_ECOH1	Methyl-accepting chemotaxis protein	IM
E3PF91_ECOH1	Phosphoglycerol transferase I	IM
E3PFF8_ECOH1	Osmotically-inducible protein Y	IM
E3PFJ4_ECOH1	Putative microcin B17 uptake protein - Peptide antibiotic transporter	IM
E3PFL6_ECOH1	Phosphate regulon two-component system, sensor kinase	IM

E3PFM4_ECOH1	Putative preprotein translocase subunit	IM
E3PFM5_ECOH1	Protein translocase subunit	IM
E3PFM6_ECOH1	Protein-export membrane protein	IM
E3PFP7_ECOH1	Cytochrome o ubiquinol oxidase subunit 1	IM
E3PFP8_ECOH1	Ubiquinol oxidase subunit 2	IM
E3PFQ7_ECOH1	Peptidylprolyl isomerase	IM
E3PFS3_ECOH1	Putative membrane protein	IM
E3PFS7_ECOH1	Acriflavin resistance protein B - Multidrug efflux pump subunit	IM
E3PFS8_ECOH1	Acriflavin resistance protein A - Multidrug efflux pump subunit	IM
E3PFT0_ECOH1	Mechanosensitive channel MscK - Potassium efflux protein	IM
E3PFU3_ECOH1	Putative transport protein	IM
E3PFU9_ECOH1	Copper-transporting P-type ATPase	IM
E3PFV1_ECOH1	Putative amino acid permease	IM
E3PFV3_ECOH1	Putative membrane protein	IM
E3PFV4_ECOH1	Putative membrane protein	IM
E3PFW1_ECOH1	Putative permease	IM
E3PFZ1_ECOH1	Polyphosphate kinase	IM
E3PFZ4_ECOH1	Putative transmembrane protein	IM
E3PG57_ECOH1	Uncharacterized protein	IM
E3PG60_ECOH1	Cytoskeleton protein	IM
E3PG64_ECOH1	Putative protease inhibitor	IM
E3PGA4_ECOH1	Phosphatidylglycerophosphatase C	IM
E3PGG9_ECOH1	Putative exported protein	IM
E3PGH7_ECOH1	Two-component system sensor kinase	IM
E3PGI4_ECOH1	Miniconductance mechanosensitive channel	IM
E3PGP0_ECOH1	Penicillin-binding protein 5 - D-alanyl-D-alanine carboxypeptidase	IM
E3PGP3_ECOH1	Peptidoglycan D,D-transpeptidase	IM
E3PGR5_ECOH1	Apolipoprotein N-acyltransferase	IM
E3PGV8_ECOH1	Signal peptidase I	IM
E3PH38_ECOH1	Putative membrane protein	IM
E3PH42_ECOH1	Uncharacterized protein	IM
E3PH48_ECOH1	Glycine betaine/proline betaine transport system permease protein	IM
E3PH54_ECOH1	Multidrug resistance protein A	IM
E3PH66_ECOH1	Glucitol/sorbitol-specific PTS system EIIC component	IM
E3PH73_ECOH1	N-acetylglucosamine-specific PTS system EIICBA components	IM
E3PH88_ECOH1	Two-component sensor kinase	IM

E3PH89_ECOH1	Potassium-transporting ATPase ATP-binding subunit	IM
E3PHB1_ECOH1	Succinate dehydrogenase hydrophobic membrane anchor subunit	IM
E3PHB2_ECOH1	Succinate dehydrogenase flavoprotein subunit	IM
E3PHB3_ECOH1	Succinate dehydrogenase iron-sulfur subunit	IM
E3PHC1_ECOH1	Cytochrome d ubiquinol oxidase subunit 1	IM
E3PHC2_ECOH1	Cytochrome d ubiquinol oxidase subunit 2	IM
E3PHC6_ECOH1	Colicin import protein - TonB dependent uptake of colicins	IM
E3PHC8_ECOH1	TolA, transporter	IM
E3PHD4_ECOH1	Zinc transporter	IM
E3PHG0_ECOH1	Putative transmembrane protein	IM
E3PHL0_ECOH1	Glucitol/sorbitol-specific PTS system EIIB component	IM
E3PHU3_ECOH1	Histidine kinase	IM
E3PHV3_ECOH1	Serine transporter	IM
E3PHY2_ECOH1	Prolipoprotein diacylglyceryl transferase	IM
E3PHY9_ECOH1	Lysophospholipid transporter	IM
E3PHZ0_ECOH1	Bifunctional protein	IM
E3PI19_ECOH1	Cardiolipin synthase B	IM
E3PI22_ECOH1	Transport permease protein	IM
E3PI38_ECOH1	Putative membrane protein - Transporter, small conductance mechanosensitive ion channel MscS family protein	IM
E3PI39_ECOH1	Glutamine ABC transporter, ATP-binding protein	IM
E3PI40_ECOH1	Glutamine ABC transporter, permease protein	IM
E3PI69_ECOH1	Penicillin-binding protein 6 - D-alanyl-D-alanine carboxypeptidase	IM
E3PI77_ECOH1	Putative transport protein	IM
E3PI91_ECOH1	Arginine ABC transporter, permease protein	IM
E3PI99_ECOH1	Uncharacterized protein - Dehydrogenase	IM
E3PIA8_ECOH1	Macrolide-specific efflux protein	IM
E3PIE2_ECOH1	Putative cell wall degradation protein	IM
E3PIJ7_ECOH1	Uncharacterized protein	IM
E3PIJ9_ECOH1	Small-conductance mechanosensitive channel	IM
E3PIM4_ECOH1	Putative membrane protein	IM
E3PIR5_ECOH1	Anaerobic dimethyl sulfoxide reductase chain A	IM
E3PIS5_ECOH1	Probable formate transporter 1	IM
E3PIS7_ECOH1	Putative membrane protein	IM
E3PIT5_ECOH1	Lipid A export ATP-binding/permease protein (LPS synthesis)	IM
E3PIT6_ECOH1	Tetraacyldisaccharide 4'-kinase (LPS synthesis)	IM
E3PIU1_ECOH1	Putative membrane protein - Envelope biogenesis factor	IM

E3PIV3_ECOH1	Aminopeptidase N	IM
E3PIW9_ECOH1	Dihydroorotate dehydrogenase - Quinone	IM
E3PIX5_ECOH1	Paraquat-inducible protein B	IM
E3PIY5_ECOH1	Putative membrane protein	IM
E3PIZ5_ECOH1	Hydrogenase-1 small subunit	IM
E3PIZ6_ECOH1	NiFeSe-hydrogenase	IM
E3PJ01_ECOH1	Cytochrome bd-II oxidase subunit 1 - Quinone	IM
E3PJ04_ECOH1	Cryptic autophosphorylating protein tyrosine kinase	IM
E3PJ29_ECOH1	Putative membrane protein (MMPL family)	IM
E3PJB8_ECOH1	Hydrogenase-2 large subunit	IM
E3PJB9_ECOH1	Probable Ni/Fe-hydrogenase 2 b-type cytochrome subunit (NfrD family)	IM
E3PJC1_ECOH1	Hydrogenase-2 small chain	IM
E3PJC7_ECOH1	Biopolymer transport protein	IM
E3PJC8_ECOH1	Biopolymer transport protein	IM
E3PJD8_ECOH1	1-acyl-sn-glycerol-3-phosphate acyltransferase	IM
E3PJI2_ECOH1	Bifunctional protein	IM
E3PJI3_ECOH1	Putative sodium/proline symporter	IM
E3PJL2_ECOH1	Glucans biosynthesis glucosyltransferase H	IM
E3PJL6_ECOH1	Lipid A biosynthesis lauryltransferase	IM
E3PJR5_ECOH1	Glucose-specific PTS system IIBC component	IM
E3PJS9_ECOH1	Lipoprotein-releasing system transmembrane protein	IM
E3PJT0_ECOH1	Lipoprotein-releasing system ATP-binding protein	IM
E3PJT1_ECOH1	Lipoprotein-releasing system transmembrane protein	IM
E3PJX0_ECOH1	Uncharacterized protein	IM
E3PK12_ECOH1	Uncharacterized protein	IM
E3PK28_ECOH1	Threonine/serine transporter	IM
E3PK85_ECOH1	Protein-export membrane protein	IM
E3PK88_ECOH1	ATP-dependent zinc metalloprotease	IM
E3PKD6_ECOH1	Spermidine/putrescine import ATP-binding protein	IM
E3PKD9_ECOH1	Two-component sensor kinase	IM
E3PKG3_ECOH1	Site-determining protein	IM
E3PKH7_ECOH1	D-amino acid dehydrogenase	IM
E3PKJ2_ECOH1	Putative membrane protein	IM
E3PKL2_ECOH1	Histidine kinase or Nitrate/nitrite sensor protein	IM
E3PKL4_ECOH1	Respiratory nitrate reductase 1 alpha chain	IM
E3PKL5_ECOH1	Respiratory nitrate reductase 1 beta chain	IM

E3PKL7_ECOH1	Respiratory nitrate reductase 1 gamma chain	IM
E3PKN0_ECOH1	Oligopeptide ABC transporter - Permease protein	IM
E3PKN1_ECOH1	Oligopeptide ABC transporter - Permease protein	IM
E3PKN2_ECOH1	Oligopeptide ABC transporter, ATP-binding protein	IM
E3PKN3_ECOH1	Oligopeptide ABC transporter, ATP-binding protein	IM
E3PKN5_ECOH1	Cardiolipin synthase A	IM
E3PKN6_ECOH1	Voltage-gated potassium channel	IM
E3PKP1_ECOH1	Putative organic solvent tolerance protein (YrbD/VpsC, Toulene transporter subunit: mm component of ABC superfamily - Phospholipid transport	IM
E3PKP2_ECOH1	Putative organic solvent tolerance protein	IM
E3PKP7_ECOH1	Lipopolysaccharide export system protein (LPS synthesis)	IM
E3PKQ8_ECOH1	Aerobic respiration control sensor protein	IM
E3PKR7_ECOH1	Sialic acid transporter	IM
E3PKS6_ECOH1	Protein YhcB	IM
E3PKS8_ECOH1	Serine endoprotease	IM
E3PKT8_ECOH1	Possible exported protein	IM
E3PKU2_ECOH1	Rod shape-determining protein	IM
E3PKU4_ECOH1	RNase E specificity factor - Signal transduction protein	IM
E3PKX3_ECOH1	Potassium transport protein - Trk system potassium uptake protein	IM
E3PKX4_ECOH1	Large-conductance mechanosensitive channel	IM
E3PKY4_ECOH1	Protein translocase subunit	IM
E3PL30_ECOH1	Probable protease	IM
E3PL39_ECOH1	Lipopolysaccharide assembly protein A (LPS synthesis)	IM
E3PL40_ECOH1	Lipopolysaccharide assembly protein B (LPS synthesis)	IM
E3PL65_ECOH1	Phage shock protein	IM
E3PL82_ECOH1	UPF0283 membrane protein	IM
E3PL91_ECOH1	Low Conductance mechanosensitive channel	IM
E3PLB2_ECOH1	Putative exported protein	IM
E3PLF8_ECOH1	Glutathione-regulated potassium-efflux system protein	IM
E3PLF9_ECOH1	Glutathione-regulated potassium-efflux system ancillary protein	IM
E3PLJ5_ECOH1	Cell division protein	IM
E3PLK3_ECOH1	Penicillin-binding protein 1A	IM
E3PLK5_ECOH1	Putative membrane protein (IgaA homolog)	IM
E3PLL1_ECOH1	Two-component sensor kinase - Osmolarity sensor protein	IM
E3PLQ2_ECOH1	sn-glycerol-3-phosphate import ATP-binding protein	IM
E3PLS2_ECOH1	MCP (Methyl-accepting chemotaxis protein III (Ribose an galactose) - Chemoreceptor protein	IM

E3PLW9_ECOH1	Respiratory nitrate reductase 2 alpha chain	IM
E3PLX6_ECOH1	Formate dehydrogenase, nitrate-inducible, iron-sulfur subunit	IM
E3PLZ2_ECOH1	Probable glutamate/gamma-aminobutyrate antiporter - Extreme acid sensitivity protein	IM
E3PM52_ECOH1	Cell division protein	IM
E3PM53_ECOH1	Cell division ATP-binding protein	IM
E3PM58_ECOH1	Putative membrane protein	IM
E3PM59_ECOH1	Lead, cadmium, zinc and mercury-transporting ATPase	IM
E3PM78_ECOH1	Putative type I secretion system, ATP-binding protein, Ribosome-associated ATPase	IM
E3PM79_ECOH1	Putative type I secretion system, inner membrane protein	IM
E3PM84_ECOH1	Low affinity inorganic phosphate transporter 1	IM
E3PM85_ECOH1	Universal stress protein B	IM
E3PMA1_ECOH1	Putative acid resistance protein	IM
E3PMA3_ECOH1	Multidrug resistance protein	IM
E3PMA4_ECOH1	Multidrug resistance protein	IM
E3PMB2_ECOH1	Putative membrane protein	IM
E3PMB4_ECOH1	Outer membrane protein assembly factor	IM
E3PMB9_ECOH1	Putative signal transduction protein	IM
E3PMC2_ECOH1	Cyclic di-GMP-binding protein (Cellulose synthase regulator subunit B)	IM
E3PMC7_ECOH1	Protein BcsG homolog	IM
E3PMD5_ECOH1	Phosphoethanolamine transferase	IM
E3PMG4_ECOH1	Putative dimethyl sulphoxide reductase- Olydopterin dinucleotide binding subunit	IM
E3PMI4_ECOH1	Two component sensor kinase	IM
E3PMI9_ECOH1	Putative exported protein	IM
E3PMK7_ECOH1	Electron transport complex subunit (RsxG)	IM
E3PMM1_ECOH1	HlyD-family secretion protein	IM
E3PMP0_ECOH1	Multidrug resistance protein	IM
E3PMW2_ECOH1	Mannitol-specific PTS system EIICBA component	IM
E3PMW9_ECOH1	L-lactate dehydrogenase	IM
E3PMY6_ECOH1	O-antigen ligase (LPS synthesis)	IM
E3PMZ5_ECOH1	3-deoxy-D-manno-octulosonic-acid transferase (LPS synthesis)	IM
E3PN15_ECOH1	Sodium/glutamate symport carrier protein - Glutamate permease	IM
E3PN72_ECOH1	Lipoprotein	IM
E3PNB3_ECOH1	Putative sodium:dicarboxylate symporter	IM
E3PND5_ECOH1	Putative lipoprotein - Ferredoxin-like	IM
E3PNF0_ECOH1	Protease 4	IM

E3PNH0_ECOH1	Putativediaguanylate cyclase	IM
E3PNK1_ECOH1	Putative transport protein	IM
E3PNK4_ECOH1	Mannose-specific PTS system EIID component	IM
E3PNK5_ECOH1	UPF0266 membrane protein	IM
E3PNL5_ECOH1	Protease	IM
E3PNL6_ECOH1	Tail-specific protease	IM
E3PNN2_ECOH1	Putative membrane protein	IM
E3PNQ4_ECOH1	Membrane protein insertase	IM
E3PNS4_ECOH1	Phosphate import ATP-binding protein	IM
E3PNS5_ECOH1	Phosphate transport system permease protein	IM
E3PNT0_ECOH1	ATP synthase epsilon chain	IM
E3PNT1_ECOH1	ATP synthase subunit beta	IM
E3PNT2_ECOH1	ATP synthase gamma chain	IM
E3PNT3_ECOH1	ATP synthase subunit alpha	IM
E3PNT4_ECOH1	ATP synthase subunit delta	IM
E3PNT5_ECOH1	ATP synthase subunit b	IM
E3PNT6_ECOH1	ATP synthase subunit c	IM
E3PNT7_ECOH1	ATP synthase subunit a	IM
E3PNU6_ECOH1	Low affinity potassium transport system protein	IM
E3PNX4_ECOH1	Undecaprenyl-phosphate alpha-N-acetylglucosaminyl 1-phosphate transferase (WecA)	IM
E3PNX5_ECOH1	ECA polysaccharide chain length modulation protein (WzzE)	IM
E3PNY5_ECOH1	UDP-N-acetyl-D-mannosaminuronic acid transferase (LPS synthesis)	IM
E3PNY9_ECOH1	Porphyrin biosynthetic protein	IM
E3PNZ0_ECOH1	Putative uroporphyrinogen-III C-methyltransferase	IM
E3PPA0_ECOH1	Putative two-partner secretion transporter	IM
ACFD_ECOH1	Putative phospholipid-binding protein	IM
E3PBR6_ECOH1	Putative glycosyl transferase	IM
E3PCE6_ECOH1	Cell division protein	IM
E3PCG6_ECOH1	Dihydrolipoyl dehydrogenase	IM
E3PDW9_ECOH1	Uncharacterized protein	IM
E3PGX5_ECOH1	CDP-diacylglycerol--serine O-phosphatidyltransferase	IM
E3PH67_ECOH1	2-octaprenyl-3-methyl-6-methoxy-1,4-benzoquinol hydroxylase	IM
E3PHC7_ECOH1	Colicin import protein - TonB receptor	IM
E3PIA1_ECOH1	Pyruvate oxidase - Pyruvate dehydrogenase - Ubiquinone	IM
E3PIQ9_ECOH1	Thioredoxin reductase	IM
E3PJP8_ECOH1	Ribonuclease E	IM

E3PKE2_ECOH1	High frequency lysogenization protein	IM
E3PKP9_ECOH1	Putative organic solvent tolerance ABC transporter, ATP-binding protein	IM
E3PL64_ECOH1	Phage shock protein	IM
E3PM54_ECOH1	Signal recognition particle receptor	IM
E3PMA7_ECOH1	Glutamate decarboxylase	IM
E3PMB8_ECOH1	C4-dicarboxylate transport protein	IM
E3PNK2_ECOH1	Mannose-specific PTS system EIIAB component	IM
E3PAV3_ECOH1	Putative Lipoprotein	OM
E3PAW1_ECOH1	Phospholipase A1_Detergent resistant phospholipase A	OM
E3PBK1_ECOH1	Putative adhesin Autotransporter_Antigen 43	OM
E3PBU3_ECOH1	Vitamin B12 transporter	OM
E3PC01_ECOH1	MaltoPorin	OM
E3PCA8_ECOH1	LPS-assembly protein	OM
E3PCK0_ECOH1	Ferrichrome-iron TonB-dependent receptor	OM
E3PCU5_ECOH1	Colicin I TonB-dependent receptor	OM
E3PD73_ECOH1	Putative adhesin Autotransporter_Antigen 43	OM
E3PDA2_ECOH1	Putative lipoprotein	OM
E3PDA9_ECOH1	Outer membrane Lipoprotein	OM
E3PDC9_ECOH1	Outer membrane protein assembly factor	OM
E3PDE5_ECOH1	Copper homeostasis protein Lipoprotein	OM
E3PDE9_ECOH1	Outer membrane Lipoprotein	OM
E3PDH4_ECOH1	Probable outer membrane Lipoprotein	OM
E3PDL9_ECOH1	Outer membrane Porin E	OM
E3PDR7_ECOH1	Outer membrane Porin C	OM
E3PDV2_ECOH1	Putative exported protein_Outer membrane Porin	OM
E3PE57_ECOH1	Putative Lipoprotein	OM
E3PE94_ECOH1	Putative outer membrane protein assembly factor	OM
E3PEW7_ECOH1	Long-chain fatty acid transport protein	OM
E3PEW9_ECOH1	Lipoprotein	OM
E3PF33_ECOH1	Putative Lipoprotein	OM
E3PFF1_ECOH1	Putative outer membrane virulence protein	OM
E3PFJ5_ECOH1	Putative Lipoprotein	OM
E3PFM8_ECOH1	Nucleoside-specific channel-forming protein	OM
E3PFM9_ECOH1	Putative Lipoprotein	OM
E3PFQ0_ECOH1	Putative Lipoprotein	OM
E3PFR9_ECOH1	Putative Lipoprotein	OM

E3PFW7_ECOH1	Outer membrane protein assembly factor	OM
E3PG56_ECOH1	Outer membrane protein assembly factor	OM
E3PG99_ECOH1	Putative lipoprotein	OM
E3PGJ2_ECOH1	Ferrienterobactin_Enterobactin_TonB-dependent receptor	OM
E3PGN1_ECOH1	Lipid A palmitoyltransferase	OM
E3PGP1_ECOH1	Endolytic peptidoglycan transglycosylase	OM
E3PGP9_ECOH1	LPS-assembly Lipoprotein	OM
E3PGY1_ECOH1	Outer membrane protein assembly factor	OM
E3PH00_ECOH1	Outer membrane protein assembly factor	OM
E3PH65_ECOH1	Membrane-bound lytic transglycosylase B	OM
E3PH76_ECOH1	Putative Lipoprotein	OM
E3PHD0_ECOH1	Peptidoglycan-associated Lipoprotein	OM
E3PHF7_ECOH1	Pectinesterase_Putative acyl-CoA thioester hydrolase	OM
E3PHI5_ECOH1	Outer membrane Porin	OM
E3PHP9_ECOH1	Murein hydrolase activator	OM
E3PHW6_ECOH1	Putative Lipoprotein	OM
E3PHX0_ECOH1	Membrane bound lytic murein transglycolase A	OM
E3PHY7_ECOH1	Possible Lipoprotein	OM
E3PI35_ECOH1	Catecholate Siderophore_TonB-dependent receptor	OM
E3PI44_ECOH1	Outer membrane Porin X	OM
E3PI95_ECOH1	Probable lipoprotein	OM
E3PI97_ECOH1	Putative N-acetylmuramoyl-L-alanine amidase	OM
E3PIL0_ECOH1	Putative peptidase	OM
E3PIN5_ECOH1	Membrane-bound lytic murein transglycosylase	OM
E3PIP3_ECOH1	Iron III dicitrate_TonB-dependent receptor	OM
E3PIP9_ECOH1	Putative lipoprotein	OM
E3PIV0_ECOH1	Outer membrane Porin F	OM
E3PIX6_ECOH1	Putative lipoprotein	OM
E3PIY1_ECOH1	Outer membrane Porin A	OM
E3PJ06_ECOH1	Predicted exopolysaccharide export protein	OM
E3PJ07_ECOH1	Uncharacterized protein	OM
E3PJ09_ECOH1	Predicted outer membrane Lipoprotein	OM
E3PJ86_ECOH1	Type II secretion system protein D	OM
E3PJ88_ECOH1	Type II secretion system Lipoprotein	OM
E3PJF6_ECOH1	Drug efflux channel component	OM
E3PJF8_ECOH1	Putative Lipoprotein	OM

E3PJM7_ECOH1	Putative Lipoprotein	OM
E3PJR6_ECOH1	FeIII-coprogen Fe(III)-ferrioxamine B and Fe(III)-hodotrulic acid_TonB-dependent receptor	OM
E3PJR8_ECOH1	Penicillin-binding protein activator	OM
E3PK59_ECOH1	Penicillin-binding protein activator	OM
E3PK62_ECOH1	Putative phospholipid-binding protein	OM
E3PK75_ECOH1	Lipoprotein for cell division	OM
E3PKJ6_ECOH1	Outer-membrane Lipoprotein	OM
E3PKV8_ECOH1	Possible Lipoprotein	OM
E3PL14_ECOH1	Outer membrane Porin W	OM
E3PL43_ECOH1	Osmotically inducible Lipoprotein B	OM
E3PLB0_ECOH1	Heat shock protein	OM
E3PLT1_ECOH1	Putative lipoprotein	OM
E3PLV2_ECOH1	Siderophore_TonB-dependent receptor	OM
E3PM96_ECOH1	Outer membrane Lipoprotein	OM
E3PMC0_ECOH1	Cellulose synthase operon protein	OM
E3PME1_ECOH1	Putative outer membrane protein	OM
E3PME3_ECOH1	Putative lipoprotein	OM
E3PMG0_ECOH1	UPF0482 protein	OM
E3PML6_ECOH1	Putative Lipoprotein_Membrane-bound lysozyme inhibitor of C-type lysozyme	OM
E3PML8_ECOH1	Outer membrane Lipoprotein	OM
E3PMQ2_ECOH1	Major outer membrane Lipoprotein	OM
E3PNC3_ECOH1	Osmotically inducible Lipoprotein E	OM
E3PNG6_ECOH1	MltA-interacting protein	OM
E3PNJ0_ECOH1	Putative Lipoprotein	OM
E3PNN6_ECOH1	Putative lipoprotein	OM
E3PNZ5_ECOH1	Putative Lipoprotein	OM
EATA_ECOH1	Serine protease	OM
TIBA_ECOH1	Adhesin/invasin TibA Autotransporter	OM
E3PAG0_ECOH1	High-affinity zinc uptake system protein	PP
E3PAK1_ECOH1	L-arabinose-binding periplasmic protein	PP
E3PAU5_ECOH1	Cystine ABC transporter, substrate-binding protein - Sulfate starvation-induced protein 7	PP
E3PAZ3_ECOH1	Thiol:disulfide interchange protein	PP
E3PB27_ECOH1	Formate dehydrogenase-O, major subunit	PP
E3PB46_ECOH1	Putative extraCYToplasmic stress resistance protein	PP
E3PB49_ECOH1	Sulfate-binding protein - Sulfate starvation-induced protein 2	PP

E3PBF3_ECOH1	5-hydroxyisourate hydrolase	PP
E3PBF4_ECOH1	Protein-methionine-sulfoxide reductase catalytic subunit	PP
E3PBF6_ECOH1	Putative exported protein	PP
E3PBZ9_ECOH1	Maltose/maltodextrin IMport ATP-binding protein	PP
E3PC02_ECOH1	Maltose operon periplasmic protein	PP
E3PCA7_ECOH1	Chaperone	PP
E3PCC1_ECOH1	Thiamine ABC transport system, substrate-binding protein	PP
E3PCH3_ECOH1	Blue copper oxidase - Copper efflux oxidase	PP
E3PCQ1_ECOH1	Putative transmembrane protein	PP
E3PCS2_ECOH1	ABC transporter, substrate-binding protein	PP
E3PCS3_ECOH1	Periplasmic beta-glucosidase	PP
E3PCU0_ECOH1	D-galactose ABC transporter, substrate-binding protein	PP
E3PCW9_ECOH1	ABC transporter, substrate-binding protein	PP
E3PD08_ECOH1	D-allose transporter subunit	PP
E3PDB4_ECOH1	Putative protease Do - Periplasmic serine endoprotease	PP
E3PDD0_ECOH1	Chaperone	PP
E3PDK0_ECOH1	Inhibitor of vertebrate lysozyme	PP
E3PDR1_ECOH1	Ecotin	PP
E3PDU0_ECOH1	Glycerophosphoryl diester phosphodiesterase	PP
E3PE14_ECOH1	Histidine ABC transporter, substrate-binding periplasmic protein	PP
E3PE15_ECOH1	Lysine-arginine-ornithine-binding periplasmic protein	PP
E3PE37_ECOH1	N-acetylmuramoyl-L-alanine amidase	PP
E3PEA5_ECOH1	Electron-transport protein of unknown function	PP
E3PEE4_ECOH1	N-acetylneuraminate epimerase	PP
E3PEQ7_ECOH1	Putative exported protein (Protein YahO (Escherichia coli G3/10))	PP
E3PF26_ECOH1	Thiosulphate ABC transporter, substrate-binding protein	PP
E3PF36_ECOH1	Probable N-acetylmuramoyl-L-alanine amidase	PP
E3PF92_ECOH1	Putative glycoprotein/receptor	PP
E3PFH4_ECOH1	Soluble lytic murein transglycosylase	PP
E3PFH9_ECOH1	Protein CreA	PP
E3PFK0_ECOH1	Alkaline phosphatase	PP
E3PFU5_ECOH1	Protein UshA [includes: UDP-sugar hydrolase 5'-nucleotidase]	PP
E3PFY4_ECOH1	Beta-barrel assembly-enhancing protease	PP
E3PG92_ECOH1	ABC transporter periplasmic-binding protein	PP
E3PGK1_ECOH1	Ferrienterobactin-binding periplasmic protein	PP
E3PGL4_ECOH1	Thiol:disulfide interchange protein	PP

E3PGM1_ECOH1	Ribonuclease I	PP
E3PGR4_ECOH1	Glutamate/aspartate ABC transporter, substrate-binding protein	PP
E3PGW1_ECOH1	Sigma-E factor regulatory protein	PP
E3PH49_ECOH1	Glycine betaine/L-proline ABC transporter, substrate-binding protein	PP
E3PHC9_ECOH1	TolB (Involved in the TonB-independent uptake of proteins)	PP
E3PHD1_ECOH1	YbgF/Tol-Pal binding - TRP repeat containing protein	PP
E3PHE5_ECOH1	Molybdate ABC transporter, substrate-binding protein	PP
E3PHX1_ECOH1	N-acetylmuramoyl-L-alanine amidase	PP
E3PHX5_ECOH1	Protease III - Pitrilysin	PP
E3PI25_ECOH1	UPF0194 membrane protein	PP
E3PI41_ECOH1	Glutamine ABC transporter, substrate-binding protein	PP
E3PI60_ECOH1	ABC transporter, substrate-binding protein	PP
E3PI84_ECOH1	Putrescine-binding periplasmic protein	PP
E3PI90_ECOH1	Arginine ABC transporter, substrate-binding protein	PP
E3PI93_ECOH1	Arginine ABC transporter, substrate-binding protein	PP
E3PIG9_ECOH1	Thiol:disulfide interchange protein	PP
E3PIL2_ECOH1	Biosynthetic arginine decarboxylase	PP
E3PIM9_ECOH1	L-asparaginase 2	PP
E3PIN0_ECOH1	Uncharacterized protein	PP
E3PIP4_ECOH1	Iron(III) dicitrate-binding periplasmic protein	PP
E3PIR2_ECOH1	Putative Lipoprotein	PP
E3PJ03_ECOH1	Periplasmic AppA protein [includes: phosphoanhydrid phosphohydrolase and 4-phytase]	PP
E3PJC0_ECOH1	Hydrogenase-2 subunit	PP
E3PJD7_ECOH1	Cell division protein	PP
E3PJE4_ECOH1	Possible exported protein	PP
E3PJH1_ECOH1	Glucose-1-phosphatase	PP
E3PJI5_ECOH1	Putative exported protein	PP
E3PJL1_ECOH1	Glucans biosynthesis protein G	PP
E3PJL8_ECOH1	Protein YceI	PP
E3PJT6_ECOH1	Putrescine-binding periplasmic protein	PP
E3PK11_ECOH1	Putative exported protein	PP
E3PKG6_ECOH1	Putative exported protein - Inhibitor of g-type lysozyme	PP
E3PKI4_ECOH1	Periplasmic trehalase	PP
E3PKM9_ECOH1	Oligopeptide ABC transporter, substrate-binding protein	PP
E3PKP8_ECOH1	LPS export system protein	PP
E3PKS7_ECOH1	Periplasmic pH-dependent serine endoprotease	PP

E3PKV9_ECOH1	Putative ABC transporter, substrate-binding protein	PP
E3PL54_ECOH1	Peptide ABC transporter, substrate-binding protein	PP
E3PL84_ECOH1	Probable thiol peroxidase	PP
E3PL90_ECOH1	Periplasmic murein tripeptide binding protein	PP
E3PLF4_ECOH1	Peptidyl-prolyl cis-trans isomerase	PP
E3PLH1_ECOH1	Peptidyl-prolyl cis-trans isomerase	PP
E3PLP9_ECOH1	Gamma-glutamyltranspeptidase	PP
E3PLQ5_ECOH1	Glycerol-3-phosphate ABC transporter, substrate-binding protein	PP
E3PLS5_ECOH1	Glucans biosynthesis protein D	PP
E3PLU1_ECOH1	ABC transporter, substrate-binding protein	PP
E3PLX5_ECOH1	Formate dehydrogenase, nitrate-inducible, major subunit	PP
E3PM16_ECOH1	ABC transporter, substrate-binding protein	PP
E3PM48_ECOH1	Leucine-specific ABC transporter, substrate-binding protein	PP
E3PM50_ECOH1	Leu/ile/val ABC transporter, substrate-binding protein	PP
E3PM62_ECOH1	Putative lipoprotein	PP
E3PM66_ECOH1	Nickel ABC transporter - Substrate-binding protein	PP
E3PM99_ECOH1	Acid stress chaperone	PP
E3PMA0_ECOH1	Acid stress chaperone	PP
E3PMB7_ECOH1	Putative protease	PP
E3PMD4_ECOH1	Dipeptide ABC transporter, substrate-binding protein	PP
E3PMM3_ECOH1	Superoxide dismutase [Cu-Zn]	PP
E3PMQ3_ECOH1	Putative peptidoglycan-binding protein (ErfK/YbiS/YcfS/YnhG)	PP
E3PNC7_ECOH1	Spheroplast protein Y	PP
E3PND8_ECOH1	Putative exported protein	PP
E3PNS7_ECOH1	Phosphate-binding protein	PP
E3PNV0_ECOH1	D-ribose ABC transporter, substrate-binding protein	PP
E3PAN8_ECOH1	Uncharacterized protein	UNK
E3PCM8_ECOH1	Uncharacterized protein	UNK
E3PCN0_ECOH1	Uncharacterized protein	UNK
E3PDG8_ECOH1	Uncharacterized protein	UNK
E3PE72_ECOH1	Predicted transporter (DctP family)	UNK
E3PED1_ECOH1	Uncharacterized protein	UNK
E3PEH1_ECOH1	Conserved hypothetical exported protein	UNK
E3PFK1_ECOH1	Phosphate starvation-inducible protein	UNK
E3PFW5_ECOH1	Putative peptidase	UNK
E3PG06_ECOH1	Uncharacterized protein	UNK

E3PH35_ECOH1	Putative peptidoglycan-binding protein (LysM/BON superfamily protein) - NlpI-like?	UNK
E3PHD5_ECOH1	Putative exported protein	UNK
E3PI32_ECOH1	Putative exported protein - Multiple stress protein	UNK
E3PI49_ECOH1	Putative exported protein (ErfK/YbiS/YcfS/YnhG) - L,D-transpeptidase linking Lpp to murein	UNK
E3PI96_ECOH1	Protein YbjQ	UNK
E3PIA7_ECOH1	Uncharacterized protein	UNK
E3PIE0_ECOH1	Uncharacterized protein	UNK
E3PJ08_ECOH1	Uncharacterized protein	UNK
E3PJ67_ECOH1	Putative exported protein	UNK
E3PL31_ECOH1	Uncharacterized protein	UNK
E3PLB3_ECOH1	Uncharacterized protein	UNK
E3PLQ0_ECOH1	Uncharacterized protein	UNK
E3PMH9_ECOH1	Putative exported protein	UNK
E3PN75_ECOH1	Putative exported protein	UNK
E3PNA9_ECOH1	Putative kinase	UNK
E3PNL0_ECOH1	Uncharacterized protein	UNK
E3PNM0_ECOH1	Uncharacterized protein	UNK
E3PNN3_ECOH1	Protein YebF	UNK
E3PP03_ECOH1	Uncharacterized protein - Macrophage stimulating factor in *Salmonella*	UNK
E3PP89_ECOH1	Uncharacterized protein - ATP binding protein	UNK
E3PIH7_ECOH1	6-phospho-beta-glucosidase - Glycosyl hydrolase (similar to BglA)	UNK
E3PIR8_ECOH1	Putative isochorismatase	UNK
E3PMG5_ECOH1	Putative anaerobic dimethyl sulfoxide reductase, Fe-S	UNK
E3PNH7_ECOH1	Uncharacterized protein	UNK
E3PPH2_ECOH1	CfaD-dependent expression extracytoplasmic protein	UNK

Table 10: Summary of all OM-associated proteins detected in proteomic analysis of OM and OMV samples from untreated and peroxide-treated cultures

Primary Protein Name	Protein abbreviation (ETEC/K12)	Description	Gene name	K12 Accession number /synonym / locus / genes	Type	Part of multiprotein complex	IM tethering	Function	Regulated by stress/role in stress conditions
E3PI97_ECOH1	AmiD	N-acetylmuramoyl-L-alanine amidase AmiD	b0867	ECK0858, ybjR, b0867, JW0851	Lipoprotein			Peptidoglycan modifying	
E3PDC9_ECOH1	BamA	Outer membrane protein assembly factor	b0177	ECK0176, bamA, ecfK, omp85 (*N. meningitidis*), yaeT, yzzN, yzzY, JW0172, b0177	Integral	x		OM protein assembly	
E3PG56_ECOH1	BamB	Outer membrane protein assembly factor BamB	b2512	ECK2508, bamB, yfgL, b2512, JW2496	Lipoprotein	x		OM protein assembly	
E3PFW7_ECOH1	BamC	Outer membrane protein assembly factor BamC	b2477	ECK2473, bamC, dapX, nlpB, b2477, JW2462	Lipoprotein	x		OM protein assembly	

E3PGY1_ ECOH1	BamD	Outer membrane protein assembly factor BamD	b2595	ECK2593, bamD, ecfD, yfiO, b2595, JW2577	Lipoprotein	x		OM protein assembly	
E3PH00_ ECOH1	BamE	Outer membrane protein assembly factor bamE	b2617	ECK2613, bamE, smpA, smqA, b2617, JW2598	Lipoprotein	x		OM protein assembly	
E3PMC0 _ECOH1	BcsC	Cellulose synthase subunit	b3530	ECK3515, bcsC, yhjL, JW5942, b3530	Integral	x	x	Cellulose synthesis	
E3PDA9_ ECOH1	Blc	Outer membrane lipoprotein	b4149	ECK4145, blc, yjeL, b4149, JW4110	Lipoprotein			Role in stress conditions	x
E3PE57_ ECOH1	BsmA	Lipoprotein BsmA	b4189	ECK4185, bsmA, yjfO, b4189, JW5743	Lipoprotein			Role in oxidative stress / Role in stres conditions	x
E3PBU3_ ECOH1	BtuB	Vitamin B12 transporter	b3966	ECK3958, btuB, bfe, cer, dcrC, JW3938, b3966	Integral	x	x	Iron homeostasis	
E3PH76_ ECOH1	ChiQ	Uncharacterized lipoprotein ChiQ	b0682	ECK0670, chiQ, ybfN, b0682, JW0668	Lipoprotein			Sugar-induced	
E3PCU5_ ECOH1	CirA	Colicin I receptor	b2155	ECK2148, cirA, cir, feuA, b2155, JW2142	Integral	x	x	Iron homeostasis /	

								Colicin binding	
E3PIP9_ECOH1	E3PIP9	Uncharacterized protein		ETEC protein	Lipoprotein			Uncharacterized	
EATA_ECOH1	EatA	Serine protease EatA		ETEC protein ETEC_p948_0020	Integral			Role in virulence	
E3PEW7_ECOH1	FadL	Long-chain fatty acid transport protein	b2344	ECK2338, fadL, ttr, b2344, JW2341	Integral			Fatty acid transport	
E3PIP3_ECOH1	FecA	Fe(3+) dicitrate transport protein FecA	b4291	ECK4281, fecA, b4291, JW4251	Integral	x	x	Iron homeostasis	
E3PGJ2_ECOH1	FepA	Ferrienterobactin receptor	b0584	ECK0576, fepA, cbr, cbt, fep, feuB, b0584, JW5086	Integral	x	x	Iron homeostasis / Colicin binding	
E3PCK0_ECOH1	FhuA	Ferrichrome-iron receptor	b0150	ECK0149, fhuA, tonA, b0150, JW0146	Integral	x	x	Iron homeostasis	
E3PJR6_ECOH1	FhuE	FhuE receptor	b1102	ECK1088, fhuE, b1102, JW1088	Integral	x	x	Iron homeostasis	
E3PI35_ECOH1	Fiu	Catecholate siderophore receptor Fiu	b0805	ECK0794, fiu, ybiL, b0805, JW0790	Integral	x	x	Iron homeostasis	

E3PBK1_ECOH1	Flu	Antigen 43	b2000	ECK1993, JW1982, agn, agn43, yeeQ, b2000	Integral			Adhesion and invasion	
E3PD73_ECOH1	Flu_2	Antigen 43 (isoform)	b2000	ECK1993, JW1982, agn, agn43, yeeQ	Integral			Adhesion and invasion	
E3PJ09_ECOH1	GfcB	Uncharacterized lipoprotein GfcB	b0986	ECK0977, ymcC, b0986, JW0969	Lipoprotein			LPS assembly	
E3PJ07_ECOH1	GfcD	Uncharacterized protein GfcD	b0984	ECK0975, ymcA, b0984, JW0967	Lipoprotein			LPS assembly	
E3PJ86_ECOH1	GspD	General secretory pathway component	b3325	ECK3312, gspD, yheF, JW5707, b3325	Integral	x		Type II secretion system	
E3PLB0_ECOH1	HslJ	Heat shock protein HslJ	b1379	ECK1376, hslJ, ydbI, b1379, JW1374	Lipoprotein			Heat shock	
E3PC01_ECOH1	LamB	Maltoporin	b4036	ECK4028, lamB, malB, malL, b4036, JW3996	Integral			Sugar transport	
E3PIL0_ECOH1	LoiP	Metalloprotease LoiP	b2936	ECK2931, loiP, yggG, b2936, JW2903	Lipoprotein			Metalloprotease / Role in stress conditions / Heat shock	x

E3PKJ6_ ECOH1	LolB	Outer-membrane Lipoprotein LolP	b1209	ECK1197, lolB, hemM, ychC, b1209, JW1200	Lipoprotein			Lipoprotein biogenesis	
E3PFF1_ ECOH1	LomR	Putative outer membrane virulence protein	b4570, b1369, b1371	ECK1366, lomR, b4570, JW5884/JW5904, b1369/b1371	Integral			Role in virulence	
E3PK59_ ECOH1	LpoA	Penicillin-binding protein activator	b3147	ECK3135, lpoA, yraM, b3147, JW3116	Lipoprotein			Peptidoglycan modification	
E3PJR8_ ECOH1	LpoB	Penicillin-binding protein activator	b1105	ECK1091, lpoB, ycfM, b1105, JW5157	Lipoprotein			Peptidoglycan modification	
E3PMQ2 _ECOH1	Lpp	Major outer membrane prolipoprotein Lpp	b1677	ECK1673, mlpA, mulI, b1677, JW1667	Lipoprotein			Petidoglycan anchoring	
E3PCA8_ ECOH1	LptD	LPS assembly OM complex	b0054	ECK0055, lptD, JW0053, imp, ostA, yabG, b0054	Integral	x	x	LPS assembly	
E3PGP9_ ECOH1	LptE	LPS-assembly lipoprotein LptE	b0641	ECK0634, lptE, rlpB, b0641, JW0636	Lipoprotein	x	x	LPS assembly	

E3PNG6 _ECOH1	MipA	MltA-interacting protein	b1782	ECK1780, mipA yeaF, b1782, JW1771	Integral	x	x	Peptidoglycan modifying	
E3PEW9 _ECOH1	MlaA	Probable phospholipid-binding lipoprotein MlaA	b2346	ECK2340, mlaA, vacJ, b2346, JW2343	Lipoprotein			OM maintenance	
E3PML6_ ECOH1	MliC	Membrane-bound lysozyme inhibitor of C-type lysozyme	b1639	ECK1635, mliC, ydhA, b1639, JW1631	Lipoprotein			LPS assembly	
E3PHX0_ ECOH1	MltA	Membrane-bound lytic murein transglycosylase C	b2813	ECK2809, mlt, ygdM, JW2784, b2813	Lipoprotein	x	x	Peptidoglycan modifying	
E3PH65_ ECOH1	MltB	Membrane-bound lytic murein transglycosylase A	b2701	ECK2696, mltB, JW2671, b2701	Lipoprotein	x		Peptidoglycan modifying	
E3PIN5_ ECOH1	MltC	Membrane-bound lytic murein transglycosylase B	b2963	ECK2958, mltC, yggZ, JW5481, b2963	Lipoprotein	x	x	Peptidoglycan modifying	

E3PHP9_ECOH1	NlpD	Murein hydrolase activator NlpD	b2742	ECK2737, nlpD, b2742, JW2712	Lipoprotein			Peptidoglycan modifying	
E3PDE5_ECOH1	NlpE	Copper homeostasis protein	b0192	ECK0192, nlpE cutF, b0192, JW0188	Lipoprotein			Copper homeostasis	x
E3PK75_ECOH1	NlpI	Lipoprotein NlpI	b3163	ECK3151, nlpI, yhbM, b3163, JW3132	Lipoprotein			Peptidoglycan modifying	
E3PHI5_ECOH1	NmpC	Putative outer membrane porin protein NmpC	b0553	ECK0544, phmA, b0553	Integral			Peptidoglycan anchoring / Transport	
E3PIY1_ECOH1	OmpA	Outer membrane protein A	b0957	ECK0948, ompA, con, tolG, tut, b0957, JW0940	Integral			Role in stress conditions / Peptidoglycan anchoring	
E3PDR7_ECOH1	OmpC	Outer membrane protein C	b2215	ECK2207, ompC, butR, meoA, par, b2215, JW2203	Integral			Transport	
E3PDL9_ECOH1	OmpE	Outer membrane pore protein E	b0241	ECK0242, ompE, phoE, b0241, JW0231	Integral			Transport	
E3PIV0_ECOH1	OmpF	Outer membrane protein F	b0929	ECK0920, ompF, cmlB, coa, cry, nfxB?, tolF, b0929, JW0912	Integral			Colicin binding / Transport / Role in stress conditions	x

E3PL14_ ECOH1	OmpW	Outer membrane protein W	b1256	ECK1250, yciD, b1256, JW1248	Integral			Colicin binding / Transport / Role in stress conditions	x
E3PI44_E COH1	OmpX	Outer membrane protein X	b0814	ECK0803, ompX, b0814, ybiG	Integral			Role in stress conditions	x
E3PL43_ ECOH1	OsmB	Osmotically inducible Lipoprotein B	b1283	ECK1278, osmB, b1283, JW1275	Lipoprotein			Osmotic regulation	
E3PNC3_ ECOH1	OsmE	Osmotically inducible Lipoprotein E	b1739	ECK1737, osmE, anr, b1739, JW1728	Lipoprotein			Osmotic regulation	
E3PGN1 _ECOH1	PagP	Lipid A palmitoyltransfer ase	b0622	ECK0615, pagP, crcA, ybeG, JW0617, b0622	Integral			LPS assembly	
E3PHD0 _ECOH1	Pal	Peptidoglycan-associated lipoprotein	b0741	ECK0730, pal, excC, b0741, JW0731	Lipoprotein			Peptidoglycan anchoring	
E3PAW1 _ECOH1	PldA	Outer membrane phospholipase A	b3821	ECK3815, JW3794, b3821	Integral			OM maintenance	x
E3PDE9_ ECOH1	RcsF	Outer membrane lipoprotein	b0196	ECK0196, rcsF, b0196, JW0192	Lipoprotein			Role in stress conditions	

E3PGP1_ECOH1	RlpA	Endolytic peptidoglycan transglycosylase RlpA	b0633	ECK0626, rlpA, b0633, JW0628	Lipoprotein			Peptidoglycan modifying	
E3PDH4_ECOH1	SilC	Cation efflux system protein CusC (in K12)	b0572	ECK0564, ETEC0219, ibeB, ylcB, b0572 (E. coli, cusC)	Lipoprotein			Silver resistance	
E3PM96_ECOH1	Slp	Outer membrane protein slp	b3506	ECK3490, b3506, JW3474	Lipoprotein			Role in stress conditions	x
E3PML8_ECOH1	SlyB	Outer membrane lipoprotein SlyB	b1641	ECK1637, slyB, b1641, JW1633	Lipoprotein			Magnesium homeostasis	
E3PE94_ECOH1	TamA	Translocation and assembly module	b4220	ECK4216, JW4179, yftM, ytfM, b4220	Integral	x	x	OM protein assembly	
TIBA_ECOH1	TibA	Adhesin/invasin TibA autotransporter		ETEC protein ETEC_2141	Integral			Adhesion and invasion	
E3PJF6_ECOH1	TolC	Outer membrane protein TolC	b3035	ECK3026, tolC, colE1-i, mtcB, mukA, refI, toc, weeA, b3035, JW5503	Integral	x	x	Drug efflux	
E3PFM8_ECOH1	Tsx	Nucleoside-specific channel-forming protein	b0411	ECK0405, nupA, T6rec, b0411, JW0401	Integral			Nucleoside transport	

E3PJ06_ECOH1	Wza	Putative polysaccharide export protein Wza	b2062	ECK2056, wza, b2062, JW2047	Lipoprotein			LPS assembly	
E3PFJ5_ECOH1	YaiW	Uncharacterized protein YaiW	b0378	ECK0373, yaiW, b0378, JW0369	Lipoprotein			Role in stress conditions	
E3PFQ0_ECOH1	YajG	Uncharacterized protein YajG	b0434	ECK0428, yajG, b0434, JW0424	Lipoprotein			Uncharacterized	
E3PFM9_ECOH1	YajI	Uncharacterized lipoprotein YajI	b0412	ECK0406, yaiJ, b0412, JW5056	Lipoprotein			Uncharacterized	
E3PFR9_ECOH1	YbaY	Uncharacterized lipoprotein YbaY	b0453	ECK0447, ybaY, b0453, JW0443	Lipoprotein			Uncharacterized	
E3PHF7_ECOH1	YbhC	Pectinesterase	b0772	ECK0761, ybhC, b0772, JW0755	Lipoprotein			Thioesterase	
E3PI95_ECOH1	YbjP	Uncharacterized Lipoprotein YbjP	b0865	ECK0856, ybjP, b0865, JW0849	Lipoprotein			Uncharacterized	
E3PJM7_ECOH1	YceB	Uncharacterized lipoprotein YceB	b1063	ECK1048, yceB, b1063, JW1050	Lipoprotein			Uncharacterized	
E3PLT1_ECOH1	YdcL	Uncharacterized lipoprotein YdcL	b1431	ECK1424, ydcL, b1431, JW1427	Lipoprotein			Uncharacterized	
E3PNJ0_ECOH1	YeaY	Uncharacterized lipoprotein YeaY	b1806	ECK1804, yeaY, b1806, JW1795	Lipoprotein			Role in stress conditions	

E3PAV3_ECOH1	YedD	Outer membrane lipoprotein	b1928	ECK1927, yedD, JW1913, b1928	Lipoprotein			Uncharacterized	
E3PDV2_ECOH1	YfaZ	Outer membrane protein YfaZ	b2250	ECK2243, yfaZ, b2250, JW5371	Integral			Transport	
E3PF33_ECOH1	YfeY	Uncharacterized protein YfeY	b2432	ECK2427, yfeY, b2432, JW2425	Lipoprotein			Role in stress conditions	x
E3PG99_ECOH1	YfhG	Uncharacterized protein YfhG	b2555	ECK2552, yfhG, qseG, b2555, JW2539	Lipoprotein			Uncharacterized	
E3PHW6_ECOH1	YgdI	Uncharacterized lipoprotein YgdI	b2809	ECK2805, ygdI, b2809, JW5448	Lipoprotein			Uncharacterized	
E3PHY7_ECOH1	YgdR	Uncharacterized lipoprotein YgdR	b2833	ECK2829, ygdR, b2833, JW2801	Lipoprotein			Uncharacterized	
E3PJ88_ECOH1	YghG	Type II secretion system Lipoprotein	b2971	ECK2966, yghG, gspSbeta, b2971, JW2938	Lipoprotein			Type II secretion system	
E3PJF8_ECOH1	YgiB	UPF0441 protein YgiB	b3037	ECK3028, ygiB, b3037, JW5927	Lipoprotein			Biofilm formation	
E3PKV8_ECOH1	YhdV	Uncharacterized protein YhdV	b3267	ECK3254, yhdV, b3267, JW3235	Lipoprotein			Uncharacterized	
E3PME1_ECOH1	YiaD	Probable lipoprotein YiaD	b3552	ECK3539, yiaD, b3552, JW5657	Lipoprotein			OM protein assembly	

E3PME3_ECOH1	YiaF	Uncharacterized protein YiaF	b3554	ECK3541, yiaF, b3554, JW5655	Lipoprotein			Role in host colonization	
E3PNN6_ECOH1	YidQ	Uncharacterized protein YidQ	b3688	ECK3680, ydiQ, ecfl, b3688, JW5633	Lipoprotein			Role in stress conditions / Extracytoplasmic function	x
E3PNZ5_ECOH1	YifL	Uncharacterized lipoprotein YifL	b4558	ECK3803, yfiL, b4558, JW3781	Lipoprotein			Uncharacterized	
E3PDA2_ECOH1	YjeI	Uncharacterized protein YjeI	b4144	ECK4138, yjeI, b4144, JW5736	Lipoprotein			Role in oxidative stress / Role in stres conditions	x
E3PIX6_ECOH1	YmbA	Paraquat-inducible/ uncharacterized protein	b0952	ECK0943, ymbA, pqiC, b0952, JW5127	Lipoprotein	x	x	Role in oxidative stress	
E3PLV2_ECOH1	YncD	Probable TonB-dependent receptor YncD	b1451	ECK1445, yncD, b1451, JW1446	Integral	x	x	Iron homeostasis	
E3PMG0_ECOH1	YnfB	UPF0482 protein	b1583	ECK1578, ynfB, b1583, JW1575	Unknown			Uncharacterized	
E3PK62_ECOH1	YraP	Uncharacterized protein YraP	b3150	ECK3138, yraP, ecfH, b3150, JW3119	Lipoprotein			Role in stress conditions	x

Table 11: GO Category analysis of OM-associated proteins at least 2-fold more retained or exported with oxidative stress

Analysis Type:	PANTHER Overrepresentation Test (Released 2020-04-07)						
Annotation Version and Release Date:	GO Ontology database (Released 2020-02-21)						
Reference List:	*Escherichia coli* (all genes in database)						
Test Type:	FISHER			**Correction:**		FDR	
Retention increased at least 2-fold with stress (From Table 3, Column 5 "down")	BamA, BamD, BcsC, BtuB, CirA, FadL, FecA, FepA, FhuA, Fiu, Flu_2, GfcD, Lpp, LptD, LptE, MlaA, OmpA, OmpE/PhoE, OmpF, OmpX, PagP, PldA, SilC, TamA, TolC, Wza, YeaY, YfaZ, YncD, YnfB						
GO biological process complete	***Escherichia coli* - REFLIST (4391)**	**upload_1 (29)**	**upload_1 (expected)**	**upload_1 (over/under)**	**upload_1 (fold Enrichment)**	**upload_1 (raw P-value)**	**upload_1 (FDR)**
siderophore transmembrane transport (GO:0044718)	10	6	0.07	+	90.85	3.52E-10	3.73E-07
iron ion transmembrane transport (GO:0034755)	15	7	0.1	+	70.66	3.83E-11	6.08E-08

siderophore transport (GO:0015891)	20	8	0.13	+	60.57	3.41E-12	1.08E-08
membrane biogenesis (GO:0044091)	13	4	0.09	+	46.59	3.36E-06	7.10E-04
membrane assembly (GO:0071709)	13	4	0.09	+	46.59	3.36E-06	6.66E-04
Gram-negative-bacterium-type cell outer membrane assembly (GO:0043165)	13	4	0.09	+	46.59	3.36E-06	6.27E-04
cell envelope organization (GO:0043163)	13	4	0.09	+	46.59	3.36E-06	5.92E-04
bacteriocin transport (GO:0043213)	10	3	0.07	+	45.42	6.95E-05	6.69E-03
iron coordination entity transport (GO:1901678)	41	8	0.27	+	29.54	4.53E-10	3.59E-07
membrane organization (GO:0061024)	28	5	0.18	+	27.04	1.77E-06	4.01E-04
iron ion transport (GO:0006826)	51	8	0.34	+	23.75	2.13E-09	1.35E-06
protein localization to membrane (GO:0072657)	21	3	0.14	+	21.63	4.69E-04	4.02E-02

iron ion homeostasis (GO:0055072)	39	5	0.26	+	19.41	7.70E-06	1.22E-03
lipid localization (GO:0010876)	40	5	0.26	+	18.93	8.62E-06	1.30E-03
lipid transport (GO:0006869)	40	5	0.26	+	18.93	8.62E-06	1.24E-03
transition metal ion transport (GO:0000041)	73	8	0.48	+	16.59	2.82E-08	1.12E-05
transition metal ion homeostasis (GO:0055076)	48	5	0.32	+	15.77	1.95E-05	2.48E-03
metal ion homeostasis (GO:0055065)	53	5	0.35	+	14.28	3.05E-05	3.46E-03
cation homeostasis (GO:0055080)	62	5	0.41	+	12.21	6.17E-05	6.53E-03
inorganic ion homeostasis (GO:0098771)	63	5	0.42	+	12.02	6.63E-05	6.79E-03
ion homeostasis (GO:0050801)	63	5	0.42	+	12.02	6.63E-05	6.57E-03
chemical homeostasis (GO:0048878)	67	5	0.44	+	11.3	8.73E-05	8.16E-03

cellular localization (GO:0051641)	56	4	0.37	+	10.82	5.66E-04	4.73E-02
metal ion transport (GO:0030001)	118	8	0.78	+	10.27	9.06E-07	2.40E-04
inorganic cation transmembrane transport (GO:0098662)	108	7	0.71	+	9.81	6.53E-06	1.09E-03
macromolecule localization (GO:0033036)	143	9	0.94	+	9.53	2.95E-07	9.37E-05
inorganic ion transmembrane transport (GO:0098660)	124	7	0.82	+	8.55	1.55E-05	2.05E-03
homeostatic process (GO:0042592)	90	5	0.59	+	8.41	3.26E-04	2.87E-02
cation transmembrane transport (GO:0098655)	150	7	0.99	+	7.07	5.04E-05	5.52E-03
ion transmembrane transport (GO:0034220)	222	10	1.47	+	6.82	1.09E-06	2.65E-04
ion transport (GO:0006811)	399	14	2.64	+	5.31	6.53E-08	2.30E-05
cation transport (GO:0006812)	244	8	1.61	+	4.96	1.50E-04	1.36E-02

establishment of localization (GO:0051234)	721	19	4.76	+	3.99	5.44E-09	2.88E-06
organic substance transport (GO:0071702)	480	12	3.17	+	3.79	2.77E-05	3.26E-03
localization (GO:0051179)	766	19	5.06	+	3.76	1.51E-08	6.85E-06
transport (GO:0006810)	713	17	4.71	+	3.61	3.08E-07	8.88E-05
transmembrane transport (GO:0055085)	557	13	3.68	+	3.53	2.25E-05	2.74E-03
nitrogen compound metabolic process (GO:0006807)	1500	0	9.91	-	< 0.01	1.02E-05	1.40E-03
Export increased at least 2-fold with stress (From Table 3, Column 5 "up")*	ChiQ, E3PIP9, LoiP, LolB, LpoA, LpoB, MliC, NlpD, OmpW, OsmE, RcsF, RlpA, TibA, YajG, YajI, YfeY, YgdI, YgdR, YgiB, YifL, YraP						
	*No statistically significant results						

References

Aguilera L, Toloza L, Giménez R, et al. Proteomic analysis of outer membrane vesicles from the probiotic strain Escherichia coli Nissle 1917. *Proteomics*. 2014;14(2-3):222-9.

Nicoloff H, Gopalkrishnan S, Ades SE. Appropriate Regulation of the σ-Dependent Envelope Stress Response Is Necessary To Maintain Cell Envelope Integrity and Stationary-Phase Survival in Escherichia coli. *J Bacteriol*. 2017;199(12)

Alves NJ, Turner KB, Daniele MA, Oh E, Medintz IL, Walper SA. Bacterial Nanobioreactors--Directing Enzyme Packaging into Bacterial Outer Membrane Vesicles. *ACS Appl Mater Interfaces*. 2015;7(44):24963-72.

Alves NJ, Turner KB, Divito KA, Daniele MA, Walper SA. Affinity purification of bacterial outer membrane vesicles (OMVs) utilizing a His-tag mutant. *Res Microbiol*. 2017;168(2):139-146.

Alves NJ, Turner KB, Medintz IL, Walper SA. Protecting enzymatic function through directed packaging into bacterial outer membrane vesicles. *Sci Rep*. 2016;6:24866.

Anand S, Samuel M, Kumar S, Mathivanan S. Ticket to a bubble ride: Cargo sorting into exosomes and extracellular vesicles. *Biochim Biophys Acta Proteins Proteom*. 2019;1867(12):140203.

Arai H. Regulation and Function of Versatile Aerobic and Anaerobic Respiratory Metabolism in Pseudomonas aeruginosa. *Front Microbiol*. 2011;2:103.

Arat S, Bullerjahn GS, Laubenbacher R. A network biology approach to denitrification in Pseudomonas aeruginosa. *PLoS ONE*. 2015;10(2):e0118235.

Aridor M, Weissman J, Bannykh S, Nuoffer C, Balch WE. Cargo selection by the COPII budding machinery during export from the ER. *J Cell Biol*. 1998;141(1):61-70.

Arts IS, Gennaris A, Collet JF. Reducing systems protecting the bacterial cell envelope from oxidative damage. *FEBS Lett*. 2015;589(14):1559-68.

Ashburner M, Ball CA, Blake JA, et al. Gene ontology: tool for the unification of biology. The Gene Ontology Consortium. *Nat Genet*. 2000;25(1):25-9.

Avila-calderón ED, Otero-olarra JE, Flores-romo L, et al. The Outer Membrane Vesicles of ATCC 7966: A Proteomic Analysis and Effect on Host Cells. *Front Microbiol*. 2018;9:2765.

Ayalew S, Confer AW, Shrestha B, Wilson AE, Montelongo M. Proteomic analysis and immunogenicity of Mannheimia haemolytica vesicles. *Clin Vaccine Immunol*. 2013;20(2):191-6.

Bachurski D, Schuldner M, Nguyen PH, et al. Extracellular vesicle measurements with nanoparticle tracking analysis - An accuracy and repeatability comparison between NanoSight NS300 and ZetaView. *J Extracell Vesicles*. 2019;8(1):1596016.

Bager RJ, Persson G, Nesta B, et al. Outer membrane vesicles reflect environmental cues in Gallibacterium anatis. *Vet Microbiol*. 2013;167(3-4):565-72.

Baik SC, Kim KM, Song SM, et al. Proteomic analysis of the sarcosine-insoluble outer membrane fraction of Helicobacter pylori strain 26695. *J Bacteriol*. 2004;186(4):949-55.

Baker LM, Poole LB. Catalytic mechanism of thiol peroxidase from Escherichia coli. Sulfenic acid formation and overoxidation of essential CYS61. *J Biol Chem*. 2003;278(11):9203-11.

Ballok AE, Filkins LM, Bomberger JM, Stanton BA, O'toole GA. Epoxide-mediated differential packaging of Cif and other virulence factors into outer membrane vesicles. *J Bacteriol*. 2014;196(20):3633-42.

Barlowe C, Helenius A. Cargo Capture and Bulk Flow in the Early Secretory Pathway. *Annu Rev Cell Dev Biol*. 2016;32:197-222.

Barrett T, Wilhite SE, Ledoux P, et al. NCBI GEO: archive for functional genomics data sets--update. *Nucleic Acids Res*. 2013;41(Database issue):D991-5.

Baumgarten T, Sperling S, Seifert J, et al. Membrane vesicle formation as a multiple-stress response mechanism enhances Pseudomonas putida DOT-T1E cell surface hydrophobicity and biofilm formation. *Appl Environ Microbiol*. 2012;78(17):6217-24.

Baumgarten T, Vazquez J, Bastisch C, et al. Alkanols and chlorophenols cause different physiological adaptive responses on the level of cell surface properties and membrane vesicle formation in Pseudomonas putida DOT-T1E. *Appl Microbiol Biotechnol*. 2012;93(2):837-45.

Bearson BL, Lee IS, Casey TA. Escherichia coli O157 : H7 glutamate- and arginine-dependent acid-resistance systems protect against oxidative stress during extreme acid challenge. *Microbiology* (Reading, Engl). 2009;155(Pt 3):805-812.

Bentley R, Meganathan R. Biosynthesis of vitamin K (menaquinone) in bacteria. *Microbiol Rev*. 1982;46(3):241-80.

Bhunia, A., 2018. Escherichia coli. In: A. Bhunia, ed., Foodborne Microbial Pathogens: Mechanisms and Pathogenesis, 2nd ed. [online] New York: Springer-Verlag New York, pp.249-269. Available at: <https://www.springer.com/gp/book/9781493973477>.

Bielaszewska M, Rüter C, Bauwens A, et al. Host cell interactions of outer membrane vesicle-associated virulence factors of enterohemorrhagic Escherichia coli O157: Intracellular delivery, trafficking and mechanisms of cell injury. *PLoS Pathog*. 2017;13(2):e1006159.

Bienert S, Waterhouse A, De beer TA, et al. The SWISS-MODEL Repository-new features and functionality. *Nucleic Acids Res*. 2017;45(D1):D313-D319.

Biller SJ, Schubotz F, Roggensack SE, Thompson AW, Summons RE, Chisholm SW. Bacterial vesicles in marine ecosystems. *Science*. 2014;343(6167):183-6.

Bishop DG, Work E. An extracellular glycolipid produced by Escherichia coli grown under lysine-limiting conditions. *Biochem J*. 1965;96(2):567-76.

Blattner FR, Plunkett G, Bloch CA, et al. The complete genome sequence of Escherichia coli K-12. *Science*. 1997;277(5331):1453-62.

Blenkiron C, Simonov D, Muthukaruppan A, et al. Uropathogenic Escherichia coli Releases Extracellular Vesicles That Are Associated with RNA. *PLoS ONE*. 2016;11(8):e0160440.

Blesa A, Berenguer J. Contribution of vesicle-protected extracellular DNA to horizontal gene transfer in Thermus spp. *Int Microbiol*. 2015;18(3):177-87.

Blount ZD. The unexhausted potential of E. coli. *Elife*. 2015;4

Bodero MD, Pilonieta MC, Munson GP. Repression of the inner membrane lipoprotein NlpA by Rns in enterotoxigenic Escherichia coli. *J Bacteriol*. 2007;189(5):1627-32.

Bomberger JM, Maceachran DP, Coutermarsh BA, Ye S, O'toole GA, Stanton BA. Long-distance delivery of bacterial virulence factors by Pseudomonas aeruginosa outer membrane vesicles. *PLoS Pathog*. 2009;5(4):e1000382.

Bonnington KE, Kuehn MJ. Protein selection and export via outer membrane vesicles. *Biochim Biophys Acta*. 2014;1843(8):1612-9.

Bonnington KE, Kuehn MJ. Outer Membrane Vesicle Production Facilitates LPS Remodeling and Outer Membrane Maintenance in Salmonella during Environmental Transitions. *mBio*. 2016;7(5)

Braun V, Rehn K. Chemical characterization, spatial distribution and function of a lipoprotein (murein-lipoprotein) of the E. coli cell wall. The specific effect of trypsin on the membrane structure. *Eur J Biochem*. 1969;10(3):426-38.

Braun V. Covalent lipoprotein from the outer membrane of escherichia coli. *Biochim Biophys Acta Biomemb*. 1975;415(3):335-377.

Bürkner P-C. brms: An R Package for Bayesian Multilevel Models Using Stan. *J Stat Softw*. 2017;80(1).

Bürkner P-C. Advanced Bayesian Multilevel Modeling with the R Package brms. *R J*. 2018;10(1):395.

Cabiscol E, Tamarit J, Ros J. Oxidative stress in bacteria and protein damage by reactive oxygen species. *Int Microbio*l. 2000;3(1):3-8.

Cai Y, Wang R, An MM, Liang BB. Iron-Depletion prevents biofilm formation in Pseudomonas Aeruginosa through twitching mobility and quorum sensing. Braz *J Microbiol*. 2010;41(1):37-41.

Cascales E, Bernadac A, Gavioli M, Lazzaroni JC, Lloubes R. Pal lipoprotein of Escherichia coli plays a major role in outer membrane integrity. *J Bacteriol*. 2002;184(3):754-9.

Caspi R, Billington R, Keseler IM, et al. The MetaCyc database of metabolic pathways and enzymes - a 2019 update. *Nucleic Acids Res*. 2020;48(D1):D445-D453.

Castro BM, Torreno-piña JA, Van zanten TS, Gracia-parajo MF. Biochemical and imaging methods to study receptor membrane organization and association with lipid rafts. *Methods Cell Biol*. 2013;117:105-22.

Caza M, Kronstad JW. Shared and distinct mechanisms of iron acquisition by bacterial and fungal pathogens of humans. *Front Cell Infect Microbiol*. 2013;3:80.

CDC. Antibiotic Resistance Threats in the United States, 2019. Atlanta, GA: U.S. Department of Health and Human Services, CDC; 2019.

Celia H, Noinaj N, Zakharov SD, et al. Structural insight into the role of the Ton complex in energy transduction. *Nature*. 2016;538(7623):60-65.

Chakravorty S, Helb D, Burday M, Connell N, Alland D. A detailed analysis of 16S ribosomal RNA gene segments for the diagnosis of pathogenic bacteria. *J Microbiol Methods*. 2007;69(2):330-9.

Chan KW, Shone C, Hesp JR. Antibiotics and iron-limiting conditions and their effect on the production and composition of outer membrane vesicles secreted from clinical isolates of extraintestinal pathogenic E. coli. *Proteomics Clin Appl*. 2017;11(1-2).

Chang W, Small DA, Toghrol F, Bentley WE. Microarray analysis of Pseudomonas aeruginosa reveals induction of pyocin genes in response to hydrogen peroxide. *BMC Genomics*. 2005;6:115.

Charrin S, Jouannet S, Boucheix C, Rubinstein E. Tetraspanins at a glance. *J Cell Sci*. 2014;127(Pt 17):3641-8.

Chatterjee SN, Das J. Electron microscopic observations on the excretion of cell-wall material by Vibrio cholerae. *J Gen Microbiol*. 1967;49(1):1-11.

Chen L, Valentine JL, Huang CJ, et al. Outer membrane vesicles displaying engineered glycotopes elicit protective antibodies. *Proc Natl Acad Sci USA*. 2016;113(26):E3609-18.

Chen T, Guo J, Yang M, Zhu X, Cao X. Chemokine-containing exosomes are released from heat-stressed tumor cells via lipid raft-dependent pathway and act as efficient tumor vaccine. *J Immunol*. 2011;186(4):2219-28.

Chen Y, Liu L, Fu H, Wei C, Jin Q. Comparative proteomic analysis of outer membrane vesicles from Shigella flexneri under different culture conditions. *Biochem Biophys Res Commun*. 2014;453(4):696-702.

Chiu CH, Lee YT, Lin YC, et al. Bacterial membrane vesicles from induced by ceftazidime are more virulent than those induced by imipenem. *Virulence*. 2020;11(1):145-158.

Choi CW, Park EC, Yun SH, et al. Proteomic characterization of the outer membrane vesicle of Pseudomonas putida KT2440. *J Proteome Res*. 2014;13(10):4298-309.

Choi DS, Kim DK, Choi SJ, et al. Proteomic analysis of outer membrane vesicles derived from Pseudomonas aeruginosa. *Proteomics*. 2011;11(16):3424-9.

Chowdhury C, Jagannadham MV. Virulence factors are released in association with outer membrane vesicles of Pseudomonas syringae pv. tomato T1 during normal growth. *Biochim Biophys Acta*. 2013;1834(1):231-9.

Chung H, Bang W, Drake M. Stress Response of Escherichia coli. Comprehensive Reviews in Food Science and Food Safety. 2006;5(3):52-64.

Chutkan H, Kuehn MJ. Context-dependent activation kinetics elicited by soluble versus outer membrane vesicle-associated heat-labile enterotoxin. *Infect Immun*. 2011;79(9):3760-9.

Chutkan H, Macdonald I, Manning A, Kuehn MJ. Quantitative and qualitative preparations of bacterial outer membrane vesicles. *Methods Mol Biol*. 2013;966:259-72.

Claiborne A, Fridovich I. Purification of the o-dianisidine peroxidase from Escherichia coli B. Physicochemical characterization and analysis of its dual catalatic and peroxidatic activities. *J Biol Chem*. 1979;254(10):4245-52.

Claiborne A, Malinowski DP, Fridovich I. Purification and characterization of hydroperoxidase II of Escherichia coli B. *J Biol Chem*. 1979;254(22):11664-8.

Clough E, Barrett T. The Gene Expression Omnibus Database. *Methods Mol Biol*. 2016;1418:93-110.

Cocucci E, Racchetti G, Meldolesi J. Shedding microvesicles: artefacts no more. *Trends Cell Biol*. 2009;19(2):43-51.

Colombo M, Moita C, Van niel G, et al. Analysis of ESCRT functions in exosome biogenesis, composition and secretion highlights the heterogeneity of extracellular vesicles. *J Cell Sci*. 2013;126(Pt 24):5553-65.

Connell TD, Metzger DJ, Wang M, Jobling MG, Holmes RK. Initial studies of the structural signal for extracellular transport of cholera toxin and other proteins recognized by Vibrio cholerae. *Infect Immun*. 1995;63(10):4091-8.

Cooke AC, Nello AV, Ernst RK, Schertzer JW. Analysis of Pseudomonas aeruginosa biofilm membrane vesicles supports multiple mechanisms of biogenesis. *PLoS ONE*. 2019;14(2):e0212275.

Coves J, Fontecave M. Reduction and mobilization of iron by a NAD(P)H:flavin oxidoreductase from Escherichia coli. *Eur J Biochem*. 1993;211(3):635-41.

Cronan JE. Escherichia coli as an Experimental Organism. *eLS*. 2014.

Crossman LC, Chaudhuri RR, Beatson SA, et al. A commensal gone bad: complete genome sequence of the prototypical enterotoxigenic Escherichia coli strain H10407. *J Bacteriol*. 2010;192(21):5822-31.

De groote MA, Ochsner UA, Shiloh MU, et al. Periplasmic superoxide dismutase protects Salmonella from products of phagocyte NADPH-oxidase and nitric oxide synthase. *Proc Natl Acad Sci USA*. 1997;94(25):13997-4001.

De lise F, Mensitieri F, Rusciano G, et al. Novosphingobium sp. PP1Y as a novel source of outer membrane vesicles. *J Microbiol*. 2019;57(6):498-508.

De SN, Bhattacharya K, Sarkar JK. A study of the pathogenicity of strains of Bacterium coli from acute and chronic enteritis. *J Pathol Bacteriol*. 1956;71(1):201-9.

Deatherage BL, Lara JC, Bergsbaken T, Barrett SLR, Lara S, Cookson BT. Biogenesis of bacterial membrane vesicles. *Mol Microbiol*. 2009;72(6):1395-1407.

Devos S, Stremersch S, Raemdonck K, Braeckmans K, Devreese B. Intra- and Interspecies Effects of Outer Membrane Vesicles from Stenotrophomonas maltophilia on β-Lactam Resistance. *Antimicrob Agents Chemother*. 2016;60(4):2516-8.

Devos S, Van oudenhove L, Stremersch S, et al. The effect of imipenem and diffusible signaling factors on the secretion of outer membrane vesicles and associated Ax21 proteins in Stenotrophomonas maltophilia. *Front Microbiol*. 2015;6:298.

Dirienzo JM, Nakamura K, Inouye M. The outer membrane proteins of Gram-negative bacteria: biosynthesis, assembly, and functions. *Annu Rev Biochem*. 1978;47:481-532.

Dizdaroglu M. Measurement of radiation-induced damage to DNA at the molecular level. *Int J Radiat Biol*. 1992;61(2):175-83.

Domingues S, Nielsen KM. Membrane vesicles and horizontal gene transfer in prokaryotes. *Curr Opin Microbiol*. 2017;38:16-21.

Dominguez M, Dejgaard K, Füllekrug J, et al. gp25L/emp24/p24 protein family members of the cis-Golgi network bind both COP I and II coatomer. *J Cell Biol*. 1998;140(4):751-65.

Donaldson JG. Multiple roles for Arf6: sorting, structuring, and signaling at the plasma membrane. *J Biol Chem*. 2003;278(43):41573-6.

Dong TG, Dong S, Catalano C, Moore R, Liang X, Mekalanos JJ. Generation of reactive oxygen species by lethal attacks from competing microbes. *Proc Natl Acad Sci USA*. 2015;112(7):2181-6.

Donta ST, Moon HW, Whipp SC. Detection of heat-labile Escherichia coli enterotoxin with the use of adrenal cells in tissue culture. *Science*. 1974;183(4122):334-6.

Dwyer DJ, Collins JJ, Walker GC. Unraveling the physiological complexities of antibiotic lethality. *Annu Rev Pharmacol Toxicol*. 2015;55:313-32.

Dwyer DJ, Kohanski MA, Hayete B, Collins JJ. Gyrase inhibitors induce an oxidative damage cellular death pathway in Escherichia coli. *Mol Syst Biol*. 2007;3:91.

Ebanks RO, Goguen M, Mckinnon S, Pinto DM, Ross NW. Identification of the major outer membrane proteins of Aeromonas salmonicida. *Dis Aquat Org*. 2005;68(1):29-38.

Ebi.ac.uk. 2020. Bioinformatics Services | European Bioinformatics Institute. [online] Available at: <https://www.ebi.ac.uk/services> .

Edgar R, Domrachev M, Lash AE. Gene Expression Omnibus: NCBI gene expression and hybridization array data repository. *Nucleic Acids Res*. 2002;30(1):207-10.

Efron B, Tibshirani R, Storey JD, Tusher V. Empirical Bayes Analysis of a Microarray Experiment. *J Am Stat Assoc*. 2001;96(456):1151-1160.

Elhenawy W, Debelyy MO, Feldman MF. Preferential packing of acidic glycosidases and proteases into Bacteroides outer membrane vesicles. *mBio*. 2014;5(2):e00909-14.

Elhenawy W, Bording-jorgensen M, Valguarnera E, Haurat MF, Wine E, Feldman MF. LPS Remodeling Triggers Formation of Outer Membrane Vesicles in Salmonella. *mBio*. 2016;7(4)

Ellis TN, Kuehn MJ. Virulence and immunomodulatory roles of bacterial outer membrane vesicles. *Microbiol Mol Biol Rev*. 2010;74(1):81-94.

Elrod-erickson MJ, Kaiser CA. Genes that control the fidelity of endoplasmic reticulum to Golgi transport identified as suppressors of vesicle budding mutations. *Mol Biol Cell*. 1996;7(7):1043-58.

Escherich T. The intestinal bacteria of the neonate and breast-fed infant. 1885. *Rev Infect Dis*. 1989;11(2):352-6.

Esoda CN, Kuehn MJ. Pseudomonas aeruginosa Leucine Aminopeptidase Influences Early Biofilm Composition and Structure via Vesicle-Associated Antibiofilm Activity. *mBio*. 2019;10(6)

Evans DJ, Evans DG. Three characteristics associated with enterotoxigenic Escherichia coli isolated from man. *Infect Immun*. 1973;8(3):322-8.

Evans DJ, Fleiszig SM. Why does the healthy cornea resist Pseudomonas aeruginosa infection?. *Am J Ophthalmol*. 2013;155(6):961-970.e2.

Farr SB, Kogoma T. Oxidative stress responses in Escherichia coli and Salmonella typhimurium. *Microbiol Rev*. 1991;55(4):561-85.

Feitosa-junior OR, Stefanello E, Zaini PA, et al. Proteomic and Metabolomic Analyses of OMV-Enriched Fractions Reveal Association with Virulence Factors and Signaling Molecules of the DSF Family. *Phytopathology*. 2019;109(8):1344-1353.

Felício DL, Almeida CE, Silva AB, Leitão AC. Hydrogen peroxide induces a specific DNA base change profile in the presence of the iron chelator 2,2' dipyridyl in Escherichia coli. Braz *J Med Biol Res*. 2009;42(11):1015-9.

Ferreira D, Seca AML, C g a D, Silva AMS. Targeting human pathogenic bacteria by siderophores: A proteomics review. *J Proteomics*. 2016;145:153-166.

Ferreira TG, Trindade CNDR, Bell P, et al. Identification of the alpha-enolase P46 in the extracellular membrane vesicles of Bacteroides fragilis. *Mem Inst Oswaldo Cruz*. 2018;113(3):178-184.

Ferrer-Navarro M, Torrent G, Mongiardini E, Conchillo-solé O, Gibert I, Daura X. Proteomic analysis of outer membrane proteins and vesicles of a clinical isolate and a collection strain of Stenotrophomonas maltophilia. *J Proteomics*. 2016;142:122-9.

Filipe V, Hawe A, Jiskoot W. Critical evaluation of Nanoparticle Tracking Analysis (NTA) by NanoSight for the measurement of nanoparticles and protein aggregates. *Pharm Res*. 2010;27(5):796-810.

Fischer E, Strehlow B, Hartz D, Braun V. Soluble and membrane-bound ferrisiderophore reductases of Escherichia coli K-12. *Arch Microbiol*. 1990;153(4):329-36.

Fisher RA, Gollan B, Helaine S. Persistent bacterial infections and persister cells. *Nat Rev Microbiol*. 2017;15(8):453-464.

Fleckenstein JM, Hardwidge PR, Munson GP, Rasko DA, Sommerfelt H, Steinsland H. Molecular mechanisms of enterotoxigenic Escherichia coli infection. *Microbes Infect*. 2010;12(2):89-98.

Florez C, Raab JE, Cooke AC, Schertzer JW. Membrane Distribution of the Quinolone Signal Modulates Outer Membrane Vesicle Production in Pseudomonas aeruginosa. *mBio*. 2017;8(4)

Fontecave M, Eliasson R, Reichard P. NAD(P)H:flavin oxidoreductase of Escherichia coli. A ferric iron reductase participating in the generation of the free radical of ribonucleotide reductase. *J Biol Chem*. 1987;262(25):12325-31.

Forsberg CW, Beveridge TJ, Hellstrom A. Cellulase and Xylanase Release from Bacteroides succinogenes and Its Importance in the Rumen Environment. *Appl Environ Microbio*l. 1981;42(5):886-96.

Frias A, Manresa A, De oliveira E, López-iglesias C, Mercade E. Membrane vesicles: a common feature in the extracellular matter of cold-adapted antarctic bacteria. *Microb Ecol*. 2010;59(3):476-86.

Fulsundar S, Harms K, Flaten GE, Johnsen PJ, Chopade BA, Nielsen KM. Gene transfer potential of outer membrane vesicles of Acinetobacter baylyi and effects of stress on vesiculation. *Appl Environ Microbiol*. 2014;80(11):3469-83.

Fulsundar S, Kulkarni HM, Jagannadham MV, et al. Molecular characterization of outer membrane vesicles released from Acinetobacter radioresistens and their potential roles in pathogenesis. *Microb Pathog*. 2015;83-84:12-22.

Gamazo C, Moriyón I. Release of outer membrane fragments by exponentially growing Brucella melitensis cells. *Infect Immun*. 1987;55(3):609-15.

Gangalum RK, Atanasov IC, Zhou ZH, Bhat SP. AlphaB-crystallin is found in detergent-resistant membrane microdomains and is secreted via exosomes from human retinal pigment epithelial cells. *J Biol Chem*. 2011;286(5):3261-9.

Gankema H, Wensink J, Guinée PA, Jansen WH, Witholt B. Some characteristics of the outer membrane material released by growing enterotoxigenic Escherichia coli. *Infect Immun*. 1980;29(2):704-13.

Garin J, Diez R, Kieffer S, et al. The phagosome proteome: insight into phagosome functions. *J Cell Biol*. 2001;152(1):165-80.

Gasperini G, Biagini M, Arato V, et al. Outer Membrane Vesicles (OMV)-based and Proteomics-driven Antigen Selection Identifies Novel Factors Contributing to Adhesion to Epithelial Cells. *Mol Cell Proteomics*. 2018;17(2):205-215.

Glowczyk I, Wong A, Potempa B, et al. Inactive Gingipains from Selectively Skews T Cells toward a Th17 Phenotype in an IL-6 Dependent Manner. *Front Cell Infect Microbiol*. 2017;7:140.

Gnopo YMD, Watkins HC, Stevenson TC, Delisa MP, Putnam D. Designer outer membrane vesicles as immunomodulatory systems - Reprogramming bacteria for vaccine delivery. *Adv Drug Deliv Rev*. 2017;114:132-142.

Gonzales-siles L, Sjöling Å. The different ecological niches of enterotoxigenic Escherichia coli. *Environ Microbiol*. 2016;18(3):741-51.

Gottardo R, Raftery AE, Yeung KY, Bumgarner RE. Bayesian robust inference for differential gene expression in microarrays with multiple samples. *Biometrics*. 2006;62(1):10-8.

Grande R, Di giulio M, Bessa LJ, et al. Extracellular DNA in Helicobacter pylori biofilm: a backstairs rumour. *J Appl Microbiol*. 2011;110(2):490-8.

Grande R, Di marcantonio MC, Robuffo I, et al. Helicobacter pylori ATCC 43629/NCTC 11639 Outer Membrane Vesicles (OMVs) from Biofilm and Planktonic Phase Associated with Extracellular DNA (eDNA). *Front Microbiol*. 2015;6:1369.

Gwinn MR, Vallyathan V. Respiratory burst: role in signal transduction in alveolar macrophages. *J Toxicol Environ Health B Crit Rev*. 2006;9(1):27-39.

Gómez MI, Prince A. Opportunistic infections in lung disease: Pseudomonas infections in cystic fibrosis. *Curr Opin Pharmacol*. 2007;7(3):244-51.

Hagemann S, Stöger L, Kappelmann M, Hassl I, Ellinger A, Velimirov B. DNA-bearing membrane vesicles produced by Ahrensia kielensis and Pseudoalteromonas marina. *J Basic Microbiol*. 2014;54(10):1062-72.

Hassett DJ, Charniga L, Bean K, Ohman DE, Cohen MS. Response of Pseudomonas aeruginosa to pyocyanin: mechanisms of resistance, antioxidant defenses, and demonstration of a manganese-cofactored superoxide dismutase. *Infect Immun*. 1992;60(2):328-36.

Haurat MF, Aduse-opoku J, Rangarajan M, et al. Selective sorting of cargo proteins into bacterial membrane vesicles. *J Biol Chem*. 2011;286(2):1269-76.

Hayakawa M, Sugiyama S, Takamura T, et al. Neutrophils biosynthesize leukotoxin, 9, 10-epoxy-12-octadecenoate. *Biochem Biophys Res Commun*. 1986;137(1):424-430.

Hirst TR, Holmgren J. Transient entry of enterotoxin subunits into the periplasm occurs during their secretion from Vibrio cholerae. *J Bacteriol*. 1987;169(3):1037-45.

Hobot, J., 2015. Bacterial Ultrastructure. In: Y. Tang, M. Sussman, D. Liu, I. Poxton and J. Schwartzman, ed., Molecular Medical Microbiology, 2nd ed. [online] Boston: Academic Press, pp.7-32. Available at: <https://www.sciencedirect.com/book/9780123971692/molecular-medical-microbiology>.

Hodgkinson JT, Galloway WR, Saraf S, et al. Microwave and flow syntheses of Pseudomonas quinolone signal (PQS) and analogues. *Org Biomol Chem*. 2011;9(1):57-61.

Horstman AL, Kuehn MJ. Enterotoxigenic Escherichia coli secretes active heat-labile enterotoxin via outer membrane vesicles. *J Biol Chem*. 2000;275(17):12489-96.

Horstman AL, Kuehn MJ. Bacterial surface association of heat-labile enterotoxin through lipopolysaccharide after secretion via the general secretory pathway. *J Biol Chem*. 2002;277(36):32538-45.

Horstman AL, Bauman SJ, Kuehn MJ. Lipopolysaccharide 3-deoxy-D-manno-octulosonic acid (Kdo) core determines bacterial association of secreted toxins. *J Biol Chem*. 2004;279(9):8070-5.

Hudault S, Guignot J, Servin AL. Escherichia coli strains colonising the gastrointestinal tract protect germfree mice against Salmonella typhimurium infection. *Gut*. 2001;49(1):47-55.

Humphries KM, Szweda LI. Selective inactivation of alpha-ketoglutarate dehydrogenase and pyruvate dehydrogenase: reaction of lipoic acid with 4-hydroxy-2-nonenal. *Biochemistry*. 1998;37(45):15835-41.

Husain F, Humbard M, Misra R. Interaction between the TolC and AcrA proteins of a multidrug efflux system of Escherichia coli. *J Bacteriol*. 2004;186(24):8533-6.

Iconfinder. 2020. 4,625,000+ Free And Premium Vector Icons In SVG, PNG, CSH And AI Format.. [online] Available at: <https://www.iconfinder.com/> .

Irene C, Fantappiè L, Caproni E, et al. Bacterial outer membrane vesicles engineered with lipidated antigens as a platform for vaccine. *Proc Natl Acad Sci USA*. 2019;116(43):21780-21788.

Ishida H, Garcia-herrero A, Vogel HJ. The periplasmic domain of Escherichia coli outer membrane protein A can undergo a localized temperature dependent structural transition. *Biochim Biophys Acta*. 2014;1838(12):3014-24.

Ito Y, Kanamaru K, Taniguchi N, Miyamoto S, Tokuda H. A novel ligand bound ABC transporter, LolCDE, provides insights into the molecular mechanisms underlying membrane detachment of bacterial lipoproteins. *Mol Microbiol*. 2006;62(4):1064-75.

Jang KS, Sweredoski MJ, Graham RL, Hess S, Clemons WM. Comprehensive proteomic profiling of outer membrane vesicles from Campylobacter jejuni. *J Proteomics*. 2014;98:90-8.

Jeong W, Cha MK, Kim IH. Thioredoxin-dependent hydroperoxide peroxidase activity of bacterioferritin comigratory protein (BCP) as a new member of the thiol-specific antioxidant protein (TSA)/Alkyl hydroperoxide peroxidase C (AhpC) family. *J Biol Chem*. 2000;275(4):2924-30.

Jin JS, Moon DC, Choi C-W, et al. A Pathogenic Potential of Acinetobacter baumannii-Derived Membrane Vesicles. *J Anal Sci Technol*. 2011;2(Supplement A).

Jun SH, Lee JH, Kim BR, et al. Acinetobacter baumannii outer membrane vesicles elicit a potent innate immune response via membrane proteins. *PLoS ONE*. 2013;8(8):e71751.

Kadurugamuwa JL, Beveridge TJ. Virulence factors are released from Pseudomonas aeruginosa in association with membrane vesicles during normal growth and exposure to gentamicin: a novel mechanism of enzyme secretion. *J Bacteriol*. 1995;177(14):3998-4008.

Kahnt J, Aguiluz K, Koch J, et al. Profiling the outer membrane proteome during growth and development of the social bacterium Myxococcus xanthus by selective biotinylation and analyses of outer membrane vesicles. *J Proteome Res*. 2010;9(10):5197-208.

Kaiser C. Thinking about p24 proteins and how transport vesicles select their cargo. *Proc Natl Acad Sci USA*. 2000;97(8):3783-5.

Kato S, Kowashi Y, Demuth DR. Outer membrane-like vesicles secreted by Actinobacillus actinomycetemcomitans are enriched in leukotoxin. *Microb Pathog*. 2002;32(1):1-13.

Keenan JI, Allardyce RA. Iron influences the expression of Helicobacter pylori outer membrane vesicle-associated virulence factors. *Eur J Gastroenterol Hepatol*. 2000;12(12):1267-73.

Kesavan D, Vasudevan A, Wu L, et al. Integrative analysis of outer membrane vesicles proteomics and whole-cell transcriptome analysis of eravacycline induced Acinetobacter baumannii strains. *BMC Microbiol*. 2020;20(1):31.

Keseler IM, Mackie A, Santos-zavaleta A, et al. The EcoCyc database: reflecting new knowledge about Escherichia coli K-12. *Nucleic Acids Res*. 2017;45(D1):D543-D550.

Kesty NC, Mason KM, Reedy M, Miller SE, Kuehn MJ. Enterotoxigenic Escherichia coli vesicles target toxin delivery into mammalian cells. *EMBO J*. 2004;23(23):4538-49.

Kitagawa R, Takaya A, Ohya M, et al. Biogenesis of Salmonella enterica serovar typhimurium membrane vesicles provoked by induction of PagC. *J Bacteriol*. 2010;192(21):5645-56.

Klimentova J, Pavkova I, Horcickova L, et al. Francisella tularensis subsp. Releases Differentially Loaded Outer Membrane Vesicles Under Various Stress Conditions. *Front Microbiol*. 2019;10:2304.

Koebnik R, Locher KP, Van gelder P. Structure and function of bacterial outer membrane proteins: barrels in a nutshell. *Mol Microbiol*. 2000;37(2):239-53.

Koeppen K, Barnaby R, Jackson AA, Gerber SA, Hogan DA, Stanton BA. Tobramycin reduces key virulence determinants in the proteome of Pseudomonas aeruginosa outer membrane vesicles. *PLoS ONE*. 2019;14(1):e0211290.

Kohanski MA, Dwyer DJ, Hayete B, Lawrence CA, Collins JJ. A common mechanism of cellular death induced by bactericidal antibiotics. *Cell*. 2007;130(5):797-810.

Kojima S, Blair DF. The bacterial flagellar motor: structure and function of a complex molecular machine. *Int Rev Cytol*. 2004;233:93-134.

Korshunov S, Imlay JA. Detection and quantification of superoxide formed within the periplasm of Escherichia coli. *J Bacteriol*. 2006;188(17):6326-34.

Kovacs-simon A, Titball RW, Michell SL. Lipoproteins of bacterial pathogens. *Infect Immun*. 2011;79(2):548-61.

Krisko A, Copic T, Gabaldón T, Lehner B, Supek F. Inferring gene function from evolutionary change in signatures of translation efficiency. Genome Biol. 2014;15(3):R44.

Kuehn MJ, Herrmann JM, Schekman R. COPII-cargo interactions direct protein sorting into ER-derived transport vesicles. *Nature*. 1998;391(6663):187-90.

Kuehn MJ, Kesty NC. Bacterial outer membrane vesicles and the host-pathogen interaction. *Genes & Development*. 2005;19(22):2645-2655.

Kulkarni HM, Swamy ChV, Jagannadham MV. Molecular characterization and functional analysis of outer membrane vesicles from the antarctic bacterium Pseudomonas syringae suggest a possible response to environmental conditions. *J Proteome Res*. 2014;13(3):1345-58.

Kulkarni HM, Nagaraj R, Jagannadham MV. Protective role of E. coli outer membrane vesicles against antibiotics. *Microbiol Res*. 2015;181:1-7.

Kulp AJ, Sun B, Ai T, et al. Genome-Wide Assessment of Outer Membrane Vesicle Production in Escherichia coli. *PLoS ONE*. 2015;10(9):e0139200.

Kulp A, Kuehn MJ. Biological functions and biogenesis of secreted bacterial outer membrane vesicles. *Annu Rev Microbiol*. 2010;64:163-84.

Kwon SO, Gho YS, Lee JC, Kim SI. Proteome analysis of outer membrane vesicles from a clinical Acinetobacter baumannii isolate. *FEMS Microbiol Lett*. 2009;297(2):150-6.

Lagos L, Tandberg JI, Repnik U, et al. Characterization and Vaccine Potential of Membrane Vesicles Produced by Francisella noatunensis subsp. orientalis in an Adult Zebrafish Model. *Clin Vaccine Immunol*. 2017;24(5)

Lajoie P, Nabi IR. Lipid rafts, caveolae, and their endocytosis. *Int Rev Cell Mol Biol*. 2010;282:135-63.

Langlete P, Krabberød AK, Winther-larsen HC. Vesicles From Contain AT-Rich DNA and Shorter mRNAs That Do Not Correlate With Their Protein Products. *Front Microbiol*. 2019;10:2708.

Lappann M, Otto A, Becher D, Vogel U. Comparative proteome analysis of spontaneous outer membrane vesicles and purified outer membranes of Neisseria meningitidis. *J Bacteriol*. 2013;195(19):4425-35.

Lavoie C, Paiement J, Dominguez M, et al. Roles for alpha(2)p24 and COPI in endoplasmic reticulum cargo exit site formation. *J Cell Biol*. 1999;146(2):285-99.

Lee EY, Bang JY, Park GW, et al. Global proteomic profiling of native outer membrane vesicles derived from Escherichia coli. *Proteomics*. 2007;7(17):3143-53.

Lee JC, Lee EJ, Lee JH, et al. Klebsiella pneumoniae secretes outer membrane vesicles that induce the innate immune response. *FEMS Microbiol Lett*. 2012;331(1):17-24.

Lee JH, Wittki S, Bräu T, et al. HIV Nef, paxillin, and Pak1/2 regulate activation and secretion of TACE/ADAM10 proteases. *Mol Cell*. 2013;49(4):668-79.

Lee J, Kim SH, Choi DS, et al. Proteomic analysis of extracellular vesicles derived from Mycobacterium tuberculosis. *Proteomics*. 2015;15(19):3331-7.

Lee J, Lee EY, Kim SH, et al. Staphylococcus aureus extracellular vesicles carry biologically active β-lactamase. *Antimicrob Agents Chemother*. 2013;57(6):2589-95.

Lekmeechai S, Su YC, Brant M, et al. Outer Membrane Vesicles Protect the Pathogen From Reactive Oxygen Species of the Respiratory Burst. *Front Microbiol*. 2018;9:1837.

Lencer WI, Hirst TR, Holmes RK. Membrane traffic and the cellular uptake of cholera toxin. *Biochim Biophys Acta*. 1999;1450(3):177-90.

Li SP, Lin ZX, Jiang XY, Yu XY. Exosomal cargo-loading and synthetic exosome-mimics as potential therapeutic tools. *Acta Pharmacol Sin*. 2018;39(4):542-551.

Li ZT, Zhang RL, Bi XG, et al. Outer membrane vesicles isolated from two clinical Acinetobacter baumannii strains exhibit different toxicity and proteome characteristics. *Microb Pathog*. 2015;81:46-52.

Licznerska K, Nejman-faleńczyk B, Bloch S, et al. Oxidative Stress in Shiga Toxin Production by Enterohemorrhagic Escherichia coli. *Oxid Med Cell Longev*. 2016;2016:3578368.

Lin MC, Chen SY, Tsai HM, et al. PGE /EP Signaling Controls the Transfer of the Mammary Stem Cell State by Lipid Rafts in Extracellular Vesicles. *Stem Cells*. 2017;35(2):425-444.

Lin X, Wang Z, Li Y, Li J. Genome-wide transcriptional response of the Arctic bacterium Pseudoalteromonas sp. A2 to oxidative stress induced by hydrogen peroxide. *Acta Oceanol Sin*. 2016;35(12):73-80.

Liu GY, Nie P, Zhang J, Li N. Proteomic analysis of the sarcosine-insoluble outer membrane fraction of Flavobacterium columnare. *J Fish Dis*. 2008;31(4):269-76.

Liu J, Hsieh CL, Gelincik O, et al. Corrigendum to "Proteomic characterization of outer membrane vesicles from gut mucosa-derived fusobacterium nucleatum". J Proteomics. 2019 Jan 8;195:125-137. *J Proteomics*. 2019;200:161.

Liu Q, Yi J, Liang K, Zhang X, Liu Q. Salmonella Choleraesuis outer membrane vesicles: Proteomics and immunogenicity. *J Basic Microbiol*. 2017;57(10):852-861.

Liu X, Marrakchi M, Jahne M, Rogers S, Andreescu S. Real-time investigation of antibiotics-induced oxidative stress and superoxide release in bacteria using an electrochemical biosensor. *Free Radic Biol Med*. 2016;91:25-33.

Lynch JB, Schwartzman JA, Bennett BD, et al. Ambient pH Alters the Protein Content of Outer Membrane Vesicles, Driving Host Development in a Beneficial Symbiosis. *J Bacteriol*. 2019;201(20)

Macdonald IA, Kuehn MJ. Stress-induced outer membrane vesicle production by Pseudomonas aeruginosa. *J Bacteriol*. 2013;195(13):2971-81.

Maldonado R, Wei R, Kachlany SC, Kazi M, Balashova NV. Cytotoxic effects of Kingella kingae outer membrane vesicles on human cells. *Microb Pathog*. 2011;51(1-2):22-30.

Manda SO, Walls RE, Gilthorpe MS. A full Bayesian hierarchical mixture model for the variance of gene differential expression. *BMC Bioinformatics*. 2007;8:124.

Manning AJ, Kuehn MJ. Contribution of bacterial outer membrane vesicles to innate bacterial defense. *BMC Microbiol*. 2011;11:258.

Mantri CK, Chen CH, Dong X, et al. Fimbriae-mediated outer membrane vesicle production and invasion of Porphyromonas gingivalis. *Microbiologyopen*. 2015;4(1):53-65.

Maredia R, Devineni N, Lentz P, et al. Vesiculation from Pseudomonas aeruginosa under SOS. *Sci World J*. 2012;2012:402919.

Martora F, Pinto F, Folliero V, et al. Isolation, characterization and analysis of pro-inflammatory potential of Klebsiella pneumoniae outer membrane vesicles. *Microb Pathog*. 2019;136:103719.

Mashburn LM, Whiteley M. Membrane vesicles traffic signals and facilitate group activities in a prokaryote. *Nature*. 2005;437(7057):422-5.

Mashburn-warren L, Howe J, Garidel P, et al. Interaction of quorum signals with outer membrane lipids: insights into prokaryotic membrane vesicle formation. *Mol Microbiol.* 2008;69(2):491-502.

Masuda K, Matsuyama S, Tokuda H. Elucidation of the function of lipoprotein-sorting signals that determine membrane localization. *Proc Natl Acad Sci USA*. 2002;99(11):7390-5.

Mcbroom AJ, Johnson AP, Vemulapalli S, Kuehn MJ. Outer membrane vesicle production by Escherichia coli is independent of membrane instability. *J Bacteriol*. 2006;188(15):5385-92.

Mcbroom AJ, Kuehn MJ. Release of outer membrane vesicles by Gram-negative bacteria is a novel envelope stress response. *Mol Microbiol*. 2007;63(2):545-58.

McCaig WD, Koller A, Thanassi DG. Production of outer membrane vesicles and outer membrane tubes by Francisella novicida. *J Bacteriol*. 2013;195(6):1120-32.

McCaig WD, Loving CL, Hughes HR, Brockmeier SL. Characterization and Vaccine Potential of Outer Membrane Vesicles Produced by Haemophilus parasuis. *PLoS ONE*. 2016;11(3):e0149132.

McDougald D, Rice SA, Barraud N, Steinberg PD, Kjelleberg S. Should we stay or should we go: mechanisms and ecological consequences for biofilm dispersal. *Nat Rev Microbiol*. 2011;10(1):39-50.

Mcmahon KJ, Castelli ME, García Vescovi E, Feldman MF. Biogenesis of outer membrane vesicles in Serratia marcescens is thermoregulated and can be induced by activation of the Rcs phosphorelay system. *J Bacteriol*. 2012;194(12):3241-9.

McMillan, HM, Zebell SG, Ristaino JB, Dong X, Kuehn MJ. Protective Plant Immune Responses are Elicited by Bacterial Membrane Vesicles. 2020. Manuscript submitted for publication.

Mei GY, Tang J, Bach S, Kostrzynska M. Changes in Gene Transcription Induced by Hydrogen Peroxide Treatment of Verotoxin-Producing O157:H7 and Non-O157 Serotypes on Romaine Lettuce. *Front Microbiol*. 2017;8:477.

Merritt EA, Pronk SE, Sixma TK, Kalk KH, Van zanten BA, Hol WG. Structure of partially-activated E. coli heat-labile enterotoxin (LT) at 2.6 A resolution. *FEBS Lett*. 1994;337(1):88-92.

Metruccio MM, Evans DJ, Gabriel MM, Kadurugamuwa JL, Fleiszig SM. Pseudomonas aeruginosa Outer Membrane Vesicles Triggered by Human Mucosal Fluid and Lysozyme Can Prime Host Tissue Surfaces for Bacterial Adhesion. *Front Microbiol*. 2016;7:871.

Meyer DH, Fives-taylor PM. Characteristics of adherence of Actinobacillus actinomycetemcomitans to epithelial cells. *Infect Immun*. 1994;62(3):928-35.

Miller MB, Bassler BL. Quorum Sensing in Bacteria. *Annu Rev Microbiol*. 2001;55(1):165-199.

Missiakas D, Raina S. Protein folding in the bacterial periplasm. *J Bacteriol*. 1997;179(8):2465-2471.

Miyamoto S, Tokuda H. Diverse effects of phospholipids on lipoprotein sorting and ATP hydrolysis by the ABC transporter LolCDE complex. *Biochim Biophys Acta*. 2007;1768(7):1848-54.

Montgomery L, Flesher B, Stahl D. Transfer of Bacteroides succinogenes (Hungate) to Fibrobacter gen. nov. as Fibrobacter succinogenes comb. nov. and Description of Fibrobacter intestinalis sp. nov. *Int J Syst Bacteriol*. 1988;38(4):430-435.

Murphy K, Park AJ, Hao Y, Brewer D, Lam JS, Khursigara CM. Influence of O polysaccharides on biofilm development and outer membrane vesicle biogenesis in Pseudomonas aeruginosa PAO1. *J Bacteriol*. 2014;196(7):1306-17.

Nakayama H, Kurokawa K, Lee BL. Lipoproteins in bacteria: structures and biosynthetic pathways. *FEBS J*. 2012;279(23):4247-68.

Narita S, Tanaka K, Matsuyama S, Tokuda H. Disruption of lolCDE, encoding an ATP-binding cassette transporter, is lethal for Escherichia coli and prevents release of lipoproteins from the inner membrane. *J Bacteriol*. 2002;184(5):1417-22.

Narita S, Tokuda H. An ABC transporter mediating the membrane detachment of bacterial lipoproteins depending on their sorting signals. *FEBS Lett*. 2006;580(4):1164-70.

Narita SI, Tokuda H. Bacterial lipoproteins; biogenesis, sorting and quality control. *Biochim Biophys Acta Mol Cell Biol Lipids*. 2017;1862(11):1414-1423.

Nevermann J, Silva A, Otero C, et al. Identification of Genes Involved in Biogenesis of Outer Membrane Vesicles (OMVs) in Salmonella enterica Serovar Typhi. *Front Microbiol*. 2019;10:104.

Nguyen Y, Sperandio V. Enterohemorrhagic E. coli (EHEC) pathogenesis. *Front Cell Infect Microbiol*. 2012;2:90.

Nikaido H. Multiple antibiotic resistance and efflux. *Curr Opin Microbiol*. 1998;1(5):516-523.

Nikaido H. The Limitations of LB Medium. Small Things Considered. https://schaechter.asmblog.org/schaechter/2009/11/the-limitations-of-lb-medium.html. Published November 9, 2009.

Nikaido H, Takatsuka Y. Mechanisms of RND multidrug efflux pumps. *Biochim Biophys Acta.* 2009;1794(5):769-81.

Nishimura N, Balch WE. A di-acidic signal required for selective export from the endoplasmic reticulum. *Science*. 1997;277(5325):556-8.

Noinaj N, Guillier M, Barnard TJ, Buchanan SK. TonB-dependent transporters: regulation, structure, and function. *Annu Rev Microbiol*. 2010;64:43-60.

Noland CL, Kattke MD, Diao J, et al. Structural insights into lipoprotein N-acylation by apolipoprotein N-acyltransferase. *Proc Natl Acad Sci USA*. 2017;114(30):E6044-E6053.

Oboeipr.com. 2020. OBOE IPR. [online] Available at: <http://oboeipr.com/>.

Okuda S, Tokuda H. Lipoprotein sorting in bacteria. *Annu Rev Microbiol*. 2011;65:239-59.

Oliveira P, Martins NM, Santos M, Couto NA, Wright PC, Tamagnini P. The Anabaena sp. PCC 7120 Exoproteome: Taking a Peek outside the Box. *Life* (Basel). 2015;5(1):130-63.

Oliver C, Hernández MA, Tandberg JI, et al. The Proteome of Biologically Active Membrane Vesicles from LF-89 Type Strain Identifies Plasmid-Encoded Putative Toxins. *Front Cell Infect Microbiol*. 2017;7:420.

Olofsson A, Vallström A, Petzold K, et al. Biochemical and functional characterization of Helicobacter pylori vesicles. *Mol Microbiol*. 2010;77(6):1539-55.

Ong SE, Mann M. Mass spectrometry-based proteomics turns quantitative. *Nat Chem Biol*. 2005;1(5):252-62.

Orench-Rivera N, Kuehn MJ. Environmentally controlled bacterial vesicle-mediated export. *Cell Microbiol*. 2016;18(11):1525-1536.

Ortiz-Suarez ML, Samsudin F, Piggot TJ, Bond PJ, Khalid S. Full-Length OmpA: Structure, Function, and Membrane Interactions Predicted by Molecular Dynamics Simulations. *Biophys J*. 2016;111(8):1692-1702.

Pagès JM, Amaral L. Mechanisms of drug efflux and strategies to combat them: challenging the efflux pump of Gram-negative bacteria. *Biochim Biophys Acta*. 2009;1794(5):826-33.

Palmieri V, Lucchetti D, Gatto I, et al. Dynamic light scattering for the characterization and counting of extracellular vesicles: a powerful noninvasive tool. *J Nanopart Res*. 2014;16(9).

Park AJ, Murphy K, Surette MD, et al. Tracking the Dynamic Relationship between Cellular Systems and Extracellular Subproteomes in Pseudomonas aeruginosa Biofilms. *J Proteome Res*. 2015;14(11):4524-37.

Park JS, Lee WC, Yeo KJ, et al. Mechanism of anchoring of OmpA protein to the cell wall peptidoglycan of the gram-negative bacterial outer membrane. *FASEB J*. 2012;26(1):219-28.

Partridge JD, Scott C, Tang Y, Poole RK, Green J. Escherichia coli transcriptome dynamics during the transition from anaerobic to aerobic conditions. *J Biol Chem*. 2006;281(38):27806-15.

Pawelek PD, Croteau N, Ng-thow-hing C, et al. Structure of TonB in complex with FhuA, E. coli outer membrane receptor. *Science*. 2006;312(5778):1399-402.

Pencer J, Hallett FR. Effects of Vesicle Size and Shape on Static and Dynamic Light Scattering Measurements. *Langmuir*. 2003;19(18):7488-7497.

Pérez-Cruz C, Carrión O, Delgado L, Martinez G, López-iglesias C, Mercade E. New type of outer membrane vesicle produced by the Gram-negative bacterium Shewanella vesiculosa M7T: implications for DNA content. *Appl Environ Microbiol*. 2013;79(6):1874-81.

Pierson T, Matrakas D, Taylor YU, et al. Proteomic characterization and functional analysis of outer membrane vesicles of Francisella novicida suggests possible role in virulence and use as a vaccine. *J Proteome Res*. 2011;10(3):954-67.

Pizarro-Cerdá J, Cossart P. Bacterial adhesion and entry into host cells. *Cell*. 2006;124(4):715-27.

Pos KM. Drug transport mechanism of the AcrB efflux pump. *Biochim Biophys Acta*. 2009;1794(5):782-93.

Prados-Rosales R, Baena A, Martinez LR, et al. Mycobacteria release active membrane vesicles that modulate immune responses in a TLR2-dependent manner in mice. *J Clin Invest*. 2011;121(4):1471-83.

Prados-Rosales R, Weinrick BC, Piqué DG, Jacobs WR, Casadevall A, Rodriguez GM. Role for Mycobacterium tuberculosis membrane vesicles in iron acquisition. *J Bacteriol*. 2014;196(6):1250-6.

Qadri F, Svennerholm A-M, Faruque ASG, Sack RB. Enterotoxigenic Escherichia coli in Developing Countries: Epidemiology, Microbiology, Clinical Features, Treatment, and Prevention. *Clin Microbiol Rev*. 2005;18(3):465-483.

Quintana M, Viele K, Lewis RJ. Bayesian Analysis: Using Prior Information to Interpret the Results of Clinical Trials. *JAMA*. 2017;318(16):1605-1606.

Raetz CR. Bacterial endotoxins: extraordinary lipids that activate eucaryotic signal transduction. *J Bacteriol*. 1993;175(18):5745-53.

Raetz CR, Dowhan W. Biosynthesis and function of phospholipids in Escherichia coli. *J Biol Chem*. 1990;265(3):1235-8.

Raivio TL. Envelope stress responses and Gram-negative bacterial pathogenesis. *Mol Microbiol.* 2005;56(5):1119-28.

Raposo G, Stoorvogel W. Extracellular vesicles: exosomes, microvesicles, and friends. *J Cell Biol*. 2013;200(4):373-83.

Rassam P, Copeland NA, Birkholz O, et al. Supramolecular assemblies underpin turnover of outer membrane proteins in bacteria. *Nature*. 2015;523(7560):333-6.

Renelli M, Matias V, Lo RY, Beveridge TJ. DNA-containing membrane vesicles of Pseudomonas aeruginosa PAO1 and their genetic transformation potential. *Microbiology (Reading, Engl).* 2004;150(Pt 7):2161-2169.

Reyes-Robles T, Dillard RS, Cairns LS, et al. Vibrio cholerae Outer Membrane Vesicles Inhibit Bacteriophage Infection. *J Bacteriol*. 2018;200(15)

Brisson AR. Comment on "Quality of extracellular vesicle images by transmission electron microscopy is operator and protocol dependent". *J Extracell Vesicles*. 2019;8(1):1648996.

Roier S, Zingl FG, Cakar F, et al. A novel mechanism for the biogenesis of outer membrane vesicles in Gram-negative bacteria. *Nat Commun*. 2016;7:10515.

Rollauer SE, Sooreshjani MA, Noinaj N, Buchanan SK. Outer membrane protein biogenesis in Gram-negative bacteria. *Philos Trans R Soc Lond, B, Biol Sci*. 2015;370(1679)

Rumbo C, Fernández-moreira E, Merino M, et al. Horizontal transfer of the OXA-24 carbapenemase gene via outer membrane vesicles: a new mechanism of dissemination of carbapenem resistance genes in Acinetobacter baumannii. *Antimicrob Agents Chemother*. 2011;55(7):3084-90.

Sack RB, Gorbach SL, Banwell JG, Jacobs B, Chatterjee BD, Mitra RC. Enterotoxigenic Escherichia coli isolated from patients with severe cholera-like disease. *J Infect Dis*. 1971;123(4):378-85.

Sakamoto C, Satou R, Tokuda H, Narita S. Novel mutations of the LolCDE complex causing outer membrane localization of lipoproteins despite their inner membrane-retention signals. *Biochem Biophys Res Commun*. 2010;401(4):586-91.

Salvachúa D, Karp EM, Nimlos CT, Vardon DR, Beckham GT. Towards lignin consolidated bioprocessing: simultaneous lignin depolymerization and product generation by bacteria. *Green Chem*. 2015;17(11):4951-4967.

Salvachúa D, Werner AZ, Pardo I, et al. Outer membrane vesicles catabolize lignin-derived aromatic compounds in KT2440. *Proc Natl Acad Sci USA*. 2020;117(17):9302-9310.

Samsudin F, Ortiz-suarez ML, Piggot TJ, Bond PJ, Khalid S. OmpA: A Flexible Clamp for Bacterial Cell Wall Attachment. *Structure*. 2016;24(12):2227-2235.

Sandkvist M, Michel LO, Hough LP, et al. General secretion pathway (eps) genes required for toxin secretion and outer membrane biogenesis in Vibrio cholerae. *J Bacteriol*. 1997;179(22):6994-7003.

Scandella CJ, Kornberg A. A membrane-bound phospholipase A1 purified from Escherichia coli. *Biochemistry*. 1971;10(24):4447-56.

Schaar V, Nordström T, Mörgelin M, Riesbeck K. Moraxella catarrhalis outer membrane vesicles carry β-lactamase and promote survival of Streptococcus pneumoniae and Haemophilus influenzae by inactivating amoxicillin. *Antimicrob Agents Chemother*. 2011;55(8):3845-53.

Schertzer JW, Brown SA, Whiteley M. Oxygen levels rapidly modulate Pseudomonas aeruginosa social behaviours via substrate limitation of PqsH. *Mol Microbiol*. 2010;77(6):1527-38.

Schertzer JW, Whiteley M. A bilayer-couple model of bacterial outer membrane vesicle biogenesis. *mBio*. 2012;3(2).

Schindler M, Osborn MJ, Koppel DE. Lateral diffusion of lipopolysaccharide in the outer membrane of Salmonella typhimurium. *Nature*. 1980;285(5762):261-3.

Schooling SR, Beveridge TJ. Membrane vesicles: an overlooked component of the matrices of biofilms. *J Bacteriol*. 2006;188(16):5945-57.

Schuh AL, Audhya A. The ESCRT machinery: from the plasma membrane to endosomes and back again. *Crit Rev Biochem Mol Biol*. 2014;49(3):242-61.

Schwechheimer C, Kuehn MJ. Synthetic effect between envelope stress and lack of outer membrane vesicle production in Escherichia coli. *J Bacteriol*. 2013;195(18):4161-73.

Schwechheimer C, Kuehn MJ. Outer-membrane vesicles from Gram-negative bacteria: biogenesis and functions. *Nat Rev Microbiol*. 2015;13(10):605-19.

Schwechheimer C, Kulp A, Kuehn MJ. Modulation of bacterial outer membrane vesicle production by envelope structure and content. *BMC Microbiol*. 2014;14:324.

Schwechheimer C, Rodriguez DL, Kuehn MJ. NlpI-mediated modulation of outer membrane vesicle production through peptidoglycan dynamics in Escherichia coli. *Microbiologyopen*. 2015;4(3):375-89.

Sears CL, Kaper JB. Enteric bacterial toxins: mechanisms of action and linkage to intestinal secretion. *Microbiol Rev*. 1996;60(1):167-215.

Seaver LC, Imlay JA. Alkyl hydroperoxide reductase is the primary scavenger of endogenous hydrogen peroxide in Escherichia coli. *J Bacteriol*. 2001a;183(24):7173-81.

Seaver LC, Imlay JA. Hydrogen peroxide fluxes and compartmentalization inside growing Escherichia coli. *J Bacteriol*. 2001b;183(24):7182-9.

Sezonov G, Joseleau-petit D, D'ari R. Escherichia coli physiology in Luria-Bertani broth. *J Bacteriol*. 2007;189(23):8746-9.

Sharpe SW, Kuehn MJ, Mason KM. Elicitation of epithelial cell-derived immune effectors by outer membrane vesicles of nontypeable Haemophilus influenzae. *Infect Immun*. 2011;79(11):4361-9.

Shen HH, Leyton DL, Shiota T, et al. Reconstitution of a nanomachine driving the assembly of proteins into bacterial outer membranes. *Nat Commun*. 2014;5:5078.

Shetty A, Chen S, Tocheva EI, Jensen GJ, Hickey WJ. Nanopods: a new bacterial structure and mechanism for deployment of outer membrane vesicles. *PLoS ONE*. 2011;6(6):e20725.

Shetty A, Hickey WJ. Effects of outer membrane vesicle formation, surface-layer production and nanopod development on the metabolism of phenanthrene by Delftia acidovorans Cs1-4. *PLoS ONE*. 2014;9(3):e92143.

Shoberg RJ, Thomas DD. Specific adherence of Borrelia burgdorferi extracellular vesicles to human endothelial cells in culture. *Infect Immun*. 1993;61(9):3892-900.

Shultis DD, Purdy MD, Banchs CN, Wiener MC. Outer membrane active transport: structure of the BtuB:TonB complex. *Science*. 2006;312(5778):1396-9.

Sies H. Damage to plasmid DNA by singlet oxygen and its protection. *Mutat Res*. 1993;299(3-4):183-91.

Sies H, Menck CF. Singlet oxygen induced DNA damage. *Mutat Research/DNAging*. 1992;275(3-6):367-375.

Silhavy TJ, Kahne D, Walker S. The Bacterial Cell Envelope. *Cold Spring Harb Perspect Biol*. 2010;2(5).

Singh AK, Shin JH, Lee KL, Imlay JA, Roe JH. Comparative study of SoxR activation by redox-active compounds. *Mol Microbiol*. 2013;90(5):983-96.

Singh PK, Parsek MR, Greenberg EP, Welsh MJ. A component of innate immunity prevents bacterial biofilm development. *Nature*. 2002;417(6888):552-5.

Sixma TK, Pronk SE, Kalk KH, et al. Crystal structure of a cholera toxin-related heat-labile enterotoxin from E. coli. *Nature*. 1991;351(6325):371-7.

Sjöström AE, Sandblad L, Uhlin BE, Wai SN. Membrane vesicle-mediated release of bacterial RNA. *Sci Rep*. 2015;5:15329.

Slauch JM. How does the oxidative burst of macrophages kill bacteria? Still an open question. *Mol Microbiol*. 2011;80(3):580-3.

Spangler BD. Structure and function of cholera toxin and the related Escherichia coli heat-labile enterotoxin. *Microbiol Rev*. 1992;56(4):622-47.

Springer S, Chen E, Duden R, et al. The p24 proteins are not essential for vesicular transport in Saccharomyces cerevisiae. *Proc Natl Acad Sci USA*. 2000;97(8):4034-4039.

Sridhar S, Steele-mortimer O. Inherent Variability of Growth Media Impacts the Ability of Salmonella Typhimurium to Interact with Host Cells. *PLoS ONE*. 2016;11(6):e0157043.

Stapleton F, Dart J. Pseudomonas keratitis associated with biofilm formation on a disposable soft contact lens. *Br J Ophthalmol*. 1995;79(9):864-5.

Staubach S, Razawi H, Hanisch FG. Proteomics of MUC1-containing lipid rafts from plasma membranes and exosomes of human breast carcinoma cells MCF-7. *Proteomics*. 2009;9(10):2820-35.

Stewart JC. Colorimetric determination of phospholipids with ammonium ferrothiocyanate. *Anal Biochem*. 1980;104(1):10-4.

Sutcliffe JA, O'brien W, Fyfe C, Grossman TH. Antibacterial activity of eravacycline (TP-434), a novel fluorocycline, against hospital and community pathogens. *Antimicrob Agents Chemother*. 2013;57(11):5548-58.

Suzuki H, Nishimura Y, Yasuda S, Nishimura A, Yamada M, Hirota Y. Murein-lipoprotein of Escherichia coli: a protein involved in the stabilization of bacterial cell envelope. *Mol Gen Genet*. 1978;167(1):1-9.

Szewczyk J, Collet JF. The Journey of Lipoproteins Through the Cell: One Birthplace, Multiple Destinations. *Adv Microb Physiol*. 2016;69:1-50.

Taboada H, Meneses N, Dunn MF, et al. Proteins in the periplasmic space and outer membrane vesicles of Rhizobium etli CE3 grown in minimal medium are largely distinct and change with growth phase. *Microbiology (Reading, Engl)*. 2019;165(6):638-650.

Taheri N, Fällman M, Wai SN, Fahlgren A. Accumulation of virulence-associated proteins in Campylobacter jejuni Outer Membrane Vesicles at human body temperature. *J Proteomics*. 2019;195:33-40.

Taheri N, Mahmud AKMF, Sandblad L, Fällman M, Wai SN, Fahlgren A. Campylobacter jejuni bile exposure influences outer membrane vesicles protein content and bacterial interaction with epithelial cells. *Sci Rep*. 2018;8(1):16996.

Tam C, Mun JJ, Evans DJ, Fleiszig SM. The impact of inoculation parameters on the pathogenesis of contact lens-related infectious keratitis. *Invest Ophthalmol Vis Sci*. 2010;51(6):3100-6.

Tamarit J, Cabiscol E, Ros J. Identification of the major oxidatively damaged proteins in Escherichia coli cells exposed to oxidative stress. *J Biol Chem*. 1998;273(5):3027-32.

Tashiro Y, Ichikawa S, Shimizu M, et al. Variation of physiochemical properties and cell association activity of membrane vesicles with growth phase in Pseudomonas aeruginosa. *Appl Environ Microbiol*. 2010;76(11):3732-9.

Tauschek M, Gorrell RJ, Strugnell RA, Robins-browne RM. Identification of a protein secretory pathway for the secretion of heat-labile enterotoxin by an enterotoxigenic strain of Escherichia coli. *Proc Natl Acad Sci USA*. 2002;99(10):7066-71.

Tenaillon O, Skurnik D, Picard B, Denamur E. The population genetics of commensal Escherichia coli. *Nat Rev Microbiol*. 2010;8(3):207-17.

Toyofuku M, Zhou S, Sawada I, Takaya N, Uchiyama H, Nomura N. Membrane vesicle formation is associated with pyocin production under denitrifying conditions in Pseudomonas aeruginosa PAO1. *Environ Microbiol*. 2014;16(9):2927-38.

Toyofuku M. Bacterial communication through membrane vesicles. *Biosci Biotechnol Biochem*. 2019;83(9):1599-1605.

Toyofuku M, Morinaga K, Hashimoto Y, et al. Membrane vesicle-mediated bacterial communication. *ISME J*. 2017;11(6):1504-1509.

Toyofuku M, Roschitzki B, Riedel K, Eberl L. Identification of proteins associated with the Pseudomonas aeruginosa biofilm extracellular matrix. *J Proteome Res*. 2012;11(10):4906-15.

Tricarico C, Clancy J, D'souza-schorey C. Biology and biogenesis of shed microvesicles. *Small GTPases*. 2017;8(4):220-232.

Tsai SC, Noda M, Adamik R, Moss J, Vaughan M. Enhancement of choleragen ADP-ribosyltransferase activities by guanyl nucleotides and a 19-kDa membrane protein. *Proc Natl Acad Sci USA*. 1987;84(15):5139-42.

Uniprot Consortium T. UniProt: the universal protein knowledgebase. *Nucleic Acids Research*. 2018;46(5):2699-2699.

Vadillo-Rodriguez V, Schooling SR, Dutcher JR. In situ characterization of differences in the viscoelastic response of individual gram-negative and gram-positive bacterial cells. *J Bacteriol*. 2009;191(17):5518-25.

Valapala M, Vishwanatha JK. Lipid raft endocytosis and exosomal transport facilitate extracellular trafficking of annexin A2. *J Biol Chem*. 2011;286(35):30911-25.

Valeru SP, Shanan S, Alossimi H, Saeed A, Sandström G, Abd H. Lack of Outer Membrane Protein A Enhances the Release of Outer Membrane Vesicles and Survival of Vibrio cholerae and Suppresses Viability of Acanthamoeba castellanii. *Int J Microbiol*. 2014;2014:610190.

Valguarnera E, Scott NE, Azimzadeh P, Feldman MF. Surface Exposure and Packing of Lipoproteins into Outer Membrane Vesicles Are Coupled Processes in Bacteroides. *mSphere*. 2018;3(6)

van de schoot R, Kaplan D, Denissen J, Asendorpf JB, Neyer FJ, Van aken MAG. A gentle introduction to bayesian analysis: applications to developmental research. *Child Dev*. 2014;85(3):842-860.

van de waterbeemd B, Zomer G, Van den ijssel J, et al. Cysteine depletion causes oxidative stress and triggers outer membrane vesicle release by Neisseria meningitidis; implications for vaccine development. *PLoS ONE*. 2013;8(1):e54314.

van der heijden J, Reynolds LA, Deng W, et al. Salmonella Rapidly Regulates Membrane Permeability To Survive Oxidative Stress. *mBio*. 2016;7(4)

Van der pol E, Hoekstra AG, Sturk A, Otto C, Van leeuwen TG, Nieuwland R. Optical and non-optical methods for detection and characterization of microparticles and exosomes. *J Thromb Haemost*. 2010;8(12):2596-607.

van der westhuizen WA, Theron CW, Boucher CE, Bragg RR. Regulation of outer-membrane proteins (OMPs) A and F, during -induced outer-membrane vesicle (OMV) biosynthesis. *Heliyon*. 2019;5(7):e02014.

Van gelder P, Steiert M, El khattabi M, Rosenbusch JP, Tommassen J. Structural and functional characterization of a His-tagged PhoE pore protein of Escherichia coli. *Biochem Biophys Res Commun*. 1996;229(3):869-75.

van hoek ML. Biofilms: an advancement in our understanding of Francisella species. *Virulence*. 2013;4(8):833-46.

Veith PD, Chen YY, Gorasia DG, et al. Porphyromonas gingivalis outer membrane vesicles exclusively contain outer membrane and periplasmic proteins and carry a cargo enriched with virulence factors. *J Proteome Res*. 2014;13(5):2420-32.

Veith PD, Glew MD, Gorasia DG, Chen D, O'brien-simpson NM, Reynolds EC. Localization of Outer Membrane Proteins in Treponema denticola by Quantitative Proteome Analyses of Outer Membrane Vesicles and Cellular Fractions. *J Proteome Res*. 2019;18(4):1567-1581.

Veith PD, Luong C, Tan KH, Dashper SG, Reynolds EC. Outer Membrane Vesicle Proteome of Porphyromonas gingivalis Is Differentially Modulated Relative to the Outer Membrane in Response to Heme Availability. *J Proteome Res*. 2018;17(7):2377-2389.

Verhoeven GS, Dogterom M, Den blaauwen T. Absence of long-range diffusion of OmpA in E. coli is not caused by its peptidoglycan binding domain. *BMC Microbiol*. 2013;13:66.

Vert M, Doi Y, Hellwich K-H, et al. Terminology for biorelated polymers and applications (IUPAC Recommendations 2012). *Pure Appl Chem*. 2012;84(2):377-410.

Vollmer W, Blanot D, De Pedro MA. Peptidoglycan structure and architecture. *FEMS Microbiol Rev*. 2008;32(2):149-67.

Wai SN, Lindmark B, Söderblom T, et al. Vesicle-mediated export and assembly of pore-forming oligomers of the enterobacterial ClyA cytotoxin. *Cell*. 2003;115(1):25-35.

Walker WL, Liao IH, Gilbert DL, et al. Empirical Bayes accomodation of batch-effects in microarray data using identical replicate reference samples: application to RNA expression profiling of blood from Duchenne muscular dystrophy patients. *BMC Genomics*. 2008;9:494.

Wallecha A, Correnti J, Munster V, Van der woude M. Phase variation of Ag43 is independent of the oxidation state of OxyR. *J Bacteriol*. 2003;185(7):2203-9.

Walther DM, Rapaport D, Tommassen J. Biogenesis of β-barrel membrane proteins in bacteria and eukaryotes: evolutionary conservation and divergence. *Cell Mol Life Sci*. 2009;66(17):2789-2804.

Wang X, Kim Y, Ma Q, et al. Cryptic prophages help bacteria cope with adverse environments. *Nat Commun*. 2010;1:147.

Wang Y. The function of OmpA in Escherichia coli. *Biochem Biophys Res Commun*. 2002;292(2):396-401.

Wang Z, Fan G, Hryc CF, et al. An allosteric transport mechanism for the AcrAB-TolC multidrug efflux pump. *Elife*. 2017;6

Werner E, Roe F, Bugnicourt A, et al. Stratified growth in Pseudomonas aeruginosa biofilms. *Appl Environ Microbiol*. 2004;70(10):6188-96.

Wessel AK, Liew J, Kwon T, Marcotte EM, Whiteley M. Role of Pseudomonas aeruginosa peptidoglycan-associated outer membrane proteins in vesicle formation. *J Bacteriol*. 2013;195(2):213-9.

Whitworth DE, Slade SE, Mironas A. Composition of distinct sub-proteomes in Myxococcus xanthus: metabolic cost and amino acid availability. *Amino Acids*. 2015;47(12):2521-31.

Wikipedia.org. 2020. Wikipedia. [online] Available at: <https://www.wikipedia.org/>.

Wimley WC. The versatile beta-barrel membrane protein. *Curr Opin Struct Biol*. 2003;13(4):404-11.

Xu KD, Stewart PS, Xia F, Huang CT, Mcfeters GA. Spatial physiological heterogeneity in Pseudomonas aeruginosa biofilm is determined by oxygen availability. *Appl Environ Microbiol*. 1998;64(10):4035-9.

Yem DW, Wu HC. Physiological characterization of an Escherichia coli mutant altered in the structure of murein lipoprotein. *J Bacteriol*. 1978;133(3):1419-26.

Yennawar NH, Fecko JA, Showalter SA, Bevilacqua PC. A High-Throughput Biological Calorimetry Core: Steps to Startup, Run, and Maintain a Multiuser Facility. *Meth Enzymol*. 2016;567:435-60.

Yonezawa H, Osaki T, Woo T, et al. Analysis of outer membrane vesicle protein involved in biofilm formation of Helicobacter pylori. *Anaerobe*. 2011;17(6):388-90.

Yu NY, Wagner JR, Laird MR, et al. PSORTb 3.0: improved protein subcellular localization prediction with refined localization subcategories and predictive capabilities for all prokaryotes. *Bioinformatics*. 2010;26(13):1608-15.

Yun SH, Lee SY, Choi CW, et al. Proteomic characterization of the outer membrane vesicle of the halophilic marine bacterium Novosphingobium pentaromativorans US6-1. *J Microbiol*. 2017;55(1):56-62.

Yun SH, Park EC, Lee SY, et al. Antibiotic treatment modulates protein components of cytotoxic outer membrane vesicles of multidrug-resistant clinical strain, DU202. *Clin Proteomics*. 2018;15:28.

Zakharzhevskaya NB, Vanyushkina AA, Altukhov IA, et al. Outer membrane vesicles secreted by pathogenic and nonpathogenic Bacteroides fragilis represent different metabolic activities. *Sci Rep*. 2017;7(1):5008.

Zavan L, Bitto NJ, Johnston EL, Greening DW, Kaparakis-liaskos M. Helicobacter pylori Growth Stage Determines the Size, Protein Composition, and Preferential Cargo Packaging of Outer Membrane Vesicles. *Proteomics*. 2019;19(1-2):e1800209.

Zgurskaya HI, Nikaido H. AcrA is a highly asymmetric protein capable of spanning the periplasm. *J Mol Biol*. 1999;285(1):409-20.

Zhang YJ, Lin H, Wang P, Chen C, Chen S. Subcellular localisation of lipoproteins of Vibrio vulnificus by the identification of outer membrane vesicles components. *Anton Leeuw Int J G*. 2018;111(11):1985-1997.

Zhou J, Rudd KE. EcoGene 3.0. *Nucleic Acids Res*. 2013;41(Database issue):D613-24.

Zielke RA, Wierzbicki IH, Weber JV, Gafken PR, Sikora AE. Quantitative proteomics of the Neisseria gonorrhoeae cell envelope and membrane vesicles for the discovery of potential therapeutic targets. *Mol Cell Proteomics*. 2014;13(5):1299-317.

Loś JM, Loś M, Wegrzyn A, Wegrzyn G. Hydrogen peroxide-mediated induction of the Shiga toxin-converting lambdoid prophage ST2-8624 in Escherichia coli O157:H7. *FEMS Immunol Med Microbiol*. 2010;58(3):322-9.

Biography

Nichole Orench-Rivera obtained her Bachelor's degree in Industrial Biotechnology from the University of Puerto Rico at Mayagüez. Since then she worked towards her doctoral degree in Biochemistry and a Certificate in College Teaching at Duke University. After participating in the Preparing Future Faculty Program at Duke, she was Adjunct Professor of Biology for two semesters at North Carolina Central University (NCCU). She is first author in a review: *Environmentally controlled bacterial vesicle-mediated export*, and the article: *Differential packaging into outer membrane vesicles upon oxidative stress reveals a general mechanism for cargo selectivity* (under review). She has also collaborated in several investigations resulting in publications where she is listed as contributing author. As a PhD Candidate she received several academic honors including being selected to travel and present her research at the meeting for the American Association of Biochemistry and Molecular Biology (ASBMB), being selected to receive the Mitchell Meritorious Research Travel Award granted by the Duke University Center for Host-Microbial Interactions (CHoMI), receiving an outstanding abstract award from the American Society for Microbiology (ASM), and being awarded the Chancellor's Scholarship granted by the Duke University Graduate School. In the Fall of 2020 she will begin working as an Assistant Professor of Biology at Lasell University.